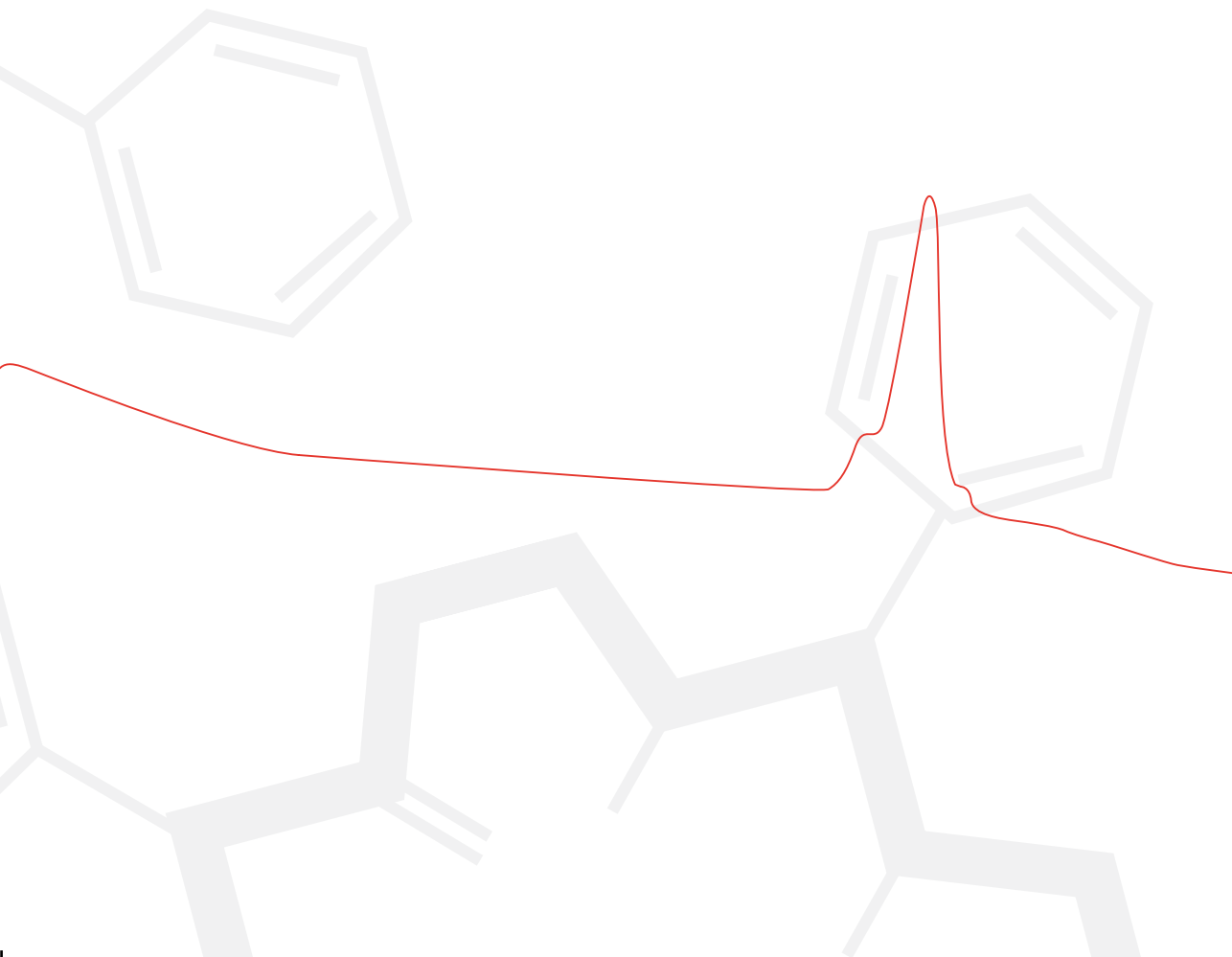# mTHPC mediated PDT of Head and Neck Cancer

Modifying pharmacokinetics using liposomal drug carriers

Sebastiaan A.H.J. de Visscher

mTHPC mediated PDT of Head and Neck Cancer
Modifying pharmacokinetics using liposomal drug carriers

thesis

Sebastiaan A.H.J. de Visscher

university of groningen

mTHPC mediated PDT of Head and Neck Cancer
Modifying pharmacokinetics using liposomal drug carriers

Proefschrift

ter verkrijging van de graad van doctor aan de
Rijksuniversiteit Groningen
op gezag van de
rector magnificus, prof. dr. E. Sterken
en volgens besluit van het College voor Promoties.

De openbare verdediging zal plaatsvinden op

woensdag 8 januari 2014 om 16.15 uur

door

Sebastiaan Antonius Hendrik Johannes de Visscher

geboren op 1 november 1981
te Nijmegen

Contents

Chapter 1

Introduction

Cancer of the head and neck

Head and neck cancer has a world wide estimated incidence of more than half a million in 2002, with approximately 350,000 patients dying of this disease each year [1]. In the Netherlands, head and neck cancer is the 7th most common cancer for men (3.8%) and the 9th most common cancer for women (2.0%) with a total incidence of almost 3000 in 2011 (source: IKNL 2013). Of these malignancies, 90% are squamous cell carcinomas (SCCs) of the mucosal lining of the upper aerodigestive tract. These tumors usually develop in elderly patients after a life long period of smoking and or consuming large amounts of alcohol. Tobacco and alcohol are the most important risk-factors for developing head and neck squamous cell carcinoma (HNSCC); a combination of both has a synergistic effect [2-5]. In the last decade it became apparent that the human papillomavirus (HPV) can also induce HNSCC, increasingly affecting young non-smokers [2,3,6,7]. Treatment strategies are based on tumor factors, patient factors and physician factors. Tumor factors affecting treatment choice are the size of the primary tumor, the location, the presence of metastases, previous treatments and the presence and depth of disruptive growth into surrounding tissues [2,3]. Classification of HNSCC is performed using the American Joint Committee on Cancer (AJCC) and the Union for International Cancer Control (UICC) staging systems [8]. The standard treatment regime for patients with early stage (stage I/II) HNSCC is surgery and/or radiotherapy, both with similar cure rates [2,3,9,10]. Most often surgery is preferred because radiotherapy side effects can be avoided and histopathological staging can be obtained [3,9]. For more advanced head and neck neoplasms (stage III/IV), treatment options consists of combinations of surgery, radiotherapy and chemotherapy [3,7,11-13].

Unfortunately, these standard treatments often induce toxicities, anatomical defects and loss of normal organ function, affecting quality of life [3,14-19]. A major challenge in the treatment of cancers within the anatomical constraints of the head and neck region, is obtaining a high cure rate while preserving its vital structures and functions [2,3,7]. This is further complicated as continuous exposure of the mucosa to smoking and alcohol induces multiple (pre)malignant lesions in this condemned mucosa [2,3]. It has been suggested that photodynamic therapy (PDT) could be an alternative, local treatment option for both patients with early and advanced stages of HNSCC [20-23].

Photodynamic therapy

As a treatment modality, light has been used in ancient societies to treat various skin diseases [24,25]. In more recent history, Finsen was awarded the Nobel prize in 1903 for "phototherapy" in which he used (ultraviolet) sun light to treat cutaneous tuberculosis and red-light to decrease formation of small-pox pustules [26]. In that same year, Tappeiner and Je-

sionek described "photodynamic action" whereby skin tumors were treated by white light illumination of topically applied eosin [27,28]. In further experimentations the use of certain light sensitive drugs, so-called photosensitizers (PS), resulted in what is presently known as "Photodynamic Therapy". PDT involves the uptake and localization of PS in tissue combined with the illumination of that same tissue with light of a sensitizer-specific wavelength to excite the PS. Excitation leads to a process in which energy is transferred from light to molecular oxygen generating intracellular cytotoxic reactive oxygen species (ROS) within the light exposed tissue which are disruptive to cells and induce cell death [29]. Porphyrins were the first widely studied photosensitizers. In 1913 Meyer-Betz was the first to use porphyrins in humans, applying it to his own skin [30]. Fifty years later haemotoporphyrin derivative (HPD) was developed which showed increased localization in tumor tissue in animal studies. In the 1970's the first patients were treated by HPD for various tumors showing some promising results in inoperable patients with early stage disease [24]. In 1993 clinical PDT was approved for the first time using the first generation photosensitizer Photofrin® (porfimer sodium, partially purified HPD) [24]. Although currently Photofrin holds the largest number of approvals for clinical use of any sensitizer, it has several limitations; the need for high drug and light concentrations for desired tumor response, lack of long wavelength absorption and therefore limited tissue penetration, poor water solubility and prolonged cutaneous photosensitivity. Moreover, its composition of numerous compounds hinders it reproduction [24,31,32]. These limitations led to the investigation of new chemically synthesized pure compounds (second generation photosensitizers) with better properties and lower toxic side-effects due to better absorption at longer wavelengths and shorter tissue accumulation [23]. Examples of second-generation PSs are 5-aminolevulinic acid (5-ALA) and its derivatives (Metvix®) which are now widely used in the treatment of actinic keratosis and cutaneous basal cell carcinoma while intravenous administered Verteporfin (Visudyne®) is used in the treatment of age-related macular degeneration [32]. Another second generation PS, *meta*-tetra(hydroxylphenyl)chlorin (mTHPC), is a chlorin-based sensitizer that can be excited with red wavelengths, resulting in a depth of light penetration of at least 10 mm and is described with a high potency [23].

mTHPC mediated PDT
The hydrophobic photosensitizer mTHPC (INN: Temoporfin) is approved and used in the European Union for palliative treatment of advanced HNSCC, using a formulation of ethanol and propylene glycol (Foscan®) [33]. mTHPC is one of the most potent clinically used photosensitizers to date; in comparison with Photofrin a 100 – 200 fold increased efficacy is estimated [34]. The current PDT protocol for HNSCC dictates an intravenous injection of 0.15 mg/kg mTHPC followed 96 hours later by illuminating tissue with non-thermal light at a wavelength of 652 nm [23]. During clinical PDT it is common practice to irradiate a margin of healthy tissue around the tumor to illuminate microscopic malignant foci, comparable to the use of a surgical margin [35,36].

Several authors described a reduction in tumor size, prolonged survival and an improved

quality of life after mTHPC mediated PDT in HNSCC patients treated with palliative intent [37]. Besides palliative treatment, mTHPC mediated PDT is also used as an alternative curative treatment for patients with early stage superficial HNSCC, supposedly with similar efficacy and decrease of treatment related morbidity [35,36,38,39].

Although mTHPC mediated PDT seems promising, it is associated with long drug-light intervals and prolonged skin photosensitivity at the injection site [23,36].

Despite possible advantages of using PDT in HNSCC, the role of mTHPC mediated PDT in treatment of HNSCC is currently not clear. Most of the literature regarding PDT of HNSCC provides insight in mechanisms of PDT and treatment results. However, the efficacy of PDT in relation to the standard treatment regimes or morbidity is seldom reported.

Mechanism of action

When photosensitizers absorb light of a PS-specific wavelength, the absorbed photons transform the PS from its ground state (S_0) via a short-lived excited singlet state (S_n) to the excited singlet state (S_1) [24,29,40,41]. The PS can return to its singlet state by either 1) emitting the absorbed energy as light of a lower energy and red-shifted (Stokes-Lommel's law) compared to the excitation light (fluorescence) or 2) transform into an excited triplet state (T_1). The excited triplet state can undergo a type I reaction whereby it reacts with a nearby substrate (molecules) and transfer electrons to form radicals which interact with oxygen to form oxygenated products (Figure 1). Alternatively a for PDT favored type II reaction can occur, in which direct transfer of energy (electrons) to oxygen ($^3O_2$) forms a highly reactive singlet oxygen species (ROS) ($^1O_2$) [29,32]. While the oxygen-dependant type I and II reactions occur simultaneously, the ratio depends on the type of photosensitizer, its concentration, drug-light interval, tissue oxygenation and the light fluence (rate). For mTHPC a high quantum yield for singlet oxygen production is known [34,42,43]. Due to the short-half life and high reactivity of singlet oxygen (10 -320 nanoseconds and 10- 55 nanometers respectively) only the tissue directly surrounding the area of ROS formation is affected [41]. Therefore, the time-dependant subcellular and macroscopic localization of a PS is an important factor that determines PDT efficacy [24]. The localization of a PS is determined by vascular permeability and time-dependant diffusion, which are influenced by interactions with plasma components, aggregation & disaggregation, molecular size, charge and hydrophobic or hydrophilic properties of a PS [23,24,44-48]. mTHPC accumulates in both normal and tumor tissue and its localization is dependant on the drug-light interval used [23]. For short drug-light intervals mTHPC is mostly localized in the vasculature, while at longer intervals diffusion into cells occurs [47,48]. Clinical mTHPC mediated PDT (Foscan) therefore relies on drug-light intervals of several days. After cellular uptake, mTHPC is preferentially accumulated in the Golgi apparatus and endoplasmic reticulum. These were also shown to be the primary sites of PDT induced damage [49-51]. As a consequence of ROS, the tumor is destroyed by a combination of direct tumor cell kill and vascular infarction of tumor tissue [29,41]. Direct tumor cell kill can be achieved by three cell death pathways; apoptosis, necrosis and stimulation of macro-autophagy induced by
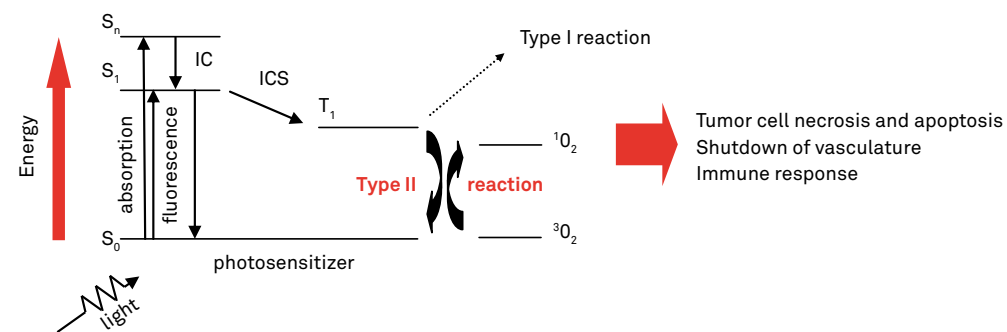

Figure 1. Modified Jablonski diagram; excitation by light of a photosensitizer in its ground state (S_0) takes it to a short lived excited state (S_n) from which internal conversion (IC) takes it to its excited singlet state (S_1). This excited molecule may undergo intersystem crossing (ICS) to an excited triplet state (T_1) subsequently, either a type I or a type II reaction can occur. The induced tissue damage is predominantly achieved by the type II reaction in which energy is transferred to molecular oxygen ($^3O_2$) to form cytotoxic singlet oxygen ($^1O_2$).

photodamage [41]. Vascular damage and infarction is supposedly induced by a combination of vasoconstriction, thrombus formation and higher sensitivity for PDT of the endothelium. Furthermore, endothelial cell response and time-dependant localization in endothelium of a PS (at short drug-light intervals) may also contribute to vascular changes [24,41,52]. Besides the aforementioned direct cell death, a response mediated by the innate immune system is described following PDT induced local inflammation [23,24,53,54]. This inflammation is characterized by generation of damage associated molecular patterns (DAMPs) and by increased permeability of tumor vasculature for proteins and inflammatory cells. Incoming neutrophils, mast cells, monocytes and macrophages attracted by DAMPs, eliminate injured or death cells from the photodamaged area by phagocytosis [40,55]. However, besides the previous immunostimulatory effect several immunosuppressive effects of PDT have been described as well [54].

Liposomes as photosensitizer carriers

Although mTHPC is described as a potent PS, it is hydrophobicity leads to poor water solubility and aggregation of mTHPC molecules. Therefore, mTHPC molecules have a tendency to aggregate under physiological conditions (vasculature) in which it is less photoactive [46,56]. In general, aggregation of PS's result in lower fluorescence and triplet-state quantum yields (T_1). Consequently a decreased quantum yield of singlet oxygen and a decreased photosensitizing efficiency follows [51,57]. Furthermore, the aggregated form of mTHPC is described with a rapid uptake by the mononuclear phagocyte system (MPS), decreasing the amount of mTHPC available for uptake in tumor tissue [23,32,58,59]. For these reasons, improved delivery and solubilisation of mTHPC by using drug-carrier systems is the subject of numerous studies [23,31,32,58,60,61]. Liposomes are amphiphilic, spherical structures which makes them suitable

for encapsulation and delivery of drugs. Over the last two decades, studies on water-soluble liposomes as drug carrier systems reported increased uptake in tumor and enhancement of therapeutic efficacy at a decreased drug dose, thus lowering toxicity of the encapsulated drug [60,62]. Therefore, encapsulation of mTHPC in liposomes has been performed to improve water solubility, prevent aggregation effects, prolong circulation time and increase mTHPC uptake in tumor. Macromolecules such as liposomes allow selective, passive accumulation in tumor tissue by the enhanced permeability and retention (EPR) effect (figure 2) [63,64]. Tumor tissue is characterized by enhanced vascular permeability due to its fast angiogenesis. Moreover, tumor tissue lacks a functional lymphatic system and macromolecules are thus retained after extravasation from its vasculature. Two liposomal mTHPC formulations that have been developed by Biolitec AG are Foslip® and Fospeg® [23,65-68]. In contrast to Foslip, the surface of the liposomes used in Fospeg is coated by a hydrophilic polymer to decrease recognition by the MPS and thus increase circulation time favoring the EPR effect [69,70]. Previous studies suggest that liposomal formulations will yield an earlier, higher availability of mTHPC in tumor tissue. However, there is a substantial lack of data to compare the kinetics of these liposomal mTHPC formulations to Foscan in (pre-clinical) animal tumor models over several days.

Measuring photosensitizer pharmacokinetics using fluorescence
Despite fixed light fluence and administered drug dose, differences in clinical PDT response may occur due to biological inter- and intra-subject variations [59]. The dose delivered during PDT (deposited PDT dose) is depended on the influence of tissue optical properties on delivered fluence (rate), uptake of photosensitizer and tissue oxygenation [71]. For instance, oxygen depletion during treatment of oxygen deprived tumor tissue, oxygen depletion due to high fluence rates or failed intravenous administration of the PS can result in suboptimal results. Therefore, insight at the complex and interdependent dynamic interactions of oxygen, light fluence (rate) and photosensitizer concentration during therapy (dosimetry) could be beneficial to optimize PDT [72,73]. The concentration and differences in distribution of a PS between tumor and surrounding normal tissue is clearly an important parameter for PDT efficacy.
In principle, photosensitizer fluorescence, although unproductive from a treatment point of view since it does not cause tissue damage, gives information on the spatial distribution and is related to both the biological activity and the concentration of the PS [23,72]. Therefore, non-invasive and *in vivo* fluorescence measurements allow for monitoring PS concentrations in tissue [74].
A major challenge in biomedical optics is quantitative measurement of emitted fluorescence intensity as it is influenced by tissue optical properties, background fluorescence, tissue thickness variations and geometric factors of the excitation and detection source.
Tissue influences the optical photon pathlength (light propagation) by way of tissue optical properties; scattering and absorption [71]. The scattering coefficient (μs) of tissue is dependant on different refractive indexes between various cell and tissue components within
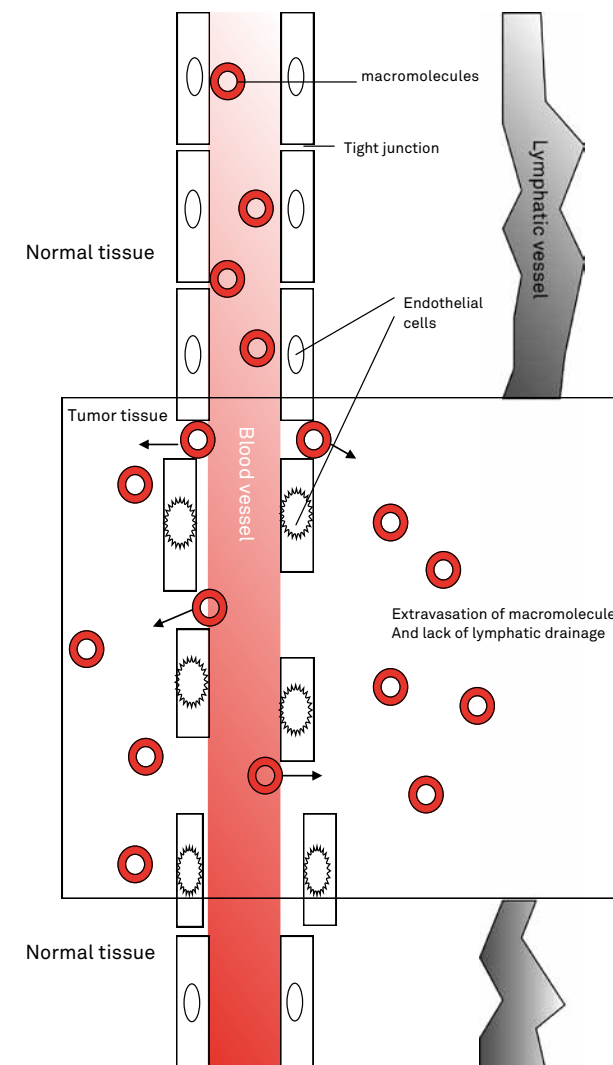

Figure 2. A schematic representation of the enhanced permeability and retention (EPR) effect. Due to both the increased fenestrae between endothelial cells and a decrease in lymphatic drainage in tumor tissue compared to normal tissue, extravasation of macromolecules occurs without drainage to the central circulation.

tissue. The absorption coefficient (μa) of tissue is related to the concentration of chromophores (e.g. melanin, bilirubin, beta-carotene, haemoglobin, water, fat) in tissue. In the visible part of the spectrum (400-700 nanometers) oxy-and deoxy-haemoglobin are the dominant absorbing molecules in tissue. Appropriate correction for these factors is important to obtain accurate information on fluorescence intensity and PS concentration in tissue [71]. Interpretation of corrected fluorescence measurement should be done with care as fluorescence emission from a PS is influenced by its environment; aggregating and binding of the PS, changes in microenvironment and photobleaching [71]. Photobleaching occurs when a fluorophore such as a PS loses the ability to fluoresce due to photon-induced photochemical destruction. Photobleaching is commonly termed "fading" of a fluorophore.

Our group developed fluorescence differential path-length spectroscopy (fDPS) [71,75,76] as a non-invasive tool to quantify microvascular oxygen saturation and photosensitizer concentration in tissue during excitation of mTHPC. fDPS is based on differential pathlength spectroscopy (DPS) which features photons pathlength contributing to a differential reflectance signal that is relatively insensitive to expected variations in tissue optical properties over a small sampling volume [76]. In previous research, we were able to show that fDPS can be used to measure the Foscan concentration *in vivo* in rat liver [74]. In contrast to the relative homogeneous liver tissue, clinically more relevant tissue of the oral cavity is optically more heterogeneous and even keratinized at some locations. Reliable *in vivo*, non-invasive mTHPC concentration measurements of tissue, could give some insight at the complex interdependent processes that is PDT. Furthermore, mTHPC concentration measurements combined with measurements of tissue physiology could guide clinical decision making on the choice of PDT parameters; fluence (rate) and drug-light interval needed [71].

Outline of this thesis

This thesis contains the results of our various studies describing the available literature on mTHPC mediated PDT for clinical treatment of HNSCC (chapter 2), the influence of two liposomal drug carrier systems on mTHPC biodistribution and (chapter 3) the performance of non-invasive fluorescence differential spectroscopy to measure *in vivo* mTHPC concentration in lip and tongue tissue (chapter 4).

The level of evidence on mTHPC mediated PDT was investigated and described in chapter 2.1 by performing an extensive systematic review of the literature up to 2012. This review was done to provide insight in the efficacy of PDT, used protocols, associated morbidity and the possible role of mTHPC mediated PDT in treatment of HNSCC. In chapter 2.2 a comparison between mTHPC mediated PDT and transoral surgery for early stage oral SCC is described. PDT patients were included from several multi-center studies while the surgically treated patients were included from our hospital database. The aim of this study was to obtain some comparative data on PDT versus surgery, as efficacy of PDT in relation to the standard treatment regimes is seldom reported.

In chapter 3.1 the influence of liposomal encapsulation of mTHPC on bioavailability was studied in the window-chamber rat model. This model allows for careful examination of photosensitizer fluorescence in vasculature, normal and (implanted) tumor tissue up to 96 hours after injection. To improve the quality of our data, we tried to correct for small changes in the thickness of tissue and to partially correct for changes in tissue optical properties by developing a ratiometric correction method, as described in chapter 3.2.

Chapter 3.3 describes the uptake of the different mTHPC formulations in both dysplastic and tumor tissue, compared to the uptake in normal oral mucosa. For this purpose, the 4-nitroquinoline-1-oxide (4NQO) oral carcinogenesis rat model was used. This model induces pre-malignant and malignant oral mucosa and is known to mimic the development of oral epithelial dysplasia in humans. By correlating mTHPC fluorescence to the dysplasia grade of the oral mucosa, a possible relation was investigated. This enabled us to grade oral tissue as normal, cancerous or precancerous in tissue exposed to the carcinogen. Moreover, a possible enhanced uptake of mTHPC in precancerous tissue could be studied. Furthermore, more in-depth analysis of mTHPC formulation specific biodistribution is possible in this induced tumor model.

In chapter 4 the mTHPC concentration of the different mTHPC formulations in tissue measured by *in vivo* fDPS was compared to the "gold standard" chemical extraction. Therefore, fDPS was tested in the clinically more relevant but optically heterogeneous oral mucosa as previous research showed encouraging performance in relatively homogeneous liver tissue. To determine the influence of liposomal encapsulation on fDPS performance, liver measurements were performed as well. The aim was to test if fDPS could be a non-invasive, *in vivo* real time instrument to measure local mTHPC concentration in optically challenging tissue. Chapter 5 contains the summary and the general discussion while chapter 6 contains the Dutch summary.

References

1. Parkin DM, Bray F, Ferlay J, Pisani P. Global cancer statistics, 2002. CA Cancer J Clin. 2005 Mar-Apr;55(2):74-108.

2. Shah JP, Gil Z. Current concepts in management of oral cancer--surgery. Oral Oncol. 2009 Apr-May;45(4-5):394-401.

3. Argiris A, Karamouzis MV, Raben D, Ferris RL. Head and neck cancer. Lancet. 2008 May 17;371(9625):1695-709.

4. Vineis P, Alavanja M, Buffler P, Fontham E, Franceschi S, Gao YT, et al. Tobacco and cancer: Recent epidemiological evidence. J Natl Cancer Inst. 2004 Jan 21;96(2):99-106.

5. Blot WJ, McLaughlin JK, Winn DM, Austin DF, Greenberg RS, Preston-Martin S, et al. Smoking and drinking in relation to oral and pharyngeal cancer. Cancer Res. 1988 Jun 1;48(11):3282-7.

6. D'Souza G, Kreimer AR, Viscidi R, Pawlita M, Fakhry C, Koch WM, et al. Case-control study of human papillomavirus and oropharyngeal cancer. N Engl J Med. 2007 May 10;356(19):1944-56.

7. Haddad RI, Shin DM. Recent advances in head and neck cancer. N Engl J Med. 2008 Sep 11;359(11):1143-54.

8. Patel SG, Shah JP. TNM staging of cancers of the head and neck: Striving for uniformity among diversity. CA Cancer J Clin. 2005 Jul-Aug;55(4):242,58; quiz 261-2, 264.

9. Wolfensberger M, Zbaeren P, Dulguerov P, Muller W, Arnoux A, Schmid S. Surgical treatment of early oral carcinoma-results of a prospective controlled multicenter study. Head Neck. 2001 Jul;23(7):525-30.

10. Ord RA, Blanchaert RH,Jr. Current management of oral cancer. A multidisciplinary approach. J Am Dent Assoc. 2001 Nov;132 Suppl:19S-23S.

11. Cohen EE, Lingen MW, Vokes EE. The expanding role of systemic therapy in head and neck cancer. J Clin Oncol. 2004 May 1;22(9):1743-52.

12. Furness S, Glenny AM, Worthington HV, Pavitt S, Oliver R, Clarkson JE, et al. Interventions for the treatment of oral cavity and oropharyngeal cancer: Chemotherapy. Cochrane Database Syst Rev. 2011 Apr 13;(4)(4):CD006386.

13. Pignon JP, le Maitre A, Maillard E, Bourhis J, MACH-NC Collaborative Group. Meta-analysis of chemotherapy in head and neck cancer (MACH-NC): An update on 93 randomised trials and 17,346 patients. Radiother Oncol. 2009 Jul;92(1):4-14.

14. Bundgaard T, Tandrup O, Elbrond O. A functional evaluation of patients treated for oral cancer. A prospective study. Int J Oral Maxillofac Surg. 1993 Feb;22(1):28-34.

15. Epstein JB, Emerton S, Kolbinson DA, Le ND, Phillips N, Stevenson-Moore P, et al. Quality of life and oral function following radiotherapy for head and neck cancer. Head Neck. 1999 Jan;21(1):1-11.

16. Finlay PM, Dawson F, Robertson AG, Soutar DS. An evaluation of functional outcome after surgery and radiotherapy for intraoral cancer. Br J Oral Maxillofac Surg. 1992 Feb;30(1):14-7.

17. Pauloski BR, Rademaker AW, Logemann JA, Colangelo LA. Speech and swallowing in irradiated and nonirradiated postsurgical oral cancer patients. Otolaryngol Head Neck Surg. 1998 May;118(5):616-24.

18. Biazevic MG, Antunes JL, Togni J, de Andrade FP, de Carvalho MB, Wunsch-Filho V. Immediate impact of primary surgery on health-related quality of life of hospitalized patients with oral and oropharyngeal cancer. J Oral Maxillofac Surg. 2008 Jul;66(7):1343-50.

19. Chandu A, Smith AC, Rogers SN. Health-related quality of life in oral cancer: A review. J Oral Maxillofac Surg. 2006 Mar;64(3):495-502.

20. Nyst HJ, Tan IB, Stewart FA, Balm AJ. Is photodynamic therapy a good alternative to surgery and radiotherapy in the treatment of head and neck cancer? Photodiagnosis Photodyn Ther. 2009 Mar;6(1):3-11.

21. Biel M. Advances in photodynamic therapy for the treatment of head and neck cancers. Lasers Surg Med. 2006 06;38(0196-8092; 5):349-55.

22. Jerjes W, Upile T, Akram S, Hopper C. The surgical palliation of advanced head and neck cancer using photodynamic therapy. Clin Oncol (R Coll Radiol). 2010 Nov;22(9):785-91.

23. Senge MO, Brandt JC. Temoporfin (foscan(R), 5,10,15,20-tetra(m-hydroxyphenyl)chlorin)--a second-generation photosensitizer. Photochem Photobiol. 2011 Nov-Dec;87(6):1240-96.

24. Dolmans DEJGJ, Fukumura D, Jain RK. Photodynamic therapy for cancer. Nat Rev Cancer. 2003 /;3(5):380-7.

25. Ackroyd R, Kelty C, Brown N, Reed M. The history of photodetection and photodynamic therapy. Photochem Photobiol. 2001 2001/11;74(5):656-69.

26. Niels ryberg finsen - biography [homepage on the Internet]. Available from: http://www.nobelprize.org/nobel_prizes/medicine/laureates/1903/finsen.html.

27. Tappeiner Hv, H.Jesionek. Therapeutische versuche mit fluoreszierenden stoffen. Munch Med Wschr. 1903;50:2042-4.

28. Jesionek H, H. von Tappeiner. Zur behandlung der hautcarcinome mit fluoreszierenden stoffen. Dtsch Arch Klin Med. 1905;82:223-6.

29. Buytaert E, Dewaele M, Agostinis P. Molecular effectors of multiple cell death pathways initiated by photodynamic therapy. Biochim Biophys Acta. 2007 Sep;1776(1):86-107.

30. Meyer-Betz F. Untersuchungen uber die biologische photodynamische wirkung des hematoporphyrins und anderer derivative des blut und galenafarbstoffs. Dtsch Arch Klin. 1913(112):476-503.

31. Senge MO. mTHPC--a drug on its way from second to third generation photosensitizer? Photodiagnosis Photodyn Ther. 2012 Jun;9(2):170-9.

32. Allison RR, Sibata CH. Oncologic photodynamic therapy photosensitizers: A clinical review. Photodiagn Photodyn Ther. 2010 /;7(2):61-75.

33. European Medicines Agencies. H-C-318 foscan european public assessment report. 2009 04/30.

34. Mitra S, Foster TH. Photophysical parameters, photosensitizer retention and tissue optical properties completely account for the higher photodynamic efficacy of meso-tetra-hydroxyphenyl-chlorin vs photofrin. Photochem Photobiol. 2005 07;81(0031-8655; 0031-8655; 4):849-59.

35. Hopper C, Kubler A, Lewis H, BingTan I, Putnam G, Foscan 01 Study Grp. mTHPC-mediated photodynamic therapy for early oral squamous cell carcinoma. International Journal of Cancer. 2004 AUG 10;111(1):138-46.

36. Karakullukcu B, van Oudenaarde K, Copper MP, Klop WM, van Veen R, Wildeman M, et al. Photodynamic therapy of early stage oral cavity and oropharynx neoplasms: An outcome analysis of 170 patients. Eur Arch Otorhinolaryngol. 2011 Feb;268(2):281-8.

37. D'Cruz AK, Robinson MH, Biel MA. mTHPC-mediated photodynamic therapy in patients with advanced, incurable head and neck cancer: A multicenter study of 128 patients. Head Neck. 2004 03;26(1043-3074; 1043-3074; 3):232-40.

38. Kubler AC, de Carpentier J, Hopper C, Leonard AG, Putnam G. Treatment of squamous cell carcinoma of the lip using foscan-mediated photodynamic therapy. Int J Oral Maxillofac Surg. 2001 12;30(0901-5027; 0901-5027; 6):504-9.

39. Jerjes W, Upile T, Hamdoon Z, Alexander Mosse C, Morcos M, Hopper C. Photodynamic therapy outcome for T1/T2 N0 oral squamous cell carcinoma. Lasers Surg Med. 2011 /;43(6):463-9.

40. Henderson BW, Dougherty TJ. How does photodynamic therapy work? Photochem Photobiol. 1992 01;55(0031-8655; 0031-8655; 1):145-57.

41. Agostinis P, Berg K, Cengel KA, Foster TH, Girotti AW, Gollnick SO, et al. Photodynamic therapy of cancer: An update. CA Cancer J Clin. 2011 /;61(4):250-81.

42. Redmond RW, Gamlin JN. A compilation of singlet oxygen yields from biologically relevant molecules. Photochem Photobiol. 1999 Oct;70(4):391-475.

43. Melnikova VO, Bezdetnaya LN, Potapenko AY, Guillemin F. Photodynamic properties of meta-tetra(hydroxyphenyl)chlorin in human tumor cells. Radiat Res. 1999 10;152(0033-7587; 0033-7587; 4):428-35.

44. Hopkinson HJ, Vernon DI, Brown SB. Identification and partial characterization of an unusual distribution of the photosensitizer meta-tetrahydroxyphenyl chlorin (temoporfin) in human plasma. Photochem Photobiol. 1999 Apr;69(4):482-8.

45. Kiesslich T, Berlanda J, Plaetzer K, Krammer B, Berr F. Comparative characterization of the efficiency and cellular pharmacokinetics of foscan- and foslip-based photodynamic treatment in human biliary tract cancer cell lines. Photochem Photobiol Sci. 2007 Jun;6(6):619-27.

46. Triesscheijn M, Ruevekamp M, Out R, Van Berkel TJ, Schellens J, Baas P, et al. The pharmacokinetic behavior of the photosensitizer meso-tetra-hydroxyphenyl-chlorin in mice and men. Cancer Chemother Pharmacol. 2007 Jun;60(1):113-22.

47. Jones HJ, Vernon DI, Brown SB. Photodynamic therapy effect of m-THPC (foscan) in vivo: Correlation with pharmacokinetics. Br J Cancer. 2003 07/21;89(0007-0920; 0007-0920; 2):398-404.

48. Cramers P, Ruevekamp M, Oppelaar H, Dalesio O, Baas P, Stewart FA. Foscan uptake and tissue distribution in relation to photodynamic efficacy. Br J Cancer. 2003 01/27;88(0007-0920; 2):283-90.

49. Teiten MH, Bezdetnaya L, Morliere P, Santus R, Guillemin F. Endoplasmic reticulum and golgi apparatus are the preferential sites of foscan localisation in cultured tumour cells. Br J Cancer. 2003 Jan 13;88(1):146-52.

50. Teiten MH, Marchal S, D'Hallewin MA, Guillemin F, Bezdetnaya L. Primary photodamage sites and mitochondrial events after foscan photosensitization of MCF-7 human breast cancer cells. Photochem Photobiol. 2003 Jul;78(1):9-14.

51. Sasnouski S, Pic E, Dumas D, Zorin V, D'Hallewin MA, Guillemin F, et al. Influence of incubation time and sensitizer localization on meta-tetra(hydroxyphenyl)chlorin (mTHPC)-induced photoinactivation of cells. Radiat Res. 2007 08;168(0033-7587; 0033-7587; 2):209-17.

52. Triesscheijn M, Ruevekamp M, Aalders M, Baas P, Stewart FA. Outcome of mTHPC mediated photodynamic therapy is primarily determined by the vascular response. Photochem Photobiol. 2005 Sep-Oct;81(5):1161-7.

53. Dougherty TJ, Gomer CJ, Henderson BW, Jori G, Kessel D, Korbelik M, et al. Photodynamic therapy. J Natl Cancer Inst. 1998 06/17;90(0027-8874; 0027-8874; 12):889-905.

54. Castano AP, Mroz P, Hamblin MR. Photodynamic therapy and anti-tumour immunity. Nat Rev Cancer. 2006 Jul;6(7):535-45.

55. Korbelik M. PDT-associated host response and its role in the therapy outcome. Lasers Surg Med. 2006 Jun;38(5):500-8.

56. Sasnouski S, Zorin V, Khludeyev I, D'Hallewin MA, Guillemin F, Bezdetnaya L. Investigation of foscan interactions with plasma proteins. Biochim Biophys Acta. 2005 Oct 10;1725(3):394-402.

57. Redmond RW, Land EJ, Truscott TG. Aggregation effects on the photophysical properties of porphyrins in relation to mechanisms involved in photodynamic therapy. Adv Exp Med Biol. 1985;193:293-302.

58. Konan YN, Gurny R, Allemann E. State of the art in the delivery of photosensitizers for photodynamic therapy. J Photochem Photobiol B. 2002 03;66(1011-1344; 1011-1344; 2):89-106.

59. Glanzmann T, Hadjur C, Zellweger M, Grosjean P, Forrer M, Ballini JP, et al. Pharmacokinetics of tetra(m-hydroxyphenyl)chlorin in human plasma and individualized light dosimetry in photodynamic therapy. Photochem Photobiol. 1998 May;67(5):596-602.

60. Decker C, Schubert H, May S, Fahr A. Pharmacokinetics of temoporfin-loaded liposome formulations: Correlation of liposome and temoporfin blood concentration. J Control Release. 2013 Mar 28;166(3):277-85.

61. Paszko E, Ehrhardt C, Senge MO, Kelleher DP, Reynolds JV. Nanodrug applications in photodynamic therapy. Photodiagn Photodyn Ther. 2011 /;8(1):14-29.

62. Lammers T, Hennink WE, Storm G. Tumour-targeted nanomedicines: Principles and practice. Br J Cancer. 2008 Aug 5;99(3):392-7.

63. Maeda H, Wu J, Sawa T, Matsumura Y, Hori K. Tumor vascular permeability and the EPR effect in macromolecular therapeutics: A review. J Control Release. 2000 03/01;65(0168-3659; 1-2):271-84.

64. Maruyama K. Intracellular targeting delivery of liposomal drugs to solid tumors based on EPR effects. Adv Drug Deliv Rev. 2011 Mar 18;63(3):161-9.

65. Buchholz J, Kaser-Hotz B, Khan T, Rohrer Bley C, Melzer K, Schwendener RA, et al. Optimizing photodynamic therapy: In vivo pharmacokinetics of liposomal meta-(tetrahydroxyphenyl)chlorin in feline squamous cell carcinoma. Clin Cancer Res. 2005 10/15;11(1078-0432; 20):7538-44.

66. Svensson J, Johansson A, Grafe S, Gitter B, Trebst T, Bendsoe N, et al. Tumor selectivity at short times following systemic administration of a liposomal temoporfin formulation in a murine tumor model. Photochem Photobiol. 2007 09;83(0031-8655; 0031-8655; 5):1211-9.

67. Berlanda J, Kiesslich T, Engelhardt V, Krammer B, Plaetzer K. Comparative in vitro study on the characteristics of different photosensitizers employed in PDT. J Photochem Photobiol B. 2010 Sep 2;100(3):173-80.

68. Lassalle HP, Dumas D, Grafe S, D'Hallewin MA, Guillemin F, Bezdetnaya L. Correlation between in vivo pharmacokinetics, intratumoral distribution and photodynamic efficiency of liposomal mTHPC. J Control Release. 2009 Mar 4;134(2):118-24.

69. Romberg B, Hennink WE, Storm G. Sheddable coatings for long-circulating nanoparticles. Pharm Res. 2008 Jan;25(1):55-71.

70. Derycke AS, de Witte PA. Liposomes for photodynamic therapy. Adv Drug Deliv Rev. 2004 01/13;56(0169-409; 1):17-30.

71. Robinson DJ, Karakullukcu MB, Kruijt B, Kanick SC, van Veen RPL, Amelink A, et al. Optical spectroscopy to guide photodynamic therapy of head and neck tumors. Ieee Journal of Selected Topics in Quantum Electronics. 2010 JUL-AUG;16(4):854-62.

72. Amelink A, van der Ploeg van den Heuvel,A., de Wolf WJ, Robinson DJ, Sterenborg HJ. Monitoring PDT by means of superficial reflectance spectroscopy. J Photochem Photobiol B. 2005 Jun 1;79(3):243-51.

73. Zhu TC, Finlay JC. The role of photodynamic therapy (PDT) physics. Med Phys. 2008 Jul;35(7):3127-36.

74. Kruijt B, Kascakova S, de Bruijn HS, van der Ploeg-van den Heuvel,A., Sterenborg HJ, Robinson DJ, et al. In vivo quantification of chromophore concentration using fluorescence differential path length spectroscopy. J Biomed Opt. 2009 May-Jun;14(3):034022.

75. Amelink A, Kruijt B, Robinson DJ, Sterenborg HJ. Quantitative fluorescence spectroscopy in turbid media using fluorescence differential path length spectroscopy. J Biomed Opt. 2008 Sep-Oct;13(5):054051.

76. Amelink A, Sterenborg HJ. Measurement of the local optical properties of turbid media by differential path-length spectroscopy. Appl Opt. 2004 May 20;43(15):3048-54.

Chapter 2

Evaluation of mTHPC mediated photodynamic therapy in clinical treatment of head and neck squamous cell carcinoma

Chapter 2.1

mTHPC mediated photodynamic therapy of squamous cell carcinoma in the head and neck: a systematic review
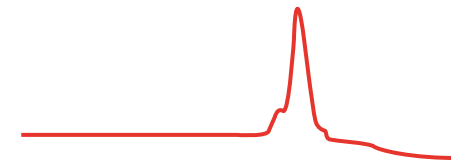
Abstract

Background and objective. Photodynamic Therapy (PDT) is used in curative and palliative treatment of head and neck squamous cell carcinoma. To evaluate available evidence on the use of mTHPC (Foscan®) mediated PDT, we conducted a review of the literature.

Materials and Methods. A systematic review was performed by searching 7 bibliographic databases on database specific mesh terms and free text words in the categories; "head and neck neoplasms", "Photodynamic Therapy" and "Foscan". Papers identified were assessed on several criteria by two independent reviewers.

Results. The search identified 566 unique papers. Twelve studies were included for our review. Six studies reported PDT with curative intent and 6 studies reported PDT with palliative intent, of which 3 studies used interstitial PDT. The studies did not compare PDT to other treatments and none exceeded level 3 using the Oxford levels of evidence. Pooling of data (n=301) was possible for 4 of the 6 studies with curative intent. T1 tumors showed higher complete response rates compared to T2 (86% vs 63%). PDT with palliative intent was predominantly used in patients unsuitable for further conventional treatment. After PDT, substantial tumor response and increase in quality of life was observed. Complications of PDT were mostly related to non-compliance to light restriction guidelines.

Conclusion. The studies on mTHPC mediated PDT for head and neck squamous cell carcinoma are not sufficient for adequate assessment of the efficacy for curative intent. To assess efficacy of PDT with curative intent, high quality comparative studies are needed. Palliative treatment with PDT seems to increase the quality of life in otherwise untreatable patients.

Introduction

Head and neck cancer has a world wide estimated incidence of 484,000 in 2002, with 262,000 patients dying of this disease [1]. Of these malignancies, 90% are squamous cell carcinomas (SCCs) arising from the lining of the oral cavity/pharynx. The standard treatment regime for patients with early stage (stage I/II) head and neck squamous cell carcinomas (HNSCC) is surgery or radiotherapy [2-7].

For more advanced head and neck neoplasms (stage III/IV), treatment options consists of combinations of surgery, radiotherapy and chemotherapy [7-11]. For recurrent or metastatic locoregional disease the only likely curative option is salvage surgery with or without re-irradiation. When the tumor is not resectable, re-irradiation alone or in combination with chemotherapy could be a possibility [12,13]. For palliative care, several chemotherapeutic agents are available without one being the standard of care [7].

A major challenge in treatment of cancers in the head and neck region, is obtaining a high cure rate while preserving its vital structures and functions [8]. Unfortunately, surgery and radiotherapy often induce anatomical defects, loss of normal function and toxicities affecting quality of life [6,7,14-18]. These side effects are often more pronounced in certain anatomical locations and in the treatment of recurrent or second primary tumors located in previously operated/irradiated fields [19-22]. Treatment regimes using platinum-based compounds are associated with severe acute and late toxicities [7-10,23-26].

It has been suggested that photodynamic therapy (PDT) could be an alternative, local treatment option for both patients with early stage HNSCC and for patients with advanced HNSCC who exhausted all treatment options [27-30]. PDT is described with limited scarring and limited loss of function after treatment without complicating other (future) treatments [27,31-38].

The basic mechanism of PDT involves the use of a light sensitive drug, photosensitizer (PS), available in the tumor, a light source and oxygen present in the target tissue [39,40]. The compound *meta*-tetra(hydroxyphenyl)chlorin (mTHPC) (INN: Temoporfin) is the most potent, clinically used PS to date [30,39,41,42]. Activation of intravenously (IV) administered mTHPC is achieved by illuminating target tissue with non-thermal laser light typically at a wavelength of 652nm [30]. The subsequent activation leads to the formation of intracellular cytotoxic reactive oxygen species which are disruptive to cells and induce cell death [43-45].

In the European union, the formulation of mTHPC in ethanol and propylene glycol (Foscan®) is approved for palliative treatment of patients suffering from incurable HNSCC [31,32,37,46,47]. Due to decreased light penetration at increased tissue depth, treatment using PDT with surface illumination is limited to tumors with < 5 - 10 mm invasion depth [30,48,49]. Larger tumor volumes can be treated by inserting optical fibers in the tissue; interstitial PDT (iPDT). Besides palliative treatment, Foscan is used in curative treatment for patients with early stage HNSCC [49-52].

Current literature regarding PDT of HNSCC provides insight in mechanisms of PDT and treatment results. However, efficacy of the therapy in relation to the standard treatment regimes or level of evidence is seldom reported. Therefore, the purpose of this study was to systematically review literature on effects of mTHPC mediated PDT of HNSCC for curative and palliative treatment.

Materials and methods

Literature search
A literature search was performed in seven bibliographical databases using a combination of "head and neck neoplasms", "photodynamic therapy" and "Foscan" in free text words, synonyms and database specific controlled vocabulary terms (Mesh and EMTREE) (table 1). No language or study type restrictions or other limits were implemented in our search. To check for unknown papers, the reference lists of the obtained papers were searched and "experts" were consulted for studies not identified in the search. To capture new publications (appearing after September 2011), the initial search was supplemented by monthly updates from PubMed throughout the project ending in June 2012.

Selection and assessment of relevant studies
The electronic and manual search results were imported into a RefWorks® database and duplicate citations were removed. Two reviewers (SV and MW) independently assessed titles and available abstracts of the papers retrieved from the searches on predefined inclusion and exclusion criteria (table 2). If inclusion criteria could not be assessed from the title or abstract, a full text analysis was performed against the criteria. After assessment, inter-observer agreement was calculated and a meeting was held to discuss discrepancies and to reach consensus. Following the first selection, the full text of the included papers was assessed independently by two observers (SV and MW) according to nineteen criteria specifically designed for this study (table 3). The authors involved in the development of the assessment criteria were 2 oral and maxillofacial surgeons specialized in oncology (JR and MW) and a clinical epidemiologist (PD). The criteria were scored on a dichotomous scale (yes or no) and inter-observer agreement was calculated. Of the assessment criteria, 9 were regarded as essential for further inclusion (table 3). Two papers were translated out of French by a native French speaker and one was read in German in order to assess quality [53-55]. A consensus meeting was held between the observers to discuss discrepancies in assessment. Furthermore, the level of evidence provided by each study was assessed according to the Levels of Evidence of the Oxford Centre for Evidence-based Medicine, enabling comparisons across different study designs [56].

Data extraction
Systematic data extraction of the included papers was performed (SV) and was checked for

Table 1. Search Strategy.

#1 head and neck neoplasms or head cancer or neck cancer or head neoplasms or neck neoplasms Or head cancers or neck cancers

#2 photochemotherapy or photobiology or phototherapy or (Light induced) or light-induced or photochemotherapies or photodynamic therapy or photodynamic therapies or PDT

#3 mesoporphyrin or mesoporphyrins or foscan or mthpc or m-thpc or (meta tetrahydroxyphenyl chlorin) or meso-tetra-hydroxyphenyl-chlorin or (meso-tetra (hydroxyphenyl) chlorin) or temoporfin

#4 #1 and #2 and #3 (In PUBMED AND WEB OF SCIENCE)

#5 photodynamic therapy or photodynamic therapies or pdt or photochemotherapy or photochemotherapies or photobiology or phototherapy or (light and induced) or light induced

#6 head and neck neoplasms or mouth tumor or head tumor or neck tumor or mouth cancer or head Cancer or neck cancer

#7 temoporfin or porphyrin or porphyrins or foscan or mthpc or m-thpc or m thpc or metatetrahydroxyphenyl chlorin or meso-tetra-hydroxyphenyl-chlorin or meso-tetra (hydroxyphenyl) chlorin

#8 #5 and #6 and #7 (In EMBASE)

#9 head and neck cancer AND (photodynamic therapy or photochemotherapy) (In INSPEC)

#10 meta tetrahydroxyphenyl chlorin or meso-tetra-hydroxyphenyl-chlorin or meso-tetra (hydroxyphenyl)chlorin or mesoporphyrines or mesoporphyrin or porphyrins or m-thpc or temoporfin or mthpc or foscan or photosensitizing agents

#11 head and neck neoplasms or head and neck cancer or head cancer or neck cancer or head Neoplasms or neck neoplasms or mouth cancer or oropharynx cancer

#12 photodynamic therapies or photodynamic therapy or pdt or photochemotherapy or photochemotherapies

#13 #10 AND #11 AND #12 (In ACADEMIC SEARCH PREMIER AND CINAHL)

#14 photochemotherapy or photodynamic therapy or PDT

#15 #10 AND #11 AND #14 (in COCHRANE CENTRAL)

Table 2. Criteria for including studies. Criteria were scored on a dichotomous scale.

Characteristics	Inclusion criteria	Exclusion criteria
Study design	• case series (n=≥10)	• single case reports (n=1) • review
Participants	• humans	• animal studies • *in vitro* studies
Tumor histology	• squamous cell carcinoma	
Tumor location	• lip or • oral cavity or • oropharynx or • hypopharynx or • nasopharynx	
Intervention	• Photodynamic therapy • mTHPC (Foscan)	

accuracy (MW). The datasheet used to collect information is based upon the 19 assessment criteria and incorporated information on the purpose and methods of a study (table 4).

Qualitative

Possible outcome measures were tumor response of the target lesion, local disease free survival (LDFS), survival, quality of life and adverse events. Tumor response was defined as "complete" when evidence of local eradication of the treated tumor was presented or was categorized as complete response (CR) according to RECIST (Response Evaluation Criteria In Solid Tumors) criteria or WHO (World Health Organization) criteria [57,58]. LDFS was defined as time in months from the day of treatment resulting in CR to the date of first local relapse (recurrence, 2nd cancer) or end of follow-up.

Overall survival (OS) was defined as percentage of patients who did not die, irrespective of cause of death. Survival was calculated in months from the day of treatment to the date of death or date of last known status. Definition of change in quality of life was possible by means of the University of Washington Quality of Life Questionnaire (UW-QOL), by the Quality of Life Questionnaire (QLQ) on head and neck cancer of the European Organisation for Research and Treatment of Cancer (EORTC) or by study specific instruments [59-61]. Adverse events were defined as complications arising as a direct result of the treatment used, further specified into transient events or events requiring treatment.

Table 3. Assessment of papers on essential criteria (*red*) and quality criteria (*black*). X = did not adhere to criteria, 1 = did adhere to criteria. For inclusion in our review studies had to fulfill all essential criteria.

Assessment criteria (columns, essential criteria in red): Description of tumor location according to ICD-10 or description; Description of tumor histology; Measurement of (maximum) tumor-depth or volume by MRI, CT, US; Description of prior treatment; Description of Foscan dose used; Description of the illumination procedure; Description of the drug-light interval; Description of follow-up; Assessment of tumor-response in % or according to RECIST.

Quality criteria (black): Description of tumor size by T-stadium or measurements; Description of NM-status or stage; Description of gender in numbers or percentages of patients; Indication for Foscan mediated PDT; Description of number of patients; Description of mean/median (range) age of patients; Description of number of PDT-treatments; Description of method of Foscan administration; Description of tumor size assessment after PDT; Description of treatment-related complications.

Studies (rows): Karakullukcu (2012)(66); Karakullukcu (2011)(52); Jerjes (2011)(64); Jerjes (2011)(68); Jerjes (2011)(67); Tan (2010)(65); Lorenz (2009)(46); Jerjes (2009)(63); Lorenz (2008)(53); Copper (2007)(34); Van Veen (2006)(82); Lou (2004)(37); Hopper (2004)(49); d'Cruz (2004)(31); Dilkes (2003)(81); Copper (2003)(50); Kubler (2001)(51); Fan (1997)(33); Grosjean (1996)(54); Grosjean (1996)(80); Dilkes (1996)(79); Dilkes (1995)(78).

Table 4. Datasheet used to extract information from selected studies.

Characteristics	Description of information collected
Cancer	Histology, stage of disease, tumor depth, location
Patients	Number of patients, age, gender, prior treatment, indication for treatment
PDT	Foscan dose, administration, drug-light interval, illumination dosage, number of PDT treatments
Study	Follow-up, study type (case series, cohort studies, clinical trials), centers involved, retrospective or prospective
Outcomes	Complete/ partial/ no response, recurrence, overall survival
Adverse events	Transient / requiring further treatment

Quantitative
Careful assessment of included studies on treatment characteristics and patient inclusion was performed to assess possible pooling of data. Of studies that could be meaningfully combined, original study databases were obtained. To exclude any double patient entries into the pooled database, similarities in patient/tumor characteristics like hospital number, date of treatment, gender and date of birth were carefully checked for between databases. To provide data on outcomes of interest information on tumor size, tumor location (oral cavity/oropharynx, nasopharynx, lip), follow-up time, treatment outcome, LDFS and OS were included in the pooled database.

Statistical analysis
Inter-observer agreement regarding inclusion and assessment of studies was calculated using Cohen's kappa (κ). Descriptive statistics and 95% confidence interval (CI) were calculated according to standard procedures [62]. Differences in outcomes were analyzed using χ^2 tests. Survival curves were constructed using the Kaplan-Meier method. Differences in curves were analyzed using the log-rank test (Mantel-Cox). All tests were conducted at a 2-sided significance level of 5% in PASW statistics 18 software package (SPSS inc.) or Graphpad Prism® (software version 5.0).

Results

Results of the search and selection process
The literature search yielded a total of 566 unique citations (appendix I), of which 22 papers were considered eligible for critical appraisal (figure 1). After appraisal using the assess-
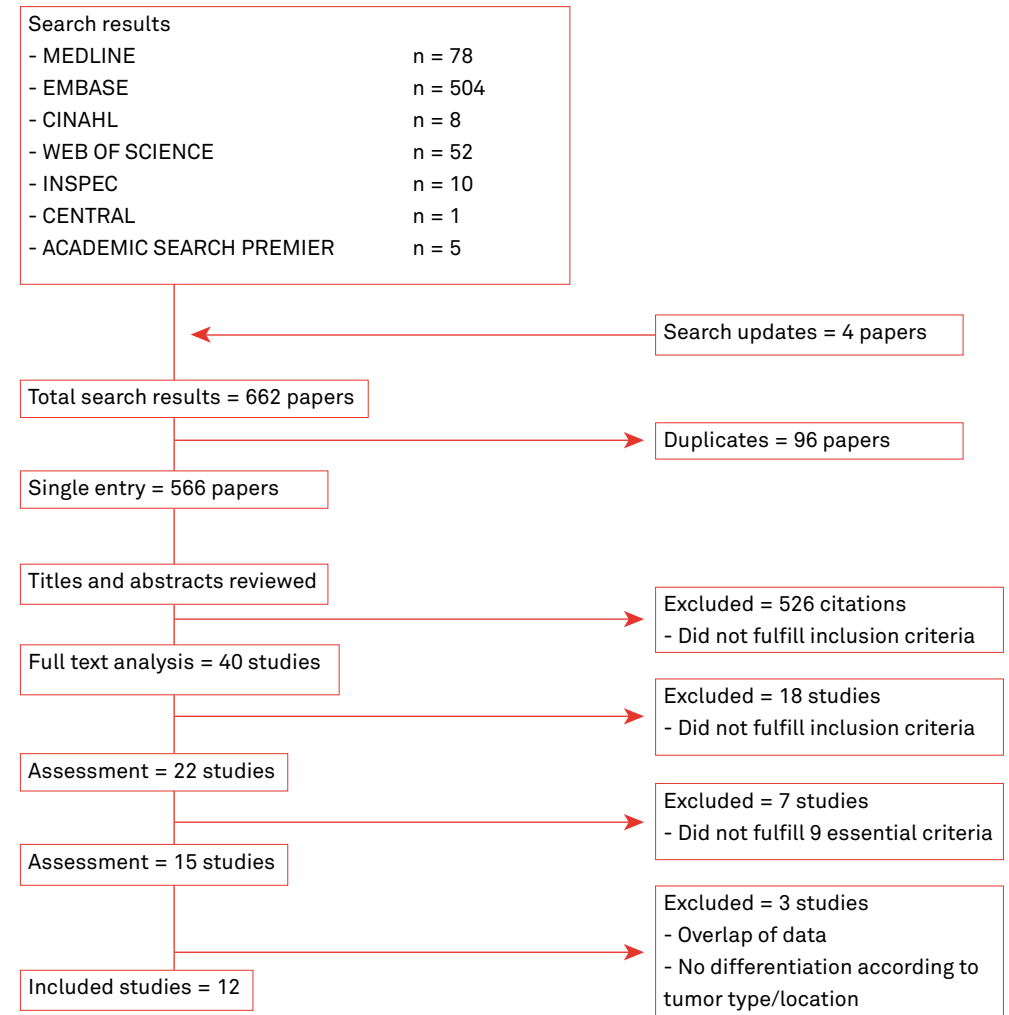
Figure 1. Algorithm of study selection.

ment criteria (table 3), 7 papers were excluded from analysis (appendix II). During the selection process, the inter-observer agreement (Cohen's κ) for inclusion criteria and assessment criteria were respectively 0.79 and 0.76. For both the use of inclusion and assessment criteria, no third party adjudication was required for reaching consensus.
Following full-text analysis of the 15 remaining studies, a further three studies were excluded. Two studies were excluded as a majority of included patients had no HNSCC [63,64]. The third study to be excluded revealed extensive overlap of data with a more recent paper [46,53]. Eventually, the search and selection process culminated in 12 papers included for our review.

Table 5a. Summary of studies describing surface illumination PDT with palliative intent.

Study authors	Cancer type	Patients	PDT treatment	Study design	Outcomes	Treatment related adverse events	Level of evidence[56]
D'cruz A, Robinson M. (2004)[31] *Note:* • Not all tumors were evaluable for different outcomes. Specified in paper.	*Histology:* Squamous cell carcinoma (100%) *Neoplasms:* 145 *Depth:* Mean: 15 mm (2.5 – 50) ≤10 mm:52/102 (51%) >10 mm:50/102 (49%) *Tumor size:* Range: 10 – 100 mm *Location of target:* Oral cavity: 95 (74%) Pharynx: 22 (17%) Larynx: 3 (2%) Nasopharynx:1 (1%) Other: 7 (5%) (further specified in paper) *NM-status:* Not reported	*Patients:* Male: 93 Female: 35 Mean age: 58 years (range: 27 – 96) Single tumor: 113 patients (88%) Multiple tumors: 15 patients (12%) *Any previous treatment:* 98% patients Surgery: 88 (69%) Radiotherapy: 113 (88%) Chemotherapy: 50 (39%) *Inclusion criteria:* recurrent/refractory HNSCC advanced disease unsuitable for conventional treatment Karnofsky score > 60% no diseases exacerbated by light	*Protocol:* Surface illumination 0.15 mg/kg mTHPC i.v. 96 hours drug-light interval 652 nm laser-light Dose: 20 J/cm² Intensity: 100 mW/cm² 200 seconds Tumors ≥ 4 cm: multiple spots ≥ 0.5 cm normal tissue *Number of treatments:* 1 session (100%)	*Cohort study* *Prospective consecutive* 1998 – 2000 29 centers *Follow-up:* Week 1, 2, 4, 6, 8, 12/16 >Week 16–1 year: every 3 months *Length:* Not reported *Tumor response assessment:* WHO-criteria *Quality of life assessment:* UW-QOL at baseline ≥ 1 assessment after PDT	*Tumor response* CR: 16/99 (16%) PR + CR: 33/86 (38%) CR ≤ 10 mm depth: 11/45 (24%) CR >10 mm depth: 5/54 (9%) *Survival* Overall survival: 8.1 months (median) CR: 11.1 months (median) Non-CR:7.1 months (median) *1-year survival rate:* 37% CR:73% Non-CR:32% *QOL* improvement week 1 – 16 (UW-QOL): Sufficient spot & ≤ 10 mm: 26/43 (61%)	*Transient events:* Pain injection site: 11 patients (11%) Phototoxicity reactions: 24 patients (19%) *Events requiring further treatment:* Not reported	3
Lorenz K, Maier, H (2009)[48] *Note:* • Lorenz et al. analyzed 35 of 43 treated patients, to ensure sufficiently long follow-up.	*Histology:* Squamous cell carcinoma (100%) *Neoplasms:* 35 *Depth:* ≤10mm:100% *Tumor size:* Median: 25 mm (10 – 50) T1: 12 tumors T2:20 tumors T3/4:3 tumors *Location of target:* oral cavity:4 (11%) oropharynx: 21 (60%) hypopharynx:5 (14%) larynx: 1 (3%) nasofarynx:1 (3%) skin:3 (9%) (further specified in paper) *NM-status:* N0M0: 100%	*Patients:* Male: 27 Female: 8 Mean age: 59.1 years (range: 48 – 81) *Any previous treatment:* 100% patients Surgery: 33 (94%) Radiotherapy:33 (94%) Chemotherapy: 4 (12%) *Inclusion criteria:* recurrent/refractory HNSCC advanced disease unsuitable for conventional treatment tumor depth: < 10mm (CT/US) diameter < 6 cm Karnofsky score > 80% N0M0	*Protocol:* Surface illumination 0.15 mg/kg mTHPC i.v. 96 hours drug-light interval 652 nm laser-light Dose: 20 J/cm² Intensity: 100 mW/cm² 200 seconds Tumors ≥ 4 cm: multiple spots ≈ 0.5 cm normal tissue *Number of treatments:* 1 session (100%)	*Case series* *Retrospective* 2003 – 2008 1 center *Follow-up:* Week 1, 2, 4, 8, 12, 24, 36, 52 *Lenght:* Not reported *Tumor response assessment:* WHO-criteria *Quality of life assessment:* UW-QOL at baseline 3 months after PDT	*Tumor response* CR: 21 (60%) PR: 10 (29%) No response: 4 (11%) *Tumor response (size):* CR T1: 12/12 (100%) CR T2: 10/20 (50%) CR T3/4:0/3 (0%) *Recurrence free Survival:* 6 months (median) *Survival* Overall survival: 11.7 months (median) CR: 17.3 months (median) PR: 11.3 months (median) *1-year survival rate:* 53.4% CR: 62.4% PR: 30% NR: 25% *QOL* improvement week 1 – 12 (UW-QOL): CR patients: 11/21 (52%) PR patients: 3/9 (30%)	*Transient events:* Phototoxicity reactions:3 patients (9%) *Events requiring further treatment:* Not reported	4
Tan I, Dolivet, G (2010)[65]	*Histology:* Squamous cell carcinoma (100%) *Neoplasms:* 39 *Depth:* Median: 6 mm (0 – 10) *Tumor size:* Median: 25 mm (2 – 65) *Location of target:* oral cavity:39 (100%) *NM-status:* Not reported	*Patients:* Male:31 Female: 8 Mean age: 60.9 years (range: 42 – 83) *Any previous treatment:* 100% patients Surgery: 39 (100%) Radiotherapy: 37 (95%) Chemotherapy: 13 (33%) *Inclusion criteria:* recurrent/refractory HNSCC advanced disease unsuitable for conventional treatment single tumors tumor depth: ≤ 10mm (MRI) performance status 0-2 (ECOG) no diseases exacerbated by light	*Protocol:* Surface illumination 0.15 mg/kg mTHPC i.v. 96 hours drug-light interval 652 nm laser-light Dose: 20 J/cm² Intensity: 100 mW/cm² 200 seconds Spotsize: ≤ 5 cm ≥ 3 illumination spots ≥ 0.5 cm normal tissue *Number of treatments:* 1 session (100%)	*Cohort study* *Prospective* *Consecutive* 2005 - 2009 13 centers *Follow-up:* Week 2, 4, 6, 8, 10, 12, 14, 16 Week 16 - 40: every 4 weeks ≥ 40 weeks: annually till death or lost to follow-up *Length:* Not reported *Tumor response assessment:* WHO-criteria *Quality of life assessment:* EORTC at baseline > week 8: every 4 weeks	*Tumor response* CR: 19 (49%) PR: 2 (5%) Stable disease: 5 (13%) Progressive disease:5 (13%) Non evaluable: 8 (20%) *Progression free Survival:* 7.2 months (median) CR+PR: 33 months (median) Non-responders: 2.6 months (median) *Survival* Overall survival: 16 months (median) CR+PR: 37 months (median) Non-responders: 7,4 months (median) *1-year survival rate:* 59% CR+PR: 86% Non-responders: 28% *QOL* improvement (EORTC): Week 16: 33 – 70% Week 40: 50 – 100%	*Transient events:* Phototoxicity reactions: 4 patients (10%) *Events requiring further treatment:* Necrosis: 2 patients (5%) Further specified in paper.	3

Table 5b. Summary of studies describing interstitial PDT with palliative intent.

Study authors	Cancer type	Patients	PDT treatment	Study design	Outcomes	Treatment related adverse events	Level of evidence[56]
Lou P, Jager H (2004)[37] *Note:* • Only 73% of included patients have SCC. • Only 65% of included patients have a tumor located in oropharynx or oral cavity. • 16% of patients were treated with curative intent for their recurrent/persistent tumor.	*Histology:* Squamous cell carcinoma: 33 (73%) Adenocystic carcinoma: 3 (7%) Other: 9 (20%) Neoplasms: 45 *Depth:* Mean volume: 38 cm³ (8 – 224) Not further specified *Size:* T2: 3 (6.5%) T3: 3 (6.5%) T4: 37 (82%) Not specified: 2 (5%) *Location of target:* Oral cavity: 21 (47%) Oropharynx: 8 (18%) Nasopharynx: 4 (8%) Other: 12 (27%) Further specified in paper *NM-status:* N2: 1 patient (2%) N3: 1 patient (2%) Not further specified	*Patients:* Male: 28 Female: 17 Median age: 58 years (range: 8 – 84) *Treatment intent:* Curative: 7 patients (16%) Palliative: 38 patients (84%) *Any previous treatment:* 100% patients *primary treatment:* 100% patients Surgery: 21 (47%) Radiotherapy: 34 (76%) Chemoradiotherapy: 7 (16%) *Further salvage treatment:* 47% patients *Inclusion criteria:* recurrent/refractory HNSCC advanced disease unsuitable for conventional treatment	*Protocol:* Interstitial illumination 0.15 mg/kg mTHPC i.v. 96 hours drug-light interval 652 nm laser-light Dose: 20 J per site Intensity: 100 mW/cm² 200 seconds *Interstitial:* US, MRI, CT guidance Interstitial fibers 15 mm apart Pull-back technique *Number of treatments:* Mean: 1.49 sessions 1 session: 30 patients (67%) 2 sessions: 10 patients (22%) 3 sessions: 4 patients (9%) 5 sessions: 1 patients (2%)	*Cohort-study* *Prospective* *consecutive* *July 1997 – december 2002* *1 center* *Follow-up:* Week 4 (assessment) Not further specified *Lenght:* Mean: 26 months (range: 8 – 45) *Tumor response assessment:* Inspection, radiographic 4 weeks after iPDT Compared to baseline *Quality of life assessment:* WHO-criteria	*Tumor response overall:* CR: 9/45 (20%) PR: 24/45 (54%) No change/stable: 6/45 (13%) Progressive disease: 6/45 (13%) *curative intent:* CR: 4/7 (57%) PR: 3/7 (43%) *palliative intent:* CR: 4/38 (11%) Stable/progressive disease: 12/38 (32%) *Survival* Overall survival: 14 months (median) Responders (PR+CR): 16 months (median) Non-responders: 2 months (median) *QOL (Symptomatic relief)* Tumor bulk: improved in 18/29 patients (62%) Breathing: improved in 1/2 patients (50%) Brachial compression: improved in 1/1 patients (100%) Bleeding: improved in 3/3 patients (100%) Pain: improved in 2/5 patients (40%)	*Transient events:* Phototoxicity reactions: 1 patient (2%) *Events requiring further treatment:* Major bleeding: 1 patient (2%)	3
Jerjes W, Upile T (2011)[97]	*Histology:* Squamous cell carcinoma: 20 (95%) Adenoid cystic carcinoma: 1 (5%) Neoplasms: 21 *Depth:* Volume measured, not stated *Size:* T3: 1 (5%) T4: 20 (95%) *Location of target:* Base of tongue: 21 (100%) *NM-status:* N0: 2 (10%) N1: 5 (25%) N2: 14 (65%) M0: 19 (90%) M1: 2 (10%)	*Patients:* Male: 15 Female: 6 Mean age: 66.8 years (range: 48 – 88) *Any previous treatment:* 100% patients Surgery + radiotherapy: 4 (19%) Surgery + chemoradiotherapy: 5 (24%) Chemoradiotherapy: 2 (9.5%) Radiotherapy: 3 (14.5%) *Inclusion criteria:* recurrent/refractory cancer base of tongue advanced disease unsuitable for conventional treatment or refusal of other treatments	*Protocol:* Interstitial illumination 0.15 mg/kg mTHPC i.v. 96 hours drug-light interval 652 nm laser-light Dose: 20 J per site Intensity: 100 mW/cm² 200 seconds *Interstitial:* US guidance interstitial PDT Interstitial fibers 7 mm apart Pull-back technique Elective tracheotomy before PDT: 8 patients (38%) Nasopharyngeal tube before PDT: 4 patients (19%). *Number of treatments:* Mean: 1.52 sessions (range: 1–3)	*Cohort study* *Prospective* *1 center* *Follow-up:* Week 6 (assessment) Not further specified *Lenght:* Mean: 36 months (range: 21 – 45) *Tumor response assessment:* Inspection, MRI 6 weeks after iPDT (MRI) *Quality of life assessment:* Assessment of symptoms Baseline vs 6 weeks after iPDT	*Tumor response* Reduced size 50 – 75%: 2 (9.5%) Reduced size < 50%: 6 (29%) Reduced size < 25%: 7 (33%) No change: 4 (19%) Progressive disease: 2 (9.5%) *Survival* *Overall survival* After 45 months: 60% *After follow-up of 36 months:* Tumor related death: 6 (29%) Non-tumor related death: 2 (9.5%) *QOL (symptomatic relief)* Breathing: improved in 9/11 patients (82%) Swallowing: improved in 19/21 patients (91%) Speaking: improved in 11/13 patients (85%) Disfigurement: improved in 1/1 patients (100%)	*Transient events:* Phototoxicity reactions: 3 patients (14%) *Events requiring further treatment:* orocutaneous fistula: 1 patient (5%) skin necrosis: 1 patient (5%) emergency airway: 2 patients (9.5%)	3
Karakullukcu B, Nyst H (2012)[66]	*Histology:* Squamous cell carcinoma (100%) Neoplasms: 20 *Depth:* ≤10mm *Size:* Median: 29,5 mm (0 – 60) *Location of target:* Base of tongue: 20 (100%) *NM-status:* M0: 100% Not further specified	*Patients:* Male: 13 Female: 7 Median age: 64 years (range: 55 – 93) *Any previous treatment:* 100% patients Surgery: 8 (40%) Radiotherapy: 20 (100%) Concomitant chemotherapy: 6 (30%) Surface PDT: 1 (5%) *Inclusion criteria:* recurrent/refractory SCC base of tongue advanced disease unsuitable for conventional treatment or refusal of other treatments nonmetastatic disease	*Protocol:* Interstitial illumination 0.15 mg/kg mTHPC i.v. 96 hours drug-light interval 652 nm laser-light Dose: 30 J/cm diffuser length Intensity: 100 mW/cm² 300 seconds *Interstitial:* MRI guidance (75%) Simulation by program (25%) Interstitial fibers <15mm apart Use of light-source diffusers Elective tracheotomy before PDT. *Number of treatments:* 1 session (100%)	*Case series* *Retrospective* *2003 – 2010* *3 centers* *Follow-up:* Week 2, 4, 6, 8 ≥ 8 weeks: every 4 weeks till death *Lenght:* Not reported *Tumor response assessment:* RECIST-criteria 6 months after iPDT (MRI) *Quality of life assessment:* Not reported	*Tumor response* CR: 9 (45%) PR: 9 (45%) Non evaluable: 2 (10%) *Survival* *Overall survival:* median: 12 months (95% CI: 6 ; 17 months) *4 patients still alive with sustainable CR:* 46 – 80 months	*Transient events:* Not reported *Events requiring further treatment:* Orocutaneous fistula: 6 patients (30%) Major bleeding: 1 patient (5%) Cutaneous metastasis at catheter injection site: 2 patients (10%)	4

Table 5c. Summary of studies describing PDT with curative intent.

Study authors	Cancer type	Patients	PDT treatment	Study design	Outcomes	Treatment related adverse events	Level of evidence[56]
Kubler A, de Carpentier (2001)[51] *Note:* • Information for 23 of 25 (92%) patients could be extracted for "cancer", "patients" and "response".	*Histology:* Squamous cell carcinoma *Neoplasms:* 23 Primary: 23 (100%) *Depth:* ≤ 5 mm Mean: 3.6 mm (0.2 – 0.5) *Size:* Tis/T1: 20 tumors (87%) T2: 3 tumors (13%) Mean: 14 mm (0.5 – 2.5) *Location of target:* Lip: 23 (100%) *NM-status:* N0M0: 100%	*Patients:* Male: 17 Female: 6 Mean age: 69.5 years (range: 44 – 99) 1 tumor: 23 patients (100%) *Any previous treatment:* None: 100% *Inclusion criteria:* SCC of the lip Early stage disease (0, I, II) Diameter ≤ 2.5 cm tumor depth: ≤ 5 mm Karnofsky score ≥70	*Protocol:* Surface illumination 0.15 mg/kg mTHPC i.v. 96 hours drug-light interval 652 nm laser-light Dose: 20 J./cm² Intensity: 100 mW/cm² 200 seconds Single spot illumination. ≥ 0.5 cm normal tissue *Number of treatments:* 1 session: 24 patients (96%) 2 sessions: 1 patient (4%)	*Cohort study* *Prospective* *1996 - 2001* *5 centers* *Follow-up:* 12 weeks: biopsy, US of neck "regular interval" (not further specified) *Lenght:* Mean: 13.95 months *Tumor response assessment:* At outpatient clinic during follow-up Biopsy of target site 12 weeks post-PDT *Change in QOL:* Maximum mouth opening Functional lip closure Compared between baseline and 12 weeks post-PDT	*Tumor response* *Overall:* CR: 22/23 (96%) PR: 1 (4%) *size:* Tis/T1 CR: 19/20 (95%) T2 CR: 3/3 (100%) *Local disease free survival:* 14.5 months: 87% *Survival:* Not reported *QOL:* Reduction in mouth opening: 0% Normal lip closing possible: 100%	*Transient events:* Phototoxicity reactions: 5/25 patients (20%) *Events requiring further treatment:* Not reported	3
Copper M, Tan I. (2003)[50] *Note:* • Majority of included patients are also included in study of "Karakallukcu B, Oudenaarde K (2010)".	*Histology:* Squamous cell carcinoma *Neoplasms:* 29 primary: 29 (100%) *Depth:* ≤ 5-7 mm Mean: 2,9 mm (0,1 – 5,0) *Size:* Tis: 3 tumors (3%) T1: 96 tumors (79%) T2: 22 tumors (18%) *Location of target:* Oral cavity: 81 (67%) Oropharynx: 11 (9%) Lip: 23 (19%) Other: 6 (5%) (further specified in paper) *NM-status:* N0M0: 100%	*Patients:* Male: 15 Female: 10 Mean age: 58.5 years (range: 40 – 82) 1 tumor: 23 patients (92%) Multiple tumors: 2 patients (8%) *Any previous treatment:* None: 100% *Inclusion criteria:* SCC of oral cavity/ oropharynx Early stage disease (0, I, II) Primary tumors tumor depth: ≤ 5 – 7 mm Karnofsky score ≥70	*Protocol:* Surface illumination 0.15 mg/kg mTHPC i.v. 96 hours drug-light interval 652 nm laser-light Dose: 20 J./cm² Intensity: 100 mW/cm² 200 seconds Unknown illumination spot size ≈ 1 cm normal tissue *Number of treatments:* Mean: 1 session	*Cohort study* *Prospective* *1996 - 2000* *1 center* *Follow-up:* First year: every month 1 – 2 year: every 2 months 2 – 4 years: every 3 months *Lenght:* Median: 29 months (range: 1 – 69) *Tumor response assessment:* At outpatient clinic during follow-up *Change in QOL:* Not assessed	*Tumor response* *overall:* CR: 25 (86%) Local recurrence: 4 (14%) *size:* T1 CR: 21 (95%) T2 CR: 4 (57%) *Survival:* Not reported	*Transient events:* Phototoxicity reactions: 1 patient (4%) Pain at injection site: 1 patient (4%) Need for nasogastric tube: 1 patient (1%) *Events requiring further treatment:* Not reported	3
Hopper C, Kubler A. (2004)[49] *Note:* • 114 of 121 (94%) patients were evaluable for efficacy analysis. • The 7 patients were withdrawn from the analysis because of major protocol violations. • Included are patients also included in "Karakallukcu B, van Oudenaarde K (2010)" and in "Kubler A, de Carpentier (2001)".	*Histology:* Squamous cell carcinoma *Neoplasms:* 121 primary: 121 (100%) *Depth:* ≤ 5 mm Mean: 2,9 mm (0,1 – 5,0) *Size:* Tis: 3 tumors (3%) T1: 96 tumors (79%) T2: 22 tumors (18%) *Location of target:* Oral cavity: 81 (67%) Oropharynx: 11 (9%) Lip: 23 (19%) Other: 6 (5%) (further specified in paper) *NM-status:* N0M0: 100%	*Patients:* Male: 72 Female: 49 Mean age: 64 years (range: 30 – 99) 1 tumor: 121 patients (100%) *Any previous treatment:* None: 100% *Inclusion criteria:* SCC lip, oral cavity, oropharynx, hypopharynx Early stage disease (0, I, II) primary tumors Diameter ≤ 2.5 cm tumor depth: ≤ 5 mm Karnofsky score ≥70	*Protocol:* Surface illumination 0.15 mg/kg mTHPC i.v. 96 hours drug-light interval 652 nm laser-light Dose: 20 J./cm² Intensity: 100 mW/cm² 200 seconds Single spot illumination. ≥ 0.5 cm normal tissue *Number of treatments:* Mean: 1 session	*Cohort study* *Prospective* *1996 - 2001* *15 centers* *Follow-up:* Days 1, 2, 7 Week 2, 4, 6, 8, 12 Total: ≤ 2 years *Lenght:* Total: ≤ 2 years *Tumor response assessment:* WHO-criteria Biopsy after 12 weeks *Change in QOL:* Karnofsky performance status data Baseline, week 12 and 16	*Tumor response* *overall:* CR: 97/114 (85%) *size:* Tis CR: 3/3 (100%) T1 CR: 83/92 (90%) T2 CR: 11/19 (58%) *Duration of CR:* > 20,4 months (mean) 1 year: 85% (95%CI: 77-93%) 2 year: 77% (95% CI: 66-87%) *Survival* *Actuarial survival:* 1 year: 89% (95% CI: 83; 95%) 2 year: 75% (95% CI: 66; 84%) *QOL:* improvement week 1 – 16 (Karnofsky): Baseline: 96% (mean) Week 12: 95% (mean) Week 16: 94% (mean)	*Transient events:* Pain at injection site: 7 patients (6%) Phototoxicity reactions: 13 patients (12%) scarring: 12 patients (11%) *Events requiring further treatment:* mouth necrosis: 1 patient (1%) significant burn: 3 patients (3%)	3
Copper M, Triesscheijn, M. (2007)[54] *Note:* • Majority of included patients are also included in study of "Karakallukcu B, van Oudenaarde K (2010)".	*Histology:* Squamous cell carcinoma *Neoplasms:* 42 Second/multiple primary: 42 (100%) *Depth:* ≤ 5 mm *Size:* Tis: 3 tumors (7%) T1: 23 tumors (55%) T2: 15 tumors (36%) T3: 1 tumor (2%) *Location of target:* Oral cavity: 21 (50%) Oropharynx: 20 (48%) Nasopharynx: 1 (2%) (further specified in paper) *NM-status:* N0M0: 100%	*Patients:* Male: 13 Female: 14 Mean age: 63 years (range: 48 – 81) Second primary tumor: 18 patients (67%) Multiple primary tumors: 9 patients (33%) *Any previous treatment:* 100% of patients Surgery: 21 patients (78%) Radiotherapy: 17 patients (81%) Chemotherapy: 5 patients (18%) PDT: 2 patients (7,5%) *Inclusion criteria:* SCC of oral cavity/ oropharynx History of HNSCC Second/multiple primary tumors tumor depth: ≤ 5 mm Karnofsky score ≥70	*Protocol:* Surface illumination 0.15 mg/kg mTHPC i.v. 96 hours drug-light interval 652 nm laser-light Dose: 20 J./cm² Intensity: 100 mW/cm² 200 seconds Number of illumination spots dependent on tumor size. ≈ 1 cm normal tissue *Number of treatments:* Mean: 1 session per tumor	*Case series* *Retrospective* *1996 - 2005* *1 center* *Follow-up:* First year: every month 1 – 2 year: every 2 months > years: every 3 months *Lenght:* Median: 35 months (range: 6 – 105) *Tumor response assessment:* At outpatient clinic during follow-up CR confirmed if > 3 months sustained *Change in QOL:* Not assessed	*Tumor response* *overall:* CR: 28 (67%) Local recurrence: 14 (33%) *size:* Tis CR: 3 (100%) T1 CR: 19 (82,5%) T2 CR: 5 (33%) T3 CR: 1 (100%) *Survival:* Not reported	*Transient events:* Phototoxicity reactions: 1 patient (4%) *Events requiring further treatment:* Not reported	4

Study authors	Cancer type	Patients	PDT treatment	Study design	Outcomes	Treatment related adverse events	Level of evidence[56]
Karakallukcu B, van Oudenaarde K (2010)[52]	*Histology:* Squamous cell carcinoma Neoplasms: 226 Primary: 95 (42%) Non-primary: 131 (58%) *Depth:* ≤ 5 mm *Size:* Tis: 73 tumors (32%) T1: 121 tumors (54%) T2: 32 tumors (14%) *Location of target:* Oral cavity: 163 (72%) Oropharynx: 55 (24%) Nasopharynx: 8 (4%) (further specified in paper) *NM-status:* N0M0: 100%	*Patients:* Male: 90 Female: 80 Mean age: 60,5 years 1 tumor: 135 patients Multiple tumors: 35 patients previous treatment within subgroup of "non-primary tumors" (131 tumors): Surgery: 75,6% Radiotherapy: 48,1% Chemoradiation: 22,7% Surface PDT: 30,6% *Inclusion criteria:* SCC of oral cavity/ oropharynx Early stage disease (0, I, II) tumor depth: ≤ 5mm Karnofsky score ≥70	*Protocol:* Surface illumination 0.15 mg/kg mTHPC i.v. 96 hours drug-light interval 652 nm laser-light Dose: 20 J/cm² Intensity: 100 mW/cm² 200 seconds Number of illumination spots dependent on tumor size. ≈ 0.5 cm normal tissue *Number of treatments:* Mean: 1 session	*Cohort study* *Retrospective* *1996 - 2008* *1 center* *Follow-up:* Week 1, 2, 4, 8, 12, 24, 36, 52 1 – 5 years: every 4 months *Lenght:* Not reported on patient level *Tumor response assessment:* WHO-criteria *Change in QOL.:* Not assessed	*Tumor response overall:* CR: 160 (71%) PR: 45 (20%) Non responding: 21 (9%) *size:* Tis CR: 58 (79,5%) T1 CR: 83 (68,6%) T2 CR: 19 (59,4%) *primary vs non-primary:* Primary CR: 74 (77,9%) Non-primary CR: 86 (65,5%) *Disease free Survival (1, 2, 5 years):* Primary: 90%, 85%, 74% Non-primary: 81%, 64%, 48% CR+PR: 33 months (median) Non-responders: 2.6 months (median) *Survival* Overall (mean): Tis: 92.2 months T1: 98.4 months T2: 78.7 months Primary: 120.4 months Non-primary: 82.1 months	*Transient events:* Phototoxicity reactions: 3 patients (2%) discoloration at injection site: 9 patients (5%) Mild trismus: 5 patients (3%) *Events requiring further treatment:* Not reported	3 –
Jerjes W, Upile T (2011)[68] *Note:* • Mean PDT treatment: 1,95 session.	*Histology:* Squamous cell carcinoma Neoplasms: 38 primary: 30 (79%) second primary: 8 (21%) *Depth:* Assessed but not specified *Size:* T1: 9 tumors (24%) T2: 29 tumors (76%) *Location of target:* Oral cavity: 37 (97%) Lip: 1 (3%) (further specified in paper) *NM-status:* N0M0: 100%	*Patients:* Male: 26 Female: 12 Mean age: 58 years (range: 51 – 69) 1 tumor: 38 patients (100%) *Performance status:* Not reported *Any previous treatment:* None: 100% *Inclusion criteria:* SCC of oral cavity Early stage disease (I, II) primary tumors	*Protocol:* Surface illumination 0.15 mg/kg mTHPC i.v. 96 hours drug-light interval 652 nm laser-light Dose: 20 J/cm² Intensity: 100 mW/cm² 200 seconds Number of illumination spots dependent on tumor size. 0.5 – 1 cm normal tissue *Number of treatments:* Mean: 1.5 sessions 1 session: 9 patients (24%) 2 sessions: 22 patients (58%) 3 sessions: 7 patients (18%)	*Cohort study* *Prospective* *Consecutive* *1998 - 2005* *1 center* *Follow-up:* Week 4, 6, 8 Not further specified *Lenght:* > 5 years *Tumor response assessment:* Inspection Biopsy of target site (post-PDT) *Change in QOL.:* Not assessed	*Tumor response after 1 PDT session:* CR: 9 patients (24%) No CR: 29 patients (76%) *Biopsy after mean of 1.95 PDT sessions:* Normal: 17 (45%) Hyperkeratinization: 5 (13%) Dysplasia: 10 (26%) SCC: 6 (16%) *Time to recurrence of SCC:* Mean: 6,4 months (3,5 – 9,2) *Survival* Survival (not specified): 3 year: 92% 5 year: 84%	*Transient events:* Phototoxicity reactions: 5 patients (13%) *Events requiring further treatment:* 3rd degree burn: 1 patient (3%)	3

Description of included studies
The publication dates of the 12 selected studies span 11 years, with the earliest published in 2001 [51]. All 12 studies were case series or cohort-studies without comparing PDT to other modalities. The included studies were conducted in 7 countries. There were 5 multi-center studies, involving between 3 and 29 centers [31,49,51,65,66]. Eight of the studies were prospective and four retrospective in design. All the selected studies combined described 692 patients with 783 cancers treated with PDT, of which 770 were SCCs (tables 5a – c). Six studies (50%) described PDT with palliative intent of advanced or recurrent incurable disease. Of these 6 palliative studies, 3 described superficial PDT and 3 interstitial PDT [31,37,46,64-67]. The remaining six studies (50%) described PDT with curative intent of early stage disease [34,49-52,68].

Palliative treatment using PDT with surface illumination
Three studies described a total of 202 patients (table 5a) [31,46,65]. All patients had a HNSCC and were unsuitable for further conventional treatment with a majority of patients (n= 198, 99%) presenting with recurrent/refractory disease after previous treatment. Mean age for the 3 studies ranged from 58.0 – 60.9 years. Treatment parameters and the use of a single treatment session were similar among studies. In one study tumor depth was not restricted, and response was stratified according to depth [31]. In both other studies the tumor depth was restricted to ≤10 mm as determined by computed tomography (CT), magnetic resonance imaging (MRI) or ultrasound (US). Stratification of tumor response according to size was performed in 1 study [46].

Palliative treatment using interstitial PDT
Three studies described a total of 86 patients (table 5b) [37,66,67]. Of these 73 (85%) had a SCC and refused or were deemed unsuitable for conventional treatment. The majority of patients (92%) were treated with palliative intent and the remaining 7 patients were treated with curative intent. All patients received previous treatment for their disease prior to PDT. Mean age ranged from 58.0 – 66.8 years.
Treatment characteristics differed among these studies. In 1 study, an elective tracheotomy was performed before treatment in all patients and a total light dose of 30 J/cm per diffuser length was used in 1 treatment session [66]. During PDT, fibers with length diffusers were used allowing treatment over a certain pre-determined length while placed interstitially [66]. Both other studies used a light dosage of 20 J/cm² and used on average 1.5 treatments sessions while elective alternative airway was only created in a selection of patients [37,67]. During PDT, a "pull-back technique" was used in which 1 fiber is retracted in predetermined step-sizes to illuminate the tumor [37,67]. Further difference between studies was the varying space between the interstitial fibers in the treatment volume (7 vs 15 mm) and the inclusion of patients with metastatic disease.

Curative treatment using PDT with surface illumination

Six studies described a total of 404 patients (cN0M0) with 479 SCCs of which almost all (n= 478) were classified as Tis, T1 or T2 (table 5c) [34,49-52,68]. Three studies included patients with multiple primary tumors [34,50,52]. Mean age for the six studies ranged from 58 – 69 years. All studies used similar treatment characteristics and assessed the tumor depth (CT, MRI, US) before treatment. Five studies limited PDT to a single treatment of tumors with a depth of ≤ 5-7 mm [34,49-52], two of these studies further limited PDT to tumors with a diameter of ≤ 2.5 cm due to the use of a single illumination spot [49,51]. A marked difference in treatment protocol was that in one study no limits on tumor depth or size were used and 76% of patients received at least 2 PDT sessions [68]. A marked difference in patient inclusion between studies was that one study only included patients with SCC of the lip [51]. For the four studies that showed similar treatment protocols and inclusion criteria, pooling of data was deemed suitable and original study-databases were obtained [34,49,50,52].

Quality of included studies

Of the 12 included studies, 9 (75%) fulfilled all criteria (table 3). The 2 criteria that were not met by the other 3 studies were; "description of tumor size" and "description of NM-status or stage". The level of evidence in the 12 studies did not exceed 3 with 5 being the lowest score [56]. Seven studies were classified as level 3 studies and 4 as level 4 studies (tables 5). One study was classified as level 3 "minus" due to study design being a historical cohort study [52]. In 7 of 12 studies, tumor response was assessed according to WHO-criteria or RECIST-criteria [31,37,46,49,52,65,66]. The other 5 studies described tumor response according to change in size compared to baseline without the use of established guidelines [34,50,51,67,68]. Additionally, some studies stratified treatment responses according to tumor size, depth and location. Five studies, all on PDT with palliative intent, reported quality of life in various ways; reported by patient, by means of UW-QOL or QLQ on head and neck cancer of the EORTC [31,37,46,65,67]. Patient survival was inconsistently reported in 9 studies, and not reported in 3 studies describing PDT with curative intent [34,50,51]. Cause-specific survival was not reported in any study. Follow-up was inconsistently reported while 5 studies did not report the follow-up time at all [31,46,52,65,66]. Treatment related adverse events were described in all curative and palliative studies.

Pooling of curative studies

A pooled database of the 4 eligible studies, included a total of 418 tumors in 343 patients [34,49,50,52]. However, rigorous analysis revealed several double patient/tumor entries in the pooled database. For instance, 16 tumors were included in 3 different study databases [49,50,52]. Furthermore, some tumors were excluded as treatment protocol was violated [49]. After the exclusion of double entries and protocol violators, 279 unique patients with 332 tumors remained. A categorization of tumors into anatomical sites, resulted in 301 tumors of the oral cavity/oropharynx, 8 nasopharyngeal tumors and 23 tumors of the lip. Due to the limited number of

nasopharyngeal tumors, no analysis on these tumors was performed. Of the 23 lip tumors, all were previously described in another original paper included in our review [51]. Therefore, these 23 lip tumors included in our pooled database were not analyzed. Instead analysis of the original paper on lip tumors was performed [51].

After exclusion of lip and nasopharyngeal tumors from analysis, 248 patients with 301 oral cavity/oropharynx tumors remained. Of the 301 tumors of the oral cavity/oropharynx 44 tumors originated from the oropharynx, of which the majority (75%) was located in the soft palate. Of the tumors originating from the oral cavity/oropharynx, 177 were 1st primary tumors (59%), 62 were second/third primary tumors (20.5%) and 62 were recurrent tumors (20.5%). Grouped according to tumor size, 73 tumors were Tis (24%), 181 T1 (60%) and 47 T2 (16%). Within the subgroup of 177 1st primary tumors, 21 were Tis (12%), 126 T1 (71%) and 30 T2 (17%). The mean follow-up (range) was 39.0 months (1.0 – 156.0) for all 301 tumors and 40.5 months (2.0 – 156.0) for 177 primary tumors.

The 248 patients analyzed had a mean age (range) of 61.4 years (25.0 – 99.0); 172 patients had primary and 76 patients had non-primary tumors. The mean follow-up (range) was 40.6 months (1.0 – 156.0) for all 248 patients. The mean follow-up (range) for patients alive at the end of the follow-up was 45.7 months (1.0 – 156.0). As PDT of early stage oral cavity SCC is a local treatment modality, we analyzed the pooled database on a tumor specific level for assessment of tumor response. For assessment of survival, we analyzed the pooled database on a patient specific level.

Tumor response

Palliative treatment using PDT with surface illumination

CR rates varied between 16 – 60% and overall response rates between 38 – 89% [31,46,65]. The study that reported the highest response rates included predominantly T1 and T2 tumors [46]. The other two studies did not report on size of the target lesion or on stage of the disease [31,65]. The only study assessing the effect of tumor depth > 10 mm on response rate, showed significantly better response rates for more superficial tumors with depth ≤ 10 mm (CR: 24%) compared to tumors with depth of > 10 mm (CR: 9%) [31].

Palliative treatment using interstitial PDT

CR rate varied between 0 – 45% and tumor response was achieved in 72 - 90% [37,66,67]. The study responsible for the highest response rates was the only study using a single treatment session, light diffusers and an increased light dosage [66]. However, tumor size was not specified while in both other studies a majority of tumors was defined as T4 (86%). None of the studies stratified treatment results according to tumor size.

Curative treatment of lip tumors using PDT

The only study on PDT of lip SCC described 23 patients (N0M0) with a single Tis, T1, or T2 tumor [51]. CR was achieved in 96% of patients, one remaining patient with T1 disease showed
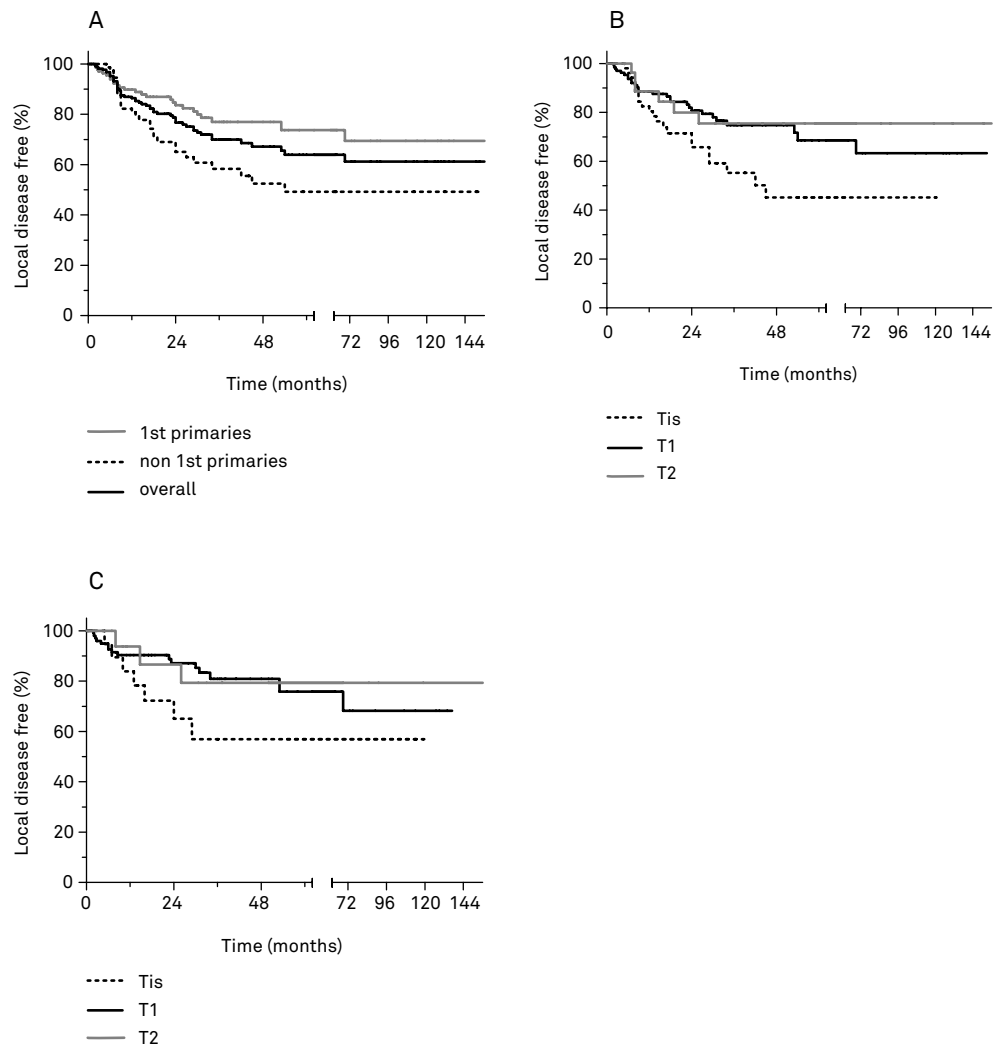
A

B

C

Figure 2. Local disease free survival curves of tumors reaching complete response. Curves depict disease free survival for primary tumors, non-primary tumors and combined (A) and local disease free survival curves by T-stage of tumors (B). Local disease free survival was significantly better for patients with primary tumors compared to those with a non-primary tumor. Additionally local disease free survival was significantly better for T1 tumors compared to Tis. Local disease free survival curves of 1st primary tumors by T-stage reaching complete response (C). No significant differences were found.

a partial response. After a mean follow-up of 14.5 months the CR rate was 87%. Two patients (8%) with T1 disease developed a local tumor recurrence and another patient was diagnosed with lymph node metastasis.

Curative treatment of early stage diseaseby multiple treatment sessions
One study reports the use of multiple rounds of PDT after failure of the initial PDT [68]. In their study, 29 of 38 (76%) patients treated had residual disease after the first round of PDT. A majority of these patients had T2 stage disease with others having T1 stage. In total, 26 of 38 treated patients had a clinical normal appearance at last follow-up of the target tissue after on average 2 treatment sessions. Further biopsy revealed recurrent SCC in 6 patients (16%); 5 patients with T4 disease and 1 patient with T2 disease.

Curative treatment of early stage disease using PDT by single treatment session
One study described significant (p<0.05) differences in response rates for different subsites in the oral cavity [52]. Oral tongue was reported with a significant better response rate and alveolar process with a significant lower response rate compared to the other subsites. For a more comprehensive analysis of PDT treatment with curative intent, a pooled database containing 301 tumors of the oral cavity/oropharynx was analyzed. The overall CR rate was 76% (95% CI: 71.1; 81.2) while the mean LDFS was 103.4 months (95% CI: 91.7; 115.0). 1-,2- and 5-year survival rates were 85%, 78% and 63% respectively.
Stratification according to primary or multiple primary/recurrent neoplasms of the 301 tumors resulted in a significant better CR rate of 83% for 1st primary tumors compared to 66-68% for non-1st primaries (table 6). The mean LDFS for the CR lesions was 114.1 months (95% CI: 99.8; 128.3) for the 1st primary tumors and 85.4 months (95% CI: 67.2; 103.6) for the non-1st primary tumors. Comparison of both Kaplan-Meier curves, showed a significant higher LDFS (p=0.0074) for the 1st primary tumors (figure 2A).
Stratification according to size of the 301 tumors showed a significant higher CR of 78% for T1 compared to 64% for T2 tumors, while CR rate for Tis was 79% (table 6). The mean local disease free survival for the CR lesions was 65.3 months (95% CI: 48.4; 82.1) for Tis, 106.6 months (95% CI: 91; 122.2) for T1 and 116.1 months (95% CI: 91.8; 140.4) for T2 (figure 2B). Comparison of the different Kaplan-Meier curves, showed a significant lower LDFS (p=0.0238) for Tis compared to T1 tumors (figure 2B).
Within the subgroup of 177 1st primary tumors, a significant higher CR rate of 86% for T1 tumors compared to 63% for T2 tumors was found, while CR rate for Tis was 95% (table 6). The mean local disease free survival for the CR lesions was 74.7 months (95% CI: 49.2; 100.2) for Tis, 102.6 months (95% CI: 86.9; 118.4) for T1 tumors and 113.8 months (95% CI: 82.3; 145.2) for T2. No significant differences between the different Kaplan-Meier curves were found (figure 2C).

Table 6. Pooled database. Complete response rates after PDT with curative intent.

	Complete response (%) (95% CI)	p-value
total tumors	76% (71.1; 81.2)	
1st primary tumors	83% (77.5; 88.6)	p=0.001
non- 1st primary tumors	67% (58.5; 75.3)	(1st primary vs
2nd/3rd primary tumors	68% (55.8; 79.7)	non-1st primary)
recurrent tumors	66% (54.0; 78.3)	
Total tumors		
Tis	79% (70.0; 89.0)	
T1 tumors	78% (72.4; 84.5) *	p=0.038
T2 tumors	64% (49.6; 78.1) #	(T1 vs T2)
1st primary tumors		
Tis	95% (77.3; 99.2)	
T1 tumors	86% (78.5; 90.8) *	p=0.005
T2 tumors	63% (45.5; 78.1) #	(T1 vs T2)

* p< 0.001 # p=0.925

Survival
Palliative treatment using PDT with surface illumination
OS and 1-year survival rates were reported by all 3 studies [31,46,65]. Median OS ranged from 8.1 – 16.0 months and 1-years survival rate ranged from 37 – 59%. Patients with CR or responders in general showed improved OS compared to non-responders.

Palliative treatment using interstitial PDT
OS as reported by 2 studies had a median of 12 and 14 months [37,66]. The study of Jerjes et al. on base of tongue tumors reported a 60% OS after 45 months [67]. One study clearly showed longer OS for responders compared to non-responders [37].

Curative treatment of lip tumors using PDT
The only study on PDT treatments of lip SCC reported no fatalities during a mean follow-up of 14.5 months [51].
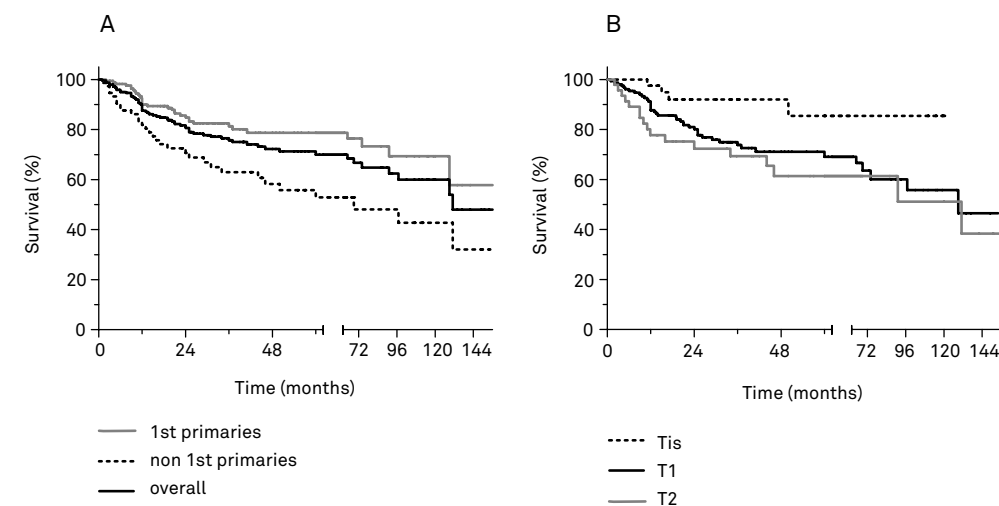
Figure 3. Overall survival. Curves depict overall survival of patients with primary tumors, non-primary tumors and combined (A) and survival by T-stage (B). Survival of patients with primary tumors was significantly better compared to those with non-primary tumors. Survival was significantly better for patients with Tis tumors compared to T1 tumors.

Multiple curative treatment sessions of early stage disease
The one study describing multiple PDT sessions of the same tumor, reported 3 tumor related deaths and 3 non-tumor related deaths [68]. This resulted in a 3- and 5-year OS of 92.1% and 84.2% respectively.

Single curative treatment session of early stage disease
For survival analysis after PDT with curative intent, Kaplan-Meier curves were calculated for 248 patients included in the pooled database. The mean OS was 105 months (95% CI: 94.4; 115.7). The 1- and 5-year survival rates were 90% and 70% respectively (Figure 3). The mean OS for the 172 patients with a 1st primary tumor was 116.5 months (95% CI: 103.8; 129.2) and 82.3 months (95% CI: 64.6; 100) for the 76 patients with a non-1st primary tumor. Comparison of the Kaplan-Meier curves, showed a significant difference (p=0.001) between patients with a 1st primary tumor and with a non-1st primary tumor. The mean OS for patients with Tis, T1 tumors and T2 tumors were 113.8 months (95% CI: 101.6; 124.4), 101.5 months (95% CI: 89.3; 113.8) and 116.9 months (95% CI: 87.7; 146.1) respectively.
Comparison of the Kaplan-Meier curves, showed a significant better OS for patients with Tis compared to patients with T1 (p=0.0255) or T2 (p=0.063) tumors.

Adverse events
PDT using surface illumination for both curative and palliative intent resulted in adverse

events that needed treatment in 7 patients (1% in a total of 606 patients); 4 developed severe burns and 3 developed necrosis of the skin [49,65,68]. With interstitial PDT 12 patients required treatment for adverse events (14% in a total of 86 patients); one developed skin necrosis, 2 developed a major bleeding, 7 developed an oro-cutaneous fistula and 2 needed an emergency airway [37,66,67]. Furthermore, 2 patients developed cutaneous metastases after iPDT at the site of catheter insertion [66]. The majority of transient events occurring in both superficial and iPDT were phototoxicity reactions; of the 692 patients described in the included papers, 58 (8%) reported blisters, erythema, hyperpigmentation or 1st/2nd degree skin burn. Other transient events reported were; pain at the injection site (3%), discoloration at the injection site (1%) and scarring/mild trismus (2%).

Quality of life

Five of 6 studies on palliative PDT analyzed quality of life. Three studies on surface PDT, all reported improvement in quality of life [31,46,65]; 2 studies used the UW-QOL scale and described an improvement of at least 30% at 3 – 4 months while the other study used the EORTC (QLQ-C30/H&N-35) scale and reported an improvement of 33% at 4 months and 50% at 10 months. Two studies on iPDT, described improvements in quality of life as symptomatic relief reported by patients [37,67]. At least 50% of tumor associated symptoms improved subjectively after iPDT.

Discussion

To the best of our knowledge, this paper is the only comprehensive systematic review of Foscan mediated PDT for the treatment of HNSCC. Of the 12 papers included in our systematic review, none compared PDT with other treatment modalities. In each of these studies a comparison of the PDT results with other treatment modalities relied on previously published data, historical control or own experience. All included studies were of either level 3 or 4 evidence [56].

Despite the absence of evidence of the highest quality, PDT with palliative intent (both surface illumination and interstitial) appears to be effective for treatment of patients with local end-stage disease with no further treatment options. Reviewed studies showed that a considerable number of patients had tumor response and improvement in quality of life or symptomatic relief after PDT with palliative intent. The application of PDT using surface illumination is limited to superficial tumors as tissue penetration of excitation light decreases with increased depth. There is evidence to limit superficial PDT with palliative intent to tumors with a depth ≤ 10 mm, as significantly lower response rates are described for tumors with a depth >10 mm [31].

For tumors with a larger volume interstitial PDT is used, whereby multiple laser fibers are guided into the tumor volume through strategically positioned needles. While differences in treatment characteristics between iPDT studies were found, its influence on outcome could not be assessed. An interesting development is the use of digital pre-treatment planning instead of intra-operative imaging for the positioning of the interstitial fibers [66]. Comparing palliative PDT to standard treatment for non-resectable local advanced disease is difficult. Standard treatment for patients unsuitable for conventional treatment is single-agent or combination chemotherapy. Chemotherapy regimes have response rates around 20 – 40%, and higher if combined with Cetuximab [9,69-73]. However, the majority of patients are treated by combination chemotherapy for its systemic use while PDT with palliative intent is purely used as a local treatment modality.

Based on currently available evidence identified by our systematic review, the value of PDT for the curative treatment of early HNSCC (stage I/II) is difficult to assess due to the absence of randomized, comparative studies. As a result, no high quality evidence could be identified in our search to substantiate the suggested better functional and aesthetic results after PDT compared to surgery. There is some evidence that tumor response after PDT differs according to anatomical subsite. In a small study, PDT of SCC of the lip showed relative high cure rates compared to response rates described for the oral cavity [51]. Within the oral cavity, the oral tongue was described with the most favorable outcomes [52]. While most studies on PDT with curative intent used 1 treatment session, it was suggested that PDT treatments could be repeated without cumulative toxicity in reaching CR [68]. Rigorous analysis was performed on our pooled database of early stage SCC of the oropharynx/oral cavity. PDT treatment of 1st primary tumors showed a higher CR rate than of both recurrent and 2nd, 3rd primary tumors. An interesting outcome described previously by others, was the response after PDT of non-1st primary tumors [52]. While these early stage tumors were located in tissue previously treated by radiotherapy, chemoradiation or surgery, still a CR rate of 66 – 68% was found. Stratification of tumor response according to size showed highest CR rates for Tis, followed by T1 and T2. Surprisingly, local disease free survival of all treated tumors reaching CR showed a trend for lowest local disease free survival for Tis and thus a higher chance of recurrence. This high recurrence rate could be explained by difficulties assessing the exact border of the lesion. Furthermore, the recurrence of Tis could be attributable to the known high rate of leukoplakia development after treatment [74]. This phenomenon was also described by Karakullukcu et al. as could be expected due to the inclusion of a majority of their patients in our pooled database [52]. Overall survival was higher for Tis compared to T1 and T2 tumors and higher for 1st primary tumors compared to non-1st primary tumors.

In comparison with surgical treatment results described in the literature, PDT showed a lower local control rate. Local control rate for surgical treatment of early stage I/II tumors is around 90% [2,75,76]. However, in most of these studies only tumors resected with clear margins were included in the local control rate. This further emphasizes the need for a comparative, randomized study to rigorously evaluate PDT against conventional treatment. Very recently and therefore not assessed by our review, a non-randomized study appeared comparing PDT of early stage HNSCC to surgery in a single institution [77]. In that historically matched cohort-study, PDT showed comparable disease control and OS to surgery. However, results

were not stratified according to tumor size nor were morbidity or aesthetic outcome compared between PDT and surgery.

The most common complication of Foscan mediated PDT described is phototoxicity. Both minor phototoxicity (burns, blisters) and severe phototoxicity (3rd degree burns, necrosis) seem preventable by adhering to the stringent light protocol. Pain or discoloration at the injection site is also common and suggests a problematic injection of the photosensitizer in the circulation. Interstitial PDT shows the most severe complications as could be expected because all patients presented with larger tumor volumes. Most notable is the incidence of oro-cutaneous fistula after PDT. One surprising finding was the need in 1 study to provide an emergency airway after interstitial PDT, while in other studies an alternative airway was provided per protocol pre-treatment.

Conclusion

Findings from this review support the use of PDT and interstitial PDT for palliative intent in patients with no further treatment options. Evaluation of PDT for early stage disease is difficult, as no comparative studies with other modalities are available. Treatment response with PDT for T1 tumors is significantly better compared to T2 tumors. Furthermore, tumor response with PDT is significantly better for 1st primary tumors versus non-1st primary tumors. No evidence for any functional or esthetic advantage of PDT over other modalities could be identified. To properly evaluate PDT for early stage disease, comparative and randomized studies are needed.

References

1. Parkin DM, Bray F, Ferlay J, Pisani P. Global cancer statistics, 2002. CA Cancer J Clin. 2005 Mar-Apr;55(2):74-108.

2. Wolfensberger M, Zbaeren P, Dulguerov P, Muller W, Arnoux A, Schmid S. Surgical treatment of early oral carcinoma-results of a prospective controlled multicenter study. Head Neck. 2001 Jul;23(7):525-30.

3. Ord RA, Blanchaert RH,Jr. Current management of oral cancer. A multidisciplinary approach. J Am Dent Assoc. 2001 Nov;132 Suppl:19S-23S.

4. Bhalavat RI, Mahantshetty UM, Tole S, Jamema SV. Treatment outcome with low-dose-rate interstitial brachytherapy in early-stage oral tongue cancers. J Cancer Res Ther. 2009 Jul-Sep;5(3):192-7.

5. Fasunla AJ, Greene BH, Timmesfeld N, Wiegand S, Werner JA, Sesterhenn AM. A meta-analysis of the randomized controlled trials on elective neck dissection versus therapeutic neck dissection in oral cavity cancers with clinically node-negative neck. Oral Oncol. 2011 May;47(5):320-4.

6. Bundgaard T, Tandrup O, Elbrond O. A functional evaluation of patients treated for oral cancer. A prospective study. Int J Oral Maxillofac Surg. 1993 Feb;22(1):28-34.

7. Argiris A, Karamouzis MV, Raben D, Ferris RL. Head and neck cancer. Lancet. 2008 May 17;371(9625):1695-709.

8. Haddad RI, Shin DM. Recent advances in head and neck cancer. N Engl J Med. 2008 Sep 11;359(11):1143-54.

9. Cohen EE, Lingen MW, Vokes EE. The expanding role of systemic therapy in head and neck cancer. J Clin Oncol. 2004 May 1;22(9):1743-52.

10. Furness S, Glenny AM, Worthington HV, Pavitt S, Oliver R, Clarkson JE, et al. Interventions for the treatment of oral cavity and oropharyngeal cancer: Chemotherapy. Cochrane Database Syst Rev. 2011 Apr 13;(4)(4):CD006386.

11. Pignon JP, le Maitre A, Maillard E, Bourhis J, MACH-NC Collaborative Group. Meta-analysis of chemotherapy in head and neck cancer (MACH-NC): An update on 93 randomised trials and 17,346 patients. Radiother Oncol. 2009 Jul;92(1):4-14.

12. Bourhis J, Temam S, Wibault P, Lusinchi A, de Crevoisier B, Janot R, et al. Locoregional recurrences of HNSCC: Place of re-irradiations. Bull Cancer. 2004 Nov;91(11):871-3.

13. Tortochaux J, Tao Y, Tournay E, Lapeyre M, Lesaunier F, Bardet E, et al. Randomized phase III trial (GORTEC 98-03) comparing re-irradiation plus chemotherapy versus methotrexate in patients with recurrent or a second primary head and neck squamous cell carcinoma, treated with a palliative intent. Radiother Oncol. 2011 Jul;100(1):70-5.

14. Epstein JB, Emerton S, Kolbinson DA, Le ND, Phillips N, Stevenson-Moore P, et al. Quality of life and oral function following radiotherapy for head and neck cancer. Head Neck. 1999 Jan;21(1):1-11.

15. Finlay PM, Dawson F, Robertson AG, Soutar DS. An evaluation of functional outcome after surgery and radiotherapy for intraoral cancer. Br J Oral Maxillofac Surg. 1992 Feb;30(1):14-7.

16. Pauloski BR, Rademaker AW, Logemann JA, Colangelo LA. Speech and swallowing in irradiated and nonirradiated postsurgical oral cancer patients. Otolaryngol Head Neck Surg. 1998 May;118(5):616-24.

17. Biazevic MG, Antunes JL, Togni J, de Andrade FP, de Carvalho MB, Wunsch-Filho V. Immediate impact of primary surgery on health-related quality of life of hospitalized patients with oral and oropharyngeal cancer. J Oral Maxillofac Surg. 2008 Jul;66(7):1343-50.

18. Chandu A, Smith AC, Rogers SN. Health-related quality of life in oral cancer: A review. J Oral Maxillofac Surg. 2006 Mar;64(3):495-502.

19. Day GL, Blot WJ. Second primary tumors in patients with oral cancer. Cancer. 1992 Jul 1;70(1):14-9.

20. Jovanovic A, van der Tol IG, Kostense PJ, Schulten EA, de Vries N, Snow GB, et al. Second respiratory and upper digestive tract cancer following oral squamous cell carcinoma. Eur J Cancer B Oral Oncol. 1994 Jul;30B(4):225-9.

21. Leon X, Quer M, Diez S, Orus C, Lopez-Pousa A, Burgues J. Second neoplasm in patients with head and neck cancer. Head Neck. 1999 May;21(3):204-10.

22. Ridge JA. Squamous cancer of the head and neck: Surgical treatment of local and regional recurrence. Semin Oncol. 1993 Oct;20(5):419-29.

23. Trotti A, Bellm LA, Epstein JB, Frame D, Fuchs HJ, Gwede CK, et al. Mucositis incidence, severity and associated outcomes in patients with head and neck cancer receiving radiotherapy with or without chemotherapy: A systematic literature review. Radiother Oncol. 2003 Mar;66(3):253-62.

24. Rosenthal DI, Lewin JS, Eisbruch A. Prevention and treatment of dysphagia and aspiration after chemoradiation for head and neck cancer. J Clin Oncol. 2006 Jun 10;24(17):2636-43.

25. Price KA, Cohen EE. Current treatment options for metastatic head and neck cancer. Curr Treat Options Oncol. 2012 Mar;13(1):35-46.

26. Hartmann JT, Lipp HP. Toxicity of platinum compounds. Expert Opin Pharmacother. 2003 Jun;4(6):889-901.

27. Nyst HJ, Tan IB, Stewart FA, Balm AJ. Is photodynamic therapy a good alternative to surgery and radiotherapy in the treatment of head and neck cancer? Photodiagnosis Photodyn Ther. 2009 Mar;6(1):3-11.

28. Biel M. Advances in photodynamic therapy for the treatment of head and neck cancers. Lasers Surg Med. 2006 06;38(0196-8092; 5):349-55.

29. Jerjes W, Upile T, Akram S, Hopper C. The surgical palliation of advanced head and neck cancer using photodynamic therapy. Clin Oncol (R Coll Radiol). 2010 Nov;22(9):785-91.

30. Senge MO, Brandt JC. Temoporfin (foscan(R), 5,10,15,20-tetra(m-hydroxyphenyl)chlorin)--a second-generation photosensitizer. Photochem Photobiol. 2011 Nov-Dec;87(6):1240-96.

31. D'Cruz AK, Robinson MH, Biel MA. mTHPC-mediated photodynamic therapy in patients with advanced, incurable head and neck cancer: A multicenter study of 128 patients. Head Neck. 2004 03;26(1043-3074; 1043-3074; 3):232-40.

32. Hopper C. Photodynamic therapy: A clinical reality in the treatment of cancer. Lancet Oncol. 2000 12;1(1470-2045):212-9.

33. Fan KF, Hopper C, Speight PM, Buonaccorsi GA, Bown SG. Photodynamic therapy using mTHPC for malignant disease in the oral cavity. Int J Cancer. 1997 Sep 26;73(1):25-32.

34. Copper MP, Triesscheijn M, Tan IB, Ruevekamp MC, Stewart FA. Photodynamic therapy in the treatment of multiple primary tumours in the head and neck, located to the oral cavity and oropharynx. Clin Otolaryngol. 2007 06;32(1749-4478; 3):185-9.

35. Henderson BW. Photodynamic therapy--coming of age. Photodermatol. 1989 Oct;6(5):200-11.

36. Yow CM, Chen JY, Mak NK, Cheung NH, Leung AW. Cellular uptake, subcellular localization and photodamaging effect of temoporfin (mTHPC) in nasopharyngeal carcinoma cells: Comparison with hematoporphyrin derivative. Cancer Lett. 2000 Sep 1;157(2):123-31.

37. Lou PJ, Jager HR, Jones L, Theodossy T, Bown SG, Hopper C. Interstitial photodynamic therapy as salvage treatment for recurrent head and neck cancer. Br J Cancer. 2004 Aug 2;91(3):441-6.

38. Yow CM, Chen JY, Mak NK, Cheung NH, Leung AW. Cellular uptake, subcellular localization and photodamaging effect of temoporfin (mTHPC) in nasopharyngeal carcinoma cells: Comparison with hematoporphyrin derivative. Cancer Lett. 2000 Sep 1;157(2):123-31.

39. Dougherty TJ, Gomer CJ, Henderson BW, Jori G, Kessel D, Korbelik M, et al. Photodynamic therapy. J Natl Cancer Inst. 1998 06/17;90(0027-8874; 0027-8874; 12):889-905.

40. Henderson BW, Dougherty TJ. How does photodynamic therapy work? Photochem Photobiol. 1992 01;55(0031-8655; 0031-8655; 1):145-57.

41. Berlanda J, Kiesslich T, Engelhardt V, Krammer B, Plaetzer K. Comparative in vitro study on the characteristics of different photosensitizers employed in PDT. J Photochem Photobiol B. 2010 Sep 2;100(3):173-80.

42. Mitra S, Foster TH. Photophysical parameters, photosensitizer retention and tissue optical properties completely account for the higher photodynamic efficacy of meso-tetra-hydroxyphenyl-chlorin vs photofrin. Photochem Photobiol. 2005 07;81(0031-8655; 0031-8655; 4):849-59.

43. Weishaupt KR, Gomer CJ, Dougherty TJ. Identification of singlet oxygen as the cytotoxic agent in photoinactivation of a murine tumor. Cancer Res. 1976 Jul;36(7 PT 1):2326-9.

44. Buytaert E, Dewaele M, Agostinis P. Molecular effectors of multiple cell death pathways initiated by photodynamic therapy. Biochim Biophys Acta. 2007 Sep;1776(1):86-107.

45. Dewaele M, Maes H, Agostinis P. ROS-mediated mechanisms of autophagy stimulation and their relevance in cancer therapy. Autophagy. 2010 Oct;6(7):838-54.

46. Lorenz KJ, Maier H. Photodynamic therapy with meta-tetrahydroxyphenylchlorin (foscan((R))) in the management of squamous cell carcinoma of the head and neck: Experience with 35 patients. Eur Arch Otorhinolaryngol. 2009 03/17(1434-4726).

47. European Medicines Agencies. H-C-318 foscan european public assessment report. 2009 04/30.

48. Plaetzer K, Krammer B, Berlanda J, Berr F, Kiesslich T. Photophysics and photochemistry of photodynamic therapy: Fundamental aspects. Lasers Med Sci. 2009 Mar;24(2):259-68.

49. Hopper C, Kubler A, Lewis H, Tan IB, Putnam G. mTHPC-mediated photodynamic therapy for early oral squamous cell carcinoma. Int J Cancer. 2004 08/10;111(0020-7136; 0020-7136; 1):138-46.

50. Copper MP, Tan IB, Oppelaar H, Ruevekamp MC, Stewart FA. Meta-tetra(hydroxyphenyl)chlorin photodynamic therapy in early-stage squamous cell carcinoma of the head and neck. Arch Otolaryngol Head Neck Surg. 2003 07;129(0886-4470; 7):709-11.

51. Kubler AC, de Carpentier J, Hopper C, Leonard AG, Putnam G. Treatment of squamous cell carcinoma of the lip using foscan-mediated photodynamic therapy. Int J Oral Maxillofac Surg. 2001 12;30(0901-5027; 0901-5027; 6):504-9.

52. Karakullukcu B, van Oudenaarde K, Copper MP, Klop WM, van Veen R, Wildeman M, et al. Photodynamic therapy of early stage oral cavity and oropharynx neoplasms: An outcome analysis of 170 patients. Eur Arch Otorhinolaryngol. 2011 Feb;268(2):281-8.

53. Lorenz KJ, Maier H. Squamous cell carcinoma of the head and neck. photodynamic therapy with foscan. HNO. 2008 Apr;56(4):402-9.

54. Grosjean P, Savary JF, Wagnieres G, Mizeret J, Woodtli A, Fontolliet C, et al. Phototherapy of pharyngeal, oesophageal and bronchial early squamous cell carcinomas after sensitisation by tetra (m-hydroxyphenyl) chlorin (mTHPC). Med Chir Dig. 1996 1996/;25(8):411-3.

55. Dequanter D, Lothaire P, Meert A-, Andry G. Photodynamic therapy in head and neck oncology. Rev Med Brux. 2008 /;29(1):23-5.

56. OCEBM Levels of Evidence Working Group. The oxford 2011 levels of evidence. 2011.

57. Miller AB, Hoogstraten B, Staquet M, Winkler A. Reporting results of cancer treatment. Cancer. 1981 Jan 1;47(1):207-14.

58. Eisenhauer EA, Therasse P, Bogaerts J, Schwartz LH, Sargent D, Ford R, et al. New response evaluation criteria in solid tumours: Revised RECIST guideline (version 1.1). Eur J Cancer. 2009 Jan;45(2):228-47.

59. Preedy VR, Watson RR. Handbook of disease burdens and quality of life measures. New York: Springer; 2010.

60. Bjordal K, de Graeff A, Fayers PM, Hammerlid E, van Pottelsberghe C, Curran D, et al. A 12 country field study of the EORTC QLQ-C30 (version 3.0) and the head and neck cancer specific module (EORTC QLQ-H&N35) in head and neck patients. EORTC quality of life group. Eur J Cancer. 2000 Sep;36(14):1796-807.

61. Bjordal K, Hammerlid E, Ahlner-Elmqvist M, de Graeff A, Boysen M, Evensen JF, et al. Quality of life in head and neck cancer patients: Validation of the european organization for research and treatment of cancer quality of life questionnaire-H&N35. J Clin Oncol. 1999 Mar;17(3):1008-19.

62. Altman DG, Machin D, Bryant T, Gardner S. Statistics with confidence: Confidence intervals and statistical guidelines. 2nd ed. London: BMJ Books; 2000.

63. Jerjes W, Upile T, Hamdoon Z, Nhembe F, Bhandari R, Mackay S, et al. Ultrasound-guided photodynamic therapy for deep seated pathologies: Prospective study. Lasers Surg Med. 2009 Nov;41(9):612-21.

64. Jerjes W, Upile T, Alexander Mosse C, Hamdoon Z, Morcos M, Morley S, et al. Prospective evaluation of 110 patients following ultrasound-guided photodynamic therapy for deep seated pathologies. Photodiagnosis Photodyn Ther. 2011 Dec;8(4):297-306.

65. Tan IB, Dolivet G, Ceruse P, Vander Poorten V, Roest G, Rauschning W. Temoporfin-mediated photodynamic therapy in patients with advanced, incurable head and neck cancer: A multicenter study. Head Neck. 2010 Dec;32(12):1597-604.

66. Karakullukcu B, Nyst HJ, van Veen RL, Hoebers FJ, Hamming-Vrieze O, Witjes MJ, et al. mTHPC mediated interstitial photodynamic therapy of recurrent nonmetastatic base of tongue cancers: Development of a new method. Head Neck. 2012 Jan 31.

67. Jerjes W, Upile T, Hamdoon Z, Abbas S, Akram S, Mosse CA, et al. Photodynamic therapy: The minimally invasive surgical intervention for advanced and/or recurrent tongue base carcinoma. Lasers Surg Med. 2011 APR;43(4):283-92.

68. Jerjes W, Upile T, Hamdoon Z, Alexander Mosse C, Morcos M, Hopper C. Photodynamic therapy outcome for T1/T2 N0 oral squamous cell carcinoma. Lasers Surg Med. 2011 /;43(6):463-9.

69. Colevas AD. Chemotherapy options for patients with metastatic or recurrent squamous cell carcinoma of the head and neck. J Clin Oncol. 2006 Jun 10;24(17):2644-52.

70. Molin Y, Fayette J. Current chemotherapies for recurrent/metastatic head and neck cancer. Anticancer Drugs. 2011 Aug;22(7):621-5.

71. Forastiere AA, Metch B, Schuller DE, Ensley JF, Hutchins LF, Triozzi P, et al. Randomized comparison of cisplatin plus fluorouracil and carboplatin plus fluorouracil versus methotrexate in advanced squamous-cell carcinoma of the head and neck: A southwest oncology group study. J Clin Oncol. 1992 Aug;10(8):1245-51.

72. Frampton JE. Cetuximab: A review of its use in squamous cell carcinoma of the head and neck. Drugs. 2010 Oct 22;70(15):1987-2010.

73. Vermorken JB, Mesia R, Rivera F, Remenar E, Kawecki A, Rottey S, et al. Platinum-based chemotherapy plus cetuximab in head and neck cancer. N Engl J Med. 2008 Sep 11;359(11):1116-27.

74. Braakhuis BJ, Tabor MP, Kummer JA, Leemans CR, Brakenhoff RH. A genetic explanation of slaughter's concept of field cancerization: Evidence and clinical implications. Cancer Res. 2003 Apr 15;63(8):1727-30.

75. Brown JS, Shaw RJ, Bekiroglu F, Rogers SN. Systematic review of the current evidence in the use of postoperative radiotherapy for oral squamous cell carcinoma. Br J Oral Maxillofac Surg. 2011 Dec 22.

76. Hicks WL,Jr, Loree TR, Garcia RI, Maamoun S, Marshall D, Orner JB, et al. Squamous cell carcinoma of the floor of mouth: A 20-year review. Head Neck. 1997 Aug;19(5):400-5.

77. Karakullukcu B, Stoker SD, Wildeman AP, Copper MP, Wildeman MA, Tan IB. A matched cohort comparison of mTHPC-mediated photodynamic therapy and trans-oral surgery of early stage oral cavity squamous cell cancer. Eur Arch Otorhinolaryngol. 2012 Jul 7.

78. Dilkes MG, DeJode ML, Gardiner Q, Kenyon GS, McKelvie P. Treatment of head and neck cancer with photodynamic therapy: Results after one year. J Laryngol Otol. 1995 1995/;109(11):1072-6.

79. Dilkes MG, DeJode ML, Rowntree-Taylor A, McGilligan JA, Kenyon GS, McKelvie P. M-THPC photodynamic therapy for head and neck cancer. LASERS MED SCI. 1996 1996/;11(1):23-9.

80. Grosjean P, Savary JF, Mizeret J, Wagnieres G, Woodtli A, Theumann JF, et al. Photodynamic therapy for cancer of the upper aerodigestive tract using tetra(m-hydroxyphenyl)chlorin. J Clin Laser Med Surg. 1996 Oct;14(5):281-7.

81. Dilkes MG, Benjamin E, Ovaisi S, Banerjee AS. Treatment of primary mucosal head and neck squamous cell carcinoma using photodynamic therapy: Results after 25 treated cases. J Laryngol Otol. 2003 /;117(9):713-7.

82. van Veen RL, Nyst H, Rai Indrasari S, Adham Yudharto M, Robinson DJ, Tan IB, et al. In vivo fluence rate measurements during foscan-mediated photodynamic therapy of persistent and recurrent nasopharyngeal carcinomas using a dedicated light applicator. J Biomed Opt. 2006 /;11(4):041107.

Appendix I. Single entry citations identified with literature search.

(1) 13th IPA World Congress - International Photo-dynamic Association in Association with EPPM and HNODS. Photodiagn Photodyn Ther 2011 /;8(2).

(2) Boehringer Ingelheim. Formulary 1999/;34(10 SUP-PL.):31-33.

(3) Comparison of haematoporphyrin derivative and new photosensitizers. Ciba Found Symp 1989 /;146:33-39.

(4) Ackroyd R, Kelty C, Brown N, Reed M. The history of photodetection and photodynamic therapy. Photochem Photobiol 2001/11;74(5):656-669.

(5) Aerts I, Leuraud P, Blais J, Pouliquen A-, Maillard P, Houdayer C, et al. In vivo efficacy of photodynamic therapy in three new xenograft models of human retinoblastoma. Photodiagn Photodyn Ther 2010 /;7(4):275-283.

(6) Agostinis P, Berg K, Cengel KA, Foster TH, Girotti AW, Gollnick SO, et al. Photodynamic therapy of cancer: An update. CA Cancer J Clin 2011 /;61(4):250-281.

(7) Akens MK, Burch S, Yee AJM. Evaluation of photo-dynamic therapy as treatment for spinal metastases. J Pain Manage 2010 /;4(1):83-91.

(8) Ali SM, Chee SK, Yuen GY, Olivo M. Photodynamic therapy induced Fas-mediated apoptosis in human carcinoma cells. Int J Mol Med 2002 /;9(3):257-270.

(9) Ali SM, Olivo M. Bio-distribution and subcellular localization of Hypericin and its role in PDT induced apoptosis in cancer cells. Int J Oncol 2002 /;21(3):531-540.

(10) Allison RR, Bagnato VS, Cuenca R, Downie GH, Sibata CH. The future of photodynamic therapy in oncology. Future Oncol 2006 /;2(1):53-71.

(11) Allison RR, Cuenca RE, Downie GH, Camnitz P, Brodish B, Sibata CH. Clinical photodynamic therapy of head and neck cancers - A review of applications and outcomes. Photodiagn Photodyn Ther 2005/09;2(3):205-222.

(12) Allison RR, Downie GH, Cuenca R, Hu X-, Childs CJH, Sibata CH. Photosensitizers in clinical PDT. Photodiagn Photodyn Ther 2004/05;1(1):27-42.

(13) Allison RR, Downie GH, Cuenca R, Sibata CH. A brief review of photodynamic therapy in oncology. AM J ONCOL REV 2006 02;5(2):111-117.

(14) Allison RR, Mota HC, Sibata CH. Clinical PD/PDT in North America: An historical review. Photodiagn Photo-dyn Ther 2004/12;1(4):263-277.

(15) Allison RR, Sibata CH. Photodynamic therapy: Mechanism of action and role in the treatment of skin disease. G Ital Dermatol Venereol 2010 /;145(4):491-507.

(16) Allison RR, Sibata CH. Oncologic photodynamic therapy photosensitizers: A clinical review. Photodiagn Photodyn Ther 2010 /;7(2):61-75.

(17) Allison RR, Sibata CH. Photofrin(registered trade-mark) photodynamic therapy: 2.0 mg/kg or not 2.0 mg/kg that is the question. Photodiagn Photodyn Ther 2008 /;5(2):112-119.

(18) Andersson-Engels S, Elner A, Johansson J, Karls-son S-, Salford LG, Stromblad L-, et al. Clinical recording of laser-induced fluorescence spectra for evaluation of tumour demarcation feasibility in selected clinical specialities. LASERS MED SCI 1991/;6(4):415-424.

(19) Andonegui J, Perez De Arcelus M, Jimenez-Lasanta L. Treatment with photodynamic therapy of circum-scribed choroidal hemangioma. Arch Soc Esp Oftalmol 2010 /;85(10):337-340.

(20) Andrejevic Blant S, Grosjean P, Ballini J-, Wagnieres G, Van Den Bergh H, Fontolliet C, et al. Localization of tetra(m-hydroxyphenyl)chlorin (Foscan) in human healthy tissues and squamous cell carcinomas of the upper aero-digestive tract, the esophagus and the bronchi: A fluorescence microscopy study. J Photochem Photobiol B Biol 2001/08;61(1-2):1-9.

(21) Andrejevic S, Savary JF, Monnier P, Fontolliet C, Braichotte D, Wagnieres G, et al. Measurements by fluo-rescence microscopy of the time-dependent distribution of meso-tetra-hydroxyphenylchlorin in healthy tissues and chemically induced «early» squamous cell carci-noma of the Syrian hamster cheek pouch. J Photochem Photobiol B 1996 Nov;36(2):143-151.

(22) Andrejevic-Blant S, Hadjur C, Ballini JP, Wagnieres G, Fontolliet C, van den Bergh H, et al. Photodynamic therapy of early squamous cell carcinoma with tetra(m-hydroxyphenyl)chlorin: optimal drug-light interval. Br J Cancer 1997;76(8):1021-1028.

(23) Andrejevic-Blant S, Woodtli A, Wagnieres G, Fontol-liet C, Van Den Bergh H, Monnier P. Interstitial photo-dynamic therapy with tetra(M-hydroxyphenyl)chlorin: Tumor versus striated muscle damage. Int J Radiat Oncol Biol Phys 1998/09;42(2):403-412.

(24) Antoniv VF, Dmitriev AA, Daikhes NA, Ivanov AV, Davudov KS, Perekosova IV, et al. Adoptive laser immu-notherapy and photodynamic therapy in ORL oncology. Vestn Otorinolaringol 1990 /(5):3-8.

(25) Arango BA, Castrellon AB, Perez CA, Raez LE, Santos ES. Nasopharyngeal carcinoma: Alternative treatment options after disease progression. Expert Rev Anticancer Ther 2010 /;10(3):377-386.

(26) Avetisov SE, Likhvantseva VG, Reshetnikov AV, Fe-dorov AA, Vereshchagina MV, Balaian ML, et al. Russian photosensitizer radachlorine in photodynamic therapy for epibulbar and choroid tumors: experimental studies. Vestn Oftalmol 2005 /;121(5):9-13.

(27) Awan MA, Tarin SA. Review of photodynamic therapy. Surgeon 2006 /;4(4):231-236.

(28) Baba T, Kitahashi M, Kubota-Taniai M, Oshitari T, Ya-mamoto S. Subretinal hemorrhage after photodynamic therapy for juxtapapillary retinal capillary hemangioma. Case Rep Ophthalmol 2011 /;2(1):134-139.

(29) Bakri SJ, Beer PM. Photodynamic therapy for maculopathy due to radiation retinopathy. Eye 2005 /;19(7):795-799.

(30) Balasubramanian S, Elangovan V, Govindasamy S. Fluorescence spectroscopic identification of 7,12-dimethylbenz[a]anthracene-induced hamster buccal pouch carcinogenesis. Carcinogenesis 1995 /;16(10):2461-2465.

(31) Balasubramanian S, Govindasamy S. In-hibitory effect of dietary flavonol quercetin on 7,12-dimethylbenz[a]anthracene-induced hamster buccal pouch carcinogenesis. Carcinogenesis 1996 /;17(4):877-879.

(32) Balmer A, Munier F, Zografos L. New strategies in the management of retinoblastoma. J Fr Ophtalmol 2002/;25(2):187-193.

(33) Barbazetto IA, Lee TC, Abramson DH. Treatment of conjunctival squamous cell carcinoma with photody-namic therapy. Am J Ophthalmol 2004 /;138(2):183-189.

(34) Barbazetto IA, Lee TC, Rollins IS, Chang S, Abramson DH. Treatment of choroidal melanoma using photody-namic therapy. Am J Ophthalmol 2003/06;135(6):898-899.

(35) Barbezetto IA, Smith RT. Vasoproliferative tumor of the retima treated with PDT. Retina 2003 /;23(4):565-567.

(36) Barth RF, Coderre JA, Vicente MGH, Blue TE. Boron neutron capture therapy of cancer: Current status and future prospects. Clin Cancer Res 2005/06;11(11):3987-4002.

(37) Belzacq A-, Brenner C. The adenine nucleotide translocator: A new potential chemotherapeutic target. Curr Drug Targets 2003 /;4(7):517-524.

(38) Berg K, Selbo PK, Weyergang A, Dietze A, Prasmick-aite L, Bonsted A, et al. Porphyrin-related photosensitiz-ers for cancer imaging and therapeutic applications. J Microsc 2005 /;218(2):133-147.

(39) Betz CS, Jager HR, Brookes JA, Richards R, Leunig A, Hopper C. Interstitial photodynamic therapy for a symp-tom-targeted treatment of complex vascular malforma-tions in the head and neck region. Lasers Surg Med 2007 Aug;39(7):571-582.

(40) Betz CS, Lai J-, Xiang W, Janda P, Heinrich P, Stepp H, et al. In vitro photodynamic therapy of nasopharyngeal carcinoma using 5-aminolevulinic acid. Photochem Photobiol Sci 2002/05;1(5):315-319.

(41) Betz CS, Rauschning W, Stranadko EP, Riabov MV, Albrecht V, Nifantiev NE, et al. Optimization of treatment parameters for Foscan-PDT of basal cell carcinomas. Lasers Surg Med 2008 Jul;40(5):300-311.

(42) Betz CS, Stepp H, Janda P, Arbogast S, Grevers G, Baumgartner R, et al. A comparative study of normal inspection, autofluorescence and 5-ALA-induced PPIX fluorescence for oral cancer diagnosis. Int J Cancer 2002/01;97(2):245-252.

(43) Bhagat N. Retinal detachments in the pediatric population: Part II. J Pediatr Ophthalmol Strabismus 2007 /;44(2):86-92.

(44) Bhattacharjee H, Deka H, Deka S, Barman MJ, Ma-zumdar M, Medhi J. Verteporfin photodynamic therapy of retinal capillary hemangioblastoma in von Hippel-Lindau disease. Indian J Ophthalmol 2010/03;58(1):73-75.

(45) Bhuvaneswari R, Gan YY, Soo KC, Olivo M. The effect of photodynamic therapy on tumor angiogenesis. Cell Mol Life Sci 2009 /;66(14):2275-2283.

(46) Bid MA. Photodynamic therapy as an adjuvant intraoperative treatment of recurrent head and neck carcinomas. ARCH OTOLARYNGOL HEAD NECK SURG 1996 /;122(11):1261-1265.

(47) Biel M. Advances in photodynamic therapy for the

treatment of head and neck cancers. Lasers Surg Med 2006 /;38(5):349-355.

(48) Biel MA. Photodynamic therapy of head and neck cancers. Methods Mol Biol 2010 /;635:281-293.

(49) Biel MA. Photodynamic therapy treatment of early oral and laryngeal cancers. Photochem Photobiol 2007 /;83(5):1063-1068.

(50) Biel MA. Photodynamic therapy in head and neck cancer. Curr Oncol Rep 2002 /;4(1):87-96.

(51) Biel MA. Photodynamic therapy and the treatment of head and neck neoplasia. Laryngoscope 1998 /;108(9):1259-1268.

(52) Biel MA. Photodynamic therapy and the treatment of head and neck cancers. J Clin Laser Med Surg 1996 /;14(5):239-244.

(53) Biel MA. Photodynamic therapy and head neck cancer treatment. MINIMALLY INVASIVE THER 1995/;4(3):153-157.

(54) Biel MA. Photodynamic therapy of head and neck cancers. Semin Surg Oncol 1995/;11(5):355-359.

(55) Biel MA, Janssen W, Trump MF. Photodynamic therapy to the oral cavity, tongue and larynx: A canine normal tissue tolerance study. LASERS MED SCI 1995/;10(1):13-18.

(56) Bischoff R, Bischoff G, Hoffmann S. Scanning force microscopy observation of tumor cells treated with hematoporphyrin IX derivatives. Ann Biomed Eng 2001 /;29(12):1092-1099.

(57) Blant SA, Glanzmann TM, Ballini JP, Wagnieres G, van den Bergh H, Monnier P. Uptake and localisation of mTHPC (Foscan) and its 14C-labelled form in normal and tumour tissues of the hamster squamous cell carcinoma model: a comparative study. Br J Cancer 2002 Dec 2;87(12):1470-1478.

(58) Blant SA, Woodtll A, Wagnieres G, Fontolliet C, Van Den Bergh H, Monnier P. In vivo fluence rate effect in photodynamic therapy of early cancers with tetra(m-hydroxyphenyl)chlorin. Photochem Photobiol 1996 /;64(6):963-968.

(59) Blasi MA, Scupola A, Tiberti AC, Sasso P, Balestrazzi E. Photodynamic therapy for vasoproliferative retinal tumors. Retina 2006 /;26(4):404-409.

(60) Blasi MA, Tiberti AC, Scupola A, Balestrazzi A, Colangelo E, Valente P, et al. Photodynamic therapy with

verteporfin for symptomatic circumscribed choroidal hemangioma: Five-year outcomes. Ophthalmology 2010 /;117(8):1630-1637.

(61) Blom D-R, Schuitmaker HJ, De Waard-Siebinga I, Dubbelman TMAR, Jager MJ. Decreased expression of HLA class I on ocular melanoma cells following in vitro photodynamic therapy. Cancer Lett 1997/01;112(2):239-243.

(62) Boixadera A, Arumi JG, Martinez-Castillo V, Encinas JL, Elizalde J, Blanco-Mateos G, et al. Prospective Clinical Trial Evaluating the Efficacy of Photodynamic Therapy for Symptomatic Circumscribed Choroidal Hemangioma. Ophthalmology 2009 /;116(1):100; 105.e1.

(63) Boniface G, Azab M. Cancer therapy with PHOTO-FRIN: overview and perspectives. EUR J CANCER CARE 1999 12/02;8:25-30.

(64) Boonkitticharoen V, Kulapaditharom B, Punnachaiya S, Kraiphibul P. Differences in in vitro photodynamic sensitivity among head and neck cancers. LASERS MED SCI 1997/09;12(3):274-279.

(65) Borle F, Radu A, Fontolliet C, Van Den Bergh H, Monnier P, Wagnieres G. Selectivity of the photosensitiser Tookad(registered trademark) for photodynamic therapy evaluated in the Syrian golden hamster cheek pouch tumour model. Br J Cancer 2003 /;89(12):2320-2326.

(66) Bown S, Rogowska A, Whitelaw D, Lees W, Lovat L, Ripley P, et al. Photodynamic therapy for cancer of the pancreas RID C-5713-2009 RID C-1986-2009. Gut 2002 APR;50(4):549-557.

(67) Braichorotte D, Savary J-, Glanzmann T, Westermann P, Folli S, Wagnieres G, et al. Clinical pharmacokinetic studies of tetra(meta-hydroxyphenyl) chlorin in squamous cell carcinoma by fluorescence spectroscopy at 2 wavelengths. Int J Cancer 1995/;63(2):198-204.

(68) Braichotte D, Savary JF, Glanzmann T, Westermann P, Folli S, Wagnieres G, et al. Clinical pharmacokinetic studies of tetra(meta-hydroxyphenyl)chlorin in squamous cell carcinoma by fluorescence spectroscopy at 2 wavelengths. Int J Cancer 1995 Oct 9;63(2):198-204.

(69) Braichotte DR, Savary JF, Monnier P, van den Bergh HE. Optimizing light dosimetry in photodynamic therapy of early stage carcinomas of the esophagus using fluorescence spectroscopy. Lasers Surg Med 1996;19(3):340-346.

(70) Braichotte DR, Wagnieres GA, Bays R, Monnier

P, Van den Bergh HE. Clinical pharmacokinetic studies of photofrin by fluorescence spectroscopy in the oral cavity, the esophagus, and the bronchi. Cancer 1995/;75(11):2768-2778.

(71) Brandt MG, Moore CC, Jordan K. Randomized control trial of fluorescence-guided surgical excision of nonmelanotic cutaneous malignancies. J Otolaryngol 2007 /;36(3):148-155.

(72) Bredell MG, Besic E, Maake C, Walt H. The application and challenges of clinical PD-PDT in the head and neck region: A short review. J Photochem Photobiol B Biol 2010/12;101(3):185-190.

(73) Brini A. Conservative treatment of melanoma of the choroid. Is enucleation an unusual step? J Fr Ophtalmol 1984 /;7(11):745-753.

(74) Brown SB, Brown EA, Walker I. The present and future role of photodynamic therapy in cancer treatment. Lancet Oncol 2004/08;5(8):497-508.

(75) Brown SB, Ibbotson SH. Photodynamic therapy and cancer. BMJ 2009/08;339(7715):251.

(76) Bruce Jr. RA. Photoradiation of choroidal malignant melanoma. Prog Clin Biol Res 1984 /;170:777-784.

(77) Bruce Jr. RA. Evaluation of hematoporphyrin photoradiation therapy to treat choroidal melanomas. Lasers Surg Med 1984/;4(1):59-64.

(78) Bryce R. Burns after photodynamic therapy - Drug point gives misleading impression of incidence of burns with temoporfin (Foscan). Br Med J 2000 JUN 24;320(7251):1731-1731.

(79) Buchanan RB, Carruth JAS, McKenzie AL, Williams SR. Photodynamic therapy in the treatment of malignant tumours of the skin and hean and neck. Eur J Surg Oncol 1989/;15(5):400-406.

(80) Calzavara F, Tomio L, Norberto L, Peracchia A, Corti L, Z orat PL, et al. Photodynamic therapy in the treatment of malignant tumours of the upper aerodigestive tract. LASERS MED SCI 1989/;4(4):279-284.

(81) Castro DJ, Saxton RE, Lufkin RB, Haugland RP, Zwarun AA, Fetterman HR, et al. Future directions of laser phototherapy for diagnosis and treatment of malignancies: Fantasy, fallacy, or reality? Laryngoscope 1991/;101(7 II SUPPL. 55):1-10.

(82) Cekic O, Bardak Y, Kapucuoglu N. Photodynamic

therapy for conjunctival ocular surface squamous neoplasia. J Ocul Pharmacol Ther 2011/04;27(2):205-207.

(83) Chan RPS, Lai TYY. Photodynamic therapy with verteporfin for vasoproliferative tumour of the retina: Diagnosis/Therapy in ophthalmology. Acta Ophthalmol 2010 /;88(6):711-712.

(84) Chang C-, Lai Y-, Wong C-. Photodynamic therapy for facial squamous cell carcinoma in cats using Photofrin(registered trademark). Chang Gung Med J 1998/;21(1):13-19.

(85) Chang C-, Wilder-Smith P. Topical application of photofrin for photodynamic diagnosis of oral neoplasms. Plast Reconstr Surg 2005 /;115(7):1877-1886.

(86) Chang KJ. EUS-Guided Fine Needle Injection and Brachytherapy. Tech Gastrointest Endosc 2007 /;9(1):55-58.

(87) Chang S-, Bown SG. Photodynamic therapy: Applications in bladder cancer and other malignancies. J Formos Med Assoc 1997 /;96(11):853-856.

(88) Chatterjee DK, Fong LS, Zhang Y. Nanoparticles in photodynamic therapy: An emerging paradigm. Adv Drug Deliv Rev 2008/12;60(15):1627-1637.

(89) Chen B, Pogue BW, Hasan T. Liposomal delivery of photosensitising agents. Expert Opin Drug Deliv 2005 /;2(3):477-487.

(90) Chen B, Pogue BW, Hoopes PJ, Hasan T. Vascular and cellular targeting for photodynamic therapy. Crit Rev Eukaryotic Gene Expr 2006/;16(4):279-306.

(91) Chen S-, Cao J-. Hemodynamic and imageological analysis of oral and maxillofacial tumor with photodynamic therapy. J Clin Rehab Tissue Eng Res 2007/02;11(5):923-925.

(92) Choi H, Lim W, Kim J-, Kim I, Jeong J, Ko Y, et al. Cell death and intracellular distribution of hematoporphyrin in a KB cell line. Photomed Laser Surg 2009/06;27(3):453-460.

(93) Chu ESM, Wu RWK, Yow CMN, Wong TKS, Chen JY. The cytotoxic and genotoxic potential of 5-aminolevulinic acid on lymphocytes: A comet assay study. Cancer Chemother Pharmacol 2006 /;58(3):408-414.

(94) Chung P-, He P, Shin J-, Hwang H-, Lee SJ, Ahn J-. Photodynamic therapy with 9-hydroxypheophorbide (alpha) on AMC-HN-3 human head and neck cancer

cells Induction of apoptosis via photoactivation of mitochondria and endoplasmic reticulum. Cancer Biol Ther 2009/07;8(14):34-42.

(95) Chung W-, Lee J-, Lee W-, Surh Y-, Park K-. Protective effects of hemin and tetrakis(4-benzoic acid)porphyrin on bacterial mutagenesis and mouse skin carcinogenesis induced by 7,12-dimethylbenz[a]anthracene. Mutat Res Genet Toxicol Environ Mutagen 2000/12;472(1-2):139-145.

(96) Cilliers H, Harper CA. Photodynamic therapy with Verteporfin for vascular leakage from a combined hamartoma of the retina and retinal pigment epithelium [6]. Clin Exp Ophthalmol 2006 /;34(2):186-188.

(97) Cohen EM, Ding H, Kessinger CW, Khemtong C, Gao J, Sumer BD. Polymeric micelle nanoparticles for photodynamic treatment of head and neck cancer cells. Otolaryngol Head Neck Surg 2010 /;143(1):109-115.

(98) Comer GM, Ciulla TA, Criswell MH, Tolentino M. Current and future treatment options for nonexudative and exudative age-related macular degeneration. Drugs Aging 2004/;21(15):967-992.

(99) Copper MP, Tan IB, Oppelaar H, Ruevekamp MC, Stewart FA. Meta-tetra(hydroxyphenyl)chlorin photodynamic therapy in early-stage squamous cell carcinoma of the head and neck. Arch Otolaryngol Head Neck Surg 2003/07;129(7):709-711.

(100) Copper MP, Triesscheijn M, Tan IB, Ruevekamp MC, Stewart FA. Photodynamic therapy in the treatment of multiple primary tumours in the head and neck, located to the oral cavity and oropharynx. Clin Otolaryngol 2007 06;32(1749-4478; 3):185-189.

(101) Coulter AH. Photodynamic therapy proves valuable in ophthalmology. J Clin Laser Med Surg 1994/;12(6):343-344.

(102) Crean DH, Liebow C, Penetrante RB, Mang TS. Evaluation of porfimer sodium fluorescence for measuring tissue transformation. Cancer 1993/;72(10):3068-3077.

(103) Csanady M, Kiss JG, Ivan L, Jori J, Czigner J. ALA (5-aminolevulinic acid)-induced protoporphyrin IX fluorescence in the endoscopic diagnostic and control of pharyngo-laryngeal cancer. Eur Arch Oto-Rhino-Laryngol 2004 /;261(5):262-266.

(104) Danjo Y, Sasabe T, Ishimoto I. Photoradiation therapy for retinoblastoma. FOLIA OPHTHALMOL JPN 1991/;42(5 II):1207-1212.

(105) Date M, Sakata I, Fukuchi K, Ohura K, Azuma Y, Shinohara M, et al. Photodynamic therapy for human oral squamous cell carcinoma and xenografts using a new photosensitizer, PAD-S31. Lasers Surg Med 2003/;33(1):57-63.

(106) Davila ML. Photodynamic therapy. Gastrointest Endosc Clin N Am 2011 Jan;21(1):67-79.

(107) Davis RK. Photodynamic therapy in otolaryngology-head and neck surgery. Otolaryngol Clin North Am 1990/;23(1):107-119.

(108) D'Cruz AK, Robinson MH, Biel MA. mTHPC-mediated photodynamic therapy in patients with advanced, incurable head and neck cancer: A multicenter study of 128 patients. Head Neck 2004 /;26(3):232-240.

(109) de Rosa A, Naviglio D, Di Luccia A. Advances in photodynamic therapy of cancer. Curr Cancer Ther Rev 2011 /;7(3):234-247.

(110) de Visscher SAHJ, Kascakova S, de Bruijn HS, van der Ploeg-van den Heuvel,Angelique, Amelink A, Sterenborg HJCM, et al. Fluorescence Localization and Kinetics of mTHPC and Liposomal Formulations of mTHPC in the Window-Chamber Tumor Model. Lasers Surg Med 2011 AUG;43(6):528-536.

(111) Dequanter D, Lothaire P, Meert A-, Andry G. Photodynamic therapy in head and neck oncology. Rev Med Brux 2008 /;29(1):23-25.

(112) Dewaele M, Maes H, Agostinis P. ROS-mediated mechanisms of autophagy stimulation and their relevance in cancer therapy. Autophagy 2010/10;6(7):838-854.

(113) Dilkes MG, Alusi G, Djaezeri BI. The treatment of head and neck cancer with photodynamic therapy: Clinical experience. Rev Contemp Pharmacother 1999/;10(1):47-57.

(114) Dilkes MG, Benjamin E, Ovaisi S, Banerjee AS. Treatment of primary mucosal head and neck squamous cell carcinoma using photodynamic therapy: Results after 25 treated cases. J Laryngol Otol 2003 /;117(9):713-717.

(115) Dilkes MG, DeJode ML, Gardiner Q, Kenyon GS, McKelvie P. Treatment of head and neck cancer with photodynamic therapy: Results after one year. J Laryngol Otol 1995/;109(11):1072-1076.

(116) Dilkes MG, DeJode ML, Rowntree-Taylor A, McGilligan JA, Kenyon GS, McKelvie P. M-THPC photodynamic

therapy for head and neck cancer. LASERS MED SCI 1996/;11(1):23-29.

(117) Dolmans DEJGJ, Fukumura D, Jain RK. Photodynamic therapy for cancer. Nat Rev Cancer 2003 /;3(5):380-387.

(118) Donald PJ, Cardiff RD, Kendall K. Monoclonal antibody-porphyrin conjugate for head and neck cancer: The possible magic bullet. Otolaryngol Head Neck Surg 1991/;105(6):781.

(119) Donaldson MJ, Lim L, Harper CA, Mackenzie J, Campbell W. Primary treatment of choroidal amelanotic melanoma with photodynamic therapy - Response [2]. Clin Exp Ophthalmol 2006/09;34(7):721-722.

(120) Donaldson MJ, Lim L, Harper CA, Mackenzie J, Campbell WG. Primary treatment of choroidal amelanotic melanoma with photodynamic therapy. Clin Exp Ophthalmol 2005 /;33(5):548-549.

(121) Donnelly RF, McCarron PA, Woolfson D. Drug delivery systems for photodynamic therapy. Recent Pat Drug Deliv Formulation 2009/;3(1):1-7.

(122) Dougherty TJ. Photosensitization of malignant tumors. Semin Surg Oncol 1986/;2(1):24-37.

(123) Dragicevic-Curic N, Grafe S, Albrecht V, Fahr A. Topical application of temoporfin-loaded invasomes for photodynamic therapy of subcutaneously implanted tumours in mice: a pilot study. J Photochem Photobiol B 2008 Apr 25;91(1):41-50.

(124) Ebrahim S, Peyman GA, Lee PJ. Applications of liposomes in ophthalmology. Surv Ophthalmol 2005 /;50(2):167-182.

(125) Economou MA. Introduction: Uveal melanoma. Acta Ophthalmol 2008 /;86(THESIS 4):7-19.

(126) Edge CJ, Carruth JAS. Photodynamic therapy and the treatment of head and neck cancer. Br J Oral Maxillofac Surg 1988/;26(1):1-11.

(127) Egorov EA, Prokof'eva MI, Egorov AE, Novoderezhkin VV, Botabekova TK. Photodynamic therapy in the treatment of diseases of the anterior and posterior eye segments. Vestn Oftalmol 2003 /;119(2):13-15.

(128) El-Far M, Setate A, El-Maddawy M. First initial clinical application of photodynamic therapy (PDT) in Egypt: Two case reports. Lasers Life Sci 1998/;8(1):27-35.

(129) Eskelin S, Tommila P, Palosaari T, Kivela T. Photodynamic therapy with verteporfin to induce regression

of aggressive retinal astrocytomas. Acta Ophthalmol 2008/;86(7):794-799.

(130) Etienne J, Dorme N, Bourg-Heckly G, Raimbert P, Fekete F. Local curative treatment of superficial adenocarcinoma in Barrett's esophagus. First results of photodynamic therapy with a new photosensitizer. Bull Acad Natl Med 2000;184(8):1731-44; discussion 1744-7.

(131) Etienne J, Dorme N, Bourg-Heckly G, Raimbert P, Flejou JF. Photodynamic therapy with green light and m-tetrahydroxyphenyl chlorin for intramucosal adenocarcinoma and high-grade dysplasia in Barrett's esophagus. Gastrointest Endosc 2004 Jun;59(7):880-889.

(132) Fan K, Hopper C, Speight P, Buonaccorsi G, Bown S. Photodynamic therapy using mTHPC for malignant disease in the oral cavity RID C-5713-2009. International Journal of Cancer 1997 SEP 26;73(1):25-32.

(133) Favilla I, Favilla ML, Gosbell AD, Barry WR, Ellims P, Hill JS, et al. Photodynamic therapy: A 5-year study of its effectiveness in the treatment of posterior uveal melanoma, and evaluation of haematoporphyrin uptake and photocytotoxicity of melanoma cells in tissue culture. Melanoma Res 1995/;5(5):355-364.

(134) Fayter D, Corbett M, Heirs M, Fox D, Eastwood A. A systematic review of photodynamic therapy in the treatment of precancerous skin conditions, Barrett's oesophagus and cancers of the biliary tract, brain, head and neck, lung, oesophagus and skin. Health Technol Assess 2010/;14(37):3-129.

(135) Ferrer E, Cole P. Ophthalmic therapeutics: New basic research and clinical studies: Highlights from the Annual Meeting of the Association for Research in Vision and Ophthalmology (ARVO) 2007: The Aging Eye. Drugs Future 2007 /;32(7):643-654.

(136) Ferriols Lisart F, Pitarch Molina J. Principles of phototherapy and its use in cancer patients. Farm Hosp 2004 /;28(3):205-213.

(137) Feyh J. Photodynamic treatment for cancers of the head and neck. J PHOTOCHEM PHOTOBIOL B BIOL 1996 /;36(2):175-177.

(138) Feyh J, Goetz A, Martin F, Lumper W, Muller W, Brendel W, et al. Photodynamic therapy with haematoporphyrin-derivative (hpd) on a spinocellular carcinoma of the auricle. LARYNGO- RHINO- OTOL 1989/;68(10):563-565.

(139) Feyh J, Goetz A, Muller W, Konigsberger R, Kas-

tenbauer E. Photodynamic therapy in head and neck surgery. J Photochem Photobiol B, Biol 1990 /;7(2-4):353-358.

(140) Feyh J, Gutmann R, Leunig A. Photodynamic therapy in head and neck surgery. LARYNGO- RHINO- OTOL 1993/;72(6):273-278.

(141) Fisher AMR, Murphree AL, Gomer CJ. Clinical and preclinical photodynamic therapy. Lasers Surg Med 1995/;17(1):2-31.

(142) Foster BS, Gragoudas ES, Young LHY. Photodynamic therapy of choroidal melanoma. Int Ophthalmol Clin 1997 /;37(4):117-126.

(143) Franken KAP, Van Delft JL, Dubbelman TMAR. Hematoporphyrin derivative photoradiation treatment of experimental malignant melanoma in the anterior chamber of the rabbit. Curr Eye Res 1985/;4(5):641-655.

(144) Fuchs O, Hrkal Z. Use of 5-Amionolevulinic acid for photodynamic diagnosis and cancer therapy. Cas Lek Cesk 1999/;138(19):584-588.

(145) Gaal M, Gyulai R, Baltas E, Kui R, Olah J, Kemeny L. Photodynamic therapy in dermatooncology. Orvosi Hetil 2007/11;148(47):2227-2233.

(146) Garcia G, Naud-Martin D, Carrez D, Croisy A, Maillard P. Microwave-mediated 'click-chemistry' synthesis of glycoporphyrin derivatives and in vitro photocytotoxicity for application in photodynamic therapy. Tetrahedron 2011/07;67(26):4924-4932.

(147) Gerber-Leszczyszyn H, Ziolkowski P, Marszalik P. Photodynamic therapy of head and neck tumors and non-tumor like disorders. Otolaryngol Pol 2004 /;58(2):339-343.

(148) Giamas G, Man YL, Hirner H, Bischof J, Kramer K, Khan K, et al. Kinases as targets in the treatment of solid tumors. Cell Signal 2010 /;22(7):984-1002.

(149) Gillenwater A, Papadimitrakopoulou V, Richards-Kortum R. Oral premalignancy: New methods of detection and treatment. Curr Oncol Rep 2006 /;8(2):146-154.

(150) Gilmour MA. Lasers in ophthalmology. Vet Clin North Am Small Anim Pract 2002/;32(3):649-672.

(151) Giuliari GP, Sadaka A, Hinkle DM, Simpson ER. Current treatments for radiation retinopathy. Acta Oncol 2011 /;50(1):6-13.

(152) Glanzmann T, Forrer M, Andrejevic Blant S, Woodtli A, Grosjean P, Braichotte D, et al. Pharmacokinetics and

pharmacodynamics of tetra(m-hydroxyphenyl)chlorin in the hamster cheek pouch tumor model: Comparison with clinical measurements. J Photochem Photobiol B Biol 2000/;57(1):22-32.

(153) Gluckman JL. Photodynamic therapy for head and neck neoplasms. Otolaryngol Clin North Am 1991/;24(6):1559-1567.

(154) Gluckman JL. Hematoporphyrin photodynamic therapy: Is there truly a future in head and neck oncology? Reflections on a 5-year experience. Laryngoscope 1991/;101(1 I):36-42.

(155) Gluckman JL, Portugal LG. Photodynamic therapy for cutaneous malignancies of the head and neck. Otolaryngol Clin North Am 1993/;26(2):311-318.

(156) Gluckman JL, Waner M, Shumrick K, Peerless S. Photodynamic therapy. A viable alternative to conventional therapy for early lesion of the upper aerodigestive tract? ARCH OTOLARYNGOL HEAD NECK SURG 1986/;112(9):949-952.

(157) Gluckman JL, Zitsch RP. Photodynamic therapy in the management of head and neck cancer. Cancer Treat Res 1990 /;52:95-113.

(158) Gomer CJ, Doiron DR, Jester JV. Hematoporphyrin derivative photoradiation therapy for the treatment of intraocular tumors: Examination of acute normal ocular tissue toxicity. Cancer Res 1983 1983/;43(2):721-727.

(159) Gomer CJ, Doiron DR, White L. Hematoporphyrin derivative photoradiation induced damage to normal and tumor tissue of the pigmented rabbit eye. Curr Eye Res 1984/;3(1):229-237.

(160) Gomer CJ, Ferrario A, Hayashi N, Rucker N, Szirth BC, Murphree AL. Molecular, cellular, and tissue responses following photodynamic therapy. Lasers Surg Med 1988/;8(5):450-463.

(161) Gomer CJ, Jester JV, Razum NJ. Photodynamic therapy of intraocular tumors examination of hematoporphyrin derivative distribution and long-term damage in rabbit ocular tissue. Cancer Res 1985 1985/;45(8):3718-3725.

(162) Gomer CJ, Murphree AL, Jester JV. Hematoporphyrin derivative photodynamic therapy for the treatment of intraocular tumors. PROC AM ASSOC CANCER RES 1985/;VOL. 26:No.937.

(163) Gomer CJ, Rucker N, Mark C, Benedict WF, Murphree AL. Tissue distribution of 3H-hematoporphyrin

derivative in athymic „nude" mice heterotransplanted with human retinoblastoma. Invest Ophthalmol Vis Sci 1982 /;22(1):118-120.

(164) Gomer CJ, Szirth BC, Doiron DR, Jester JV, Lingua RW, Mark C, et al. Preclinical evaluation of hematoporphyrin derivative for the treatment of intraocular tumors: a preliminary report. Adv Exp Med Biol 1983 /;160:109-114.

(165) Gonzalez VH, Li Kuan Hu , Theodossiadis PG, Flotte TJ, Gragoudas ES, Young LHY. Photodynamic therapy of pigmented choroidal melanomas. Invest Ophthalmol Vis Sci 1995 1995/;36(5):871-878.

(166) Gossner L, May A, Sroka R, Ell C. A new long-range through-the-scope balloon applicator for photodynamic therapy in the esophagus and cardia. Endoscopy 1999 Jun;31(5):370-376.

(167) Grant WE, Hopper C, MacRobert AJ, Speight PM, Bown SG. Photodynamic therapy of oral cancer: Photosensitisation with systemic aminolaevulinic acid. Lancet 1993/;342(8864):147-148.

(168) Grant WE, Hopper C, Speight PM, Path MRC, MacRobert AJ, Bown SG. Photodynamic therapy of malignant and premalignant lesions in patients with ‚field cancerization' of the oral cavity. J Laryngol Otol 1993/;107(12):1140-1145.

(169) Grant WE, Speight PM, Hopper C, Bown SG. Photodynamic therapy: An effective, but non-selective treatment for superficial cancers of the oral cavity. Int J Cancer 1997/;71(6):937-942.

(170) Gravier J, Korchowiec B, Schneider R, Rogalska E. Interaction of amphiphilic chlorin-based photosensitizers with 1,2-dipalmitoyl-sn-glycero-3-phosphocholine monolayers. Chem Phys Lipids 2009 APR;158(2):102-109.

(171) Gravier N, Ducournau Y, Patrice T, Quere MA, Pechereau A. Photochemotherapy for intraocular tumours. Effects of laser fractioning on healthy retina in the rabbit. Ophtalmologie 1994/;8(4):342-345.

(172) Gregory GF, Hopper C, Fan K, Grant WE, Bown SG, Speight PM. Photodynamic therapy and lip vermilion dysplasia: A pilot study. EUR J CANCER PART B ORAL ONCOL 1995/;31(5):346-347.

(173) Grosjean P, Savary JF, Mizeret J, Wagnieres G, Woodtli A, Theumann JF, et al. Photodynamic therapy for cancer of the upper aerodigestive tract using tetra(m-

hydroxyphenyl)chlorin. J Clin Laser Med Surg 1996 Oct;14(5):281-287.

(174) Grosjean P, Savary JF, Wagnieres G, Mizeret J, Woodtli A, Fontolliet C, et al. Phototherapy of pharyngeal, oesophageal and bronchial early squamous cell carcinomas after sensitisation by tetra (m-hydroxyphenyl) chlorin (mTHPC). Med Chir Dig 1996/;25(8):411-413.

(175) Gross DJ, Waner M, Schosser RH, Dinehart SM. Squamous cell carcinoma of the lower lip involving a large cutaneous surface. Photodynamic therapy as an alternative therapy. Arch Dermatol 1990/;126(9):1148-1150.

(176) Gross SA, Wolfsen HC. The role of photodynamic therapy in the esophagus. Gastrointest Endosc Clin N Am 2010 Jan;20(1):35-53, vi.

(177) Gunther JB, Altaweel MM. Bevacizumab (Avastin) for the Treatment of Ocular Disease. Surv Ophthalmol 2009 /;54(3):372-400.

(178) Gupta M, Singh AD, Rundle PA, Rennie IG. Efficacy of photodynamic therapy in circumscribed choroidal haemangioma. Eye 2004 /;18(2):139-142.

(179) Hamad LO, Vervoorts A, Hennig T, Bayer R. Ex vivo photodynamic diagnosis to detect malignant cells in oral brush biopsies. Lasers Med Sci 2010 /;25(2):293-301.

(180) Hamdoon Z, Jerjes W, Upile T, Akram S, Hopper C. Metastatic renal cell carcinoma to the orofacial region: A novel method to alleviate symptoms and control disease progression. Photodiagn Photodyn Ther 2010 /;7(4):246-250.

(181) Hamdoon Z, Jerjes W, Upile T, Akram S, Hopper C. Cystic hygroma treated with ultrasound guided interstitial photodynamic therapy: case study. Photodiagnosis Photodyn Ther 2010 Sep;7(3):179-182.

(182) Hamdoon Z, Jerjes W, Upile T, Hoonjan P, Hopper C. Endoluminal carotid stenting prior to photodynamic therapy to pericarotid malignant disease: Technical advance. Photodiagn Photodyn Ther 2010 /;7(2):126-128.

(183) Hamdoon Z, Jerjes W, Upile T, Hopper C. Optical coherence tomography-guided photodynamic therapy for skin cancer: case study. Photodiagnosis Photodyn Ther 2011 Mar;8(1):49-52.

(184) Hamdoon Z, Jerjes W, Upile T, Osher J, Hopper C. Lacrimal gland mantle lymphoma treated with photodynamic therapy: Overview and report of a case. Photodiagn Photodyn Ther 2010 /;7(2):129-133.

(185) Harbour JW. Photodynamic therapy for choroidal metastasis from carcinoid tumor. Am J Ophthalmol 2004 /;137(6):1143-1145.

(186) Harris DM, Hill JH, Werkhaven JA. Porphyrin fluorescence and photosensitization in head and neck cancer. ARCH OTOLARYNGOL HEAD NECK SURG 1986/;112(11):1194-1199.

(187) Harris DM, Werkhaven J. Endogenous porphyrin fluorescence in tumors. Lasers Surg Med 1987/;7(6):467-472.

(188) Harris F, Chatfield LK, Phoenix DA. Phenothiazinium based photosensitisers - Photodynamic agents with a multiplicity of cellular targets and clinical applications. Curr Drug Targets 2005 /;6(5):615-627.

(189) Harrod-Kim P. Tumor ablation with photodynamic therapy: Introduction to mechanism and clinical applications. J Vasc Intervent Radiol 2006 /;17(9):1441-1448.

(190) Heijl A, Algvere PV, Alm A, Andersen N, Bauer B, Carlsson J-, et al. Nordic research in ophthalmology. Acta Ophthalmol Scand 2005 /;83(3):278-288.

(191) Heimann H, Damato B. Congenital vascular malformations of the retina and choroid. Eye 2010 /;24(3):459-467.

(192) Herzog M, Horch HH, Senekowitsch R, Schroder E. Experimental studies on laser diagnosis and therapy of oral carcinomas following tumor-selective photosensitization to a hematoporphyrin derivative (HPD). Preliminary report. Dtsch Z Mund Kiefer Gesichtschir 1987 /;11(1):18-22.

(193) Hill JH, Plant RL, Harris DM. The nude mouse xenograft system: A model for photodetection and photodynamic therapy in head and neck squamous cell carcinoma. AM J OTOLARYNGOL HEAD NECK MED SURG 1986/;7(1):17-27.

(194) Hill JH, Plant RL, Harris DM, Paniello RC. Photodynamic therapy for head and neck cancer xenografts in athymic mice. Otolaryngol Head Neck Surg 1986/;95(5):602-605.

(195) Hintschich C, Feyh J, Beyer-Machule C, Riedel K, Ludwig K. Photodynamic laser therapy of basal-cell carcinoma of the lid. Ger J Ophthalmol 1993 /;2(4-5):212-217.

(196) Hirst LW. Treatment of conjunctival squamous cell carcinoma with photodynamic therapy. Am J Ophthalmol 2005 /;139(4):759; 760; author reply 760.

(197) Hoerauf H, Huttmann G, Diddens H, Thiele B, Laqua H. Photodynamic therapy of basal cell carcinoma of the lid after topical application of delta-aminolevulinic acid. Ophthalmologe 1994 1994/;91(6):824-829.

(198) Hofman JW, Carstens MG, van Zeeland F, Helwig C, Flesch FM, Hennink WE, et al. Photocytotoxicity of mTHPC (temoporfin) loaded polymeric micelles mediated by lipase catalyzed degradation. Pharm Res 2008 Sep;25(9):2065-2073.

(199) Hogikyan ND, Hayden RE, McLear PW. Cutaneous photoprotection using a hydroxyl radical scavenger in photodynamic therapy. AM J OTOLARYNGOL HEAD NECK MED SURG 1991/;12(1):1-5.

(200) Hopper C. The role of photodynamic therapy in the management of oral cancer and precancer. EUR J CANCER PART B ORAL ONCOL 1996/;32(2):71-72.

(201) Hopper C, Kubler A, Lewis H, Tan IB, Putnam G, Patrice T, et al. mTHPC-mediated photodynamic therapy for early oral squamous cell carcinoma. Int J Cancer 2004 /;111(1):138-146.

(202) Hopper C, Niziol C, Sidhu M. The cost-effectiveness of Foscan mediated photodynamic therapy (Foscan-PDT) compared with extensive palliative surgery and palliative chemotherapy for patients with advanced head and neck cancer in the UK. Oral Oncol 2004 /;40(4):372-382.

(203) Horsman MR, Winther J. Vascular effects of photodynamic therapy in an intraocular retinoblastoma-like tumour. Acta Oncol 1989/;28(5):693-697.

(204) Huang Z. Photodynamic therapy in China: Over 25 years of unique clinical experience. Part two-Clinical experience. Photodiagn Photodyn Ther 2006 2006/06;3(2):71-84.

(205) Huang Z. A review of progress in clinical photodynamic therapy. Technol Cancer Res Treat 2005 /;4(3):283-293.

(206) Hussain N, Das T. Verteporfin therapy for subfoveal choroidal neovascularisation associated with choroidal osteoma. Int J Ophthalmol 2005/10;5(5):838-840.

(207) Inaguma M, Hashimoto K. Porphyrin-like fluorescence in oral cancer: In vivo fluorescence spectral characterization of lesions by use of a near-ultraviolet excited autofluorescence diagnosis system and separation of fluorescent extracts by capillary electrophoresis. Cancer 1999/12;86(11):2201-2211.

(208) Jain N, Sharma PK, Banik A, Bhardwaj V. Applications of photosensitizer in therapy. Pharmacogn J 2011 /;3(22):11-17.

(209) Javaid B. Photodynamic therapy (PDT) for oesophageal dysplasia and early carcinoma with mTHPC (m-Tetrahidroxyphenyl chlorin): a preliminary study. Lasers Med Sci 2002;17(2):135.

(210) Jayanthi JL, Mallia RJ, Shiny ST, Baiju KV, Mathews A, Kumar R, et al. Discriminant analysis of autofluorescence spectra for classification of oral lesions in vivo. Lasers Surg Med 2009 /;41(5):345-352.

(211) Jerjes W, Upile T, Akram S, Hopper C. The surgical palliation of advanced head and neck cancer using photodynamic therapy. Clin Oncol 2010 /;22(9):785-791.

(212) Jerjes W, Upile T, Alexander Mosse C, Hamdoon Z, Morcos M, Morley S, et al. Prospective evaluation of 110 patients following ultrasound-guided photodynamic therapy for deep seated pathologies. Photodiagnosis Photodyn Ther 2011 Dec;8(4):297-306.

(213) Jerjes W, Upile T, Betz CS, El Maaytah M, Abbas S, Wright A, et al. The application of photodynamic therapy in the head and neck. Dent Update 2007 /;34(8):478; 480, 483-484, 486.

(214) Jerjes W, Upile T, Hamdoon Z, Abbas S, Akram S, Mosse CA, et al. Photodynamic therapy: The minimally invasive surgical intervention for advanced and/or recurrent tongue base carcinoma. Lasers Surg Med 2011 /;43(4):283-292.

(215) Jerjes W, Upile T, Hamdoon Z, Alexander Mosse C, Morcos M, Hopper C. Photodynamic therapy outcome for T1/T2 N0 oral squamous cell carcinoma. Lasers Surg Med 2011 /;43(6):463-469.

(216) Jerjes W, Upile T, Hamdoon Z, Mosse CA, Akram S, Hopper C. Photodynamic therapy outcome for oral dysplasia. Lasers Surg Med 2011 /;43(3):192-199.

(217) Jerjes W, Upile T, Hamdoon Z, Nhembe F, Bhandari R, Mackay S, et al. Ultrasound-guided photodynamic therapy for deep seated pathologies: prospective study. Lasers Surg Med 2009 Nov;41(9):612-621.

(218) Jerjes W, Upile T, Vincent A, Abbas S, Shah P, Mosse CA, et al. Management of deep-seated malformations with photodynamic therapy: a new guiding imaging modality. Lasers Med Sci 2009 Sep;24(5):769-775.

(219) Jerjes W, Upile T, Hamdoon Z, Mosse CA, Akram S, Morley S, et al. Interstitial PDT for Vascular Anomalies.

Lasers Surg Med 2011 JUL;43(5):357-365.

(220) Ji H-, Zhang F, Gao L-, Jia L-, Xiong Y, Liang C, et al. Photodynamic therapy of pigmented choroidal melanomas in rabbits using hematoporphyrin monomethyl ether. Chin J Ophthalmol 2007 /;43(3):212-216.

(221) Jiang G. Hematoporphyrin derivative-laser induced changes in dehydrogenases in tumor-bearing mice and patients with nasopharyngeal carcinoma. Zhonghua Er Bi Yan Hou Ke Za Zhi 1988 /;23(1):42; 45, 62.

(222) Jin C, Wu Z, Li Y, Li Y, Chen H, North J. The killing effect of photodynamic therapy using benzoporphyrin derivative on retinoblastoma cell line in vitro. Yan Ke Xue Bao 1999 /;15(1):1-6.

(223) Jin H, Zhong X, Wang ZW, Huang X, Ye H, Ma S, et al. Sonodynamic effects of hematoporphyrin monomethyl ether on CNE-2 cells detected by atomic force microscopy. J Cell Biochem 2011 /;112(1):169-178.

(224) Jones GC, Cortese DA, Neel III HB. Effect of bleomycin on hematoporphyrin derivative phototherapy of solid tumors. Ann Otol Rhinol Laryngol 1990/;99(12):941-944.

(225) Josefsen LB, Boyle RW. Photodynamic therapy and the development of metal-based photosensitisers. Met-Based Drugs 2008.

(226) Juarranz A, Jaen P, Sanz-Rodriguez F, Cuevas J, Gonzalez S. Photodynamic therapy of cancer. Basic principles and applications. Clin Transl Oncol 2008/;10(3):148-154.

(227) Jurklies B, Anastassiou G, Ortmans S, Schuler A, Schilling H, Schmidt-Erfurth U, et al. Photodynamic therapy using verteporfin in circumscribed choroidal haemangioma. Br J Ophthalmol 2003/01;87(1):84-89.

(228) Juzeniene A, Peng Q, Moan J. Milestones in the development of photodynamic therapy and fluorescence diagnosis. Photochem Photobiol Sci 2007/;6(12):1234-1245.

(229) Kaneko A. Japanese contributions to ocular oncology. Int J Clin Oncol 1999/12;4(6):321-326.

(230) Kanick SC, Karakullukcu B, Gamm UA, Aans JB, Bing I, Sterenborg HJCM, et al. Monitoring photodynamic therapy using quantitative reflectance and fluorescence spectroscopic measurements performed with a single optical fiber. Photodiagn Photodyn Ther 2011 /;8(2):227.

(231) Kapoor S. The therapeutic benefits of heme oxygenase (HO-1) inhibition in the management of systemic

malignancies besides hepatocellular carcinomas. Int J Cancer 2009/08;125(3):736.

(232) Karakullukcu B, De Boer JP, Van Veen R, Wegman J, Tan B. Surgical debulking combined with photodynamic therapy to manage residual extramedullary plasmacytoma of the nasopharynx. Photodiagnosis Photodyn Ther 2011 Sep;8(3):264-266.

(233) Karakullukcu B, Kanick C, Amelink A, Sterenborg D, Tan B, Robinson D. Non-invasive monitoring of photodynamic therapy of oral cancers by fluorescence differential path-length spectroscopy. Photodiagn Photodyn Ther 2011 /;8(2):227-228.

(234) Karakullukcu B, Kanick SC, Aans JB, Sterenborg HJ, Tan IB, Amelink A, et al. Clinical feasibility of monitoring m-THPC mediated photodynamic therapy by means of fluorescence differential path-length spectroscopy. J Biophotonics 2011 Aug 22.

(235) Karakullukcu B, Nyst HJ, van Veen RL, Hoebers FJ, Hamming-Vrieze O, Witjes MJ, et al. mTHPC mediated interstitial photodynamic therapy of recurrent nonmetastatic base of tongue cancers: Development of a new method. Head Neck 2012 Jan 31.

(236) Karakullukcu B, Van Oudenaarde K, Copper MP, Klop WMC, Van Veen R, Wildeman M, et al. Photodynamic therapy of early stage oral cavity and oropharynx neoplasms: An outcome analysis of 170 patients. Eur Arch Oto-Rhino-Laryngol 2011 /;268(2):281-288.

(237) Kecik T, Switka-Wieclawska I, Kasprzak J, Graczyk A, Pratnicki A. Experimental studies on the usefulness of photodynamic method in diagnosis and treatment of melanoma. Klin Oczna 1993 /;95(8):293-295.

(238) Keller GS, Doiron DR, Fisher GU. Photodynamic therapy in otolaryngology - Head and neck surgery. Arch Otolaryngol 1985/;111(11):758-761.

(239) Kelley EE, Domann FE, Buettner CR, Oberley LW, Burns CP. Increased efficacy of in vitro Photofrin(registered trademark) photosensitization of human oral squamous cell carcinoma by iron and ascorbate. J PHOTOCHEM PHOTOBIOL B BIOL 1997 /;40(3):273-277.

(240) Kelloff GJ, Sullivan DC, Baker H, Clarke LP, Nordstrom R, Tatum JL, et al. Workshop on imaging science development for cancer prevention and preemption. Cancer Biomarkers 2007/;3(1):1-33.

(241) Ken Kang-Hsin Wang, Mitra S, Foster TH. Photo-

dynamic dose does not correlate with long-term tumor response to mTHPC-PDT performed at several drug-light intervals. Med Phys 2008 08;35(8):3518-3526.

(242) Ken Kang-Hsin Wang, Mitra S, Foster TH. Photodynamic dose does not correlate with long-term tumor response to mTHPC-PDT performed at several drug-light intervals. Med Phys 2008 08;35(8):3518-3526.

(243) Kennedy J. HPD photoradiation therapy for cancer at Kingston and Hamilton. Adv Exp Med Biol 1983 /;160:53-62.

(244) Kennedy JC, Marcus SL, Pottier RH. Photodynamic therapy (PDT) and photodiagnosis (PD) using endogenous photosensitization induced by 5-aminolevulinic acid (ALA): Mechanisms and clinical results. J Clin Laser Med Surg 1996 /;14(5):289-304.

(245) Kenyon JN, Fulle RJ, Lewis TJ. Activated cancer therapy using light and ultrasound - A case series of sonodynamic photodynamic therapy in 115 patients over a 4 year period. Curr Crug Ther 2009 /;4(3):179-193.

(246) Kessel D. Photodynamic therapy of neoplastic disease. DRUGS TODAY 1996/;32(5):385-396.

(247) Kiesslich T, Krammer B, Plaetzer K. Cellular mechanisms and prospective applications of hypericin in photodynamic therapy. Curr Med Chem 2006 /;13(18):2189-2204.

(248) Kilpatrick DC. Lectin-glycoconjugate interactions in health and disease. Biochem Soc Trans 2008/;36(6):1453-1456.

(249) Kim RY, Gragroudas ES, Young LHY. Future laser approaches in melanoma treatment. Int Ophthalmol Clin 2006 /;46(1):27-39.

(250) Kim RY, Hu L-, Foster BS, Gragoudas ES, Young LHY. Photodynamic therapy of pigmented choroidal melanomas of greater than 3- mm thickness. Ophthalmology 1996/;103(12):2029-2036.

(251) Kim RY, Young LHY. Use of photodynamic therapy for treatment of ocular malignancies. Ophthalmol Clin North Am 1999/;12(2):167-176.

(252) Kobayashi W, Liu Q, Nakagawa H, Sakaki H, Teh B, Matsumiya T, et al. Photodynamic therapy with mono-l-aspartyl chlorin e6 can cause necrosis of squamous cell carcinoma of tongue: Experimental study on an animal model of nude mouse. Oral Oncol 2006 /;42(1):46-50.

(253) Komerik N. A novel approach to cancer treatment:

Photodynamic therapy. Turk J Cancer 2002/07;32(3):83-91.

(254) Konomi U, Yoshida T, Ito H, Shimizu A, Shimizu S, Okamoto I, et al. Clinical photodynamic diagnosis and therapy efficiency in oropharyngeal cancer. J Otolaryngol Jpn 2009 /;112(5):429-433.

(255) Kost KM. Endoscopic percutaneous dilatational tracheotomy: A prospective evaluation of 500 consecutive cases. Laryngoscope 2005 /;115(10 II):1-30.

(256) Kozacko MF, Mang TS, Schally AV, Priore RL, Liebow C. Bombesin antagonist prevents CO2 laser-induced promotion of oral cancer. Proc Natl Acad Sci U S A 1996/04;93(7):2953-2957.

(257) Krishnamurthy S, Powers SK. Lasers in neurosurgery. Lasers Surg Med 1994/;15(2):126-167.

(258) Kubicka-Trzaska A, Romanowska-Dixon B. Photodynamic therapy of circumscribed choroidal hemangioma. Klin Oczna 2006 /;108(4-6):209-213.

(259) Kubler A, Niziol C, Sidhu M, Dunne A, Werner JA. Analysis of cost effectiveness of photodynamic therapy with Foscan (Foscan-PDT) in comparison with palliative chemotherapy in patients with advanced head-neck tumors in Germany. Laryngorhinootologie 2005 Oct;84(10):725-732.

(260) Kubler A, Niziol C, Sidhu M, Dunne A, Werner J. Cost-effectivity analysis of photodynamic therapy with Foscan (R) (Foscan (R)-PDT) compared with a palliative chemotherapy in patients with advanced head and neck tumors in Germany. Laryngo-Rhino-Otologie 2005 OCT;84(10):725-732.

(261) Kubler AC. Photodynamic therapy. Med Laser Appl 2005 2005/05;20(1):37-45.

(262) Kubler AC, de Carpentier J, Hopper C, Leonard AG, Putnam G. Treatment of squamous cell carcinoma of the lip using Foscan-mediated photodynamic therapy. Int J Oral Maxillofac Surg 2001 /;30(6):504-509.

(263) Kubler AC, Haase T, Staff C, Kahle B, Rheinwald M, Muhling J. Photodynamic therapy of primary nonmelanomatous skin tumours of the head and neck. Lasers Surg Med 1999/;25(1):60-68.

(264) Kubler AC, Reuther T. Photodynamic therapy: Possibilities and limits for head and neck carcinomas. Onkologe 2007 /;13(2):158-164.

(265) Kubler AC, Reuther T, Staff C, Haase T, Flechten-

macher C, Benner A, et al. Clinical effectiveness of m-THPC-PEG in a new xenogenic animal tumor model for human squamous epithelial carcinomas. Mund Kiefer Gesichtschir 2001 /;5(2):105-113.

(266) Kubler AC, Scheer M, Zoller JE. Photodynamic therapy of head and neck cancer. Onkologie 2001/;24(3):230-237.

(267) Kubler AC, Stenzel W, Ruhling M, Meul B, Fischer J-. Experimental Evaluation of Possible Side Effects of Intra-operative Photodynamic Therapy on Rabbit Blood Vessels and Nerves. Lasers Surg Med 2003/;33(4):247-255.

(268) Kudinova NV, Berezov TT. Photodynamic therapy of cancer: Search for ideal photosensitizer. Biochem (Moscow) Suppl Ser B Biomed Chem 2010 /;4(1):95-103.

(269) Kulapaditharom B, Boonkitticharoen V. Photodynamic therapy for residual or recurrent cancer of the nasopharynx. J Med Assoc Thailand 1999/;82(11):1111-1117.

(270) Kulapaditharom B, Boonkitticharoen V. Photodynamic therapy in the treatment of head and neck cancers: A two-year experience. J MED ASSOC THAILAND 1996/;79(4):229-235.

(271) Kuntsche J, Freisleben I, Steiniger F, Fahr A. Temoporfin-loaded liposomes: physicochemical characterization. Eur J Pharm Sci 2010 Jul 11;40(4):305-315.

(272) Kvaal SI, Warloe T. Photodynamic treatment of oral lesions. J Environ Pathol Toxicol Oncol 2007/;26(2):127-133.

(273) Lai J, Cooney M. History of photodynamic therapy. Int Ophthalmol Clin 1999 /;39(4):163-174.

(274) Lai J, Tao Z, Xiao J, Yan Y, Wang X, Wang C, et al. Effect of photodynamic therapy (PDT) on the expression of pro-apoptotic protein bak in nasopharyngeal carcinoma (NPC). Lasers Surg Med 2001/;29(1):27-32.

(275) Lantry LE. Ranibizumab, a mAb against VEGF-A for the potential treatment of age-related macular degeneration and other ocular complications. Curr Opin Mol Ther 2007 /;9(6):592-602.

(276) Latkowski B, Gryczynski M, Murlewska A. Use of sensitizers and photo laser for diagnosis and treatment of malignant tumors. Otolaryngol Pol 1995 /;49 Suppl 20:205-208.

(277) Laville I, Pigaglio S, Blais J-, Doz F, Loock B, Maillard

P, et al. Photodynamic efficiency of diethylene glycol-linked glycoconjugated porphyrins in human retinoblastoma cells. J Med Chem 2006/04;49(8):2558-2567.

(278) Lee J, Moon C. Current status of experimental therapeutics for head and neck cancer. Exp Biol Med 2011 /;236(4):375-389.

(279) Leunig A, Betz CS, Mehlmann M, Stepp H, Arbogast S, Grevers G, et al. Detection of squamous cell carcinoma of the oral cavity by imaging 5- aminolevulinic acid-induced protoporphyrin IX fluorescence. Laryngoscope 2000 /;110(1):78-83.

(280) Leunig A, Mehlmann M, Betz C, Stepp H, Arbogast S, Grevers G, et al. Fluorescence staining of oral cancer using a topical application of 5-aminolevulinic acid: Fluorescence microscopic studies. J Photochem Photobiol B Biol 2001 2001/;60(1):44-49.

(281) Leunig A, Rick K, Stepp H, Goetz A, Baumgartner R, Feyh J. Fluorescence photodetection of neoplastic lesions in the oral cavity following topical application of 5-aminolevulinic acid. LARYNGO- RHINO- OTOL 1996/;75(8):459-464.

(282) Leunig A, Rick K, Stepp H, Gutmann R, Alwin G, Baumgartner R, et al. Fluorescence imaging and spectroscopy of 5-aminolevulinic acid induced protoporphyrin IX for the dectection of neoplastic lesions in the oral cavity. Am J Surg 1996/;172(6):674-677.

(283) Li B, Chen Z, Liu L, Huang Z, Huang Z, Xie S. Differences in sensitivity to HMME-mediated photodynamic therapy between EBV+ C666-1 and EBV- CNE2 cells. Photodiagn Photodyn Ther 2010 /;7(3):204-209.

(284) Li JH. Hematoporphyrin derivatives and laser photodynamic reactions in the diagnosis and treatment of malignant tumors. Zhonghua Yi Xue Za Zhi 1986 /;66(7):388; 391, 446.

(285) Li KM, Sun X, Koon HK, Leung WN, Fung MC, Wong RNS, et al. Apoptosis and expression of cytokines triggered by pyropheophorbide-a methyl ester-mediated photodynamic therapy in nasopharyngeal carcinoma cells. Photodiagn Photodyn Ther 2006 /;3(4):247-258.

(286) Li L-, Luo R-, Liao W-, Zhang M-, Luo Y-, Miao J-. Clinical study of Photofrin photodynamic therapy for the treatment of relapse nasopharyngeal carcinoma. Photodiagn Photodyn Ther 2006 /;3(4):266-271.

(287) Li W-. Nanotechology-based strategies to enhance the efficacy of photodynamic therapy for cancers. Curr Drug Metab 2009 /;10(8):851-860.

(288) Lim H-, Oh C-. Effect of high fluence light emitting diode mediated photodynamic therapy with Photofrin II on high-grade solid tumor model. Photodiagn Photodyn Ther 2011 /;8(2):185.

(289) Lippert BM, Teymoortash A, Kuilkens C, Folz BJ, Werner JA. Photodynamic effects of anthracyclin derivatives on squamous cell carcinoma cell lines of the head and neck. Lasers Surg Med 2004 2004/;34(5):391-397.

(290) Liu LHS, Ni C. Hematoporphyrin phototherapy for experimental intraocular malignant melanoma. Arch Ophthalmol 1983/;101(6):901-903.

(291) Liu W, Zhang Y, Xu G, Qian J, Jiang C, Li L. Optical coherence tomography for evaluation of photodynamic therapy in symptomatic circumscribed choroidal hemangioma. Retina 2011 /;31(2):336-343.

(292) Loew K, Knobloch T, Wagner S, Wiehe A, Engel A, Langer K, et al. Comparison of intracellular accumulation and cytotoxicity of free mTHPC and mTHPC-loaded PLGA nanoparticles in human colon carcinoma cells. Nanotechnology 2011 MAY 17;22(24):245102.

(293) Lofgren L. Lasersurgery and photodynamic therapy. Acta Oto-Laryngol Suppl 1988/;106(449):51-52.

(294) Lofgren LA, Hallgren S, Nilsson E, Westerborn A, Nilsson C, Reizenstein J. Photodynamic therapy for recurrent nasopharyngeal cancer. ARCH OTOLARYNGOL HEAD NECK SURG 1995/;121(9):997-1002.

(295) Lofgren LA, Ronn AM, Abramson AL, Shikowitz MJ, Nouri M, Lee CJ, et al. Photodynamic therapy using m-tetra(hydroxyphenyl) chlorin. An animal model. Arch Otolaryngol Head Neck Surg 1994 Dec;120(12):1355-1362.

(296) Lorenz KJ, Maier H. Photodynamic therapy with meta-tetrahydroxyphenylchlorin (Foscan) in the management of squamous cell carcinoma of the head and neck: experience with 35 patients. Eur Arch Otorhinolaryngol 2009 Dec;266(12):1937-1944.

(297) Lorenz KJ, Maier H. Squamous cell carcinoma of the head and neck. Photodynamic therapy with Foscan. HNO 2008 /;56(4):402-409.

(298) Lou P-, Jager HR, Jones L, Theodossy T, Bown SG, Hopper C. Interstitial photodynamic therapy as salvage treatment for recurrent head and neck cancer. Br J Cancer 2004/08;91(3):441-446.

(299) Lou P-, Jones L, Hopper C. Clinical outcomes of photodynamic therapy for head-and-neck cancer. Technol Cancer Res Treat 2003 /;2(4):311-317.

(300) Loumlw K, Knobloch T, Wagner S, Wiehe A, Engel A, Langer K, et al. Comparison of Intracellular Accumulation and Cytotoxicity of free mTHPC and mTHPC-loaded PLGA nanoparticles in human colon carcinoma cells. Nanotechnology 17 17 June 2011;22(24):245102 (12 pp.);

(301) Lovat LB, Jamieson NF, Novelli MR, Mosse CA, Selvasekar C, Mackenzie GD, et al. Photodynamic therapy with m-tetrahydroxyphenyl chlorin for high-grade dysplasia and early cancer in Barrett's columnar lined esophagus. Gastrointest Endosc 2005 Oct;62(4):617-623.

(302) Lu YG, Wu JJ, Lei X, Zhu TY, He Y, Chen L, et al. Treatment of oral florid papillomatosis with systemic administration of photocarcinorin: an effective photodynamic therapy. Photomed Laser Surg 2010 /;28(6):831-833.

(303) Lucroy MD. Squamous cell carcinoma of dogs and cats: an ideal test system for human head and neck PDT protocols. Proc SPIE - Int Soc Opt Eng (USA) 2006;6078(1):519; 519-525

(304) Lucroy MD. Photodynamic therapy for companion animals with cancer. Vet Clin North Am Small Anim Pract 2002/;32(3):693-702.

(305) Lupu M, Thomas CD, Maillard P, Loock B, Chauvin B, Aerts I, et al. 23Na MRI longitudinal follow-up of PDT in a xenograft model of human retinoblastoma. Photodiagnosis Photodyn Ther 2009 /;6(3-4):214-220.

(306) Lutty GA, Fortune M, Hochheimer F. Improving the efficiency of hematoporphyrin phototherapy of ocular tumors. Photochem Photobiol 1987 /;46(3):383-392.

(307) Ma G, Ikeda H, Inokuchi T, Sano K. Effect of photodynamic therapy using 5-aminolevulinic acid on 4- nitroquinoline-1-oxide-induced premalignant and malignant lesions of mouse tongue. Oral Oncol 1999 /;35(1):120-124.

(308) Ma H-, Yang X-, Liu J-, Niu D-, Zhang F-, Zhao S-. Effect of 5-aminolevulinic acid mediated photodynamic therapy on CNE2 and CNE2/DDP in vitro. Chin J Cancer Prev Treat 2008 /;15(22):1702-1705.

(309) Maillard P, Lupu M, Thomas CD, Mispelter J. Towards a new treatment of retinoblastoma? Ann Pharm Fr 2010 /;68(3):195-202.

(310) Maillard P, Loock B, Grierson DS, Laville I, Blais J, Doz F, et al. In vitro phototoxicity of glycoconjugated porphyrins and chlorins in colorectal adenocarcinoma (HT29) and retinoblastoma (Y79) cell lines. Photodiagn Photodyn Ther 2007 /;4(4):261-268.

(311) Mak N-, Li K-, Leung W-, Wong RN-, Huang DP, Lung

ML, et al. Involvement of both endoplasmic reticulum and mitochondria in photokilling of nasopharyngeal carcinoma cells by the photosensitizer Zn-BC-AM. Biochem Pharmacol 2004/12;68(12):2387-2396.

(312) Makky A, Michel JP, Ballut S, Kasselouri A, Maillard P, Rosilio V. Effect of cholesterol and sugar on the penetration of glycodendrimeric phenylporphyrins into biomimetic models of retinoblastoma cells membranes. Langmuir 2010/07;26(13):11145-11156.

(313) Mallia RJ, Subhash N, Mathews A, Kumar R, Thomas SS, Sebastian P, et al. Clinical grading of oral mucosa by curve-fitting of corrected autofluorescence using diffuse reflectance spectra. Head Neck 2010 /;32(6):763-779.

(314) Mallia RJ, Subhash N, Sebastian P, Kumar R, Thomas SS, Mathews A, et al. In vivo temporal evolution of ALA-induced normalized fluorescence at different anatomical locations of oral cavity: Application to improve cancer diagnostic contrast and potential. Photodiagn Photodyn Ther 2010 /;7(3):162-175.

(315) Mang T, Kost J, Sullivan M, Wilson BC. Autofluorescence and Photofrin-induced fluorescence imaging and spectroscopy in an animal model of oral cancer. Photodiagn Photodyn Ther 2006/09;3(3):168-176.

(316) Mang TS. Dosimetric concepts for PDT. Photodiagn Photodyn Ther 2008 /;5(3):217-223.

(317) Mang TS. Lasers and light sources for PDT: Past, present and future. Photodiagn Photodyn Ther 2004/05;1(1):43-48.

(318) Mang TS, Sullivan M, Cooper M, Loree T, Rigual N. The use of photodynamic therapy using 630 nm laser light and porfimer sodium for the treatment of oral squamous cell carcinoma. Photodiagn Photodyn Ther 2006 /;3(4):272-275.

(319) Marchal S, Fadloun A, Maugain E, D'Hallewin M, Guillemin F, Bezdetnaya L. Necrotic and apoptotic features of cell death in response to Foscan((R)) photosensitization of HT29 monolayer and multicell spheroids. Biochem Pharmacol 2005 APR 15;69(8):1167-1176.

(320) Marchal S, Francois A, Dumas D, Guillemin F, Bezdetnaya L. Relationship between subcellular localisation of Foscan (R) and caspase activation in photosensitised MCF-7 cells. Br J Cancer 2007 MAR 26;96(6):944-951.

(321) Marchiori C, Zorat PL, Canaviglia G. Photodynamic therapy with hematoporphyrin and red light for the treatment of head and neck cancer. OTORINOLARINGO-

LOGIA 1985/;35(4):289-294.

(322) Mason M. Far-reaching benefits. Nurs Stand 2010 05/12;24(36):22-23.

(323) Mauget-Faysse M, Gambrelle J, Quaranta-El Maftouhi M, Moullet I. Photodynamic therapy for choroidal metastasis from lung adenocarcinoma. Acta Ophthalmol Scand 2006 /;84(4):552-554.

(324) Maunoury V, Mordon S, Bulois P, Mirabel X, Hecquet B, Mariette C. Photodynamic therapy for early oesophageal cancer. Dig Liver Dis 2005 /;37(7):491-495.

(325) McBride G. Studies expand potential uses of photodynamic therapy. J Natl Cancer Inst 2002/12;94(23):1740-1742.

(326) McCaughan Jr. JS. Photodynamic therapy of malignant tumors. Prog Clin Biol Res 1988 /;278:163-169.

(327) McCaughan Jr. JS. Photoradiation of malignant tumors presensitized with hematoporphyrin derivative. Prog Clin Biol Res 1984 /;170:805-827.

(328) McCaughan Jr. JS, Guy JT, Hawley P. Hematoporphyrin-derivative and photoradiation therapy of malignant tumors. Lasers Surg Med 1983/;3(3):199-209.

(329) Mennel S, Barbazetto I, Meyer CH, Peter S, Stur M. Ocular photodynamic therapy - Standard applications and new indications (part 2): Review of the literature and personal experience. Ophthalmologica 2007 /;221(5):282-291.

(330) Michels S, Michels R, Simader C, Schmidt-Erfurth U. Verteporfin therapy for choroidal hemangioma: A long-term follow-up. Retina 2005 /;25(6):697-703.

(331) Michels S, Schmidt-Erfurth U. Photodynamic therapy with verteporfin: A new treatment in ophthalmology. Semin Ophthalmol 2001 /;16(4):201-206.

(332) Mioc S, Mycek M-. Selected laser-based therapies in otolaryngology. Otolaryngol Clin North Am 2005 /;38(2):241-254.

(333) Misiuk-Hojlo M, Krzyzanowska-Berkowska P, Hill-Bator A. Therapeutic application of lasers in ophthalmology. Adv Clin Exp Med 2007/;16(6):801-805.

(334) Mitchell DA. Oral Cancer-pertinent papers 2003-2004. A personal view. Br J Oral Maxillofac Surg 2006/12;44(6):558-561.

(335) Mitton D, Ackroyd R. A brief overview of photodynamic therapy in Europe. Photodiagn Photodyn Ther 2008 /;5(2):103-111.

(336) Mlkvy P, Messmann H, Regula J, Conio M, Pauer M, Millson CE, et al. Photodynamic therapy for gastrointestinal tumors using three photosensitizers--ALA induced PPIX, Photofrin and MTHPC. A pilot study. Neoplasma 1998;45(3):157-161.

(337) Moan J, Peng Q. An Outline of the Hundred-Year History of PDT. Anticancer Res 2003 /;23(5 A):3591-3600.

(338) Moghissi K. Annual Conference of BMLA, and the First Meeting of the UK-PDPDT Interest Group, Manchester Museum of Science and Technology, 7-8 June, 2007. Photodiagn Photodyn Ther 2007 /;4(3):221.

(339) Moghissi K, Dixon K, Campbell A. Adeno-carcinoma of the pharyngo-oesophageal junction and cervical oesophagus in a patient with an oesophagus lined entirely by columnar epithelium. Report of a case treated by photodynamic therapy (PDT). Photodiagn Photodyn Ther 2008 /;5(3):224-227.

(340) Molinari A, Bombelli C, Mannino S, Stringaro A, Toccacieli L, Calcabrini A, et al. m-THPC-mediated photodynamic therapy of malignant gliomas: Assessment of a new transfection strategy RID A-2667-2008 RID E-7144-2010. International Journal of Cancer 2007 SEP 1;121(5):1149-1155.

(341) Monnier Ph. , Savary M, Fontolliet Ch. , Wagnieres Chatelain GA, Cornaz P, Depeursinge Ch. , et al. Photodetection and photodynamic therapy of 'early' squamous cell carcinomas of the pharynx, oesophagus and tracheo-bronchial tree. LASERS MED SCI 1990/;5(2):149-168.

(342) Monnier P, Fontolliet C, Wagnieres G, Braichotte D, Van Den Bergh H. Photodetection and phototherapy of early epidermoid carcinomas of the pharynx, the esophagus and bronchi. REV FR GASTRO-ENTEROL 1992/;28(277):103-112.

(343) Monnier P, Fontolliet C, Wagnieres G, Van Den Bergh H. The possibilities and limitations of the endoscopic and photodynamic treatments of early squamous cell cancer of the upper aero-digestive tract, bronchi and eosophagus. ACTA ENDOSC 1991/;21(5):641-653.

(344) Moon SJ, Wirostko WJ. Photodynamic therapy for extrafoveal choroidal neovascularization associated with choroidal nevus. Retina 2006 /;26(4):477-479.

(345) Moon Y-, Park J-, Kim S-, Lee J-, Ahn S-, Yoon J-. Anticancer effect of photodynamic therapy with hexenyl

ester of 5-aminolevulinic acid in oral squamous cell carcinoma. Head Neck 2010 /;32(9):1136-1142.

(346) Morawiec-Bajda A, Niedzwiecka I, Kaczmarczyk D, Peszynski-Drews C. Diagnosing head and neck cancer using the photodynamic method. Proc SPIE - Int Soc Opt Eng (USA) 2007;6598:659804 (3 pp.); 659804(3.)-659804 (3 pp.)659804 (3 pp.).

(347) Morris K. Ray of light for treatment of head and neck cancer. Lancet Oncol 2000 /;1(1):10.

(348) Morton CA, Burden AD. Treatment of multiple scalp basal cell carcinoma by photodynamic therapy. Clin Exp Dermatol 2001/;26(1):33-36.

(349) Nagy EM, Via LD, Ronconi L, Fregona D. Recent advances in PUVA photochemotherapy and PDT for the treatment of cancer. Curr Pharm Des 2010/;16(16):1863-1876.

(350) Naim R. Photodynamic therapy using m-THPC (Foscan (R)). HNO 2008 MAY;56(5):490-492.

(351) Nakagawa H, Matsumiya T, Sakaki H, Imaizumi T, Kubota K, Kusumi A, et al. Expression of vascular endothelial growth factor by photodynamic therapy with mono-l-aspartyl chlorin e6 (NPe6) in oral squamous cell carcinoma. Oral Oncol 2007 /;43(6):544-550.

(352) Nauta JM, Speelman OC, Van Leengoed HLLM, Nikkels PGJ, Roodenburg JLN, Star WM, et al. In vivo photodetection of chemically induced premalignant lesions and squamous cell carcinoma of the rat palatal mucosa. J PHOTOCHEM PHOTOBIOL B BIOL 1997 /;39(2):156-166.

(353) Nauta JM, van Leengoed HL, Star WM, Roodenburg JL, Witjes MJ, Vermey A. Photodynamic therapy of oral cancer. A review of basic mechanisms and clinical applications. Eur J Oral Sci 1996 /;104(2):Pt 1.

(354) Nauta JM, van Leengoed HL, Witjes MJ, Nikkels PG, Star WM, Vermey A, et al. Photofrin-mediated photodynamic therapy of chemically-induced premalignant lesions and squamous cell carcinoma of the palatal mucosa in rats. Int J Oral Maxillofac Surg 1997 /;26(3):223-231.

(355) Nauta JM, Van Leengoed HLLM, Witjes MUH, Roodenburg JLN, Nikkels PGJ, Thomsen SL, et al. Photofrin-mediated photodynamic therapy of rat Palatal Mucosa: Normal tissue effects and light dosimetry. LASERS MED SCI 1996/09;11(3):163-174.

(356) Navarro FP, Bechet D, Delmas T, Couleaud P, Frochot C, Verhille M, et al. Preparation, characteriza-

tion, and cellular studies of photosensitizer-loaded lipid nanoparticles for photodynamic therapy. Proc SPIE - Int Soc Opt Eng (USA) 2011;7886:78860Y (12 pp.); 78860Y(12.)-78860Y (12 pp.)78860Y (12 pp.).

(357) Nhembe F, Jerjes W, Upile T, Hamdoon Z, Vaz F, Hopper C. Subglottic carcinoma treated with surgery and adjuvant photodynamic therapy. Photodiagnosis Photodyn Ther 2010 Dec;7(4):284-287.

(358) Nicolo M, Ghiglione D, Polizzi A, Calabria G. Choroidal hemangioma treated with photodynamic therapy using verteporfin: Report of a case. Eur J Ophthalmol 2003 /;13(7):656-661.

(359) Norum O-, Selbo PK, Weyergang A, Giercksky K-, Berg K. Photochemical internalization (PCI) in cancer therapy: From bench towards bedside medicine. J Photochem Photobiol B Biol 2009/08;96(2):83-92.

(360) Nowak-Sliwinska P, Wagnieres G, Van Den Bergh H, Griffioen AW. Angiostasis-induced vascular normalization can improve photodynamic therapy. Cell Mol Life Sci 2010 /;67(9):1559-1560.

(361) Nyman ES, Hynninen PH. Research advances in the use of tetrapyrrolic photosensitizers for photodynamic therapy. J Photochem Photobiol B Biol 2004/01;73(1-2):1-28.

(362) Nyst HJ, Tan IB, Stewart FA, Balm AJM. Is photodynamic therapy a good alternative to surgery and radiotherapy in the treatment of head and neck cancer? Photodiagn Photodyn Ther 2009 /;6(1):3-11.

(363) Nyst HJ, Van Veen RLP, Tan IB, Peters R, Spaniol S, Robinson DJ, et al. Performance of a dedicated light delivery and dosimetry device for photodynamic therapy of nasopharyngeal carcinoma: Phantom and volunteer experiments. Lasers Surg Med 2007 /;39(8):647-653.

(364) Obana A, Goto Y, Ikoma M. A case of von Hippel-Lindau disease with papillary capillary hemangioma treated by photodynamic therapy. Nippon Ganka Gakkai Zasshi 2004 /;108(4):226-232.

(365) Ofner JG, Bartl B, Konig S, Thumfart WF. Photodynamic therapy in selected cases at the ENT Clinic, Innsbruck: Case reports. J PHOTOCHEM PHOTOBIOL B BIOL 1996 /;36(2):185-187.

(366) Ogasawara T, Miyoshi N, Sano K, Kitagawa Y, Yamada T, Ogawa T, et al. Influence of administration methods on the accumulation of ALA-induced Pp-IX in mouse tongue tumors. Oral Dis 2006 /;12(4):415-419.

(367) Ohnishi Y. Laser photoradiation therapy for intraocular malignant tumors using a hematoporphyrin derivative. FOLIA OPHTHALMOL JPN 1988/;39(5):743-747.

(368) Ohnishi Y, Marukami M, Wakeyama H. Effects of hematoporphyrin derivative and light on Y79 retinoblastoma cells in vitro. Invest Ophthalmol Vis Sci 1990 1990/;31(5):792-797.

(369) Ohnishi Y, Yamana Y, Ishibashi T. Effect of argon laser photoradiation on monkey retina treated with hematoporphyrin derivative. Fluorescein angiographic and light microscopic study. Jpn J Ophthalmol 1987/;31(1):160-170.

(370) Oliveros E, Bottiroli G, Vidoczy T. In this issue. J Photochem Photobiol B Biol 2000/;57(1):vii.

(371) Onizawa K, Okamura N, Saginoya H, Yusa H, Yanagawa T, Yoshida H. Analysis of fluorescence in oral squamous cell carcinoma. Oral Oncol 2002/;38(4):343-348.

(372) O'Reilly Zwald F, Brown M. Skin cancer in solid organ transplant recipients: Advances in therapy and management: Part II. Management of skin cancer in solid organ transplant recipients. J Am Acad Dermatol 2011 /;65(2):253-261.

(373) Orvis AK, Wesson SK, Breza Jr. TS, Church AA, Mitchell CL, Watkins SW. Mycophenolate mofetil in dermatology. J Am Acad Dermatol 2009 /;60(2):183-199.

(374) Osaki T, Takagi S, Hoshino Y, Okumura M, Kadosawa T, Fujinaga T. Efficacy of antivascular photodynamic therapy using benzoporphyrin derivative monoacid ring A (BPD-MA) in 14 dogs with oral and nasal tumors. J Vet Med Sci 2009 /;71(2):125-132.

(375) Osher J, Jerjes W, Upile T, Hamdoon Z, Morley S, Hopper C. Adenoid cystic carcinoma of the tongue base treated with ultrasound-guided interstitial photodynamic therapy: A case study. Photodiagn Photodyn Ther 2011 /;8(1):68-71.

(376) Osman SA, Aylin Y, Gul A, Celikel H. Photodynamic treatment of a secondary vasoproliferative tumour associated with sector retinitis pigmentosa and Usher syndrome type I. Clin Exp Ophthalmol 2007 /;35(2):191-193.

(377) Ota J, Giuliano EA, Cohn LA, Lewis MR, Moore CP. Local photodynamic therapy for equine squamous cell carcinoma: Evaluation of a novel treatment method in a murine model. Vet J 2008 /;176(2):170-176.

(378) Palumbo G. Photodynamic therapy and cancer: A brief sightseeing tour. Expert Opin Drug Deliv 2007

/;4(2):131-148.

(379) Pass HI. Photodynamic therapy in oncology: Mechanisms and clinical use. J Natl Cancer Inst 1993/;85(6):443-456.

(380) Paszko E, Ehrhardt C, Senge MO, Kelleher DP, Reynolds JV. Nanodrug applications in photodynamic therapy. Photodiagn Photodyn Ther 2011 /;8(1):14-29.

(381) Pathak I, Davis NL, Hsiang YN, Quenville NF, Palcic B. Detection of squamous neoplasia by fluorescence imaging comparing porfimer sodium fluorescence to tissue autofluorescence in the hamster cheek-pouch model. Am J Surg 1995/;170(5):423-426.

(382) Pathania D, Millard M, Neamati N. Opportunities in discovery and delivery of anticancer drugs targeting mitochondria and cancer cell metabolism. Adv Drug Deliv Rev 2009/11;61(14):1250-1275.

(383) Patrice T, Olivier D, Bourre L. PDT in clinics: Indications, results, and markets. J Environ Pathol Toxicol Oncol 2006/;25(1-2):467-485.

(384) Pe MB, Ikeda H, Inokuchi T. Tumour destruction and proliferation kinetics following periodic, low power light, haematoporphyrin oligomers mediated photodynamic therapy in the mouse tongue. EUR J CANCER PART B ORAL ONCOL 1994/;30(3):174-178.

(385) Peng Q. Editorial: Photodynamic therapy and detection. J Environ Pathol Toxicol Oncol 2006/;25(1-2):1-5.

(386) Perria C, Teatini G, Tanda F, Bozzo C, Casu G, Masala W, et al. Photodynamic treatment of cholesteatoma of the ear induced experimentally in rabbits: Preliminary report. LASERS MED SCI 1989/;4(2):111-113.

(387) Pervaiz S, Olivo M. Art and science of photodynamic therapy. Clin Exp Pharmacol Physiol 2006 /;33(5-6):551-556.

(388) Phillips AMR, Browne BH, Allan D, Szczesny PJ, Lee WR, Foulds WS. Haematoporphyrin photosensitisation treatment of experimental choroidal melanoma. Eye 1987/;1(6):680-685.

(389) Poate TW, Dilkes MG, Kenyon GS. Use of photodynamic therapy for the treatment of squamous cell carcinoma of the soft palate. Br J Oral Maxillofac Surg 1996 Feb;34(1):66-68.

(390) Poon C-, Chan P-, Man C, Jiang F-, Wong RNS, Mak N-, et al. An amphiphilic ruthenium(II)-polypyridyl appended porphyrin as potential bifunctional two-photon tumor-imaging and photodynamic therapeutic agent. J

Inorg Biochem 2010 /;104(1):62-70.

(391) Porrini G, Giovannini A, Amato G, Ioni A, Pantanetti M. Photodynamic therapy of circumscribed choroidal hemangioma. Ophthalmology 2003/04;110(4):674-680.

(392) Postiglione I, Chiaviello A, Palumbo G. Enhancing photodynamyc therapy efficacy by combination therapy: Dated, current and oncoming strategies. Cancers 2011 /;3(2):2597-2629.

(393) Prajapati PM, Shah Y, Sen DJ. Photodynamic therapy in cancer treatment. Pharma Times 2010 /;42(5):11-15.

(394) Prince S, Bailey BMW. Squamous carcinoma of the tongue: Review. Br J Oral Maxillofac Surg 1999 /;37(3):164-174.

(395) Qiang Y-, Zhang X-, Li J, Huang Z. Photodynamic therapy for malignant and non-malignant diseases: Clinical investigation and application. Chin Med J 2006/05;119(10):845-857.

(396) Quon H, Finlay J, Cengel K, Zhu T, O'Malley B, Weinstein G. Transoral robotic photodynamic therapy for the oropharynx. Photodiagn Photodyn Ther 2011 /;8(1):64-67.

(397) Quon H, Grossman CE, Finlay JC, Zhu TC, Clemmens CS, Malloy KM, et al. Photodynamic therapy in the management of pre-malignant head and neck mucosal dysplasia and microinvasive carcinoma. Photodiagn Photodyn Ther 2011 /;8(2):75-85.

(398) Radu A, Conde R, Fontolliet C, Wagnieres G, Van den Bergh H, Monnier P. Mucosal ablation with photodynamic therapy in the esophagus: optimization of light dosimetry in the sheep model. Gastrointest Endosc 2003 Jun;57(7):897-905.

(399) Radu A, Grosjean P, Fontolliet C, Wagnieres G, Woodtli A, Bergh HV, et al. Photodynamic therapy for 101 early cancers of the upper aerodigestive tract, the esophagus, and the bronchi: a single-institution experience. Diagn Ther Endosc 1999;5(3):145-154.

(400) Radu A, Wagnieres G, van den Bergh H, Monnier P. Photodynamic therapy of early squamous cell cancers of the esophagus. Gastrointest Endosc Clin N Am 2000 Jul;10(3):439-460.

(401) Radu A, Zellweger M, Grosjean P, Monnier P. Pulse oximeter as a cause of skin burn during photodynamic therapy. Endoscopy 1999 Nov;31(9):831-833.

(402) Rai P, Mallidi S, Zheng X, Rahmanzadeh R, Mir

Y, Elrington S, et al. Development and applications of photo-triggered theranostic agents. Adv Drug Deliv Rev 2010/08;62(11):1094-1124.

(403) Ramasubramanian A, Shields CL, Sinha N, Shields JA. Ocular Surface Squamous Neoplasia After Corneal Graft. Am J Ophthalmol 2010 /;149(1):62; 65.e1.

(404) Rand Simpson E, Wilson BC, Corriveau C, Murphy J. Thermal damage and haematoporphyrin-derivative-sensitized photochemical damage in laser irradiation of rabbit retina. LASERS MED SCI 1987/;2(1):33-40.

(405) Rauschning W, Tan I, Dolivet G. Photodynamic therapy (PDT) with mTHPC in the palliation of advanced head and neck cancer in patients who have failed prior therapies and are unsuitable for radiotherapy, surgery or systemic chemotherapy. Journal of Clinical Oncology 2004 JUL 15;22(14):512S-512S.

(406) Reeves KJ, Reed MWR, Brown NJ. Is nitric oxide important in photodynamic therapy? J Photochem Photobiol B Biol 2009/06;95(3):141-147.

(407) Retel VP, Hummel MJM, van Harten WH. Review on early technology assessments of nanotechnologies in oncology. Mol Oncol 2009 /;3(5-6):394-401.

(408) Reuther T, Kubler AC, Zillmann U, Flechtenmacher C, Sinn H. Comparison of the in vivo efficiency of photofrin II-, mTHPC-, mTHPC-PEG- and mTHPCnPEG-mediated PDT in a human xenografted head and neck carcinoma. Lasers Surg Med 2001/;29(4):314-322.

(409) Rigual NR, Thankappan K, Cooper M, Sullivan MA, Dougherty T, Popat SR, et al. Photodynamic therapy for head and neck dysplasia and cancer. Arch Otolaryngol Head Neck Surg 2009 /;135(8):784-788.

(410) Ris H-, Li Q, Krueger T, Lim CK, Reynolds B, Althaus U, et al. Photosensitizing effects of m-tetrahydroxyphenylchlorin on human tumor xenografts: Correlation with sensitizer uptake, tumor doubling time and tumor histology. Int J Cancer 1998/06;76(6):872-874.

(411) Rivellese MJ, Baumal CR. Photodynamic therapy of eye diseases. Ophthalmic Surg Lasers 1999 /;30(8):653-661.

(412) Roberts JE, Roy D, Dillon J. The photosensitized oxidation of the calf lens main intrinsic protein (MP26) with hematoporphyrin. Curr Eye Res 1985/;4(3):181-185.

(413) Robinson DJ, Karakullukccedilu MB, Kruijt B, Kanick SC, van Veen RPL, Amelink A, et al. Optical Spectroscopy to Guide Photodynamic Therapy of Head and Neck Tumors. IEEE J Sel Top Quantum Electron (USA)

2010 July-Aug. 2010;16(4):854; 854-862862; 862.

(414) Ronn AM, Nouri M, Lofgren LA, Steinberg BM, Westerborn A, Windahl T, et al. Human tissue levels and plasma pharmacokinetics of Temoporfin (Foscan(registered trademark), mTHPC). LASERS MED SCI 1996/12;11(4):267-272.

(415) Rudolf M, Michels S, Schlotzer-Schrehardt U, Schmidt-Erfurth U. Expression of angiogenic factors by photodynamic therapy. Klin Monatsbl Augenheilkd 2004 /;221(12):1026-1032.

(416) Ruiz-Galindo E, Arenas-Huertero F, Ramon-Gallegos E. Expression of genes involved in heme biosynthesis in the human retinoblastoma cell lines WERI-Rb-1 and Y79: Implications for photodynamic therapy. J Exp Clin Cancer Res 2007 /;26(2):195-200.

(417) Sanchez CG, Caballero Chavez YV, Plazola S. Photodynamic therapy for palpebral and conjunctival proliferative vascular tumors: Clinical case report. Orbit 2009 /;28(6):420-421.

(418) Sardella A, Carrassi A, Tarozzi M, Lodi G. Bisphosphonate-related osteonecrosis of the jaws associated with photodynamic therapy. J Oral Maxillofac Surg 2011 Oct;69(10):e314-6.

(419) Savary JF, Grosjean P, Monnier P, Fontolliet C, Wagnieres G, Braichotte D, et al. Photodynamic therapy of early squamous cell carcinomas of the esophagus: a review of 31 cases. Endoscopy 1998 Mar;30(3):258-265.

(420) Savary J-, Monnier P, Fontolliet C, Mizeret J, Wagnieres G, Braichotte D, et al. Photodynamic therapy for early squamous cell carcinomas of the esophagus, bronchi, and mouth with m-tetra(hydroxyphenyl) chlorin. ARCH OTOLARYNGOL HEAD NECK SURG 1997 /;123(2):162-168.

(421) Saxton RE, Paiva MB, Lufkin RB, Castro DJ. Laser photochemotherapy: A less invasive approach for treatment of cancer. Semin Surg Oncol 1995/;11(4):283-289.

(422) Scheglmann D, Fahr A, Grafe S, Neuberger W, Albrecht V. Temoporfin and its liposomal formulations Foslip and Fospeg - Properties and behaviour. Photodiagn Photodyn Ther 2011 /;8(2):195.

(423) Schlotzer-Schrehardt U, Viestenz A, Naumann GOH, Laqua H, Michels S, Schmidt-Erfurth U. Dose-related structural effects of photodynamic therapy on choroidal and retinal structures of human eyes. Graefe's Arch Clin Exp Ophthalmol 2002/;240(9):748-757.

(424) Schmidt-Erfurth U, Bauman W, Gragoudas E, Flotte TJ, Michaud NA, Birngruber R, et al. Photodynamic therapy of experimental choroidal melanoma using lipoprotein- delivered benzoporphyrin. Ophthalmology 1994/;101(1):89-99.

(425) Schmidt-Erfurth U, Diddens H, Birngruber R, Hasan T. Photodynamic targeting of human retinoblastoma cells using covalent low-density lipoprotein conjugates. Br J Cancer 1997/;75(1):54-61.

(426) Schmidt-Erfurth U, Flotte TJ, Gragoudas ES, Schomacker K, Birngruber R, Hasan T. Benzoporphyrin-lipoprotein-mediated photodestruction of intraocular tumors. Exp Eye Res 1996 /;62(1):1-10.

(427) Schmidt-Erfurth U, Kiss C, Sacu S. The role of choroidal hypoperfusion associated with photodynamic therapy in neovascular age-related macular degeneration and the consequences for combination strategies. Prog Retinal Eye Res 2009 /;28(2):145-154.

(428) Schmidt-Erfurth UM, Kusserow C, Barbazetto IA, Laqua H, Shields CL. Benefits and complications of photodynamic therapy of papillary capillary hemangiomas. Evid -Based Eye Care 003 2003/01;4(1):36-37.

(429) Schmidt-Erfurth UM, Michels S, Kusserow C, Shields CL. Photodynamic therapy for symptomatic choroidal hemangioma. Evid -Based Eye Care 2003/04;4(2):72-73.

(430) Schuitmaker JJ, Van Best JA, Van Delft JL, Dubbelman TMAR, Oosterhuis JA, De Wolff-Rouendaal D. Bacteriochlorin a, a new photosensitizer in photodynamic therapy. In vivo results. Invest Ophthalmol Vis Sci 1990/;31(8):1444-1450.

(431) Schuitmaker JJ, Vrensen GFJM, Van Delft JL, De Wolff-Rouendaal D, Dubbelman TMAR, De Wolf A. Morphologic effects of bacteriochlorin a and light in vivo on intraocular melanoma. Invest Ophthalmol Vis Sci 1991/;32(10):2683-2688.

(432) Schuller DE, McCaughan Jr. JS, Rock RP. Photodynamic therapy in head and neck cancer. Arch Otolaryngol 1985/;111(6):351-355.

(433) Schweitzer VG. PHOTOFRIN-mediated photodynamic therapy for treatment of early stage oral cavity and laryngeal malignancies. Lasers Surg Med 2001/;29(4):305-313.

(434) Schweitzer VG. Photodynamic therapy for treatment of head and neck cancer. Otolaryngol Head Neck

Surg 1990/;102(3):225-232.

(435) Schweitzer VG, Somers ML. PHOTOFRIN-mediated photodynamic therapy for treatment of early stage (Tis-T2N0M0) SqCCa of oral cavity and oropharynx. Lasers Surg Med 2010 /;42(1):1-8.

(436) Sears KS, Rundle PR, Mudhar HS, Rennie IG. The effects of photodynamic therapy on conjunctival in situ squamous cell carcinoma - A review of the histopathology. Br J Ophthalmol 2008 /;92(5):716-717.

(437) Selvasekar CR, Birbeck N, McMillan T, Wainwright M, Walker SJ. Review article: Photodynamic therapy and the alimentary tract. Aliment Pharmacol Ther 2001/;15(7):899-915.

(438) Separovic D, Bielawski J, Pierce JS, Merchant S, Tarca AL, Bhatti G, et al. Enhanced tumor cures after Foscan photodynamic therapy combined with the ceramide analog LCL29. Evidence from mouse squamous cell carcinomas for sphingolipids as biomarkers of treatment response. Int J Oncol 2011 Feb;38(2):521-527.

(439) Sery TW, Shields JA, Augsburger JJ, Shah HG. Photodynamic therapy of human ocular cancer. Ophthalmic Surg 1987/;18(6):413-418.

(440) Sharma S, Jajoo A, Dube A. 5-Aminolevulinic acid-induced protoporphyrin-IX accumulation and associated phototoxicity in macrophages and oral cancer cell lines. J Photochem Photobiol B Biol 2007/09;88(2-3):156-162.

(441) Sharwani A, Jerjes W, Hopper C, Lewis MP, El-Maaytah M, Khalil HSM, et al. Photodynamic therapy down-regulates the invasion promoting factors in human oral cancer. Arch Oral Biol 2006 /;51(12):1104-1111.

(442) Sheikh O, Lee Y, Sultan A, Vaz F, Hopper C. Endoscope guided interstitial photodynamic therapy for treatment of recurrent nasopharyngeal carcinoma. Photodiagn Photodyn Ther 2011 /;8(2):167.

(443) Sheleg S, Zhavrid E, Khodina T, Kochubeev G, Istomin Y, Chalov V, et al. Photodynamic therapy with chlorin e(6) for skin metastases of melanoma. Photodermatology Photoimmunology & Photomedicine 2004 FEB;20(1):21-26.

(444) Shetler AC. Photodynamic therapy may be alternative to head and neck surgery... this article is based on a presentation at the 42nd annual conference of AORN in March 1995. Todays Surg Nurse 1996;18(4):19-22.

(445) Shields CL, Materin MA, Mehta S, Foxman BT, Shields JA. Regression of extrafoveal choroidal osteoma

following photodynamic therapy. Arch Ophthalmol 2008 /;126(1):135-137.

(446) Shields CL, Shields JA. Ocular melanoma: relatively rare but requiring respect. Clin Dermatol 2009 /;27(1):122-133.

(447) Shikowitz MJ, Abramson AL, Steinberg BM, DeVoti J, Bonagura VR, Mullooly V, et al. Clinical trial of photodynamic therapy with meso-tetra (hydroxyphenyl) chlorin for respiratory papillomatosis. Arch Otolaryngol Head Neck Surg 2005 Feb;131(2):99-105.

(448) Sieron A, Namyslowski G, Misiolek M, Adamek M, Kawczyk-Krupka A. Photodynamic therapy of premalignant lesions and local recurrence of laryngeal and hypopharyngeal cancers. Eur Arch Oto-Rhino-Laryngol 2001/;258(7):349-352.

(449) Simoes A, Eduardo FP, Luiz AC, Campos L, Pedro Henrique RN, Cristofaro M, et al. Laser phototherapy as topical prophylaxis against head and neck cancer radiotherapy-induced oral mucositis: comparison between low and high/low power lasers. Lasers Surg Med April 2009;41(4):264; 264-270270; 270.

(450) Singh AD, Kaiser PK, Sears JE. Choroidal hemangioma. Ophthalmol Clin North Am 2005 /;18(1):151-161.

(451) Smith RP, Hahn SM, Johnstone PAS. Photodynamic therapy. Curr Probl Cancer 2002/03;26(2):61-108.

(452) Song JM, Jagannathan R, Stokes DL, Kasili PM, Panjehpour M, Phan MN, et al. Development of a Fluorescence Detection System Using Optical Parametric Oscillator (OPO) Laser Excitation for In Vivo Diagnosis. Technol Cancer Res Treat 2003 /;2(6):515-523.

(453) Songca SP, Mbatha B. Solubilization of meso-tetraphenylporphyrin photosensitizers by substitution with fluorine and with 2,3-dihydroxy-1-propyloxy groups. J Pharm Pharmacol 2000/;52(11):1361-1367.

(454) Soucek P, Cihelkova I. Primary treatment of choroidal amelanotic melanoma with photodynamic therapy - Comment [1]. Clin Exp Ophthalmol 2006/09;34(7):721.

(455) Soucek P, Cihelkova I. Photodynamic therapy with verteporfin in subfoveal amelanotic choroidal melanoma (A controlled case). Neuroendocrinol Lett 2006 /;27(1-2):145-148.

(456) Soucek P, Souckova I. Photodynamic therapy with verteporfin: From neovascularization to hemangioma. Ceska Slov Oftalmol 2010 /;66(3):146-151.

(457) Soukos NS, Hamblin MR, Keel S, Fabian RL,

Deutsch TF, Hasan T. Epidermal growth factor receptor-targeted immunophotodiagnosis and photoimmunotherapy of oral precancer in vivo. Cancer Res 2001/06;61(11):4490-4496.

(458) Spaide RF, Goldbaum M, Wong DWK, Tang KC, Iida T. Serous detachment of the retina. Retina 2003 /;23(6):820-846.

(459) Spangler C, Starkey J, Dubinina G, Rebane A, Drobizhev M, Fahlstrom C. Optimization of a two-photon-activated porphyrin PDT agent incorporating imaging and targeting moieties for the treatment of head and neck cancers. Photodiagn Photodyn Ther 2011 /;8(2):195-196.

(460) Spinelli P, Dal Fante M. Photodynamic therapy of solid tumors. Semin Hematol 1992/;29(2):142-154.

(461) Sroka R, Schaffer M, Fuchs C, Pongratz T, Schrader-Reichard U, Busch M, et al. Effects on the mitosis of normal and tumor cells induced by light treatment of different wavelengths. Lasers Surg Med 1999/;25(3):263-271.

(462) Stanescu D, Wattenberg S, Cohen SY. Photodynamic therapy for choroidal neovascularization secondary to choroidal nevus. Am J Ophthalmol 2003 2003/09;136(3):575-576.

(463) Steele Keller G, Razum NJ, Doiron DR. Photodynamic therapy for nonmelanoma skin cancer. Facial Plast Surg 1989/;6(3):180-184.

(464) Stefansson E, Zetterstrom C, Ehlers N, Kiilgaard JF, la Cour M, Sigurdsson H, et al. Nordic research in ophthalmology. Acta Ophthalmol Scand 2003 /;81(6):556-566.

(465) Stell A. Photodynamic therapy in cats [2]. Vet Rec 1998/10;143(18):512.

(466) Stephan H, Boeloeni R, Eggert A, Bornfeld N, Schueler A. Photodynamic therapy in retinoblastoma: Effects of verteporfin on retinoblastoma cell lines. Invest Ophthalmol Vis Sci 2008 /;49(7):3158-3163.

(467) Sterenborg HJCM, Robinson DJ. Photodynamic therapy: Clinical applications. EJHP Pract 2010/;16(5):56-58.

(468) Stewart F, Baas P, Star W. What does photodynamic therapy have to offer radiation oncologists (or their cancer patients)? Radiother Oncol 1998 /;48(3):233-248.

(469) Stockert JC, Canete M, Juarranz A, Villanueva A, Horobin RW, Borrell JI, et al. Porphycenes: Facts and

prospects in photodynamic therapy of cancer. Curr Med Chem 2007 /;14(9):997-1026.

(470) Sturgis EM, Miller RH. Second primary malignancies in the head and neck cancer patient. Ann Otol Rhinol Laryngol 1995/;104(12):946-954.

(471) Sturgis EM, Spitz MR, Wei Q. DNA repair and genomic instability in tobacco induced malignancies of the lung and upper aerodigestive tract. J Environ Sci Health Part C Environ Carcinog Ecotoxicol Rev 1998/;16(1):1-30.

(472) Suh SC, Jin SY, Bae SH, Kim CG, Kim JW. Retinal capillary hemangioma treated with verteporfin photodynamic therapy and intravitreal triamcinolone acetonide. Korean J Ophthalmol 2007 /;21(3):178-184.

(473) Suhr MAA, Hopper C, Jones L, George JGD, Bown SG, MacRobert AJ. Optical biopsy systems for the diagnosis and monitoring of superficial cancer and precancer. Int J Oral Maxillofac Surg 2000 /;29(6):453-457.

(474) Sun JK, Miller JW. Medical treatment of choroidal neovascularization secondary to age-related macular degeneration. Int Ophthalmol Clin 2005 /;45(4):115-132.

(475) Sun Z. Photodynamic therapy of nasopharyngeal carcinoma by argon or dye laser. An analysis of 137 cases. CHIN J ONCOL 1992/;14(4):290-292.

(476) Sun Z. Hematoporphyrin derivative (HPD) plus laser photodynamic therapy for nasopharyngeal carcinoma - Analysis of 57 cases. CHIN J ONCOL 1990/;12(2):120-122.

(477) Sunar U, Rohrbach D, Rigual N, Tracy E, Keymel K, Cooper MT, et al. Monitoring photobleaching and hemodynamic responses to HPPH-mediated photodynamic therapy of head and neck cancer: a case report. Opt Express (USA) 5 5 July 2010;18(14):14969; 14969-14978

(478) Sunar U, Rohrbach D, Rigual N, Tracy E, Keymel K, Cooper MT, et al. Monitoring photobleaching and hemodynamic responses to HPPH-mediated photodynamic therapy of head and neck cancer: a case report. Opt Express 2010 /;18(14):14969-14978.

(479) Svanberg K, Klinteberg CAF, Nilsson A, Wang I, Andersson-Engels S, Svanberg S. Laser-based spectroscopic methods in tissue characterization. Ann New York Acad Sci 1998/02;838:123-129.

(480) Swinson B, Jerjes W, El-Maaytah M, Norris P, Hopper C. Optical techniques in diagnosis of head and neck malignancy. Oral Oncol 2006 /;42(3):221-228.

(481) Tammilmani V, Yee KKL, Heng PWS, Soo KC, Olivo M. An evaluation of exogenous application of protoporphyrin IX and its dimethyl ester as a photodynamic diagnostic agent in poorly differentiated human nasopharyngeal carcinoma. Photochem Photobiol 2004 /;80(3):596-601.

(482) Tan IB, Dolivet G, Ceruse P, Poorten VV, Roest G, Rauschning W. Temoporfin-mediated photodynamic therapy in patients with advanced, incurable head and neck cancer: A multicenter study. Head Neck 2010 /;32(12):1597-1604.

(483) Tan, Balm, Hilgers, Timmers, Oppelaar, Stewart. First experience with Foscan[sup ®] mediated photodynamic therapy for head and neck tumours. Clinical Otolaryngology & Allied Sciences 1998 08;23(4):376.

(484) Tanaka H, Hashimoto K, Yamada I, Masumoto K, Ohsawa T, Murai M, et al. Interstitial photodynamic therapy with rotating and reciprocating optical fibers: Clinical trial of three patients with squamous cell carcinoma of the tongue. Cancer 2001/05;91(9):1791-1796.

(485) Tandon YK, Yang MF, Baron ED. Role of photodynamic therapy in psoriasis: A brief review. Photodermatol Photoimmunol Photomed 2008/;24(5):222-230.

(486) Taquet J-, Frochot C, Manneville V, Barberi-Heyob M. Phthalocyanines covalently bound to biomolecules for a targeted photodynamic therapy. Curr Med Chem 2007 /;14(15):1673-1687.

(487) Teatini GP, Perria C, Iora G, Meloni F, Tanda F. Hematoporphyrin uptake by experimentally induced cholesteatomas in an animal model. ARCH OTO-RHINO-LARYNGOL 1989/;246(1):53-55.

(488) Theodossy T, Chapman M, Mitchell V, Hopper C. Anaesthetic considerations for patients receiving photodynamic therapy in head and neck surgery. Eur J Anaesthesiol 2007 /;24(3):225-229.

(489) Toll A, Parera ME, Velez M, Pujol RM. Photodynamic therapy with methyl aminolevulinate induces phototoxic reactions on areas of the nose adjacent to basal cell carcinomas and actinic keratoses. Dermatol Surg 2008 /;34(8):1145-1147.

(490) Tomio L, Corti L, Polico C, Maluta S, Calzavara F, Norberto L, et al. Laser-photo-radiotherapy in the treatment malignant tumors. Radiol Med (Torino) 1987 /;73(4):313-316.

(491) Tong MCF, Van Hasselt CA, Woo JKS. Preliminary results of photodynamic therapy for recurrent nasopha-

ryngeal carcinoma. EUR ARCH OTO-RHINO-LARYNGOL 1996/;253(3):189-192.

(492) Trichopoulos N, Damato B. Photodynamic therapy for recurrent hyphema after proton beam radiotherapy of iris melanoma. Graefe's Arch Clin Exp Ophthalmol 2007 /;245(10):1573-1575.

(493) Triesscheijn M, Baas P, Schellens JHM, Stewart FA. Photodynamic therapy in oncology. Oncologist 2006 /;11(9):1034-1044.

(494) Triesscheijn M, Ruevekamp M, Aalders M, Baas P, Stewart FA. Outcome of mTHPC mediated photodynamic therapy is primarily determined by the vascular response. Photochem Photobiol 2005 /;81(5):1161-1167.

(495) Triesscheijn M, Ruevekamp M, Out R, Van Berkel TJC, Schellens J, Baas P, et al. The pharmacokinetic behavior of the photosensitizer meso-tetra- hydroxyphenyl-chlorin in mice and men. Cancer Chemother Pharmacol 2007 /;60(1):113-122.

(496) Tse DT, Dutton JJ, Weingeist TA. Hematoporphyrin photoradiation therapy for intraocular and orbital malignant melanoma. Arch Ophthalmol 1984/;102(6):833-838.

(497) Uekusa M, Omura K, Nakajima Y, Hasegawa S, Harada H, Morita K-, et al. Uptake and kinetics of 5-aminolevulinic acid in oral squamous cell carcinoma. Int J Oral Maxillofac Surg 2010 /;39(8):802-805.

(498) Unlu N, Hazirolan D, Acar MA, Demir N, Kasim R. Photodynamic therapy in a case of choroidal hemangioma. Retina-Vitreus 2009 /;17(4):295-297.

(499) Uusitalo M, Wheeler S, O'Brien JM. New approaches in the clinical management of retinoblastoma. Ophthalmol Clin North Am 1999/;12(2):255-264.

(500) Vaidyanathan V, Wiggs R, Stohl J, Baxi M. ALA-induced fluorescence in the canine oral cavity. Photomed Laser Surg 2006 /;24(3):383-388.

(501) Vakulovskaya EG. Photodynamic therapy and fluorescent diagnostics of head and neck cancer with second-generation photosensitizers. Proc SPIE - Int Soc Opt Eng (USA) 8 8 Aug. 2005;5973(1):597308-1; 597308-6;

(502) van Rijt SH, Sadler PJ. Current applications and future potential for bioinorganic chemistry in the development of anticancer drugs. Drug Discov Today 2009 /;14(23-24):1089-1097.

(503) van Veen RL, Nyst H, Rai Indrasari S, Adham Yudharto M, Robinson DJ, Tan IB, et al. In vivo fluence rate

measurements during Foscan-mediated photodynamic therapy of persistent and recurrent nasopharyngeal carcinomas using a dedicated light applicator. J Biomed Opt 2006 /;11(4):041107.

(504) Vargas A, Delie F. Potential use of biodegradable nanoparticles for the photodynamic therapy of eye diseases. Arch Soc Esp Oftalmol 2009 /;84(4):169; 171, 173-175.

(505) Vaupel P, Mayer A, Hockel M. Impact of hemoglobin levels on tumor oxygenation: The higher, the better? Strahlenther Onkol 2006 /;182(2):63-71.

(506) Verbraak FD, Schlingemann RO, de Smet MD, Keunen JEE. Single spot PDT in patients with circumscribed choroidal haemangioma and near normal visual acuity. Graefe's Arch Clin Exp Ophthalmol 2006 /;244(9):1178-1182.

(507) Verbraak FD, Schlingemann RO, Keunen JEE, de Smet MD. Longstanding symptomatic choroidal hemangioma managed with limited PDT as initial or salvage therapy. Graefe's Arch Clin Exp Ophthalmol 2003 /;241(11):891-898.

(508) Vogl TJ, Eichler K, Mack MG, Zangos S, Herzog C, Thalhammer A, et al. Interstitial photodynamic laser therapy in interventional oncology. Eur Radiol 2004 /;14(6):1063-1073.

(509) von Buelow M, Pape S, Hoerauf H. Systemic bevacizumab treatment of a juxtapapillary retinal haemangioma. Acta Ophthalmol Scand 2007 /;85(1):114-116.

(510) Vrouenraets MB, Visser GW, Stigter M, Oppelaar H, Snow GB, van Dongen GA. Comparison of aluminium (III) phthalocyanine tetrasulfonate- and meta-tetrahydroxyphenylchlorin-monoclonal antibody conjugates for their efficacy in photodynamic therapy in vitro. Int J Cancer 2002 Apr 10;98(5):793-798.

(511) Vrouenraets MB, Visser GWM, Snow GB, Van Dongen GAMS. Basic principles, applications in oncology and improved selectivity of photodynamic therapy. Anticancer Res 2003 /;23(1 B):505-522.

(512) Vrouenraets M, Visser G, Stewart F, Stigter M, Oppelaar H, Postmus P, et al. Development of meta-tetrahydroxyphenylchlorin-monoclonal antibody conjugates for photoimmunotherapy. Cancer Res 1999 APR 1;59(7):1505-1513.

(513) Wachtlin J, Bechrakis NE, Foerster MH. Photodynamic therapy with verteporfin for uveal melanoma. A

clinical histopathological pilot study. Ophthalmologe 2005 /;102(3):241-246.

(514) Wang C-, Lou P-, Lo F-, Shieh M-. m-THPC mediated photodynamic therapy inhibits the migration and invasion of nasopharyngeal carcinoma cells. Oral Oncol 2011 /;47:S111.

(515) Wang I, Bauer B, Andersson-Engels S, Svanberg S, Svanberg K. Photodynamic therapy utilising topical (delta)-aminolevulinic acid in non-melanoma skin malignancies of the eyelid and the periocular skin. Acta Ophthalmol Scand 1999 /;77(2):182-188.

(516) Wang I, Clemente LP, Pratas RMG, Cardoso E, Clemente MP, Montan S, et al. Fluorescence diagnostics and kinetic studies in the head and neck region utilizing low-dose (delta)-aminolevulinic acid sensitization. Cancer Lett 1998/;135(1):11-19.

(517) Wang KK, Mitra S, Foster TH. Photodynamic dose does not correlate with long-term tumor response to mTHPC-PDT performed at several drug-light intervals. Med Phys 2008 Aug;35(8):3518-3526.

(518) Wang KK, Wongkeesong M, Buttar NS. American gastroenterological association technical review on the role of the gastroenterologist in the management of esophageal carcinoma. Gastroenterology 2005 /;128(5):1471-1505.

(519) Wenig BL, Kurtzman DM, Grossweiner LI, Mafee MF, Harris DM, Lobraico RV, et al. Photodynamic therapy in the treatment of squamous cell carcinoma of the head and neck. ARCH OTOLARYNGOL HEAD NECK SURG 1990/;116(11):1267-1270.

(520) White L, Gomer CJ, Doiron DR, Szirth BC. Ineffective photodynamic therapy (PDT) in a poorly vascularized xenograft model. Br J Cancer 1988/;57(5):455-458.

(521) Wiedmann MW, Caca K. General principles of photodynamic therapy (PDT) and gastrointestinal applications. Curr Pharm Biotechnol 2004 /;5(4):397-408.

(522) Wile AG, Novotny J, Mason GR, Passy V, Berns MW. Photoradiation therapy of head and neck cancer. Prog Clin Biol Res 1984 /;170:681-691.

(523) Williams G, Pazdur R, Temple R. Assessing Tumor-Related Signs and Symptoms to Support Cancer Drug Approval. J Biopharm Stat 2004/;14(1):5-21.

(524) Winther J. Photodynamic therapy effect in an intraocular reginoblastoma-like tumour assessed by an in vivo to in vitro colony forming assay. Br J Cancer

1989/;59(6):869-872.

(525) Winther J. Effect of photofrin II and light energy on retinoblastoma-like cells in vitro. Dose-response relationships, effect of light dose rate and recovery ratio. J Cancer Res Clin Oncol 1989/;115(1):73-78.

(526) Winther J. Porphyrin photodynamic therapy in an experimental retinoblastoma model. Ophthalmic Paediatr Genet 1987/;8(1):49-52.

(527) Winther J, Ehlers N. Histopathological changes in an intraocular retinoblastoma-like tumour following photodynamic therapy. Acta Ophthalmol 1988/;66(1):69-78.

(528) Winther J, Overgaard J. Photodynamic therapy of experimental intraocular retinoblastomas - Dose-response relationships to light energy and photofrin II. Acta Ophthalmol 1989/;67(1):44-50.

(529) Winther J, Overgaard J. Experimental studies of photodynamic therapy in a retinoblastoma-like tumour. Acta Ophthalmol Suppl 1987 /;182:140-143.

(530) Winther J, Overgaard J, Ehlers N. The effect of photodynamic therapy alone and in combination with misonidazole or X-rays for management of a retinoblastoma-like tumour. Photochem Photobiol 1988 /;47(3):419-423.

(531) Winther JB. The effect of photodynamic therapy on a retinoblastoma-like tumour. An experimental in vitro and in vivo study on the potential use of photodynamic therapy in the treatment of retinoblastoma. Acta Ophthalmol 1990/;68(SUPPL. 197):3-37.

(532) Witjes M, Gamm U, Kanick C, Roodenburg J, Sterenborg D, Robinson D, et al. Single fiber reflectance measurements of cervical lymph nodes for identifying metastasis from oral carcinoma. Photodiagn Photodyn Ther 2011 /;8(2):229.

(533) Witjes MJH, Speelman OC, Nikkels PGJ, Nooren CAAM, Nauta JM, Van Der Holt B, et al. In vivo fluorescence kinetics and localisation of aluminium phthalocyanine disulphonate in an autologous tumour model. Br J Cancer 1996/;73(5):573-580.

(534) Wittenberg L, Ma P. Treatment of a von Hippel-Lindau retinal capillary hemangioma with photodynamic therapy. Can J Ophthalmol 2008 /;43(5):605-606.

(535) Wright KE, Liniker E, Loizidou M, Moore C, MacRobert AJ, Phillips JB. Peripheral neural cell sensitivity to mTHPC-mediated photodynamic therapy in a 3D in vitro model. Br J Cancer 2009 AUG 11;101(4):658-665.

(536) Wu RWK, Chu ESM, Yow CMN, Chen JY. Photodynamic effects on nasopharyngeal carcinoma (NPC) cells with 5-aminolevulinic acid or its hexyl ester. Cancer Lett 2006/10;242(1):112-119.

(537) Wu RWK, Huang Z, Yow CMN. FosPeg(registered trademark)-mediated photocytotoxicity suppresses cancer cell growth through down-regulation of MEK pathways. Photodiagn Photodyn Ther 2011 /;8(2):188.

(538) Wu SE. Photo-chemical therapy in the treatment of basal cell carcinoma of the eyelid. Zhonghua Yan Ke Za Zhi 1986 /;22(4):213-214.

(539) Wustrow TPU, Jocham D, Schramm A, Unsold E. Photodynamic destruction of in vitro cultured squamous cell carcinomas of the head and neck. Laryngol Rhinol Otol 1988/;67(10):532-538.

(540) Wustrow TPU, Schramm A, Jocham D, Unsold E. Laser light induced cytotoxicity of cultured squamous cell carcinomas of the head and neck after photosensitization. LARYNGO- RHINO- OTOL 1989/;68(1):44-50.

(541) Xia Y, Zhang E, Hu Y. Influence of HPD on immunological functions in patients with nasopharyngeal carcinoma treated by radiotherapy. Zhonghua Er Bi Yan Hou Ke Za Zhi 1996 /;31(3):168-170.

(542) Xu D-. Research and development of photodynamic therapy photosensitizers in China. Photodiagn Photodyn Ther 2007 /;4(1):13-25.

(543) Yamada I, Hashimoto K, Nakano K, Hsieh KJ, Tomitsuka K, Miyamoto T, et al. An experimental study of the photodynamic therapy for oral cancer. Laser Dentistry 1989; 295–300.

(544) Yamamoto N, Sery TW, Hoober JK, Willett NP, Lindsay DD. Effectiveness of photofrin II in activation of macrophages and in vitro killing of retinoblastoma cells. Photochem Photobiol 1994 /;60(2):160-164.

(545) Yamana Y, Ohnishi Y, Minei M. Argon-laser photochemotherapy with hematoporphyrin derivative in the treatment of a case of retinoblastoma. FOLIA OPHTHALMOL JPN 1982/;33(11):2208-2216.

(546) Yang X-, Luo R-, Li L-, Ding XM, Yan X, Lu CW, et al. Killing effect of hematoporphyrin derivative mediated photodynamic therapy on CNE-2 cell line of human nasopharyngeal carcinoma cultured in vitro. J Clin Rehab Tissue Eng Res 2007/03;11(9):1707-1709.

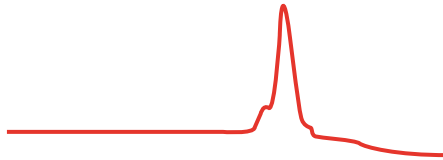(547) Yang XM, Luo RC, Ma HJ, Li LB, Ding XM, Yan X, et al. Hematoporphyrin derivative-mediated photodynamic

therapy for human nasopharyngeal carcinoma: a comparative study with CNE2 and C666-1 cell lines in vitro. Nan Fang Yi Ke Da Xue Xue Bao 2007 /;27(2):165-167.

(548) Yang Z-, Li M-, Zhang Y-, Xiang D-, Dai N, Zeng L-, et al. Knock down of the dual functional protein apurinic /apyrimidinic endonuclease 1 enhances the killing effect of hematoporphrphyrin derivative-mediated photodynamic therapy on non-small cell lung cancer cells in vitro and in a xenograft model. Cancer Sci 2010 /;101(1):180-187.

(549) Yee KKL, Soo KC, Bay BH, Olivo M. A comparison of protoporphyrin IX and protoporphyrin IX dimethyl ester as a photosensitizer in poorly differentiated human nasopharyngeal carcinoma cells. Photochem Photobiol 2002/12;76(6):678-682.

(550) Yoshida T, Kato H, Okunaka T, Saeki T, Ohashi S, Okudaira T, et al. Photodynamic therapy for head and neck cancer. DIAGN THER ENDOSC 1996/;3(1):41-51.

(551) Yoshida T, Saeki T, Ohashi S, Okudaira T, Lee M, Yoshida H, et al. Clinical study of photodynamic therapy for laryngeal cancer. Nippon Jibiinkoka Gakkai Kaiho 1995 /;98(5):795-804.

(552) Yoshida T, Tokashiki R, Ito H, Shimizu A, Nakamura K, Hiramatsu H, et al. Therapeutic effects of a new photosensitizer for photodynamic therapy of early head and neck cancer in relation to tissue concentration. Auris Nasus Larynx 2008 /;35(4):545-551.

(553) Young LHY, Howard MA, Hu LK, Kim RY, Gragoudas ES. Photodynamic therapy of pigmented choroidal melanomas using a liposomal preparation of benzoporphyrin derivative. Arch Ophthalmol 1996 /;114(2):186-192.

(554) Yow CMN, Chen JY, Mak NK, Cheung NH, Leung AWN. Cellular uptake, subcellular localization and photodamaging effect of Temoporfin (mTHPC) in nasopharyngeal carcinoma cells: Comparison with hematoporphyrin derivative. Cancer Lett 2000/09;157(2):123-131.

(555) Yow CMN, Mak NK, Leung AWN, Huang Z. Induction of early apoptosis in human nasopharyngeal carcinoma cells by mTHPC-mediated photocytotoxicity. Photodiagn Photodyn Ther 2009 /;6(2):122-127.

(556) Yow CMN, Mak NK, Szeto S, Chen JY, Lee YL, Cheung NH, et al. Photocytotoxic and DNA damaging effect of Temoporfin (mTHPC) and merocyanine 540 (MC540) on nasopharyngeal carcinoma cell. Toxicol Lett 2000/04;115(1):53-61.

(557) Zellweger M, Grosjean P, Monnier P, van den Bergh H, Wagnieres G. Stability of the fluorescence measurement of Foscan in the normal human oral cavity as an indicator of its content in early cancers of the esophagus and the bronchi. Photochem Photobiol 1999 May;69(5):605-610.

(558) Zhang Y, Liu W, Fang Y, Qian J, Xu G, Wang W, et al. Photodynamic therapy for symptomatic circumscribed macular choroidal hemangioma in Chinese patients. Am J Ophthalmol 2010 /;150(5):710; 715.e1.

(559) Zhao FY. Use of a hematoporphyrin derivative as a sensitizer to radiotherapy in the treatment of oral and maxillofacial malignant tumors. Zhonghua Kou Qiang Yi Xue Za Zhi 1988 /;23(1):52-53.

(560) Zhao FY. Application of a hematoporphyrin derivative (HpD) and the laser technic in diagnosis and treatment of oral tumors. Zhonghua Kou Qiang Ke Za Zhi 1985 /;20(1):8; 11, 62.

(561) Zhao FY, Jiang F. Hematoporphyrin derivative (HpD) and lasers in the treatment of lip cancer: with report of 41 cases. Zhonghua Kou Qiang Ke Za Zhi 1986 /;21(2):96; 98, 128.

(562) Zhao FY, Zhang KH, Jiang F, Wu MJ. Photodynamic therapy for treatment of cancers in oral and maxillofacial regions: A long-term follow-up study in 72 complete remission cases. LASERS MED SCI 1991 1991/;6(2):201-204.

(563) Zharov VP, Vesnin SG, Harms SE, Suen JY, Vaisblat AV, Tikhomirova N. Combined interstitial laser therapy for cancer using microwave radiometric sensor and RODEO MRI feedback. 1.Microwave radiometry. Proc SPIE - Int Soc Opt Eng (USA) 2001 2001;4257:370; 370-376376; 376.

(564) Zheng W, Olivo M, Soo KC. The use of digitized endoscopic imaging of 5-ALA-induced PPIX fluorescence to detect and diagnose oral premalignant and malignant lesions in vivo. Int J Cancer 2004 2004/06;110(2):295-300.

(565) Zheng W, Soo KC, Sivanandan R, Olivo M. Detection of squamous cell carcinomas and pre-cancerous lesions in the oral cavity by quantification of 5-aminolevulinic acid induced fluorescence endoscopic images. Lasers Surg Med 2002 2002/;31(3):151-157.

(566) Zheng X, Pandey RK. Porphyrin-carbohydrate conjugates: Impact of carbohydrate moieties in photodynamic therapy (PDT). Anti-Cancer Agents Med Chem 2008 /;8(3):241-268.

Authors, **Journal,** (year published)	*Main reason for exclusion*	
	Inadequate	
Dilkes MG, DeJode ML **J Laryngol Otol** (1995)[78]	-	measurement of tumor depth or volume
Dilkes MG, DeJode ML **Lasers Med Sci** (1996)[79]	- -	description of previous treatment measurement of tumor depth or volume
Grosjean P, Savary JF **Med Chir Dig** (1996)[54]	- -	description of previous treatment description of tumor localization
Grosjean P, Savary JF **J Clin Laser Med Surg** (1996)[80]	- - -	description of previous treatment description of tumor localization measurement of tumor depth or volume
Fan, KFM, Hopper C **International Journal of Cancer** (1997)[33]	-	measurement of tumor depth or volume
Dilkes MG, Benjamin E. **J Laryngol Otol** (2003)[81]	-	measurement of tumor depth or volume
Van Veen R, Nyst H **J Biomed Opt** (2006)[82]	- - -	description of previous treatment measurement of tumor depth or volume description of tumor response

mTHPC mediated photodynamic therapy of early stage oral squamous cell carcinoma: a comparison to surgical treatment

Abstract

Background and objective. mTHPC mediated (Foscan®) Photodynamic Therapy (PDT) is used for treatment of early head and neck squamous cell carcinoma. This study is a retrospective comparison of PDT with transoral surgery in the treatment of early primary squamous cell carcinoma of the oral cavity/oropharynx.

Materials and Methods. PDT data were retrieved from four study databases while surgical results were retrieved from our institutional database. To select similar primary tumors, infiltration depth was restricted to 5mm for the surgery group. A total of 126 T1 and 30 T2 tumors were included in the PDT group and 58 T1 and 33 T2 tumors were included in the surgically treated group.

Results. Complete response rates with PDT and surgery were 86% and 76% for T1 respectively, and for T2 63% and 78%. Lower local disease free survival for PDT compared to surgery was found. However, when comparing the need for local retreatment no significant difference for T1 tumors were found, while for T2 tumors surgery resulted in significantly less frequent need for local retreatment. No significant differences in overall survival between surgery and PDT were observed.

Conclusion. PDT for T1 tumors results in a similar need for retreatment compared to surgery, while for T2 tumors PDT performs worse. Local disease-free survival for surgery is better than for PDT. This may be influenced by the benefit surgery has of having histology available. This allows an early decision on reintervention while for PDT one has to follow a wait-and-see policy. Future prospective studies should compare efficacy as well as morbidity.

Introduction

The treatment of early stage (stage I/II) head and neck squamous cell carcinomas (HNSCC) is local resection or radiotherapy [1-3]. In retrospective studies, radiotherapy and surgery in patients with stage I/II disease have similar cure rates [4-6]. Usually, surgery is preferred because radiotherapy side-effects can be avoided and histopathological staging can be obtained [2,5,7-9]. However, surgery has disadvantages such as impairment of speech, impairment of swallowing and poor aesthetic outcome [10,11]. It has been suggested that photodynamic therapy (PDT) could be a primary treatment option with similar efficacy and without some of the disadvantages associated with standard treatment [12-16].

The photosensitizer *meta*-tetra(hydroxyphenyl)chlorin (mTHPC, INN: Temoporfin, Foscan®) is licensed for palliation of advanced HNSCC but can also be used for curative treatment of early HNSCC [12,14,15,17-19]. Activation of mTHPC is achieved by illuminating tissue with non-thermal light at a wavelength of 652 nm. Intracellular cytotoxic reactive oxygen species are induced which cause cell death [20-24].

Effective light penetration for PDT is approximately 10 mm at 652 nm. Therefore, curative treatment with surface illumination is limited to tumors with ≤ 5 mm invasion depth [14,25,26]. A suggested advantage of PDT is the limited scarring and limited loss of function after treatment [13,27-31]. It is assumed that long-term morbidity is less than surgery or radiotherapy in similar cases as a result of less deformation and the insensitivity of nearby nerves [32,33]. Another benefit could be the possibility for repeated treatments of the same anatomical area without complications for any other (future) treatments [28,34,35].

Despite these possible advantages, the role of mTHPC mediated PDT in curative treatment of early stage HNSCC is not clear. A systematic review failed to identify any comparative studies of PDT with other modalities [19]. Therefore, any claim of similar efficacy to surgery could not be confirmed or refuted. However, the review did identify four studies that described treatment results after PDT of early stage oral squamous cell carcinoma (OSCC) [12-15]. The similar treatment protocols and inclusion criteria of these studies allowed pooling of the obtained original PDT study databases [19]. In an effort to assess the efficacy of PDT for early stage primary OSCC, we compared PDT with surgery on tumor response and survival. Outcomes after transoral surgical resection were retrieved from our hospital database.

Materials and methods

In this retrospective study on the treatment of early stage OSCC, a comparison was made between databases on PDT treatments (a pooled, multicenter database) and surgical treatment (single institutions database of University Medical Center Groningen). The emphasis of our study was on the results after the initial treatment by either PDT or surgery, not on

Table 1. Patient and tumor characteristics.

	PDT	Surgery	PDT vs Surgery
Patients	152	91	
Sex[a]			
Male	67 (55%)	52 (57%)	
Female	54 (45%)	39 (43%)	
Age (mean in years)[a]	61.1 (SD: 12.6)	61.2 (SD:12.5)	
Years of treatment	1996 - 2008	1997 - 2008	
Follow-up (median in months)	33.0 (IQR: 37.3)	67.0 (IQR: 65.0)	
Tumors	156	91	
T1 tumors	126 (81%)	58 (64%)	
T2 tumors	30 (19%)	33 (36%)	
Complete response (CR) (95% CI)			
T1 tumors (95% CI)	86% (78.5; 90.8)	76% (63.5; 85.0)	p=0.101 [b]
T2 tumors (95% CI)	63% (45.5; 78.1)	79% (62.2; 89.3)	p=0.175 [b]
	p=0.005 [b]	p=0.750 [b]	
LDFS after CR (mean in months)			
T1 tumors (95% CI)	102.6 (86.9; 118.4)	152.7 (140.5; 164.9)	p=0.0084 [c]
T2 tumors (95% CI)	113.8 (82.3; 145.2)	152.8 (140.9; 164.7)	p=0.0260 [c]
	p=0.593 [c]	p=0.695 [c]	
Need for further treatment (no CR or recurrence)			
T1 tumors (95% CI)	28.6% (21.4; 37.0)	29.3% (19.2; 42.0)	p=0.918 [b]
T2 tumors (95% CI)	53.3% (36.1; 69.8)	24.2% (12.8; 41.0)	p=0.018 [b]
	p=0.010 [b]	p=0.603 [b]	
Overall survival (mean in months)			
Patients T1 tumors (95% CI)	101.5 (89.3; 113.8)	122.6 (106.9; 138.2)	p=0.237 [c]
Patients T2 tumors (95% CI)	116.9 (87.7; 146.1)	109.5 (87.1; 132.0)	p=0.713 [c]
	p=0.842 [c]	p=0.450 [c]	
Alive after salvage treatment(s)			
Patients T1 tumors (95% CI)	48.3% (65.6; 79.6)	70.6% (46.9; 86.7)	p=0.724 [b]
Patients T2 tumors (95% CI)	75.0% (50.5; 89.8)	62.5% (30.6; 86.3)	p=0.525 [b]
	p=0.509 [b]	p=0.686 [b]	

PDT mTHPC mediated photodynamic therapy, SD standard deviation, IQR Inter quartile range, CI confidence interval, CR complete response, LDFS local disease free survival

[a] gender and age of 31 patients was unknown.

[b] χ^2 tests

[c] Mantel-Cox analysis

Table 2. Definition of complete response after initial therapy for both surgery and PDT.

	PDT	Surgery
Complete response	Clinical examination: - Treatment site is macroscopically normal with no evidence of tumor. (Observed on 2 occasions at least 4 wk apart)	Histological examination- Negative surgical margin: - Surgical margin free of tumor - Surgical margin with low dysplasia
No complete response	Clinical examination - Presence of tumor after treatment - Partial response - No response - Progressive disease	Histological examination- positive surgical margin: - Involved surgical margin (< 1mm) - Close surgical margin (1- 4 mm) - Surgical margin with severe dysplasia

subsequent salvage treatments. The study design required that all cases with a first primary cT1-2N0 OSCC could be identified and extracted from both the pooled PDT database and the surgical database. All tumors in the pooled database had a clinical tumor depth of ≤ 5mm as assessed by imaging. Imaging in the PDT group consisted of computed tomography, magnetic resonance imaging or ultrasound.

To ensure adequate comparison, tumors with a pathologically assessed infiltration depth of ≤ 5 mm were selected from the surgical treatment database.

A total of 91 surgically treated tumors met the study criteria (table 1). The initial local treatment was transoral resection. Tumor response after surgery was determined by histopathology and classified as a complete response (CR) or as no CR (table 2). Sixty-two patients (68%), including all 33 patients with stage II disease, underwent elective neck dissection (level I – III). Where CR was not achieved (positive margin, table 2) or when patients developed a local recurrence, retreatment by surgery or radiotherapy was performed.

For assessment of the initial PDT treatment result (CR or not), information was extracted from a pooled database of four original study databases, originating from studies using the standard and thus comparable treatment protocols and inclusion criteria [12-15].

After rigorous investigation of the database, a total of 126 T1 and 30 T2 first primary oral cavity/oropharyngeal tumors in 152 patients remained (table 1) [19]. All 17 oropharyngeal tumors were located on the soft palate. Of 31 patients originating from one study database, age and gender was missing [14].

PDT was identical for all patients and included intravenous injection of 0.15 mg/kg mTHPC followed by surface illumination after 96 hours. Light was delivered by a 652 nm diode laser to a visible and accessible tumor. The calculated dose delivered was 20 J/cm² with a fluence rate of 100mW/cm². The tumor and a margin of at least 5 mm of normal appearing surrounding mucosa were illuminated. The database included data on tumor response (CR or non- CR) recorded by the authors of the included pooled studies after clinical examination (table 2). To be classified as a CR, no evidence of tumor had to be observed on 2 separate examinations (> 4 weeks apart). In contrast to the surgically treated group, no elective neck treatment was performed; all patients were subject to watchful waiting policy [36]. As in the surgical cases, when CR was not reached or patients developed a local recurrence they received retreatment by surgery, radiotherapy or repeated PDT.

Statistical analysis
Local CR rate, need for local retreatment, incidence of regional metastases and death of the patient marked the end points of our study. Local disease free survival (LDFS) was defined as absence of tumor recurrence after observation of a CR. The need for local retreatment was defined as absence of CR or recurrence of tumor after an initial CR. For survival analysis, overall survival on a patient specific level was determined. Additionally, survival after local salvage treatment was calculated.

Descriptive statistics and 95% confidence interval (CI) were calculated [37]. Differences in local CR rate, incidence of regional metastases and need for further local treatment were analyzed using χ^2 tests. Survival curves for LDFS, need for re-treatment and overall survival were constructed using the Kaplan-Meier method. Differences in survival curves were analyzed using the log-rank test (Mantel-Cox). All tests were conducted at a two-sided significance level of 5% in PASW statistics 18 software package (SPSS Inc.) or Graphpad Prism® (software version 5.0).

Results

Tumor response
Of the 156 tumors treated by PDT, the CR rate was 86% for T1, and 63% for T2 tumors (table 1, p=0.005, χ^2 test). For the 91 surgically treated tumors no significant difference in CR between T1 (76%) and T2 (79%) was found. Of the 17 surgically treated tumors without CR, 7 had involved surgical margins (margin less than 1 mm), 4 margins with severe dysplasia and 10 with close margins (1-4 mm margin). A comparison in CR rate between PDT and surgery for different T-stage showed no significant difference.

Local disease free survival
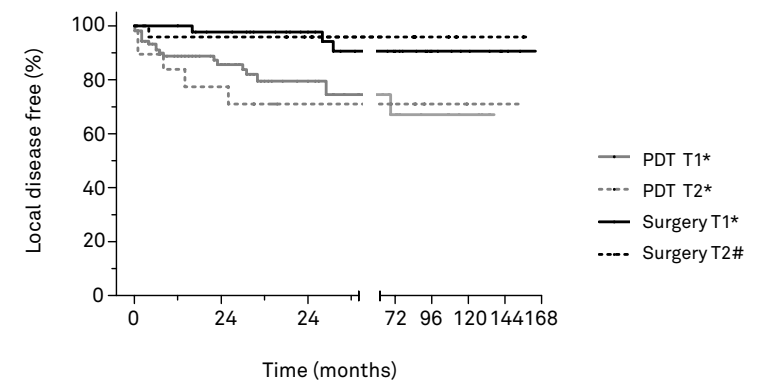For the 127 tumors in which PDT resulted in a CR, the mean LDFS was 102.6 months for T1

Figure 1. Kaplan-Meier curve depicting LDFS after CR per T-stage for PDT and Surgery. Mantel-Cox analysis; * p= 0.0084, # p= 0.0260.

and 113.8 months for T2 tumors (table 1). Comparison of the survival curves using Mantel-Cox analysis, showed no significant differences (figure 1, p=0.593). For the 70 tumors in which surgery resulted in a CR, the mean LDFS is 152.7 months for T1 and 152.8 months for T2 tumors. Comparison of the survival curves, showed no significant differences (p=0.695). When comparing curves of surgery with PDT, surgery showed a significant better outcome for both T1 (p=0.0084) and T2 tumors (p=0.0260) (table 1, figure 1).

Need for local retreatment
For the 156 tumors treated by PDT, T2 tumors needed significantly (p=0.010, χ^2 test) more additional treatment than T1 tumors (table 1). For the 91 surgically treated tumors, no significant difference in need for further treatment was found between T1 and T2 tumors (p=0.603). A comparison in need for further treatment between surgery and PDT showed a significant (p=0.018) better outcome for surgically treated T2 tumors and no difference for T1 tumors (p=0.918, table 1). A comparison of Kaplan-Meier curves using Mantel-Cox analysis again showed significant better results for T2 tumors using surgery and no difference for T1 tumors (figure 2, p=0.018 and p=0.55 respectively).

Regional status
After PDT, 22 of 152 (14%) patients were diagnosed with regional metastases and received salvage treatment. While 68 of the 91 surgically treated patients received elective neck dissection, a total of 7 patients (8%) developed regional metastases. Of those 7 regional metastases, 5 developed in patients treated initially with an elective neck dissection. Overall, no significant difference in occurrence of regional metastases between surgery and PDT was found (p=0.1155, χ^2 test).
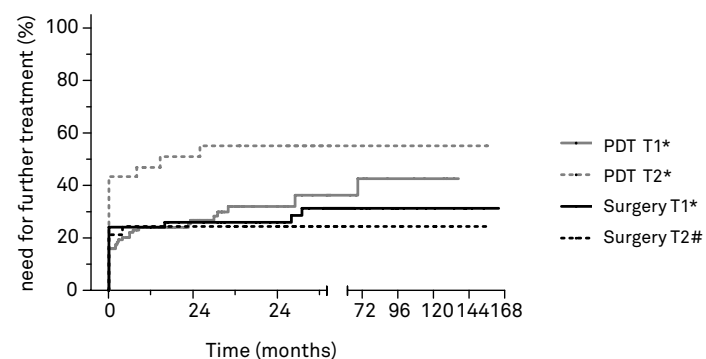
Figure 2. Kaplan-Meier of one minus curve depicting the need for further treatment. An event is defined as a need for further treatment. Mantel-Cox analysis; * p= 0.55, # p= 0.018.
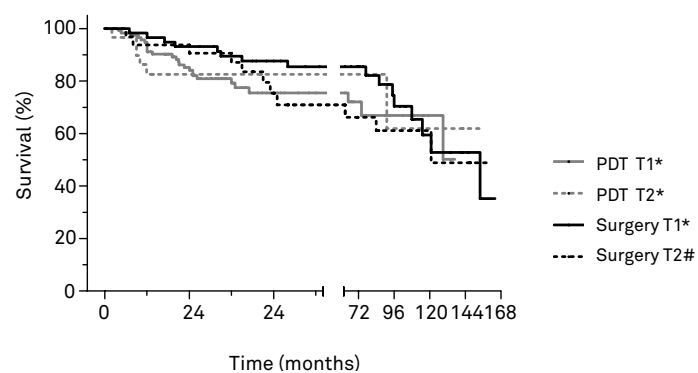

Figure 3. Kaplan-Meier curve depicting overall survival of patients after initial treatment with surgery and PDT. Mantel-Cox analysis; * p=0.237, # p= 0.713.

Overall survival

For the 152 patients treated by PDT, the overall mean survival time was 101.5 months for patients with T1 tumors and 116.9 months for patients with T2 tumors (table 1). Comparison of the survival curves using Mantel-Cox analysis, showed no significant difference in survival between patients with T1 or T2 tumors (figure 3, p=0.842).

For the 91 patients that were surgically treated the overall mean survival time was 122.6 months for T1 and 109.5 months for T2 tumors. Comparison of the survival curves, showed no significant difference between T1 and T2 tumors (p=0.450).

A comparison of overall survival between patients treated by PDT or surgery for their primary tumor, showed no significant differences (table 1, figure 3). Comparing overall survival between the PDT and surgically treated patients after additional local salvage treatment(s) showed no significant differences stratified for T1 and T2 tumors (table 1).

Discussion

In an analysis of the efficacy of PDT versus surgery, the definition of what the primary endpoint should be is strongly influenced by the difference in posttreatment strategies. The assessment of CR after PDT is performed by visual inspection while for surgery this is performed by histopathological analysis. In the surgery group, it is therefore possible that a need for retreatment is established and executed when surgical margins are shown to be compromised. Consequently, interpretation of LDFS is different for PDT and surgery. A major portion (76%) of the retreatment in the surgery group has taken place at the start of the assessment of the LDFS, whereas the retreatment in the PDT group takes place at the end of the LDFS period. Therefore, one needs to carefully draw conclusions from these data. In this study, there was no significant difference in CR when PDT was compared to surgery for the treatment of T1 and T2 tumors, respectively. When comparing LDFS, PDT was significantly less effective than surgery for both T1 and T2 tumors. This is an immediate consequence of a difference in posttreatment strategies between PDT and surgery. Because of the visual determination of CR for PDT, the chance of false-negatives is higher than in the surgery group resulting eventually in lower LDFS for PDT. We therefore think that the essential endpoint in our study should be the need for retreatment and disease-free survival. For T1 tumors, PDT and surgery showed a similar need for further treatment after initial PDT or surgery. However, for T2 tumors, the PDT-treated cases needed a significantly higher number of retreatments. Also, within the group of PDT-treated tumors, a lower CR and LDFS for T2 versus T1 tumors proved statistically significant. This was not found in surgically treated patients. The lower efficacy of PDT for T2 compared to T1 tumors was described previously by others [12,14]. We therefore conclude that in the treatment of T1 tumors the efficacy of PDT is similar to surgery. In the treatment of T2 tumors surgery is more effective.

As a result of the possibility of salvage treatment, overall survival was not different for PDT and surgery. As described in literature, patients who did not experience a CR still had the option of successful salvage treatment [12,14]. In a subanalysis we studied whether the location of the primary OSCC was relevant, since especially PDT outcomes could be influenced by the location of the OSCC. Our data show that exclusion of tongue or soft palate tumors did not significantly change CR, LDFS, or overall survival [15].

Comparison of our results with literature is difficult; as often only local control rates of tumors excised with clear surgical margins are described [3,5,38]. Exclusion of patients with involved or close margins will influence prognosis, as status of surgical margins is widely known to influence local (regional) recurrences and survival [38-41]. In a study that did describe the surgical margins after excision, 60% of stage I/II tumors were resected with clear margins and could be considered a CR according to our definition [40]. This is a lower CR compared to our results. An explanation could be our inclusion of patients with tumors with an infiltration depth of ≤5mm, which is associated with a better clinical outcome [41-45].

Even though the majority of surgically treated patients received an elective neck dissection, this did not result in differences in survival as described in literature [7-9]. This might be due to the inclusion of only tumors with an infiltration depth ≤5mm, where the additional value of an elective neck dissection is low [46]. Although our results show that the treatment results of PDT for T1 tumors are comparable to surgical treatment, the added benefit of PDT is not adequately studied in literature [19]. Several studies describe possible advantages of PDT compared to standard treatment such as decreased morbidity and possibility of repeated treatments [13,15,27-31,34,35].

Our study has some limitations; all PDT data are retrospectively derived from different centers, whereas all surgically treated patients are derived from our own institution. Although our inclusion criteria were chosen so that the cases from this surgical database optimally reflect the cases from the PDT database, differences in both groups are to be expected. For instance, for surgery infiltration depth ≤5mm was histologically assessed and can differ from tumor depth assessed by imaging as used for PDT. The pathologically assessed infiltration depth could be influenced by tissue shrinkage associated with fixation and pathological processing [47]. A further difficulty is what constitutes a positive resection margin. Many studies regard close or involved margins as a positive margin [40,47,48]. In our current study we adhered to our institution's protocol whereby severe dysplasia at the margins is considered a "positive" margin and thus as a failure of initial excision. As a consequence, our CR rate described for surgery is underestimated. No disease specific survival could be calculated as a result of insufficient data on cause of death for the PDT group. A recent non-randomized matched control study described similar local disease control and survival for PDT and surgery in treatment of early stage squamous cell carcinoma of the oral cavity [16]. However, that study did not stratify according to T1 or T2 tumors. It is clear that a future prospective, comparative study should assess the efficacy of PDT compared to standard treatment on a group of well-defined tumors. More importantly, the differences in long-term morbidity of PDT should be further explored.

Conclusion

In summary, treatment of primary T1 tumors of the oral cavity by either mTHPC mediated PDT or trans-oral surgery seems to result in similar need for retreatment. Local disease-free survival for surgery is better than for PDT. This may be influenced by the benefit surgery has of having histology available.

For T2 tumors, PDT seemed less effective; PDT and surgery showed similar overall survival rates for both T1 and T2 tumors. Besides the need for prospective and comparative studies to assess the efficacy of PDT compared to standard treatment, further emphasis should be placed on the comparison of morbidity between modalities.

References

1. Haddad RI, Shin DM. Recent advances in head and neck cancer. N Engl J Med. 2008 Sep 11;359(11):1143-54.

2. Argiris A, Karamouzis MV, Raben D, Ferris RL. Head and neck cancer. Lancet. 2008 May 17;371(9625):1695-709.

3. Brown JS, Shaw RJ, Bekiroglu F, Rogers SN. Systematic review of the current evidence in the use of postoperative radiotherapy for oral squamous cell carcinoma. Br J Oral Maxillofac Surg. 2011 Dec 22.

4. Inagi K, Takahashi H, Okamoto M, Nakayama M, Makoshi T, Nagai H. Treatment effects in patients with squamous cell carcinoma of the oral cavity. Acta Otolaryngol Suppl. 2002;(547)(547):25-9.

5. Wolfensberger M, Zbaeren P, Dulguerov P, Muller W, Arnoux A, Schmid S. Surgical treatment of early oral carcinoma-results of a prospective controlled multicenter study. Head Neck. 2001 Jul;23(7):525-30.

6. Shah JP, Gil Z. Current concepts in management of oral cancer--surgery. Oral Oncol. 2009 Apr-May;45(4-5):394-401.

7. Bessell A, Glenny AM, Furness S, Clarkson JE, Oliver R, Conway DI, et al. Interventions for the treatment of oral and oropharyngeal cancers: Surgical treatment. Cochrane Database Syst Rev. 2011 Sep 7;(9)(9):CD006205.

8. Capote A, Escorial V, Munoz-Guerra MF, Rodriguez-Campo FJ, Gamallo C, Naval L. Elective neck dissection in early-stage oral squamous cell carcinoma--does it influence recurrence and survival? Head Neck. 2007 Jan;29(1):3-11.

9. Fasunla AJ, Greene BH, Timmesfeld N, Wiegand S, Werner JA, Sesterhenn AM. A meta-analysis of the randomized controlled trials on elective neck dissection versus therapeutic neck dissection in oral cavity cancers with clinically node-negative neck. Oral Oncol. 2011 May;47(5):320-4.

10. Biazevic MG, Antunes JL, Togni J, de Andrade FP, de Carvalho MB, Wunsch-Filho V. Immediate impact of primary surgery on health-related quality of life of hospitalized patients with oral and oropharyngeal cancer. J Oral Maxillofac Surg. 2008 Jul;66(7):1343-50.

11. Chandu A, Smith AC, Rogers SN. Health-related quality of life in oral cancer: A review. J Oral Maxillofac Surg. 2006 Mar;64(3):495-502.

12. Copper MP, Tan IB, Oppelaar H, Ruevekamp MC, Stewart FA. Meta-tetra(hydroxyphenyl) chlorin photodynamic therapy in early-stage squamous cell carcinoma of the head and neck. Arch Otolaryngol Head Neck Surg. 2003 07;129(0886-4470; 7):709-11.

13. Copper MP, Triesscheijn M, Tan IB, Ruevekamp MC, Stewart FA. Photodynamic therapy in the treatment of multiple primary tumours in the head and neck, located to the oral cavity and oropharynx. Clin Otolaryngol. 2007 06;32(1749-4478; 3):185-9.

14. Hopper C, Kubler A, Lewis H, Tan IB, Putnam G. mTHPC-mediated photodynamic therapy for early oral squamous cell carcinoma. Int J Cancer. 2004 08/10;111(0020-7136; 0020-7136; 1):138-46.

15. Karakullukcu B, van Oudenaarde K, Copper MP, Klop WM, van Veen R, Wildeman M, et al. Photodynamic therapy of early stage oral cavity and oropharynx neoplasms: An outcome analysis of 170 patients. Eur Arch Otorhinolaryngol. 2011 Feb;268(2):281-8.

16. Karakullukcu B, Stoker SD, Wildeman AP, Copper MP, Wildeman MA, Tan IB. A matched cohort comparison of mTHPC-mediated photodynamic therapy and trans-oral surgery of early stage oral cavity squamous cell cancer. Eur Arch Otorhinolaryngol. 2012 Jul 7.

17. European Medicines Agencies. H-C-318 foscan european public assessment report. 2009 04/30.

18. Kubler AC, de Carpentier J, Hopper C, Leonard AG, Putnam G. Treatment of squamous cell carcinoma of the lip using foscan-mediated photodynamic therapy. Int J Oral Maxillofac Surg. 2001 12;30(0901-5027; 0901-5027; 6):504-9.

19. de Visscher SA, Dijkstra PU, Tan IB, Roodenburg JL, Witjes MJ. mTHPC mediated photodynamic therapy (PDT) of squamous cell carcinoma in the head and neck: A systematic review. Oral Oncol. 2013 Mar;49(3):192-210.

20. Weishaupt KR, Gomer CJ, Dougherty TJ. Identification of singlet oxygen as the cytotoxic agent in photoinactivation of a murine tumor. Cancer Res. 1976 Jul;36(7 PT 1):2326-9.

21. Dewaele M, Maes H, Agostinis P. ROS-mediated mechanisms of autophagy stimulation and their relevance in cancer therapy. Autophagy. 2010 Oct;6(7):838-54.

22. Buytaert E, Dewaele M, Agostinis P. Molecular effectors of multiple cell death pathways initiated by photodynamic therapy. Biochim Biophys Acta. 2007 Sep;1776(1):86-107.

23. Dougherty TJ, Gomer CJ, Henderson BW, Jori G, Kessel D, Korbelik M, et al. Photodynamic therapy. J Natl Cancer Inst. 1998 06/17;90(0027-8874; 0027-8874; 12):889-905.

24. Henderson BW, Dougherty TJ. How does photodynamic therapy work? Photochem Photobiol. 1992 01;55(0031-8655; 0031-8655; 1):145-57.

25. Senge MO, Brandt JC. Temoporfin (foscan(R), 5,10,15,20-tetra(m-hydroxyphenyl)chlorin)--a second-generation photosensitizer. Photochem Photobiol. 2011 Nov-Dec;87(6):1240-96.

26. Plaetzer K, Krammer B, Berlanda J, Berr F, Kiesslich T. Photophysics and photochemistry of photodynamic therapy: Fundamental aspects. Lasers Med Sci. 2009 Mar;24(2):259-68.

27. D'Cruz AK, Robinson MH, Biel MA. mTHPC-mediated photodynamic therapy in patients with advanced, incurable head and neck cancer: A multicenter study of 128 patients. Head Neck. 2004 03;26(1043-3074; 1043-3074; 3):232-40.

28. Hopper C. Photodynamic therapy: A clinical reality in the treatment of cancer. Lancet Oncol. 2000 12;1(1470-2045):212-9.

29. Fan KF, Hopper C, Speight PM, Buonaccorsi GA, Bown SG. Photodynamic therapy using mTHPC for malignant disease in the oral cavity. Int J Cancer. 1997 Sep 26;73(1):25-32.

30. Henderson BW. Photodynamic therapy--coming of age. Photodermatol. 1989 Oct;6(5):200-11.

31. Yow CM, Chen JY, Mak NK, Cheung NH, Leung AW. Cellular uptake, subcellular localization and photodamaging effect of temoporfin (mTHPC) in nasopharyngeal carcinoma cells: Comparison with hematoporphyrin derivative. Cancer Lett. 2000 Sep 1;157(2):123-31.

32. Kubler AC, Stenzel W, Ruhling M, Meul B, Fischer J-. Experimental evaluation of possible side effects of intra-operative photodynamic therapy on rabbit blood vessels and nerves. Lasers Surg Med. 2003 2003/;33(4):247-55.

33. Wright KE, Liniker E, Loizidou M, Moore C, Macrobert AJ, Phillips JB. Peripheral neural cell sensitivity to mTHPC-mediated photodynamic therapy in a 3D in vitro model. Br J Cancer. 2009 Aug 18;101(4):658-65.

34. Hornung R, Walt H, Crompton NE, Keefe KA, Jentsch B, Perewusnyk G, et al. m-THPC-mediated photodynamic therapy (PDT) does not induce resistance to chemotherapy, radiotherapy or PDT on human breast cancer cells in vitro. Photochem Photobiol. 1998 Oct;68(4):569-74.

35. Dougherty TJ, Marcus SL. Photodynamic therapy. Eur J Cancer. 1992;28A(10):1734-42.

36. Nieuwenhuis EJ, Castelijns JA, Pijpers R, van den Brekel MW, Brakenhoff RH, van der Waal I, et al. Wait-and-see policy for the N0 neck in early-stage oral and oropharyngeal squamous cell carcinoma using ultrasonography-guided cytology: Is there a role for identification of the sentinel node? Head Neck. 2002 Mar;24(3):282-9.
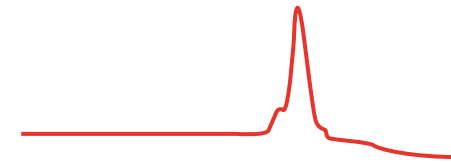
37. Altman DG, Machin D, Bryant T, Gardner S. Statistics with confidence: Confidence intervals and statistical guidelines. 2nd ed. London: BMJ Books; 2000.

38. Hicks WL,Jr, Loree TR, Garcia RI, Maamoun S, Marshall D, Orner JB, et al. Squamous cell carcinoma of the floor of mouth: A 20-year review. Head Neck. 1997 Aug;19(5):400-5.

39. Nason RW, Binahmed A, Pathak KA, Abdoh AA, Sandor GK. What is the adequate margin of surgical resection in oral cancer? Oral Surg Oral Med Oral Pathol Oral Radiol Endod. 2009 May;107(5):625-9.

40. Sutton DN, Brown JS, Rogers SN, Vaughan ED, Woolgar JA. The prognostic implications of the surgical margin in oral squamous cell carcinoma. Int J Oral Maxillofac Surg. 2003 Feb;32(1):30-4.

41. Woolgar JA. Histopathological prognosticators in oral and oropharyngeal squamous cell carcinoma. Oral Oncol. 2006 Mar;42(3):229-39.

42. Spiro RH, Huvos AG, Wong GY, Spiro JD, Gnecco CA, Strong EW. Predictive value of tumor thickness in squamous carcinoma confined to the tongue and floor of the mouth. Am J Surg. 1986 Oct;152(4):345-50.

43. Shingaki S, Suzuki I, Nakajima T, Kawasaki T. Evaluation of histopathologic parameters in predicting cervical lymph node metastasis of oral and oropharyngeal carcinomas. Oral Surg Oral Med Oral Pathol. 1988 Dec;66(6):683-8.

44. O-charoenrat P, Pillai G, Patel S, Fisher C, Archer D, Eccles S, et al. Tumour thickness predicts cervical nodal metastases and survival in early oral tongue cancer. Oral Oncol. 2003 Jun;39(4):386-90.

45. Po Wing Yuen A, Lam KY, Lam LK, Ho CM, Wong A, Chow TL, et al. Prognostic factors of clinically stage I and II oral tongue carcinoma-A comparative study of stage, thickness, shape, growth pattern, invasive front malignancy grading, martinez-gimeno score, and pathologic features. Head Neck. 2002 Jun;24(6):513-20.

46. Melchers LJ, Schuuring E, van Dijk BA, de Bock GH, Witjes MJ, van der Laan BF, et al. Tumour infiltration depth >/=4 mm is an indication for an elective neck dissection in pT1cN0 oral squamous cell carcinoma. Oral Oncol. 2012 Apr;48(4):337-42.

47. Batsakis JG. Surgical excision margins: A pathologist's perspective. Adv Anat Pathol. 1999 May;6(3):140-8.

48. Woolgar JA, Triantafyllou A. A histopathological appraisal of surgical margins in oral and oropharyngeal cancer resection specimens. Oral Oncol. 2005 Nov;41(10):1034-43.

Chapter 3

Comparison of mTHPC fluorescence pharmacokinetics between liposomal mTHPC drug-carrier systems and free mTHPC

Fluorescence localization and kinetics of mTHPC
and liposomal formulations of mTHPC in the
window-chamber tumor model

Abstract

Background and objective. Foslip® and Fospeg® are liposomal formulations of the photosensitizer meta-tetra(hydroxyphenyl)chlorin (mTHPC), intended for use in Photodynamic Therapy (PDT) of malignancies. Foslip consists of mTHPC encapsulated in conventional liposomes, Fospeg consists of mTHPC encapsulated in pegylated liposomes. Possible differences in tumor-fluorescence and vasculature kinetics between Foslip, Fospeg and Foscan® were studied using the rat window-chamber model.

Materials and methods. In 18 rats a dorsal skinfold window-chamber was installed and a mammary carcinoma was transplanted in the subcutaneous tissue. The dose used for intravenous injection was 0.15 mg/kg mTHPC for each formulation. At 7 time points after injection (5 minutes – 96 hours) fluorescence images were made with a Charge-coupled device (CCD). The achieved mTHPC fluorescence images were corrected for tissue optical properties and autofluorescence by the ratio fluorescence imaging technique of Kascakova et al. Fluorescence intensities of 3 different regions of interest were assessed; tumor tissue, vasculature and surrounding connective tissue.

Results. The three mTHPC formulations showed marked differences in their fluorescence kinetic profile. After injection, vascular mTHPC fluorescence increased for Foslip and Fospeg but decreased for Foscan. Maximum tumor fluorescence is reached at 8 hours for Fospeg and at 24 hours for Foscan and Foslip with overall higher fluorescence for both liposomal formulations. Foscan showed no significant difference in fluorescence intensity between surrounding tissue and tumor tissue (selectivity). However, Fospeg showed a trend towards tumor selectivity at early time points, while Foslip reached significantly ($p<0.05$) better tumor selectivity at these time points.

Conclusion. Our results showed marked differences in fluorescence intensities of Fospeg, Foslip and Foscan, which suggests overall higher bioavailability for the liposomal formulations. Pegylated liposomes seemed most promising for future application; as Fospeg showed highest tumor fluorescence at the earlier time points.

Introduction

Photodynamic therapy (PDT) has been established as a local treatment modality for several kinds of malignancies in various organs [1-7]. PDT is based on the use of a light sensitive drug, a photosensitizer, which is locally applied or systemically administered. Excitation of a photosensitizer with non-thermal light of an appropriate wavelength leads to a process in which energy is transferred to molecular oxygen. This leads to the formation of intracellular cytotoxic reactive oxygen species and subsequent cell death [8-11]. As a consequence, the tumor is destroyed by a combination of direct tumor cell kill and by vascular damage [4,9,12-14]. Next to parameters such as the presence of oxygen and the use of a sufficient amount of light, the amount of a photosensitizer in the target tissue is an important parameter.

One of the most potent clinically used photosensitizers to date is the compound *meta*-tetra(hydroxyphenyl)chlorin (mTHPC, INN: Temoporfin) [9,15,16]. In the European Union, a formulation of ethanol and propylene glycol with mTHPC (Foscan®) is approved and used for palliative treatment of advanced squamous cell carcinoma (SCC) of the head and neck [8,17-20]. Several authors described a reduction in tumor size, prolonged survival and an improved quality of life after mTHPC mediated PDT in patients treated with palliative intent [8,17,19-21]. Besides palliative treatment, mTHPC mediated PDT is also used as an effective curative treatment for patients with superficial oral SCCs [16,22-24]. The efficacy of mTHPC mediated PDT in these patients is similar to surgery and radiotherapy, while the long-term morbidity is limited [16,22]. Potentially important features of PDT are the possibility of repeated treatment of the target tissue, the restriction of the induced damage to the illuminated area and the potential for a good functional and aesthetic result [2,8,16,22,23,25].

The current PDT protocol for head and neck SCCs dictates an intravenous (i.v.) injection of 0.15 mg/kg mTHPC followed 96 hours later by illumination. This protocol is effective, but is also demanding for the patients as it involves long drug-light intervals, skin photosensitivity and in some patients, pain and discoloration at the site of drug injection [7,19,21,22,24,26,27]. A protocol with comparable high efficacy but with a shorter drug-light interval, lower skin accumulation and less adverse side effects at the injection site would be beneficial for patients. Furthermore, the basic form of mTHPC is highly hydrophobic and lipophilic, which complicates its formulation and administration [28,29]. Due to its hydrophobic nature, mTHPC aggregates will form in the vasculature, which decreases its biodistribution [30-34]. Due to its lipophilic nature, mTHPC adheres to endothelium of the injected vein and to the surrounding subcutaneous tissue. That could explain the discoloration at the injection site as reported in some patients [24,27].

Previously, PEG-mTHPC conjugates were developed to improve the characteristics of mTHPC with some success [29]. However, the therapeutic effect of these conjugates was at best similar to the basic form of mTHPC [35].

The encapsulation of mTHPC into liposomes may offer further improvements in clinical PDT;

other liposomal photosensitizer formulations showed higher tumor uptake, superior water solubility and higher photosensitizing efficacy compared to the original formulations [31-33,36-39]. Water-soluble liposomes are thought to allow selective accumulation in tumor tissue by the enhanced permeability and retention (EPR) effect and by the increased binding to low-density lipoprotein (LDL) receptors [31,37,38]. The higher PDT efficacy attributed to the use of this approach is due to the non-aggregated form of photosensitizer encapsulated in liposomes. If proven for mTHPC, these characteristics could result in optimization of clinical PDT with a shorter drug-light interval and less skin photosensitivity.

Two formulations of mTHPC encapsulated into liposomes are available. One mTHPC formulation (Foslip®) consists of plain or conventional liposomes based on dipalmitoylphosphatidylcholine (DPPC). The other mTHPC formulation (Fospeg®) consists of liposomes with a pegylated (poly-ethylene glycol) layer on the surface. This hydrophilic pegylated layer is thought to prevent uptake by the mononuclear phagocyte system (MPS) thereby increasing the circulation time [31,37]. It is suggested that this longer circulation time should increase the EPR effect [29,31,40].

The fluorescence pharmacokinetics of Foslip and Fospeg have been investigated before in a small number of studies using various models [26,41-43]. Encapsulation of mTHPC in plain liposomes (Foslip) and in pegylated liposomes (Fospeg) resulted, *in vitro*, in similar cellular uptake compared to Foscan [44,45]. Pegaz et al. compared Fospeg and Foslip in an *in vivo*, non-tumor, chick chorioallantoic membrane model [42]. During the experimental time of 20 minutes, they found no differences in kinetics between the two liposomal formulations. In a study in mice, Foslip was found to have a slightly higher tumor-to-muscle ratio compared to Foscan, with high tumor concentrations 4 hours post injection and at their last measurement, 8 hours post injection [26,29].

An interesting study of Buchholz et al. compared the pharmacokinetics of Fospeg with Foscan in 10 cats with spontaneous SCCs of the nose [41]. They found that mTHPC encapsulated in pegylated liposomes (Fospeg) showed higher bioavailability in tumor, earlier maximal tumor accumulation and higher tumor-to-skin fluorescence ratio compared to Foscan. However, tumor fluorescence intensity was measured by point fiber optic measurements without correcting for autofluorescence.

The previously described *in vivo* studies suggest that liposomal formulations will yield an earlier, higher availability of mTHPC. However, there is a substantial lack of data to compare the kinetics of these liposomal mTHPC formulations to Foscan at long time-intervals with appropriate correction for tissue optical properties.

In this study the *in vivo* fluorescence kinetics of two liposomal mTHPC formulations and Foscan are investigated in a mammary adenocarcinoma xenograft tumor model (rat skin fold window chamber model). Fluorescence imaging is used to determine mTHPC levels at various time points and tissue types. A ratiometric correction method [46] was used to correct for changes of tissue optical properties and changes in the thickness of tissue. Our aim is to study whether the use of liposome encapsulated mTHPC will enhance the fluorescence

uptake of mTHPC in tumor tissue and if the time to reach maximal tumor fluorescence is altered.

Materials and methods

Animal and tumor model
Seven weeks old Female Fisher-344 rats, weighing approximately 100 – 140 g, were purchased from Harlan Netherlands B.V. (Horst, The Netherlands). The window chamber model has been described elsewhere [47,48]. In brief, over a series of 4 operations a thin layer of subcutaneous tissue from a dorsal skin flap was prepared and fixed in a plastic frame, to form a skin fold chamber. After a short healing time the final step in the procedure was the implantation of an isogeneic mammary adenocarcinoma (R3230AC) into the subcutaneous tissue. All operations were carried out under general Isoflurane®/O_2/N_2O anesthesia. The animals were kept in a temperature controlled cabinet at 27 °C with a 12/12 hour light/dark interval. Tumor growth, the general condition of the chamber and the blood circulation were followed using a microscope at low magnification. This was done to determine the best day to start the experiment. Most experiments started approximately 5-7 days after tumor implantation. After injection with a photosensitizer the animals were kept under reduced light conditions (< 100 lux). Through all procedures and measurements Isoflurane was used as a general inhalation anesthetic. In between measurements, the animals were conscious and kept in the same reduced light conditions. At the end of the experiments the animals were terminated by cervical dislocation.

Materials
Foscan (4 mg mTHPC/ml), Fospeg (1.5 mg mTHPC/ml) and Foslip (1.38 mg mTHPC/ml) were kindly provided by Biolitec AG (Jena, Germany) in the described stock concentrations. Pegylated liposomal mTHPC (Fospeg) consists of dipalmitoylphosphatidylcholine (DPPC), dipalmitoylphosphatidylglycerol (DPPG) and Pegylated distearoylphosphatidylethanolamine. Conventional liposomal mTHPC (Foslip) consists of DPPC, DPPG, mTHPC and Glucose (Foslip). Determined by others, the particle size of Fospeg ≈140 nm and of Foslip ≈ 120 nm [41,43]. All solutions were prepared before the start of the experiments. Foscan was made by dissolving the stock-solution (4 mg/ml mTHPC in water-free PEG-EtOH) in a solution of PEG400: EtOH: water = 3:2:5 (v/v). Foslip and Fospeg were dissolved as recommended by the manufacturer for intravenous injection in 5% aqueous glucose solution and in sterile water respectively. Polyethylene glycol 400 (PEG400) was obtained from Sigma-Aldrich (Zwijndrecht, the Netherlands) and 96% ethanol (EtOH) from Merck (Amsterdam, The Netherlands). All photosensitizers were diluted to reduce errors when injecting a small volume. Depending on the weight of the rat, the average amount of injected solution was 0.25 ml. All solutions were prepared with minimal light and kept at 4 °C in the dark prior to the experiments.
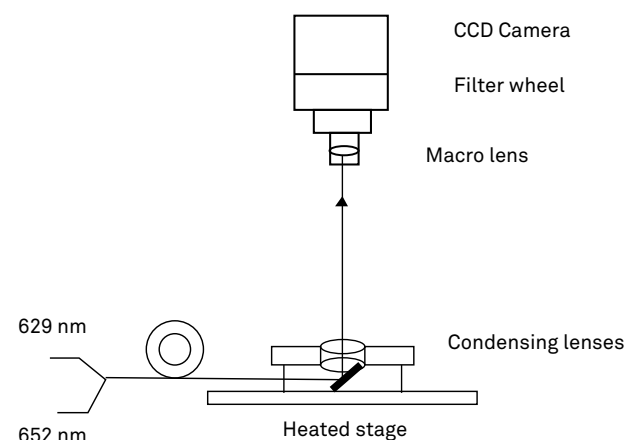
Figure 1. Experimental setup.

Experimental procedures

Experiments were performed after the tumors in the skin fold chamber had visibly grown and adequate blood circulation in the window chamber was observed. The animals were sedated and placed on a temperature controlled positioning stage, allowing reproducible positioning of the animal under the camera using a customized imaging program. A schematic diagram of experimental setup is presented in figure 1. An autofluorescence image was made and subsequently one of the photosensitizers was injected via a tail vein of the animal. The mTHPC fluorescence pharmacokinetics in the chamber model was investigated in time after intravenous mTHPC administration. The dose used for intravenous injection was 0.15 mg/kg of mTHPC for each formulation. Eight rats were injected with Foscan, 5 with Fospeg and 5 with Foslip. At T=0 (before mTHPC injection), 5 minutes, 2, 4, 8, 24, 48 and 96 hours p.i. (post injection) fluorescence images of the chamber were recorded. Before imaging, the position of the chamber relative to the charge-coupled device (CCD) was checked to be the same compared to previous measurements. After 96 hours all animals were terminated by cervical dislocation. Animal experiments were performed under protocols approved by the experimental welfare committee of the Erasmus MC and conformed to Dutch and European regulations for animal experimentation.

Experimental setup

To obtain quantification of fluorescence images, the experimental setup (figure 1) and correction method of Kascakova et al. [(46)] was used. Briefly, the localization of mTHPC within the chamber was visualized by acquiring fluorescence and transmission images with a combination of two excitation light sources: dye laser 629 nm (Spectra physics, Darmstadt,

Germany, model 171 argon laser, pumping a model 375 dye laser with DCM as lasing medium) and 652 nm diode laser (Biolitec pharma, Edinburgh, The United Kingdom). Light was coupled from a bifurcated optical fiber into the base of a heated stage. Using a system of condensing lenses, a uniform and equal excitation field has been obtained. The fluence rate of both excitation wavelengths was 0.6 mW cm^{-2}. The light transmitted through the chamber was collected using a f2.8/105 mm macro lens coupled to a CCD camera (ORCA-ER, Hamamatsu, Japan). The macro lens can be used to zoom in on a specific area within the sample resulting in a square field of view of 4.5 mm. For fluorescence and transmission imaging, the filter wheel (L.O.T.-Oriel, Stratford, USA) has been placed between the macro lens and CCD camera. Details on specification of filters, which were placed into the filter wheel, are provided by Kascakova et al [46]. Note, three detection channels have been used in order to obtain fluorescence and transmission: 1) the band pass filter 720 ± 10 nm; 2) the long pass filter 763 nm; and 3) the neutral density filter with 10% transmission for both excitation wavelength lights. The integration time of the camera was 30 s for each excitation and filter combination used to visualize tissue fluorescence. The fluence delivered during these measurements was approximately 0.072 J cm^{-2} per measured time point and the total fluence for each chamber was approximately 0.504 J cm^{-2}

Principle of ratio fluorescence imaging technique

To accurately quantify the fluorescence intensity for mTHPC, a correction for the autofluorescence, tissue optical properties and thickness variation between chambers and between different tissues in chamber, is important. This correction was done according to the ratio fluorescence imaging technique developed by Kascakova et al. [46] This method is based on dual-wavelength excitation and dual-wavelength detection in near infrared (NIR): One excitation wavelength is chosen to be at an absorption maximum of mTHPC ($\lambda = 652$ nm) and the other at its absorption minimum ($\lambda = 629$ nm)). The two emission wavelengths are chosen to be at the secondary fluorescence maximum of mTHPC (at $\lambda = 720$ nm, e.g. band pass filter 720 ± 10 nm) and in the region of no photosensitizer fluorescence (long pass filter 763 nm). The correction is then provided according to the equation:

$$R = \frac{F(\lambda_{exc\,652nm}, \lambda_{emisBP720nm}) - F(\lambda_{exc\,629nm}, \lambda_{emisBP720nm})}{F(\lambda_{exc\,629nm}, \lambda_{emisLP763nm})}$$

$F(\lambda_{exc}652nm, \lambda_{emis}BP720nm)$ is the fluorescence image detected by excitation light source of 652 nm in the wavelength region 720 ± 10 nm, i.e. it is the fluorescence image detected by excitation at an absorption maximum of mTHPC and detected at the secondary fluorescence maximum of mTHPC. Since the fluorescence emission detected in the band pass filter 720 ± 10 nm by 652 nm excitation will lead to both: high mTHPC fluorescence emission as well as background autofluorescence excited by this wavelength, a correction for background auto-
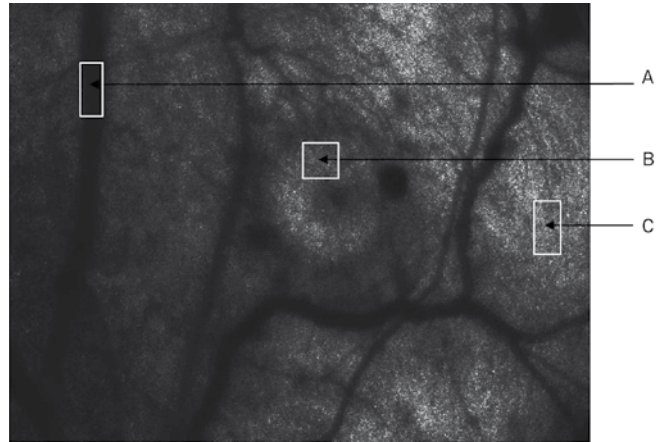
Figure 2. Example of regions of interest in a transmission image taken by confocal microscopy of the window-chamber model, showing vasculature (A), tumor tissue (B) and normal tissue (C).
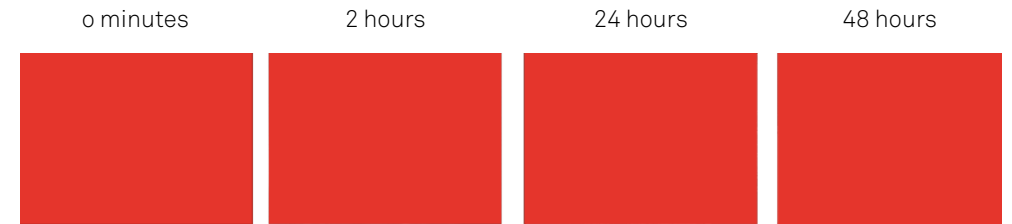

Figure 3. The time dependent evolution of the corrected fluorescence images of the chamber model after mTHPC administration, in this case Foscan. Fluorescence diffusion in time out of the vasculature can be seen.

fluorescence in the band pass filter 720 ± 10 nm is necessary. For this purpose, the subtraction of fluorescence signal detected in the band pass filter 720 ± 10 nm by excitation at 629 nm was included, e.g. $F(\lambda_{exc}629nm, \lambda_{emis}BP720nm)$. Thus the $F(\lambda_{exc}629nm, \lambda_{emis}BP720nm)$ is the fluorescence image detected by excitation at an absorption minimum of mTHPC and detected at a fluorescence maximum of mTHPC. It will lead to low mTHPC fluorescence emission and background autofluorescence excited by this wavelength. Assuming that excitation at 629 nm and 652 nm leads to the same autofluorescence, subtraction of the fluorescence signals detected in the 720 nm band pass filter will be corrected for autofluorescence. Subsequently, this difference is divided by the $F(\lambda_{exc}629nm, \lambda_{emis}LP763nm)$. $F(\lambda_{exc}629nm, \lambda_{emis}LP763nm)$ is the fluorescence image detected by excitation at an absorption minimum of mTHPC and detected at a fluorescence minimum of mTHPC. This will lead only to autofluorescence detection. Assuming that the autofluorescence is influenced by tissue absorbers, scatters and chamber thickness the same way as mTHPC fluorescence is, the division for autofluorescence will correct for tissue optical properties and chamber thickness.

Image analysis
In the present study, 18 rats were injected with an mTHPC formulation. However, due to presence of inflammation or absence of tumor tissue, only 11 rats were suitable for image analysis. All fluorescence images were first corrected for differences in background fluorescence and variations in laser output of both excitation light sources. Both background fluorescence and laser-output were determined before each measurement.
Images were co-registered at each of the 7 time points by translating and rotating the fluorescence images using anatomical landmarks in transmission images (figures 2 and 3). Af-

ter the procedure, the signal-to-noise ratio was increased by binning of the pixels (4x4). After the binning, the images were resized on the same size of 16-bit image at a resolution of 1344 x 1024 pixels. According to determined square field of view of macro lens, one picture element (pixel) corresponds to approximately 3 micrometer. In the corresponding transmission image the regions of interest were chosen for each tissue type. Tumor and normal tissue regions of interest were chosen so that no large vessels were in, or near the region. Each animal had on average three regions of interest for normal tissue, three regions of interest selected inside the tumor, and three up to five regions of interest for vasculature.
Finally, the subtraction and division of the fluorescence images was done according to the ratio fluorescence imaging technique. Image analysis was done using Labview 7.1 (National Instruments Corporation, Austin, USA).

Statistical analysis
After the corrections, average grey scale values of selected regions of interest (ROIs) were measured. Normal tissue, vessels and tumor could be selected by the transmission image of the window chamber (figure 2). Fluorescence intensities of these ROIs were arranged by tissue type and photosensitizer formulation. Average fluorescence ratios of Foscan were determined from 3 animals, for Foslip and for Fospeg from 4 animals. Statistical analysis was done to compare means of measured fluorescence by performing the two-tailed t-test (α=0.05) using Microcal Origin®, version 6.0 (Microcal Software, Inc., Northampton, MA).

Results

Figures 4-8 show the "fluorescence ratio of mTHPC corrected for tissue optical properties" (from here on termed; "fluorescence intensity") in tumor tissue, normal tissue and vasculature. Figure 4 shows the fluorescence intensity after the administration of Foscan. In vasculature, fluorescence intensity has a peak at 5 minutes and decreases significantly
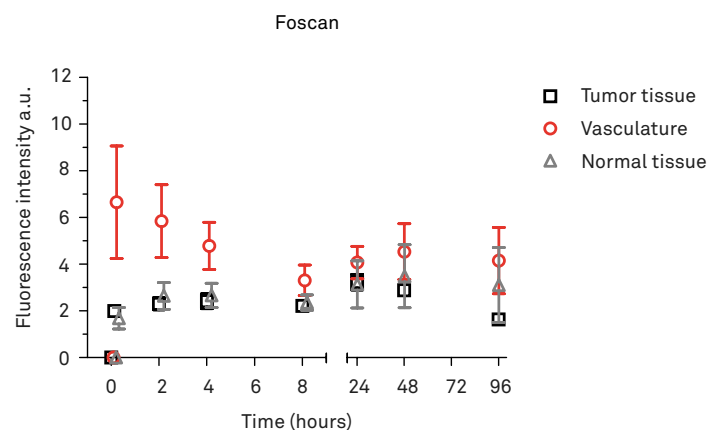
Foscan

Figure 4. mTHPC fluorescence kinetic profile (corrected fluorescence signal) of Foscan within the different tissue types. Error-bars indicate standard deviation of uncertainty.
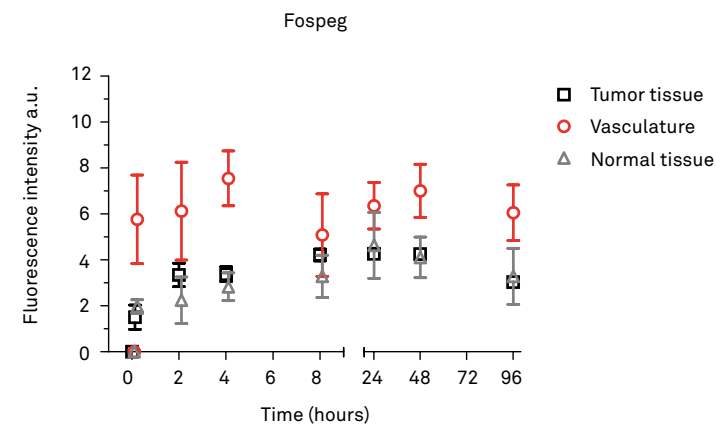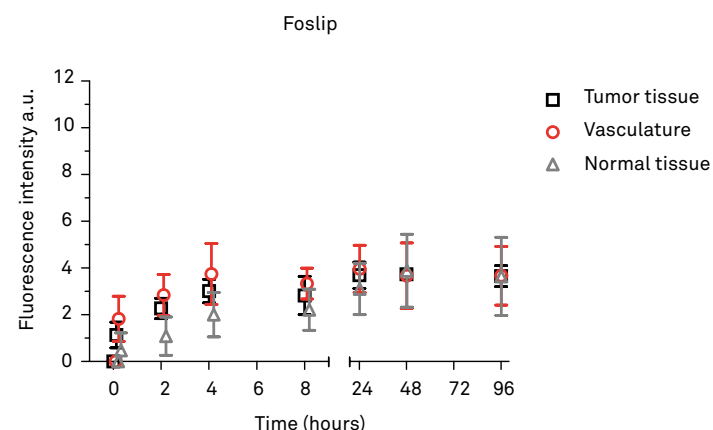
Foslip

Figure 5. mTHPC fluorescence kinetic profile (corrected fluorescence signal) of Foslip within the different tissue types. Error-bars indicate standard deviation of uncertainty.

Fospeg

Figure 6. mTHPC fluorescence kinetic profile (corrected fluorescence signal) of Fospeg within the different tissue types. Error-bars indicate standard deviation of uncertainty.
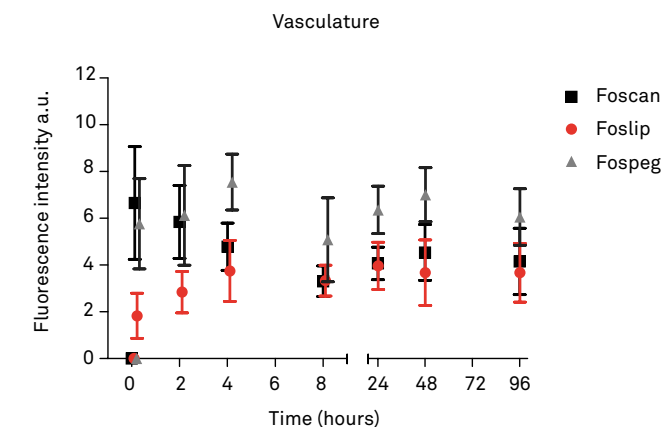
Vasculature

Figure 7. Comparison of mTHPC fluorescence kinetic profile (corrected fluorescence signal) of the three different formulations within the vasculature. Difference in fluorescence-kinetic profile between the different formulations of mTHPC is clear. Error-bars indicate standard deviation of uncertainty.

($p < 0.001$) from 5 minutes to 8 hours p.i. After this decrease, intensities increased significantly ($p = 0.022$) until 24 hours, with a positive trend towards a second peak at 48 hours for vasculature. In tumor tissue, the fluorescence intensity increased significantly ($p = 0.019$) between 2 and 24 hours p.i., reached a maximum between 24 – 48 hours and decreased significantly ($p < 0.001$) after 48-hours. During the experiment we found significant ($p < 0.05$) higher fluorescence intensity for vasculature compared to tumor tissue, except for the 24-hour time point ($p = 0.075$). However, no time points showed a significant ($p < 0.05$) difference in fluorescence intensity between normal tissue and tumor tissue (tumor selectivity).

Figure 5 shows the fluorescence intensity after the administration of Foslip. In vasculature,

fluorescence intensity increased significantly ($p = 0.025$) in the first 2 hours with a trend ($p = 0.085$) towards a further increase at 4 hours. Between 4 and 96 hours, the intensities remained stable except for a small dip at 8 hours. In tumor tissue, fluorescence intensity increased significantly ($p < 0.05$) in the first 4 hours and again ($p = 0.041$) between 8 and 24 hours p.i. After 24 hours, intensities in tumor tissue remained at a maximum for at least the 96-hour time point. For the first 8 hours, intensities in the vasculature were significantly higher than in normal tissue. Interestingly, tumor selectivity ($p < 0.05$) was shown for the 2- and 4-hour time points.

Figure 6 shows the fluorescence intensity after administration of Fospeg. In the vasculature,
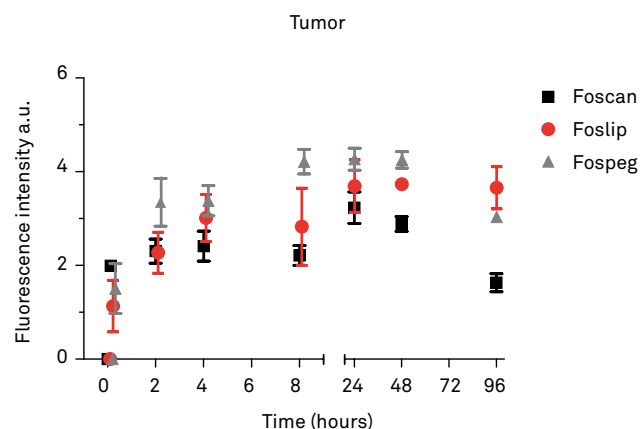
Figure 8. Comparison of mTHPC fluorescence kinetic profile (corrected fluorescence signal) of the three different formulations within tumor tissue. Fospeg has a tendency for highest intensities from 2 – 48 hrs with Foslip showing highest intensity at 96 hrs p.i. Error-bars indicate standard deviation of uncertainty.

the fluorescence intensity remains stable throughout the experiment, with a positive trend (p=0.411) towards a 4-hour maximum. In tumor tissue, the intensity increased (p<0.05) significantly for the 2- and 8-hour time points. From then until the 48-hour time point, a plateau of maximum fluorescence intensity is reached. After 48 hours, the intensity in tumor decreases significantly. For the duration of the experiment, excluding the 8- and 24-hour time points, a significant (p<0.05) difference in fluorescence intensities was observed between the vasculature and (tumor) tissue. Unfortunately, no significant (p<0.05) difference between normal and tumor tissue (tumor selectivity) was found. However, the p-value of the 5-minute, 2- and 4-hour time points nearly reached significance (p=0.075, 0.137 and 0.089 respectively).

Figure 7 shows a comparison of the fluorescence intensities of Foscan, Foslip and Fospeg in vasculature. Overall, the fluorescence intensity of Fospeg is higher than both other formulations, in particular (p<0.05) at the 4, 8, 24 and 48 time points. A marked difference between formulations is that in the first 4 hours the intensity of Foscan decreases, while the intensity of both liposomal formulations increases to their maximum intensity. After 24 hours, all 3 formulations reach a stable intensity in vasculature.

Figure 8 shows a comparison of the fluorescence intensities of the three formulations in tumor tissue. Fospeg shows the overall highest fluorescence intensity between 2 – 48 hours, particularly (p<0.05) at the 2, 8 and 48 hour time points, whereas Foscan has the lowest tumor intensities. An interesting difference between the formulations is the time at which the maximum fluorescence intensity in tumor is reached; both Foscan and Foslip reach their maximum at the 24 hour time point, while Fospeg reaches its maximum already at the 4 hour

time point. However, before its 24 hour maximum, Foslip has a smaller peak at the same 4 hour time point. This smaller peak has approximately the same intensity as the maximum fluorescence intensity of Foscan.

Discussion

In this study, we investigated the fluorescence kinetic profile of mTHPC after systemic administration of liposomal formulations (Foslip and Fospeg) and the ethanol based formulation (Foscan) in the window chamber model. With the ratio fluorescence imaging technique we used a combination of dual-wavelength excitation and dual-wavelength detection in the NIR region to correct for changes of tissue optical properties and thickness in time [46].
Fospeg showed overall high fluorescence intensities in tumor and normal tissue for all time points compared to the other formulations. Foslip reached fluorescence intensities in between Foscan and Fospeg. Our findings suggest that liposomal bound mTHPC enhances the bioavailability of mTHPC in vasculature and tumor tissue, in particular that of mTHPC encapsulated in pegylated liposomes (Fospeg). Furthermore, when comparing the times at which maximum fluorescence intensities were reached in tumor tissue, Fospeg showed an earlier maximum peak at 8 hours p.i., with both Foscan and Foslip reaching their maximum peak at 24 hours p.i. This suggests that Fospeg not only has increased fluorescence uptake in tumor tissue but also reaches this earlier compared to Foscan and Foslip. In our model, both Foslip and Fospeg showed high tumor-to- normal tissue ratios (tumor selectivity) at 2 and 4 hours p.i. However, only with Foslip the differences in fluorescence intensity between tumor and normal tissue proved to be significant at these time points.
In agreement with others, Foscan showed a first fluorescence peak in vasculature direct post injection with a second peak 24 hours post injection as described extensively by others [12,49]. Interestingly, Fospeg showed overall higher vascular fluorescence intensities compared to Foscan as was seen by others [41]. The higher intensity can be explained by a low recognition and thus low uptake of pegylated liposomes by the MPS, which enhances circulation time [31,37,42,43,50].

Another effect that increases the fluorescence intensity is the relatively higher amount of non-aggregated mTHPC molecules in liposomal formulations [31]. However, despite the monomeric form of mTHPC within liposomes, Foslip showed fluorescence intensities in vasculature comparable to Foscan. This was also observed in an *in vitro* model by Kiesslich et al. as they found no difference in the relative amount of plasma protein bound Foscan or Foslip [44]. A possible explanation is the rapid opsonization by plasma proteins or phagocytosis of conventional liposomes (like Foslip). Subsequent transportation to the MPS, thus decreasing the plasma half-life in vasculature [26,37]. These effects could explain the observed low fluorescence in vasculature and the stable fluorescence pharmacokinetics in tissue with Foslip, according to Svensson et al. [26]. Interestingly, Pegaz et al. found similar vascular kinetic

profile for Fospeg and Foslip during their experimental time of 30 minutes p.i. [42]. This suggests that the conventional liposomes are intact for at least 30 minutes, after which Foslip is rapidly transferred from the vasculature. However, in our model the fluorescence intensity in the vasculature is also low, but does not decrease as rapidly as reported by Svensson et al. [26] The most interesting findings of our experiments were the higher and the earlier tumor fluorescence peaks with Fospeg and to a lesser extent with Foslip compared to Foscan. Our results were in agreement with other *in vivo* studies which also showed higher uptake of the liposomal mTHPC formulations in tumor tissue [26,41]. The observed higher tumor fluorescence of the liposomal formulations compared to Foscan has several explanations. Aggregation of mTHPC molecules in Foscan has been observed and is more likely to occur than with liposomal bound mTHPC [34]. This aggregation is associated with diminished fluorescence, increased uptake by the MPS and delayed uptake into tissue. As only when the aggregates are disassociated, mTHPC can bind to plasma proteins [34,51]. Next to aggregation of the standard Foscan formulation, the increased circulation half-life of Fospeg may explain its higher uptake into (tumor) tissue and subsequently leads to higher fluorescence intensities. This way, the shorter circulation half-life of Foslip and especially Foscan is likely to be responsible for the lower tumor fluorescence.

The 24 hour time point at which Foscan reached its maximum tumor fluorescence in our study was in agreement with the study of Jones et al. [12]. For Fospeg Bucholz et al. found its maximum slightly earlier at 4 hours [41]. For Foslip a comparison with Svensson et al. was difficult due to the short experimental times they investigated [(26)].

As we mentioned previously, other studies have reported on higher tumor-to-normal tissue ratio's (tumor selectivity) for other photosensitizers encapsulated in liposomes compared to the original formulation [31-33,36-39]. We observed significant tumor selectivity for Foslip at early time points, as did Svensson et al [26]. For Fospeg we found a non-significant, trend towards tumor selectivity at early time points. In contrast, Buchholz et al. did find significant tumor selectivity for Fospeg, but they did not correct their optical measurements for variations in thickness or for tissue optical properties [41]. The absence of tumor selectivity for Foscan we found, is in agreement with other studies [13,52]. Our results thus suggest some tumor selectivity for liposomal formulations compared to ethanol based formulation, but limited to early time points.

Passive accumulation of mTHPC can have several explanations. One explanation is the tendency of proliferating cells (tumor) to show an increased number of LDL receptors, while liposomes serve as donors of photosensitizers to these lipoproteins [31,37]. Thus, tumor cells would attract LDLs with entrapped photosensitizers. A second explanation for passive accumulation is the EPR effect [31,37,38]. This effect is present when the vasculature becomes more permeable for larger molecules due to local biochemical changes in tumor tissue or due to the often poor quality of tumor vessels originated from tumor-angiogenesis. The increased retention of the larger molecules is present when lymphatic drainage is diminished, which is characteristic of tumor tissue. This EPR effect can lead to accumulation of high molecular drugs, like liposomes, in tumor tissue [29,31,40].

A surprising finding was the significant ($p < 0.05$) higher mTHPC fluorescence of Foslip at 96 hours compared to both other formulations. Detailed analysis of this time point shows that while the fluorescence of both Foscan and Fospeg decrease, the fluorescence of Foslip remains stable. A possible explanation for this finding could be the described association of conventional liposomes with the MPS [26]. This potentially causes association of conventional liposomes to inflammatory cells close to tumor tissue. With Fospeg this is much less, as pegylated liposomes are harder to recognize by the MPS.

The exact effects of mTHPC aggregates on the optical fluorescence measurements are not fully known. While mTHPC molecules are in monomeric form when incorporated into liposomes, aggregates can form when distributed within cells at high concentrations [53]. These aggregates can not be accurately measured by optical fluorescence measurements, and could result in underestimation of the amount of mTHPC molecules. However, one might assume that only mTHPC molecules that are capable to fluoresce are potentially important for PDT.

In future experiments, it is important to consider that higher fluorescence intensities may not necessarily lead to higher PDT efficacy response. Although it is known that other hydrophobic drugs encapsulated into liposomes display a higher photosensitizing efficacy compared to the original formulation [31-33,36], only two *in vivo* studies briefly describe at least similar efficacy for liposomal mTHPC compared to Foscan [41,42]. Very little conclusions can be drawn from these studies since they did not systematically investigate the PDT response of the different formulations. Therefore studies should be undertaken to demonstrate the (pre) clinical relevance of the different fluorescence kinetics.

Beyond the scope of this study but interesting nonetheless, is the superior biocompatibility of liposomal formulations. Besides the water-soluble formulation of liposomal mTHPC, a lower dark toxicity *in vitro* compared to Foscan is described, i.e. a low cytotoxic effect without irradiation [44,45].

Conclusion

In summary, our study showed that both liposomal mTHPC formulations reached higher tumor fluorescence intensities at earlier time points compared to the ethanol based mTHPC. This was more pronounced with the pegylated liposomes. At early time points, both liposomal formulations showed higher fluorescence in tumor compared to normal tissue, even reaching significant levels for Foslip. These characteristics of the liposomal mTHPC formulations are interesting as it suggests a possibility for a lower drug dose and a shorter drug-light interval in the future. Our findings suggest that for photodynamic therapy, Foslip and especially Fospeg have interesting advantages over Foscan. Therefore, further experiments designed for evaluating the PDT effect with liposomal mTHPC are needed.
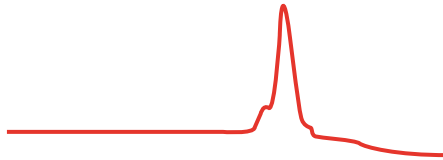
References

1. Dougherty TJ. An update on photodynamic therapy applications. J Clin Laser Med Surg. 2002 02;20(1044-5471; 1044-5471; 1):3-7.

2. Brown SB, Brown EA, Walker I. The present and future role of photodynamic therapy in cancer treatment. Lancet Oncol. 2004 08;5(1470-2045; 1470-2045; 8):497-508.

3. Schuitmaker JJ, Baas P, van Leengoed HL, van der Meulen FW, Star WM, van Zandwijk N. Photodynamic therapy: A promising new modality for the treatment of cancer. J Photochem Photobiol B. 1996 06;34(1011-1344; 1011-1344; 1):3-12.

4. Wilson BC, Patterson MS. The physics, biophysics and technology of photodynamic therapy. Phys Med Biol. 2008 05/07;53(0031-9155; 0031-9155; 9):R61-109.

5. De Rosa FS, Bentley MV. Photodynamic therapy of skin cancers: Sensitizers, clinical studies and future directives. Pharm Res. 2000 12;17(0724-8741; 0724-8741; 12):1447-55.

6. Moore CM, Pendse D, Emberton M, Medscape. Photodynamic therapy for prostate cancer--a review of current status and future promise. Nat Clin Pract Urol. 2009 Jan;6(1):18-30.

7. Bown SG, Rogowska AZ, Whitelaw DE, Lees WR, Lovat LB, Ripley P, et al. Photodynamic therapy for cancer of the pancreas. Gut. 2002 Apr;50(4):549-57.

8. Hopper C. Photodynamic therapy: A clinical reality in the treatment of cancer. Lancet Oncol. 2000 12;1(1470-2045):212-9.

9. Dougherty TJ, Gomer CJ, Henderson BW, Jori G, Kessel D, Korbelik M, et al. Photodynamic therapy. J Natl Cancer Inst. 1998 06/17;90(0027-8874; 0027-8874; 12):889-905.

10. Henderson BW, Dougherty TJ. How does photodynamic therapy work? Photochem Photobiol. 1992 01;55(0031-8655; 0031-8655; 1):145-57.

11. Melnikova VO, Bezdetnaya LN, Potapenko AY, Guillemin F. Photodynamic properties of meta-tetra(hydroxyphenyl)chlorin in human tumor cells. Radiat Res. 1999 10;152(0033-7587; 0033-7587; 4):428-35.

12. Jones HJ, Vernon DI, Brown SB. Photodynamic therapy effect of m-THPC (foscan) in vivo: Correlation with pharmacokinetics. Br J Cancer. 2003 07/21;89(0007-0920; 0007-0920; 2):398-404.

13. Cramers P, Ruevekamp M, Oppelaar H, Dalesio O, Baas P, Stewart FA. Foscan uptake and tissue distribution in relation to photodynamic efficacy. Br J Cancer. 2003 01/27;88(0007-0920; 2):283-90.

14. Pass HI. Photodynamic therapy in oncology: Mechanisms and clinical use. J Natl Cancer Inst. 1993 Mar 17;85(6):443-56.

15. Mitra S, Foster TH. Photophysical parameters, photosensitizer retention and tissue optical properties completely account for the higher photodynamic efficacy of meso-tetra-hydroxyphenyl-chlorin vs photofrin. Photochem Photobiol. 2005 07;81(0031-8655; 0031-8655; 4):849-59.

16. Copper MP, Tan IB, Oppelaar H, Ruevekamp MC, Stewart FA. Meta-tetra(hydroxyphenyl) chlorin photodynamic therapy in early-stage squamous cell carcinoma of the head and neck. Arch Otolaryngol Head Neck Surg. 2003 07;129(0886-4470; 7):709-11.

17. Lorenz KJ, Maier H. Photodynamic therapy with meta-tetrahydroxyphenylchlorin (foscan((R))) in the management of squamous cell carcinoma of the head and neck: Experience with 35 patients. Eur Arch Otorhinolaryngol. 2009 03/17(1434-4726).

18. European Medicines Agencies. H-C-318 foscan european public assessment report. 2009 04/30.

19. D'Cruz AK, Robinson MH, Biel MA. mTHPC-mediated photodynamic therapy in patients with advanced, incurable head and neck cancer: A multicenter study of 128 patients. Head Neck. 2004 03;26(1043-3074; 1043-3074; 3):232-40.

20. Lou PJ, Jager HR, Jones L, Theodossy T, Bown SG, Hopper C. Interstitial photodynamic therapy as salvage treatment for recurrent head and neck cancer. Br J Cancer. 2004 Aug 2;91(3):441-6.

21. Jerjes W, Upile T, Akram S, Hopper C. The surgical palliation of advanced head and neck cancer using photodynamic therapy. Clin Oncol (R Coll Radiol). 2010 Nov;22(9):785-91.

22. Hopper C, Kubler A, Lewis H, Tan IB, Putnam G. mTHPC-mediated photodynamic therapy for early oral squamous cell carcinoma. Int J Cancer. 2004 08/10;111(0020-7136; 0020-7136; 1):138-46.

23. Kubler AC, de Carpentier J, Hopper C, Leonard AG, Putnam G. Treatment of squamous cell carcinoma of the lip using foscan-mediated photodynamic therapy. Int J Oral Maxillofac Surg. 2001 12;30(0901-5027; 0901-5027; 6):504-9.

24. Karakullukcu B, van Oudenaarde K, Copper MP, Klop WM, van Veen R, Wildeman M, et al. Photodynamic therapy of early stage oral cavity and oropharynx neoplasms: An outcome analysis of 170 patients. Eur Arch Otorhinolaryngol. 2011 Feb;268(2):281-8.

25. Jerjes W, Upile T, Betz CS, El Maaytah M, Abbas S, Wright A, et al. The application of photodynamic therapy in the head and neck. Dent Update. 2007 10;34(0305-5000; 8):478,4, 486.

26. Svensson J, Johansson A, Grafe S, Gitter B, Trebst T, Bendsoe N, et al. Tumor selectivity at short times following systemic administration of a liposomal temoporfin formulation in a murine tumor model. Photochem Photobiol. 2007 09;83(0031-8655; 0031-8655; 5):1211-9.

27. Triesscheijn M, Ruevekamp M, Antonini N, Neering H, Stewart FA, Baas P. Optimizing meso-tetra-hydroxyphenyl-chlorin-mediated photodynamic therapy for basal cell carcinoma. Photochem Photobiol. 2006 Nov-Dec;82(6):1686-90.

28. Hofman JW, Carstens MG, van Zeeland F, Helwig C, Flesch FM, Hennink WE, et al. Photocytotoxicity of mTHPC (temoporfin) loaded polymeric micelles mediated by lipase catalyzed degradation. Pharm Res. 2008 Sep;25(9):2065-73.

29. Westerman P, Glanzmann T, Andrejevic S, Braichotte DR, Forrer M, Wagnieres GA, et al. Long circulating half-life and high tumor selectivity of the photosensitizer meta-tetrahydroxyphenylchlorin conjugated to polyethylene glycol in nude mice grafted with a human colon carcinoma. Int J Cancer. 1998 06/10;76(0020-7136; 6):842-50.

30. Sasnouski S, Pic E, Dumas D, Zorin V, D'Hallewin MA, Guillemin F, et al. Influence of incubation time and sensitizer localization on meta-tetra(hydroxyphenyl)chlorin (mTHPC)-induced photoinactivation of cells. Radiat Res. 2007 08;168(0033-7587; 0033-7587; 2):209-17.

31. Derycke AS, de Witte PA. Liposomes for photodynamic therapy. Adv Drug Deliv Rev. 2004 01/13;56(0169-409; 1):17-30.

32. Chen B, Pogue BW, Hasan T. Liposomal delivery of photosensitising agents. Expert Opin Drug Deliv. 2005 05;2(1742-5247; 1742-5247; 3):477-87.

33. Damoiseau X, Schuitmaker HJ, Lagerberg JW, Hoebeke M. Increase of the photosensitizing efficiency of the bacteriochlorin a by liposome-incorporation. J Photochem Photobiol B. 2001 04;60(1011-1344; 1011-1344; 1):50-60.

34. Hopkinson HJ, Vernon DI, Brown SB. Identification and partial characterization of an unusual distribution of the photosensitizer meta-tetrahydroxyphenyl chlorin (temoporfin) in human plasma. Photochem Photobiol. 1999 Apr;69(4):482-8.

35. Reuther T, Kubler AC, Zillmann U, Flechtenmacher C, Sinn H. Comparison of the in vivo efficiency of photofrin II-, mTHPC-, mTHPC-PEG- and mTHPCnPEG-mediated PDT in a human xenografted head and neck carcinoma. Lasers Surg Med. 2001;29(4):314-22.

36. Richter AM, Waterfield E, Jain AK, Canaan AJ, Allison BA, Levy JG. Liposomal delivery of a photosensitizer, benzoporphyrin derivative monoacid ring A (BPD), to tumor tissue in a mouse tumor model. Photochem Photobiol. 1993 06;57(0031-8655; 0031-8655; 6):1000-6.

37. Konan YN, Gurny R, Allemann E. State of the art in the delivery of photosensitizers for photodynamic therapy. J Photochem Photobiol B. 2002 03;66(1011-1344; 1011-1344; 2):89-106.

38. Maeda H, Wu J, Sawa T, Matsumura Y, Hori K. Tumor vascular permeability and the EPR effect in macromolecular therapeutics: A review. J Control Release. 2000 03/01;65(0168-3659; 1-2):271-84.

39. Bourre L, Thibaut S, Fimiani M, Ferrand Y, Simonneaux G, Patrice T. In vivo photosensitizing efficiency of a diphenylchlorin sensitizer: Interest of a DMPC liposome formulation. Pharmacol Res. 2003 Mar;47(3):253-61.

40. Huwyler J, Drewe J, Krahenbuhl S. Tumor targeting using liposomal antineoplastic drugs. Int J Nanomedicine. 2008;3(1176-9114; 1):21-9.

41. Buchholz J, Kaser-Hotz B, Khan T, Rohrer Bley C, Melzer K, Schwendener RA, et al. Optimizing photodynamic therapy: In vivo pharmacokinetics of liposomal meta-(tetrahydroxyphenyl)chlorin in feline squamous cell carcinoma. Clin Cancer Res. 2005 10/15;11(1078-0432; 20):7538-44.

42. Pegaz B, Debefve E, Ballini JP, Wagnieres G, Spaniol S, Albrecht V, et al. Photothrombic activity of m-THPC-loaded liposomal formulations: Pre-clinical assessment on chick chorioallantoic membrane model. Eur J Pharm Sci. 2006 05;28(0928-0987; 1-2):134-40.

43. Kachatkou D, Sasnouski S, Zorin V, Zorina T, D'Hallewin MA, Guillemin F, et al. Unusual photoinduced response of mTHPC liposomal formulation (foslip). Photochem Photobiol. 2009 05;85(0031-8655; 0031-8655; 3):719-24.

44. Kiesslich T, Berlanda J, Plaetzer K, Krammer B, Berr F. Comparative characterization of the efficiency and cellular pharmacokinetics of foscan- and foslip-based photodynamic treatment in human biliary tract cancer cell lines. Photochem Photobiol Sci. 2007 Jun;6(6):619-27.

45. Berlanda J, Kiesslich T, Engelhardt V, Krammer B, Plaetzer K. Comparative in vitro study on the characteristics of different photosensitizers employed in PDT. J Photochem Photobiol B. 2010 Sep 2;100(3):173-80.

46. Kascakova S, de Visscher S, Kruijt B, de Bruijn HS, van der Ploeg-van den Heuvel,A., Sterenborg HJ, et al. In vivo quantification of photosensitizer fluorescence in the skin-fold observation chamber using dual-wavelength excitation and NIR imaging. Lasers Med Sci. 2011 Nov;26(6):789-801.

47. van der Veen N, van Leengoed HL, Star WM. In vivo fluorescence kinetics and photodynamic therapy using 5-aminolaevulinic acid-induced porphyrin: Increased damage after multiple irradiations. Br J Cancer. 1994 11;70(0007-0920; 5):867-72.

48. Reinhold HS, Blachiewicz B, Berg-Blok A. Reoxygenation of tumours in "sandwich" chambers. Eur J Cancer. 1979 04;15(0014-2964; 4):481-9.

49. Glanzmann T, Hadjur C, Zellweger M, Grosiean P, Forrer M, Ballini JP, et al. Pharmacokinetics of tetra(m-hydroxyphenyl)chlorin in human plasma and individualized light dosimetry in photodynamic therapy. Photochem Photobiol. 1998 May;67(5):596-602.

50. Immordino ML, Dosio F, Cattel L. Stealth liposomes: Review of the basic science, rationale, and clinical applications, existing and potential. Int J Nanomedicine. 2006;1(1176-9114; 3):297-315.

51. Sasnouski S, Zorin V, Khludeyev I, D'Hallewin MA, Guillemin F, Bezdetnaya L. Investigation of foscan interactions with plasma proteins. Biochim Biophys Acta. 2005 Oct 10;1725(3):394-402.

52. Peng Q, Moan J, Ma LW, Nesland JM. Uptake, localization, and photodynamic effect of meso-tetra(hydroxyphenyl)porphine and its corresponding chlorin in normal and tumor tissues of mice bearing mammary carcinoma. Cancer Res. 1995 Jun 15;55(12):2620-6.

53. Noiseux I, Mermut O, Bouchard JP, Cormier JF, Desroches P, Fortin M, et al. Effect of liposomal confinement on photochemical properties of photosensitizers with varying hydrophilicity. J Biomed Opt. 2008 07;13(1083-3668; 1083-3668; 4):041313.

Chapter 3.2

In vivo quantification of photosensitizer fluorescence in the window-chamber tumor model using dual wavelength excitation and near infrared imaging

Abstract

Background and objective. A major challenge in biomedical optics is the accurate quantification of *in vivo* fluorescence images. Fluorescence imaging is often used to determine the pharmacokinetics of photosensitizers used for photodynamic therapy. Often, however, this type of imaging does not take into account differences in and changes to tissue volume and optical properties of the tissue under interrogation. To address this problem, a ratiometric quantification method is developed and applied to monitor photosensitizer *meta*-tetra(hydroxyphenyl) chlorin (mTHPC) pharmacokinetics in the rat skin-fold observation chamber.

Materials and Methods. The quantification method employs a combination of dual-wavelength excitation and dual-wavelength detection. Excitation and detection wavelengths were selected in the near-infrared region. One excitation wavelength was chosen to be at the Q band of mTHPC, whereas the second excitation wavelength was close to its absorption minimum. Two fluorescence emission bands were used; one at the secondary fluorescence maximum of mTHPC centered on 720 nm and one in a region of tissue autofluorescence. The first excitation wavelength was used to excite the mTHPC and autofluorescence and the second to excite only autofluorescence, so that this could be subtracted. Subsequently the autofluorescence-corrected mTHPC image was divided by the autofluorescence signal to correct for variations in tissue optical properties.

Discussion. This correction algorithm in principle results in a linear relation between the corrected fluorescence and photosensitizer concentration. The limitations of the presented method and comparison with previously published and validated techniques are discussed.

Introduction

The primary response to photodynamic therapy (PDT) is determined by the tissue oxygenation, light fluence (rate) and local concentration of photosensitizer. The biological activity of the photosensitizer within the illuminated volume is related to the concentration of fluorescent active form of photosensitizer. Thus optical imaging of photosensitizer fluorescence (using light doses much lower than are necessary for PDT damage) aids the understanding of PDT by monitoring the photosensitizer spatial distribution and its fluorescence activity. For many years, observation chambers implanted in various animal species and in humans have been used for intravital microscopy of living tissue [1-12]. Through the possibility to transplant neoplastic tissue within the chamber, the skin-fold observation chamber, also known as the window chamber model, was especially developed to monitor the early vascular events, anti-tumor effects and pharmacokinetics of photosensitizers.

However, the ability to accurately quantify the *in vivo* measured fluorescence is critical [13,14]. The fluorescence signal originates not only from the photosensitizer, but also from various other fluorescent molecules naturally present in the tissue, that can cause an unknown and variable amount of background autofluorescence [15]. Moreover, the measured fluorescence signal is also influenced by geometric factors (the distance and the angle of the excitation and detection source relative to tissue surface) and the tissue optics (scattering and absorption of the excitation and fluorescence emission light in the tissue). For example, tissues with higher background absorption coefficients, e.g. due to high melanin or blood content, can decrease the propagation of both the excitation and fluorescence emission light. This is further complicated by the fact that the absorption spectrum of blood depends on its oxygenation. In addition, tumor tissue is less scattering than normal tissue [16-18] and the thickness for the different types of tissue within the chamber varies as well. In general, the tumor within the chamber is thicker than the normal tissue. Furthermore, normal tissue can also show variability in thickness at the different sites within the chamber. Since the collected fluorescence image is influenced by all of the factors discussed above (optical properties of the tissue, tissue autofluorescence, chamber thickness variations and geometric illumination and collection factors), an imaging methodology that corrects for these factors is necessary to obtain quantitative photosensitizer fluorescence images.

Several techniques have been developed to correct the measured fluorescence for tissue autofluorescence, absorption and scattering properties of the tissue and variations in irradiance, excitation geometry and detection efficiency. Profio [19] calculated the ratio of fluorescence marker signal over the reference autofluorescence. Baumgartner et al. [20] and Witjes et al. [21] described a subtraction method, where the autofluorescence background signal is subtracted using dual-wavelength excitation. In our group, Sinaasappel and Sterenborg developed the double ratio technique based on dual-wavelength excitation and dual-wavelength detection [15] and more recently Saarnak et al. [22] published a ratiometric method based

on measuring the autofluorescence signal prior to marker administration.

Bogaards et al. [14] reviewed the performance of these correction methods for various input parameters over ranges that can be expected during *in vivo* imaging around a standard set of optical properties representing those for human skin. The study revealed that the subtraction method of Baumgartner et al. [20] corrected the detected fluorescence signal of marker for variations in autofluorescence, but applied subtraction is not sufficient to correct for variations in irradiance, excitation geometry and tissue optical properties. The ratiometric methods of Profio [19], Sinaasappel and Sterenborg [15] and Saarnak et al. [22] completely corrected for variations in irradiance, excitation geometry and detection efficiency. The correction for tissue optical properties was to a great extent also achieved using ratiometric methods. However, the method of Profio [19] remained dependent on changes in autofluorescence. The method of Saarnak et al. [22] demonstrated the best quantification performance, as it depends only on the concentration of the fluorophore. This method is based on image acquisition before and after fluorophore administration, and it requires that these subsequent images are taken from the same tissue site under an identical geometry. Here the assumption was made, that the optical properties and autofluorescence may change spatially within the image, but remain constant over the time interval between image acquisitions. However, these conditions are typically not met during window chamber pharmacokinetics experiments. Especially the assumption that autofluorescence, tissue optical properties and tissue thickness remain constant over the time period for which marker pharmacokinetics is studied (typically over periods of up to 7 days) may not be valid. In this case, the method of Sinaasappel and Sterenborg [15], which does not have such restrictive conditions with respect to window chamber changes over time, was revealed to be a better option for fluorophore quantification. However, the double ratio method of Sinaasappel and Sterenborg [15] suffers from a significant drawback: the relation between marker fluorescence and marker concentration is non-linear and saturates for high marker concentrations. This severely limits the applicability of the double ratio correction technique for determining absolute fluorophore concentrations for the study of photosensitizer pharmacokinetics, where large variations (several orders of magnitude) in fluorophore concentrations need to be quantified [14,22].

In summary, two important factors limit the quantification performance of state-of-the-art ratiometric methods: 1) the remaining dependence of the methods on time-dependent variations in autofluorescence, tissue optical properties and tissue thickness [14] and 2) the relation between marker fluorescence and marker concentration is non-linear and saturates for high marker concentrations. In the present study we address both issues using a novel ratiometric method that corrects for time-dependent variations in tissue thickness and tissue optical properties and features a linear response even for high photosensitizer concentrations. In addition, in our method we minimize the dependence of the fluorescence signal on tissue optical properties by selecting the excitation and emission wavelengths in the red and in the near infrared (NIR), where the tissue absorption and scattering coefficients are relatively small and do not vary much with wavelength [14]. We have applied our method to measure the pharmacokinetics of the second–generation photosensitizer *meta*-tetra(hydroxyphenyl)chlorin (mTHPC, INN: Temoporfin, Foscan®) in the rat skin-fold observation chamber (window chamber model).

Materials and methods

Materials

mTHPC (Foscan) (c = 4 mg mTHPC/ml dissolved in PEG, EtOH, water free solution) was obtained from Biolitec pharma (Edinburgh, The United Kingdom). Alexa Fluor 720 was obtained from Invitrogen (Breda, The Netherlands). Polyethylene glycol 400 (PEG400), Evans Blue and Titanium dioxide (TiO_2) were obtained from Sigma-Aldrich (Zwijndrecht, The Netherlands) and 96% ethanol (EtOH) was purchased from Merck (Amsterdam, The Netherlands). Stock solution of mTHPC was dissolved in a solution of PEG400:EtOH:water = 3:2:5 (v/v) to a concentration c = 0.126 mg/ml. The solution was stored in the dark for at least 30 minutes prior to injection, after which the sample was determined to be stable, i.e. no changes in fluorescence peak intensity were detected. To investigate the state of photosensitizer after 30 minutes from mixing with PEG:EtOH:H_2O mixture, the absorption spectra of mTHPC were recorded in the concentration range c = 0.11 – 200 μM. Over the concentration range the spectrum of mTHPC did not change and the solution accurately followed Beer's law with no evidence of spectral peak broadening or shifts in absorption maxima. The same species of mTHPC, i.e. the monomer, is present at the concentration administrated to the animal. The prepared mTHPC solution was administered intravenously at a dose of 0.15 mg kg^{-1} body weight under Isoflurane/O_2/N_2O anesthesia.

Animal model

The animal experiment committee of the Erasmus Medical Center approved the experimental design for this study. Skin-fold observation chambers were prepared using a slightly modified technique to the one that has been described previously [10,23]. Briefly, the chamber was prepared on the back of female Fisher-344 rats (weight m = 144 ± 3 g) in four operations (carried out under general Isoflurane/O_2/N_2O anesthesia) during the period of two weeks. As a result of these operations a thin layer of subcutaneous tissue was clamped between mice and cover slide. In the first operation sterile air (12 ml) was subcutaneously injected on the back of the rat to gently separate the skin from underlying tissue. In the second operation plastic ring and cover slide was positioned under the skin above the subcutaneous tissue matching the vessels. The third operation was proceeding on the second week. During this operation, the skin was folded, prepared and fixed in the splint. Finally, during the last operation, the mammary adenocarcinoma (R3230AC) tumor was transplanted in the layer of normal tissue, reached by unscrewing the cover slide on top of the chamber. Within five to seven days the chamber was ready for treatment, i.e. the tumor was supported by blood ves-
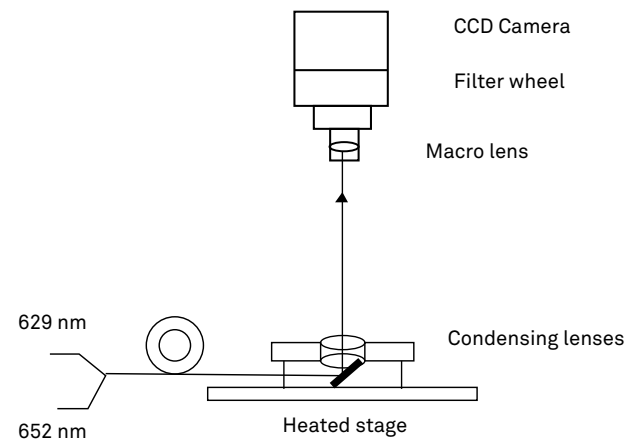
Figure 1. The schematic diagram of the experimental setup.

Figure 2. Schematic excitation (*black line*) and emission spectra (excitation wavelength 652 nm) (*grey line*) of mTHPC based on *in vivo* measurement from rat muscle tissue 16 hours after i.v. injection of mTHPC (c = 0.15 mg.kg-1). The *red line* shows the tissue autofluorescence (excitation wavelength 652 nm) measured in vivo from rat muscle tissue. Presented spectra are based on previous measurements monitoring mTHPC in muscle tissue using differential pathlength spectroscopy (DPS) and fluorescence differential pathlength spectroscopy (fDPS) [32]. The figure includes also transmission characteristics of band pass filter 720 ± 10 nm (*dash dot grey line*) and long pass filter 763 nm (*dash dot red line*) in combination with short wave pass filter 850 nm (used to shield the CCD camera from very long wavelength light).

sels and had visibly grown. Ideally the chamber contained fat cells and capillaries over an area of approximately 1 cm in diameter with some supporting arterioles and venules.

Experimental setup
A schematic diagram of the experimental setup is presented in figure 1. The mTHPC fluorescence pharmacokinetics in the chamber model was investigated in time after intravenous mTHPC administration. The experimental time points were: 0 min (before mTHPC administration) and 5 min, 2 hours, 4 hours, 8 hours, 24 hours, 48 hours and 96 hours after mTHPC i.v. injection. The localization of photosensitizer within the chamber was visualized by acquiring fluorescence and transmission images with two excitation laser light sources: dye laser 629 nm pumped by argon ion laser (Spectra Physics, Darmstadt, Germany) and 652 nm diode laser (Biolitec pharma, Edinburgh, The United Kingdom). Light was coupled from a bifurcated optical fiber using a system of condensing lenses into the base of a heated X-Y stage to produce a uniform distribution of both excitation wavelength lights through the sample. The fluence rate of each excitation illumination was 0.6 mW/cm^2 and the excitation fields were uniform and equal. For fluorescence and transmission imaging light transmitted through the chamber was collected using an f2,8/105 mm macro lens and imaged onto a charge-coupled device (CCD) camera (ORCA-ER, Hamamatsu, Japan). The macro lens can be used to zoom in on a specific area within the sample resulting in a square field of view of 4.5 mm. Detection filters were placed in a filter wheel (L.O.T.-Oriel, Stratford, USA) between the macro lens and the CCD camera in order to obtain the fluorescence (band pass filter 720 ± 10 nm (Omega Optical, Blattleboro, USA), long pass filter 763 nm (transmission: 763 nm – 1050 nm, Omega Optical, Blattleboro, USA) and transmission (neutral density filter with 10% transmission for excitation wavelength light sources 652 nm and 629 nm, Omega Optical,
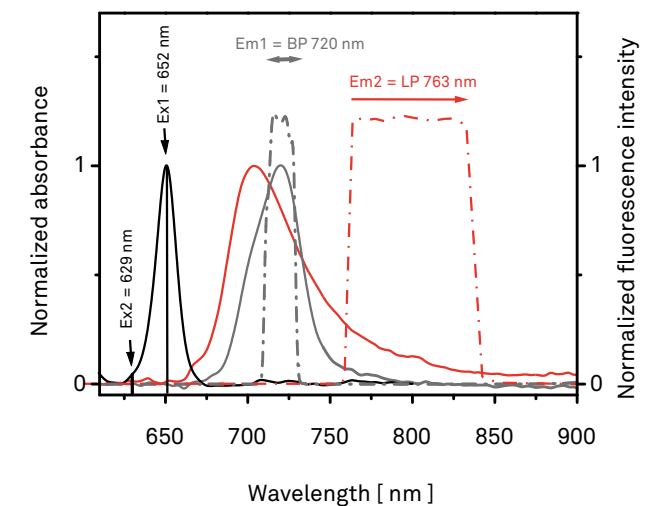
Blattleboro, USA). To eliminate the presence of excitation light in the fluorescence detection channels, the identical long pass filters 690 nm (transmission: 690 nm – 1050 nm, Omega Optical, Blattleboro, USA), were placed together with band pass filter 720 ± 10 nm and long pass filter 763 nm. In addition, to shield the CCD camera from very long wavelength light, a short pass filter 850 nm (transmission: 845 nm – 585 nm, blocking: 880 nm – 1100 nm, L.O.T.-Oriel, Stratford, USA) was placed between the exit of the filter wheel and the CCD camera. The integration time of the camera was 30 s for each excitation and filter combination used to visualize tissue fluorescence. The fluence delivered during these measurements was approximately 0.072 J cm^{-2} per measurement time point. The total fluence delivered to each chamber was approximately 0.504 J cm^{-2} during the course of the experiment. Between measured time points, animals were conscious and placed in a dark and warm environment.

Principle of correction method
The ratiometric method used in this study is illustrated in figure 2, where the *in vivo* absorption and emission spectra of mTHPC are presented with the combined transmission characteristics of the filters used for fluorescence detection.

The method presented here is based on dual-wavelength excitation and dual-wavelength detection: One excitation wavelength is chosen to be at an absorption maximum of mTHPC and the other at its absorption minimum. The two emission wavelengths are chosen to be at the secondary fluorescence maximum of mTHPC (at λ = 720 nm) and in the region of no photosensitizer fluorescence. The reason for such a wavelength selection was to detect the changes in amount of mTHPC fluorescence and monitor the autofluorescence changes in real time. The excitation of mTHPC with 652 nm wavelength (Q band absorption maximum of mTHPC (figure 2) will produce the highest fluorescence compared to excitation by any other wavelength in the red region of the mTHPC spectra. The second excitation wavelength was 629 nm. This excitation wavelength corresponds to an absorption minimum of mTHPC (figure 2). Therefore, excitation of mTHPC with 629 nm wavelength leads to only small amounts of mTHPC fluorescence emission at 720 nm. Furthermore, the fluorescence of mTHPC decreases rapidly beyond 730 nm (with a minimal fluorescence for wavelengths above 750). Therefore, excitation at 629 nm and detection of fluorescence for wavelengths longer than 763 nm will give us information on how background autofluorescence changes with time. It is important to note, that fluorescence emission detected in the band pass filter 720 ± 10 nm (λ_{exc} = 652 nm) is a spectral convolution of mTHPC fluorescence and background autofluorescence. Therefore, correction for background autofluorescence in the band pass filter 720 ± 10 nm is necessary. For this purpose, the subtraction of fluorescence signal detected in the band pass filter 720 ± 10 nm by excitation at 629 nm was included. Subsequently, to ensure correction for tissue optical properties, this difference is divided by the autofluorescence signal excited by 629 nm wavelength and detected in the region of wavelengths longer than 763 nm.

Two assumptions are made: 1) the excitation at 629 nm and 652 nm wavelengths lead to the same autofluorescence, i.e. difference in yield of fluorescence for the tissue fluorescence by excitation at 652 nm and 629 nm is minimal; 2) the excitation by 629 nm wavelength does not lead to mTHPC fluorescence detection at wavelengths longer than 763 nm.

Subtraction and division of the images was performed according to the following equation:

$$R = \frac{F(\lambda_{exc\,652nm}, \lambda_{emisBP720nm}) - F(\lambda_{exc\,629nm}, \lambda_{emisBP720nm})}{F(\lambda_{exc\,629nm}, \lambda_{emisLP763nm})} \quad (1)$$

where $F(\lambda_{exc\,652\,nm}, \lambda_{emis\,BP\,720\,nm})$ is the fluorescence image detected by excitation light source of 652 nm in the wavelength region 720 ± 10 nm; $F(\lambda_{exc\,629\,nm}, \lambda_{emis\,BP\,720\,nm})$ is fluorescence image registered by excitation light of 629 nm wavelength and fluorescence detected in the wavelength region 720 ± 10 nm and $F(\lambda_{exc\,629\,nm}, \lambda_{emis\,LP\,763\,nm})$ is the image excited by wavelength 629 nm, fluorescence detection for the wavelength region > 763 nm.

Image analysis
Image analysis was performed using the Labview 7.1 (National Instruments Corporation, Austin, USA). Images were first corrected for background and minor variations in fluence rate of the corresponding excitation light sources. In the second step, the sequence of fluorescence images from each animal was registered by translation and rotation using anatomical landmarks identified in the corresponding transmission images. In the next step, binning of the pixels was performed (4x4) to increase the signal to noise ratio. After the pixel binning the images were resized on the same size of 16-bit image at a resolution of 1344x1024 pixels. The registration of images from the second step of analysis enabled us to determine the fluorescence intensity of each tissue type from the same area as follows: in the corresponding transmission image the regions of interest were chosen for each tissue type. Tumor and normal tissue regions of interest were chosen so that no large vessels were in, or close to the region. Thus in every animal, three regions of interest were chosen for normal tissue, three regions of interest selected inside the tumor and depending on vessels content, three up to five regions of interest were selected within the vessels. The same selected regions of interest were also applied for images corrected by ratio imaging technique, where the subtraction and division of the images was done according to the equation (1).
To investigate the validity of our ratiometric imaging correction technique, we analyzed vessels of various diameters. Blood vessel diameter was estimated from the transmission images. According to determined square field of view of macro lens, one picture element (pixel) corresponds to approximately 3 µm.

Statistical analysis
In the present study, 3 female Fisher-344 rats were used to determine autofluorescence and transmission intensity profiles. However, the mTHPC pharmacokinetics profile was evaluated just in one animal. The aim of our current study is to present the correction method and not to validate the mTHPC pharmacokinetics profile. Presentation of the results from one animal avoids the increase in standard deviations due to intra-animal (biological) variations. A two-tailed t-test was used to determine significance for the difference in autofluorescence signal measured by two different excitation light sources. Results with a p value below 0.05 were considered significant. Statistical analysis was done using Microcal Origin®, version 6.0 (Microcal Software, Inc., Northampton, MA).

Results

Window chamber tissue optical properties and autofluorescence
Figure 3 shows the white light images of the chamber model immediately before mTHPC injection and 96 hours later. Tumor tissue is easily recognized as a circular area of higher light transmission compared to the surrounding normal tissue. Vessels can be recognized as
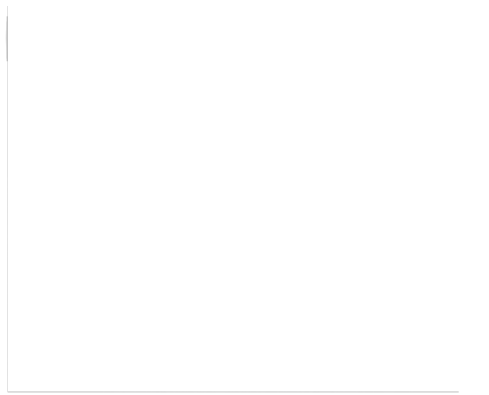
Figure 3. White light reflection images of a chamber acquired (A) before and (B) 96 hours after mTHPC administration.
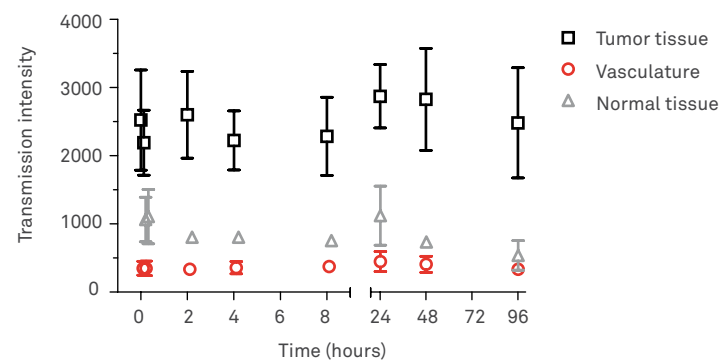

Figure 4. Transmission intensity time profile of 652 nm excitation light collected from different tissue types: vasculature, normal tissue and tumor tissue. The standard deviation for time point within the tissue type was calculated from region of interests of three control animals (in every animal, three up to five regions of interest were selected for each tissue type).

visually darker tissue, i.e. more light absorbing areas. In comparison with the first day of the experiment (figure 3A), after 96 hours (figure 3B), the natural changes in the chamber model are clearly visible. The tumor size increased and the position of the vessels surrounding the tumor changed.

Figure 4 demonstrates the transmission intensity time profile of 652 nm excitation light collected from different tissue types within the transmission images of the chamber. In comparison with the vessels and normal tissue, the transmission intensity of the light is highest for the tumor tissue. The lowest light transmission is detected from the vessels area. The
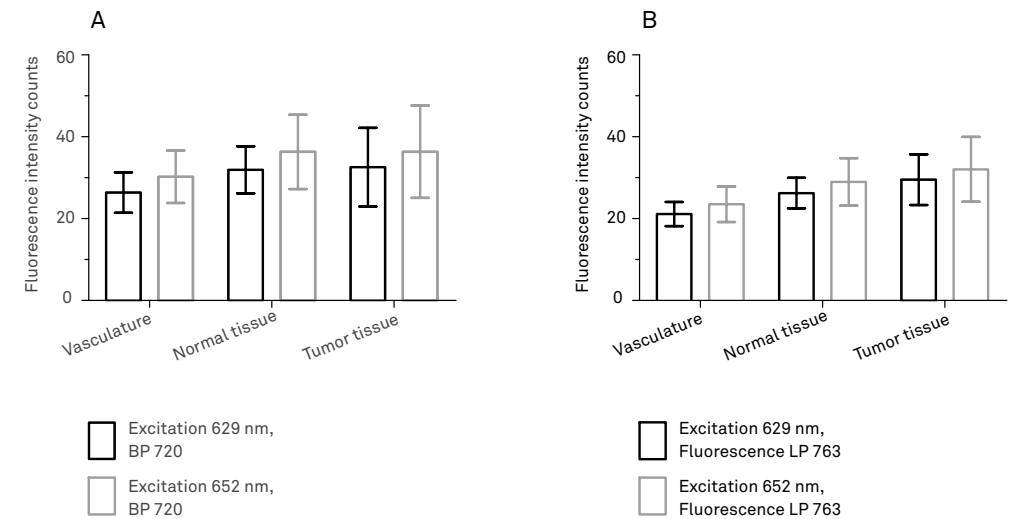
Figure 5. Fluorescence intensity collected from different tissue types in control animals (without mTHPC, corresponding to the time 0 hours from the chamber preparation) using (A) band pass filter 720 ± 10 nm, (B) long pass filter 763 nm. Black and gray columns represent 629 nm and 652 nm excitation respectively. The standard deviation was calculated from region of interests of three control animals (in every animal, three up to five regions of interest were selected for each tissue type).
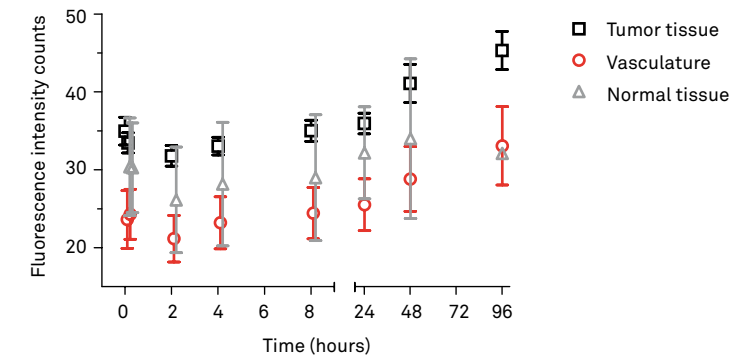

Figure 6. Fluorescence pharmacokinetics of autofluorescence (629 nm excitation, > 763 nm detection) for different tissue types: vasculature, normal tissue and tumor tissue. The standard deviations represent variations between a minimum of three regions of interest for each tissue type within the chamber model of one animal.
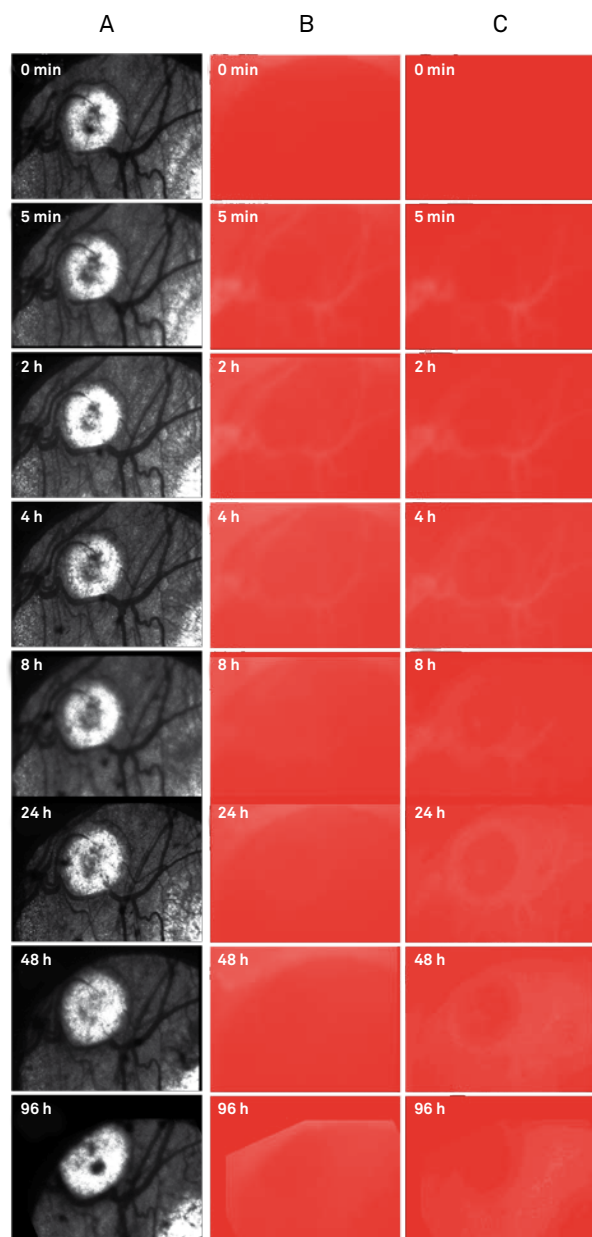
Figure 7. The time profile of the chamber model (the same window chamber as analyzed for Figure 6) after mTHPC administration:
A) Time profile of chamber transmission images after mTHPC administration.
B) Time profile of uncorrected fluorescence emission images (652 nm excitation, 720 ± 10 nm detection) of a chamber after mTHPC administration.
C) The time dependent evolution of the corrected fluorescence images of chamber model after mTHPC administration.
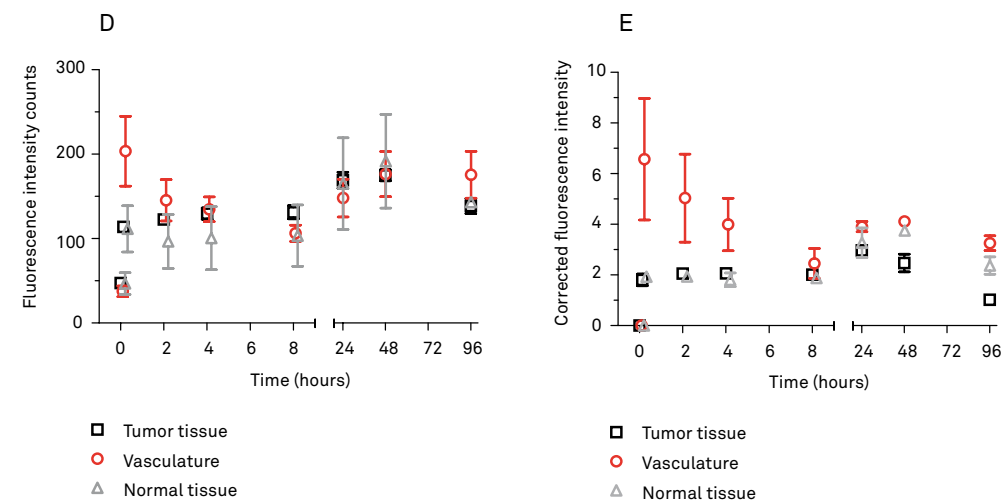
D) mTHPC pharmacokinetic profile (uncorrected fluorescence signal: 652 nm excitation, 720 ± 10 nm detection) for different tissue types: vasculature, normal tissue and tumor tissue.
E) mTHPC pharmacokinetic profile (corrected fluorescence signal) within the different tissue types: vasculature, normal tissue and tumor tissue.

difference is visible for all observation time points. Within the time no significant changes in the transmission profile of 652 nm excitation light are detected in any of the tissue types, i.e. the intensity of the transmission light does not change in time.

In figure 5, the difference between fluorescence intensities of the background autofluorescence (measured before mTHPC administration) excited by wavelengths 629 nm and 652 nm, detected in the emission channels (band pass 720 ± 10 nm and long pass 763 nm) is presented. For both detection channels, for the same tissue type, the fluorescence intensity using 652 nm excitation was not significantly different ($p > 0.05$) from 629 nm excitation.

Figure 6 shows the autofluorescence kinetics (excitation at 629 nm, long pass filter 763 nm). The fluorescence kinetics for all tissues changed in the same manner, i.e. from the measurement time points beyond 24 hours an increase in fluorescence intensity is detected. The autofluorescence signal from the vasculature is 1.2 times lower than for normal tissue and 1.5 times lower in comparison with fluorescence intensity detected in the tumor area.

Fluorescence pharmacokinetics of mTHPC
In figure 7, the time profile of the chamber model after mTHPC administration is demonstrated. Figure 7A shows the time profile of chamber transmission images. The time-dependent evolution of the uncorrected fluorescence images (excitation 652 nm, detection BP 720) of mTHPC pharmacokinetics within the chamber model is shown in figure 7B. In all uncorrected fluorescence images the borders of the chamber are clearly visible due to the
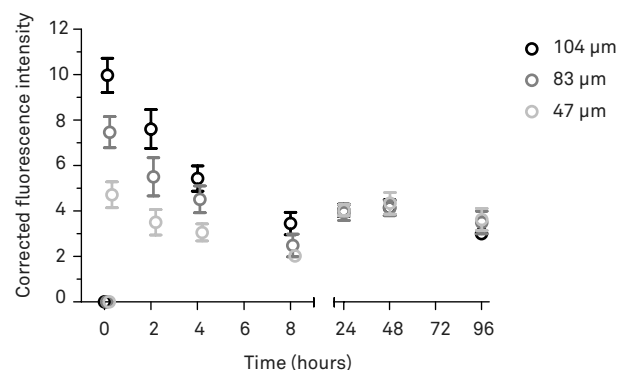
Figure 8. Corrected fluorescence signal as a function of the time after mTHPC administration, detected in vessels of different diameters: 104 μm, 83 μm and 47 μm.

fluorescence properties of the plastic ring surrounding the chamber.

Figure 7D shows the mTHPC uncorrected fluorescence pharmacokinetic profile within the different tissue types. Five minutes after mTHPC administration, the fluorescence intensity is highest in the vessels and decreases for longer time points. Four hours after mTHPC administration the difference of fluorescence observed in vessels and other tissue types reduces and from time points beyond 8 hours after mTHPC administration the fluorescence distribution in tumor and normal tissue is similar. Normal and tumor tissue showed no significant difference in fluorescence intensity over the investigated period and follow the same type of kinetic profile (figure 7D): between 5 min and 8 hours, the fluorescence intensity does not change significantly, while above the 8 hour time point, an increase in fluorescence is observed. The intensity increased up to 48 hours after mTHPC administration and decreased for the 96 hours time point. For all incubation time points, the standard deviations are higher for normal tissue than for tumor tissue or vessel area.

The time-dependent evolution of the corrected fluorescence images of mTHPC (images corrected by ratio imaging technique, Equation (1)) within the chamber is shown in figure 7C. According to transmission images (figure 7A), at time point 5 min from mTHPC administration, only vessels show fluorescence. The intensity of fluorescence within the vessels decreased for longer incubation time points. At t = 4 hours the contours of the vessels are not as clear anymore due to mTHPC penetration through vessel walls into the tissue. For t > 8 hours after mTHPC administration the fluorescence is now within all structures of the chamber. Note that the fluorescence of the plastic ring (figure 7B) is not visible in any of corrected images (figure 7C). The time dependence of the corrected fluorescence intensity for the different tissue types is plotted in figure 7E. The signal detected from the vessels shows high variations (large error bars) for times below 24 hours. The variation was highest for 5 min followed by decreasing

variations for longer incubation time points. Beyond 24 hours these variations minimized. In contrast, variations of the corrected fluorescence signal for normal tissue and tumor tissue are small throughout the time-course of the experiment.

Vessel diameter
Figure 8 shows the corrected fluorescence signal as a function of time from mTHPC administration detected in vessels of different diameters. The pharmacokinetic profile of mTHPC fluorescence is similar for all vessels: 5 min after mTHPC administration, the fluorescence intensity appears to be the highest, followed by a decrease for longer time points. Between 24 and 96 hours no significant changes of fluorescence intensity are detected. However, the corrected fluorescence signal in figure 8 demonstrates large differences in fluorescence intensity for the different vessel diameters. With decreasing vessel diameter, the fluorescence intensity decreases. The difference of fluorescence intensity is highest for early time points after mTHPC i.v. administration (t < 24 hours): the highest difference is detected for the 5 minute time point followed by a decrease in difference up to 8 hours. Between 24 and 96 hours time points the fluorescence intensity does not show any dependence on vessel diameter.

Discussion

We have investigated the use of a ratiometric imaging technique for monitoring the kinetics of mTHPC fluorescence in the rat skin-fold observation chamber. The chamber model was specifically designed for monitoring the pharmacokinetics of photosensitizers used in PDT. However, a problem associated with fluorescence measurements is the difficulty of obtaining quantitative fluorophore fluorescence, due to varying optical properties of tissues and differences in tissue thickness. This has important consequences for the general interpretation of fluorescence measurements in the window chamber. For example, in a previous study, our group determined the spatial distribution of the kinetics of protoporphyrin IX (PpIX) fluorescence during ALA-PDT [11]. PpIX fluorescence kinetics were measured in different tissue types and conclusions were based on data that was not corrected for differences in tissue optical properties and differences in the thickness within and between window chambers. Although the conclusions were based on determining the rate of fluorescence increase in each tissue type separately, temporal variations in tissue optical properties and differences in the thickness of different tissues were not considered. This may be of particular importance, especially when the relationship between the increase of PpIX fluorescence with distance from an arteriole and venule was investigated. Thus in the present study our intention was to investigate the difference in optical properties of different types of tissue and its time changes in the chamber model. The methodology proposed here accounts for the wavelength dependence of tissue optical properties and overcomes the non-linearity of previously published ratiometric methods.

Tissue optical properties of chamber
Figures 4 - 6 clearly show the differences between the fluorescence and transmission intensity acquired from different types of tissue during the course of the experiment. The fluorescence intensity detected from vessels was lower than that from normal or tumor tissue. Considering the blood content within these vessels and the absorption spectra of oxy- and deoxy hemoglobin, the result observed in figure 5A or 5B is not surprising. The same effect is also evident in the transmission intensity profile from different tissue types (figure 4), and in the transmission images of the chamber (figure 7A). The chamber vasculature represents the tissue with the highest absorption coefficient, which significantly attenuates the propagation of light. In contrast, tumor tissue exhibits higher autofluorescence intensity than the normal tissue area (figure 5, figure 6). This might be caused by 1) a lower absorption coefficient of tumor tissue, 2) a different scattering coefficient of tumor tissue (it is not evident whether a higher or lower scattering coefficient would result in a higher fluorescence yield), 3) a larger thickness of tumor tissue, 4) a higher native fluorophore concentration in tumor tissue. Most likely a combination of these factors results in the observed difference. Since the raw fluorescence signal is confounded by each of these factors, the differences in and changes to optical properties of the tissue under interrogation will lead to significant quantification errors of photosensitizer fluorescence within the chamber. Clearly, a method, which corrects for the influence of these effects, would be a step forward.

Validation of assumptions
In the study of Bogaards et al. [24] it was shown, that the performance of imaging techniques can be improved by selecting the excitation and emission wavelengths towards the NIR. Thus in this study, the excitation wavelengths were carefully selected between 620 and 840 nm; where the tissue absorption and scattering are relatively small. In addition, the combination of exciting tissue fluorescence at a wavelength where the photosensitizer absorbs minimally and detection at the wavelength of no photosensitizer fluorescence, allowed us to monitor kinetics of tissue autofluorescence during the course of the experiment. According to the principle of the method we have presented (Equation 1), the assumption was made, that both excitation wavelengths used in this study lead to the same autofluorescence. This assumption is confirmed in figure 5 where the fluorescence intensity detected from different tissue types of control animals is plotted. Within the same tissue type, the fluorescence intensity was not significantly different using 629 and 652 nm excitation.
The second assumption underlying our correction algorithm is that only signal from tissue autofluorescence can be detected in the wavelength region > 763 nm, using 629 nm wavelength excitation. This choice of wavelengths was based on the minimal absorption of mTHPC at the excitation wavelength and on the lack of mTHPC emission in the wavelength region > 763 nm (figure 2). In figure 6, we did not detect any changes of autofluorescence within the first measured time points in any of the tissue types. In contrast, mTHPC fluorescence pharmacokinetics profile (excitation 652 nm, fluorescence detection at 720 ± 10 nm (figure 7D),

revealed large differences in fluorescence intensity within the vessels 5 minutes after the mTHPC administration. It is very unlikely, that there are changes of tissue autofluorescence over the timescale of these first few measurements compared to the first measurement of autofluorescence (at t = 0). Therefore, we conclude that the increase of fluorescence intensity observed in chamber vessels in the band pass filter 720 ± 10 nm (figure 7B, 7D) is due to fluorescence emission of mTHPC. The fact that this effect was not seen in figure 6, confirmed that the signal detected in the wavelength region > 763 nm (using 629 nm wavelength excitation) is solely due to tissue autofluorescence.

Temporal changes of tissue optical properties within the chamber
The detection of autofluorescence within the timeframe of the experiment (figure 6) revealed that the autofluorescence kinetics for all tissues changed in the same manner, i.e. for measurement time points above 24 hours there is a (steady) increase in autofluorescence intensity. The cause of the observed effect might be chamber thickness changes and/or the changes in tissue optical properties at later time points. Unfortunately our data does not present conclusive evidence as to which of these effects is dominant. The fact that these changes occur within the time-course of the experiment demonstrates the necessity for a correction method, since the marker fluorescence will be affected by these chamber changes similar to the autofluorescence.

Fluorescence pharmacokinetics of mTHPC
Figures 4, 5 and 6 clearly illustrate the necessity of an appropriate correction technique for quantitative measurement of photosensitizer fluorescence in the window chamber. If we were to base conclusions on the pharmacokinetics profile of mTHPC from figure 7D (uncorrected fluorescence profile), then the tumor/normal tissue ratio is significantly higher at early time points after mTHPC administration. Taking into account figures 4, 5 and 6, this is actually due to a larger thickness and/or smaller absorption/scattering content of tumor tissue, rather than due to a higher mTHPC concentration within the tumor. The larger standard deviation associated with data detected from normal tissue can be explained by thickness inhomogeneities and due to the presence or absence of micro-capillaries. These variations are only visible at high magnification and are difficult to avoid in a model, where normal tissue has a significant component of microvasculature.
The correction of raw fluorescence data using the ratiometric correction method that we presented, results in a significant decrease in the spatial variation associated with a single measurement time point (evidenced by smaller error bars) and does not report a significant difference between the profile of mTHPC pharmacokinetics between tumor and normal tissue up to 24 hours after the administration of mTHPC (figure 7E). In addition, we observe that in all uncorrected images, a fluorescent boarder to the chamber is clearly visible (figure 7B). This is due to the presence of a fluorescent plastic ring on which the chamber is mounted. Corrected fluorescence images do not show this artifact (figure 7C).
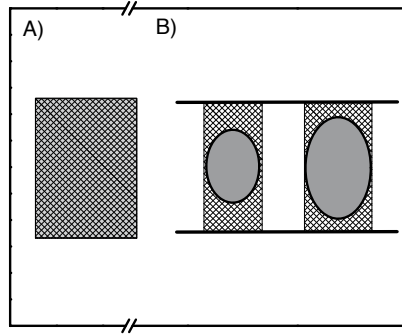
Figure 9. Schematic representation of technique limitation:
A) the same distribution pattern of fluorescence signal for fluorophore (filled *gray* area) and background tissue (hashed area)
B) Vertical profile of tissue with vessels of different diameter. Vessel is shown as an ellipse within the tissue. Localization of fluorophore (*gray*) is inhomogeneous compared to the tissue background fluorescence (open hashed area).

Figure 10. mTHPC pharmacokinetic profile (corrected fluorescence signal by double ratio fluorescence imaging technique of Sinaasappel and Sterenborg [15]) within the different tissue types: vasculature, normal tissue and tumor tissue.

Limitations of the correction method
As expected, the uncorrected signals (figure 7D) showed larger intra-chamber variations (visible as error bars) than the signal corrected using the ratiometric technique (figure 7E). The exception to this trend was observed in vessels, where the error bars were still high at early time points. These large error bars for mTHPC in vessels at early time points are caused by averaging contributions from small and large vessels, combined with vessel-diameter dependent mTHPC fluorescence yields for early time points. The dependence of corrected mTHPC fluorescence pharmacokinetics profile as a function of vessel diameter (figure 8) shows that for larger diameter vessels we obtained a higher fluorescence intensity of mTHPC, than for small vessels. We believe that the origin of this effect is due to a limitation of our correction method, which is illustrated by considering the spatial distribution of absorbers and fluorophores within the vasculature at early time points (figure 9). While it is well known that there are a number of circulating endogenous fluorophores within the vessels, such as water-soluble porphyrins and erythrocytes themselves [25-27], the autofluorescence from the window chamber vasculature is likely to be dominated by the contribution from connective tissue of vessel walls (in particular the tunica media) and the surrounding tissue. For early time points mTHPC is primarily localized in the blood plasma [28-31]. Thus localization of mTHPC is inhomogeneous with respect to the tissue background autofluorescence (figure 9B). Since our ratiometric method corrects for tissue optical properties and chamber thickness using the background autofluorescence, our method is most suitable for situations where the marker fluorescence and autofluorescence are co-localized; a condition that is not met in case of mTHPC at early time points. A confirmation of our hypothesis is the absence of a de-
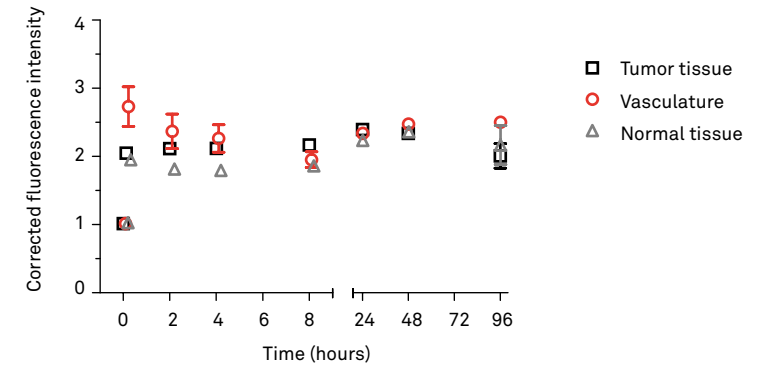
pendence of mTHPC fluorescence on vessel diameter for later time points (between 24 and 96 hours). Here the progressive re-distribution of mTHPC from the plasma into and through the vasculature into normal tissue results in a correction that is not influenced by the different spatial distribution of autofluorescence and marker fluorophore. This re-distribution of mTHPC is in accordance with the previously published pharmacokinetic profile of mTHPC in blood and other tissues [28-31]. Plasma mTHPC levels are high immediately after mTHPC injection (5 min after i.v. administration) and decrease exponentially thereafter. In mice and rats, mTHPC shows a bi-exponential decline with half-life values of 0.5 -1.3 h for the initial decline and 6.9-20.9 hours for the elimination phase [28-31].

Optical phantoms and Double ratio imaging
We tested the performance of our correction algorithm in optical phantoms. To maintain the geometry of our transmission measurements and to avoid the precipitation of scattering centers we prepared solid silicone phantoms containing mTHPC. We chose to use the absorber Evans Blue and TiO_2 to simulate tissue absorption and scattering. Preparing solid phantoms with spectral properties that match those of mTHPC and tissue autofluorescence *in vivo* proved to be very challenging. Unfavorable spectral shifts and changes in extinction coefficients and fluorescence quantum yield were observed in dyes we selected to match the optical properties of tissue. For example the choice of phantom autofluorophore was particular difficult. We found that in silicone Alexa-Fluor 720 had a negligible fluorescence quantum yield whereas Evans Blue showed significant fluorescence at both excitation wavelengths. Given these problems we chose to compare our correction algorithm with a

previously validated ratiometric technique, in which a double ratio (DR) is formed using two excitation and two detection wavelengths [15]. The result of this analysis can be seen in figure 10, where the mTHPC pharmacokinetic profile within the different tissue types is presented. A comparison of the present correction method (figure 7E) shows a similar pharmacokinetics profile for all tissue types. However, there is an important difference between DR profiles in areas of very high fluorescence intensity, in particular for short administration times in vessels. The non-linear relationship between double ratio and fluorophore concentration is a well-understood effect of double ratio imaging [14]. This saturation effect is a significant limitation of the DR correction technique for determining absolute fluorophore concentrations that are necessary for the study of pharmacokinetics, as discussed previously.

It is clear, that the method we present as well as the DR correction technique have important limitations [14] and it is important to stress, that the choice of fluorescence detection technique and correction method should be based on a specific application. This is particularly true for the most appropriate selection of excitation wavelengths and detection wavelength bands. It is important to note, that we have applied our correction method in a study investigating mTHPC detection. The application of this technique to different photosensitizers (or other fluorescent species) should involve the careful consideration of the spectroscopic properties of the photosensitizer, so that autofluorescence can be measured during the course of the study in real time and the method remains linearly dependent on photosensitizer concentration.

Conclusion

In summary, we have shown that the raw fluorescence intensity collected from tissues in the skin-fold observation chamber varied significantly between different tissue types and during the period of the investigation. Therefore any method, which does not correct for tissue optical properties and changes in autofluorescence, leads to fluorescence quantification errors. We have shown, that a ratiometric imaging method utilizing NIR autofluorescence detection can be applied and corrects for differences and changes in tissue optical properties and thickness. A limitation of our method is that for very early time points after the photosensitizer administration, a dependence on vessel size was found due to a mismatch in localization of marker fluorophore and background autofluorescence. Other than this limitation, the method we present shows a high sensitivity even for high photosensitizer concentrations.
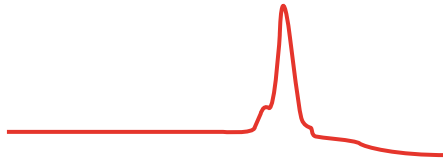
References

1. Lehr HA, Leunig M, Menger MD, Nolte D, Messmer K. Dorsal skinfold chamber technique for intravital microscopy in nude mice. Am J Pathol. 1993 Oct;143(4):1055-62.

2. Clark ER, Kirby-Smith HT, Rex RO, Williams RG. Recent modifications in the method of studying living cells and tissues in transparent chambers inserted in the rabbit's ear. Anat Rec. 1930;47:187-211.

3. Algire GH. An adaptation of the transparent chamber technique to the mouse. J Natl Cancer Inst. 1943;4:1-11.

4. Branemark PK, Aspegren K, Breine U. Microcirculatory studies in man by high resolution vital microscopy. Angiology. 1964;15:329-32.

5. Greenblatt M, Shubik P. Hamster cheek pouch chamber. Cancer Bull. 1967;19:65-81.

6. Arfors KE, Jonsson JA, McKenzie FN. A titanium rabbit ear chamber: Assembly, insertion and results. Microvasc Res. 1970 Oct;2(4):516-8.

7. Hobbs JB, Chusilp S, Hua A, Kincaid-Smith P, McIver MA. The pathogenesis of hypertensive vascular changes in the rat: Microscopic and ultrastructural correlation in vivo. Clin Sci. 1976(51):71-5.

8. Papenfuss HD, Gross JF, Intaglietta M, Treese FA. A transparent access chamber for the rat dorsal skin fold. Microvasc Res. 1979 Nov;18(3):311-8.

9. Kruijt B, de Bruijn HS, van der Ploeg-van den Heuvel,A., Sterenborg HJ, Robinson DJ. Laser speckle imaging of dynamic changes in flow during photodynamic therapy. Lasers Med Sci. 2006 Dec;21(4):208-12.

10. van der Veen N, van Leengoed HL, Star WM. In vivo fluorescence kinetics and photodynamic therapy using 5-aminolaevulinic acid-induced porphyrin: Increased damage after multiple irradiations. Br J Cancer. 1994 Nov;70(5):867-72.

11. de Bruijn HS, Kruijt B, van der Ploeg-van den Heuvel,A., Sterenborg HJ, Robinson DJ. Increase in protoporphyrin IX after 5-aminolevulinic acid based photodynamic therapy is due to local re-synthesis. Photochem Photobiol Sci. 2007 Aug;6(8):857-64.

12. van Leengoed HL, van der Veen N, Versteeg AA, Ouellet R, van Lier JE, Star WM. In vivo fluorescence kinetics of phthalocyanines in a skin-fold observation chamber model: Role of central metal ion and degree of sulfonation. Photochem Photobiol. 1993 Aug;58(2):233-7.

13. Cherry SR. In vivo molecular and genomic imaging: New challenges for imaging physics. Phys Med Biol. 2004 Feb 7;49(3):R13-48.

14. Bogaards A, Sterenborg HJCM, Bogaards., Wilson BC. In vivo quantification of fluorescent molecular markers in real-time: A review to evaluate the performance of five existing methods. Photodiagnosis and Photodynamic Therapy. 2007;4:170-8.

15. Sinaasappel M, Sterenborg HJ. Quantification of the hematoporphyrin derivative by fluorescence measurementusing dual-wavelength excitation anddual-wavelength detection. Appl Opt. 1993 Feb 1;32(4):541-8.

16. Bard MP, Amelink A, Hegt VN, Graveland WJ, Sterenborg HJ, Hoogsteden HC, et al. Measurement of hypoxia-related parameters in bronchial mucosa by use of optical spectroscopy. Am J Respir Crit Care Med. 2005 May 15;171(10):1178-84.

17. Amelink A, Kaspers OP, Sterenborg HJ, van der Wal JE, Roodenburg JL, Witjes MJ. Non-invasive measurement of the morphology and physiology of oral mucosa by use of optical spectroscopy. Oral Oncol. 2008 Jan;44(1):65-71.

18. Beauvoit B, Chance B. Time-resolved spectroscopy of mitochondria, cells and tissues under normal and pathological conditions. Mol Cell Biochem. 1998 Jul;184(1-2):445-55.

19. Profio A. Laser excited fluorescence of hematoporphyrinderivative for diagnosis of cancer. IEE Quant Electron. 1984;QE20:1502-7.

20. Baumgartner R, Fisslinger H, Jocham D, Lenz H, Ruprecht L, Stepp H, et al. A fluorescence imaging device for endoscopic detection of early stage cancer--instrumental and experimental studies. Photochem Photobiol. 1987 Nov;46(5):759-63.

21. Witjes MJ, Speelman OC, Nikkels PG, Nooren CA, Nauta JM, van der Holt B, et al. In vivo fluorescence kinetics and localisation of aluminum phthalocyanine disulphonate in an autologous tumour model. Br J Cancer. 1996 Mar;73(5):573-80.

22. Saarnak AE, Rodrigues T, Schwartz J, Moore AL, Gust D, van Gernert MJC, et al. Influence of tumour depth, blood absorption and autofluorescence on measurement of exogenous fluorophores in tissue. Lasers Med Sci. 1998;13:22-31.

23. Reinhold HS, Blachiewicz B, Berg-Blok A. Reoxygenation of tumours in "sandwich" chambers. Eur J Cancer. 1979 Apr;15(4):481-9.

24. Bogaards A, Sterenborg HJ, Trachtenberg J, Wilson BC, Lilge L. In vivo quantification of fluorescent molecular markers in real-time by ratio imaging for diagnostic screening and image-guided surgery. Lasers Surg Med. 2007 Aug;39(7):605-13.

25. Kruijt B, de Bruijn HS, van der Ploeg-van den Heuvel,A., de Bruin RW, Sterenborg HJ, Amelink A, et al. Monitoring ALA-induced PpIX photodynamic therapy in the rat esophagus using fluorescence and reflectance spectroscopy. Photochem Photobiol. 2008 Nov-Dec;84(6):1515-27.

26. De Veld DC, Witjes MJ, Sterenborg HJ, Roodenburg JL. The status of in vivo autofluorescence spectroscopy and imaging for oral oncology. Oral Oncol. 2005 Feb;41(2):117-31.

27. De Veld DC, Skurichina M, Witjes MJ, Duin RP, Sterenborg DJ, Star WM, et al. Autofluorescence characteristics of healthy oral mucosa at different anatomical sites. Lasers Surg Med. 2003;32(5):367-76.

28. Triesscheijn M, Ruevekamp M, Out R, Van Berkel TJ, Schellens J, Baas P, et al. The pharmacokinetic behavior of the photosensitizer meso-tetra-hydroxyphenyl-chlorin in mice and men. Cancer Chemother Pharmacol. 2007 Jun;60(1):113-22.

29. Jones HJ, Vernon DI, Brown SB. Photodynamic therapy effect of m-THPC (foscan) in vivo: Correlation with pharmacokinetics. Br J Cancer. 2003 Jul 21;89(2):398-404.

30. Triesscheijn M, Ruevekamp M, Aalders M, Baas P, Stewart FA. Outcome of mTHPC mediated photodynamic therapy is primarily determined by the vascular response. Photochem Photobiol. 2005 Sep-Oct;81(5):1161-7.

31. Cramers P, Ruevekamp M, Oppelaar H, Dalesio O, Baas P, Stewart FA. Foscan uptake and tissue distribution in relation to photodynamic efficacy. Br J Cancer. 2003 Jan 27;88(2):283-90.

32. Kruijt B, van der Ploeg-van den Heuvel,A., de Bruijn HS, Sterenborg HJ, Amelink A, Robinson DJ. Monitoring interstitial m-THPC-PDT in vivo using fluorescence and reflectance spectroscopy. Lasers Surg Med. 2009 Nov;41(9):653-64.

Chapter 3.3

Localization of liposomal mTHPC formulations within normal epithelium, dysplastic tissue, and carcinoma of oral epithelium in the 4NQO-carcinogenesis rat model

Abstract

Background and objective. Foslip® and Fospeg® are liposomal formulations of the photo-sensitizer *meta*-tetra(hydroxyphenyl)chlorin (Foscan®), which is used for Photodynamic Therapy (PDT) of malignancies. Literature suggests that liposomal mTHPC formulations have better properties and increased tumor uptake compared to Foscan. To investigate this, we used the 4-nitroquinoline-1-oxide (4NQO) induced carcinogen model to compare the lo-calization of the different mTHPC formulations within normal, precancerous and cancerous tissue. In contrast to xenograft models, the 4NQO model closely mimics the carcinogenesis of human oral dysplasia.

Materials and Methods. 54 rats drank water with the carcinogen 4NQO. When oral examina-tion revealed tumor, the rats received 0.15 mg/kg mTHPC (Foscan, Foslip or Fospeg). At 2, 4, 8, 24, 48 or 96 hours after injection the rats were sacrificed. Oral tissue was sectioned for hematoxylin and eosin (HE) slides and for fluorescence confocal microscopy. The HE slides were scored on the severity of dysplasia by the Epithelial Atypia Index (EAI). The calibrated fluorescence intensity per formulation or time point was correlated to EAI.

Results. Fospeg showed higher mTHPC fluorescence in normal and tumor tissue compared to both Foscan and Foslip. Significant differences in fluorescence between tumor and normal tissue were found for all formulations. However, at 4, 8 and 24 hours only Fospeg showed a significant higher fluorescence in tumor. The Pearson's correlation between EAI and mTHPC fluorescence proved weak for all formulations.

Conclusion. In our induced carcinogenesis model, Fospeg exhibited a tendency for higher fluorescence in normal and tumor tissue compared to Foslip and Foscan. In contrast to Foscan and Foslip, Fospeg showed significantly higher fluorescence in tumor vs normal tis-sue at earlier time points, suggesting a possible clinical benefit compared to Foscan. Low correlation between grade of dysplasia and mTHPC fluorescence was found.

Introduction

Photodynamic therapy (PDT) has been established as a local anticancer treatment that is based on the excitation of a light sensitive drug, a photosensitizer (PS). Upon illumina-tion with light of an appropriate wavelength the excitation of the sensitizer yields reactive oxygen species (ROS) which induces tissue necrosis. The PS *meta*-tetra(hydroxyphenyl) chlorin (mTHPC INN: temoporfin) in a formulation with propylene glycol, ethanol and water (Foscan®) is one of the most potent clinically used PSs and is approved for treatment of head and neck squamous cell carcinoma (HNSCC) [1-4].

For a high PDT effect sufficient uptake of sensitizer in tumor is necessary. Uptake of mTHPC in tumor tissue is considered relatively inefficient because of the lipophillic nature of this sensitizer. As a consequence of the low water solubility, mTHPC can aggregate in biological media, resulting in a decreased photodynamic efficacy. These solubility issues of mTHPC (Foscan) are also related to serious PDT induced side-effects such as prolonged photosen-sitivity at the site of injection due to aggregates precipitating [5]. In recent years, water soluble liposomal mTHPC formulations have been introduced as drug-carrier systems (nanocar-riers) [2,6-10]. Two liposomal mTHPC formulations that have been developed are Foslip® and Fospeg® [9,11,12].

Foslip consists of plain or conventional liposomes based on dipalmitoylphosphatidylcholine (DPPC), while Fospeg consists of liposomes with a poly-ethylene glycol layer on the surface. This hydrophilic pegylated layer is thought to prevent uptake by the mononuclear phagocyte system (MPS) thereby increasing the circulation time [2,10,13]. It is suggested that this longer circulation time should increase the enhanced permeability and retention (EPR) effect [10,14,15]. The EPR effect is described as the increased uptake of large (liposomal) formulations in tumor tissue due to altered structure of the endothelial cells in tumor tissue [10,16,17]. Further-more, the EPR effect supposedly decreases lymphatic drainage due to its structural altera-tions resulting in retention of mTHPC. Several *in vitro* studies on liposomal formulations of mTHPC showed that both Foslip and Fospeg have the potential for higher efficacy and bio-availability compared to Foscan [1,12,18,19].

In a previous study we investigated the influence of (liposomal) formulations on mTHPC pharmacokinetic profile using an *in vivo*, xenograft tumor model [20]. At several time points over 96 hours after injection, corrected mTHPC fluorescence intensity measurements were performed of the implanted tumor tissue, normal tissue and vasculature. In accordance with other studies, our findings suggested an enhanced uptake in tumor tissue at earlier time points for both liposomal mTHPC formulations compared to Foscan [8,9,20,21].

However, most of these studies were limited by either the experimental model used or by the method of measuring mTHPC in tissue. In literature, xenograft tumor models are widely used to investigate the biodistribution of liposomal mTHPC formulations [8,20-22]. The pharmacoki-netics in these xenograft models are influenced by the properties of the well vascularised,

fast growing, implanted tumors. Therefore, xenograft models do not mimic the clinical situation as the process of normal carcinogenesis leading to precancerous and eventual cancerous tissue is absent. Moreover, the influence of precancerous tissue on both the mTHPC distribution and the uptake of the different mTHPC formulations is unknown. In a study on fluorescence kinetics and localization of disulphonate aluminum phthalocyanines in an induced tumor model (4NQO) consisting of precancerous stages, a relationship between increasing severity of dysplasia and the increased sensitizer fluorescence was found [23]. We therefore were interested if this would be observed for mTHPC. Only one study described mTHPC kinetics in an acquired squamous cell carcinoma model in cats, albeit with a small sample size and fluorescence measurements not corrected for autofluorescence (AF) [9]. Non-invasive fluorescence measurements or extraction techniques are typically used to describe mTHPC tissue distribution. Complicating these measurements is the known non-uniformity and spatial variability of mTHPC distribution and uptake within (tumor) tissue [22,24-26]. In a previous study we even observed large spatial differences in mTHPC uptake in healthy (non-cancerous) oral tissue [24]. While that study was aimed at validating *in vivo* fluorescence using differential pathlength spectroscopy (fDPS) as a non-invasive instrument to measure mTHPC tissue concentration in optically heterogeneous tissue using a small interrogation volume, it raised questions about the validity of "bulk" tissue measurements. These measurements interrogate much bigger tissue volumes thereby averaging mTHPC fluorescence over that volume. As both the extraction technique and fluorescence measurements interrogate a "bulk" tissue volume, no specific information can be reported on the mTHPC distribution and uptake in tissue compartments such as epithelial and sub-epithelial tissue (stroma). Furthermore, slight local differences in mTHPC distribution possibly related to the various grades of dysplasia present in an interrogated volume might be unnoticed. It is to be expected that spatial differences in mTHPC distribution will only increase in even more heterogeneous (pre)cancerous tissue [22,25,26].

In our current study, we used the 4NQO rat model in which a squamous cell carcinoma (SCC) was generated in the mucosa of the oral cavity by the administration of the carcinogen 4-nitroquinoline-1-oxide (4NQO) in drinking water. 4NQO induces intracellular oxidative stress by generating reactive oxygen species (ROS) and its metabolic product binds to DNA at guanine residues [27-30]. Similar exertion of ROS and binding to DNA is inducted by carcinogens present in tobacco [27]. We used the 4NQO rat model because it exhibits all stages of human oral carcinogenesis with similar histological and molecular changes [27,31-35]. In the clinical situation, the presence and treatment of precancerous tissue besides cancerous tissue is of clinical relevance [36]. The major advantage of this 4NQO tumor model compared to xenograft models, is that both cancerous and precancerous lesions of tongue and palate are induced [27,33,37]. Therefore, the 4NQO model makes for an appropriate model to study the distribution of a PS in both precancerous and cancerous tissue. This is particularly important since tumor type and staging of the tumor are known to influence time-dependent uptake, retention and elimination of a PS [38,39].

To assess the stage of 4NQO induced carcinogenesis in the rat, microscopic analysis using the Epithelial Atypia Index (EAI) is appropriate to allow for a consistent *ex-vivo* grading of epithelial tissue [34,40]. This microscopic analysis facilitates the identification of tissue compartments (epithelium, stroma), besides staging of the induced oral carcinogenesis.

To obtain information on spatial mTHPC distribution within healthy, pre-cancerous or cancerous mucosa and stroma of the 4NQO rat-model, confocal fluorescence spectral imaging was used. Fluorescence microscopy enables exact localization of emitted mTHPC fluorescence. The use of a *confocal* microscope permits more reliable measurements within the center of a thicker slide, minimizing artifacts and bleaching. To further enhance the reliability of our measurements, the influence of changes in experimental setup, background and autofluorescence have to be taken into consideration.

By relating the microscopic tissue analysis (EAI & tissue compartment) with the fluorescence attributed to mTHPC, information on stage or tissue dependant selectivity of mTHPC formulations is gathered. To thoroughly investigate the differences in mTHPC distribution between the formulations, multiple time point were used for assessment of the fluorescence pharmacokinetic profile.

The aim of the present study was to investigate distribution and accumulation of Foslip, Fospeg and Foscan within time in a tumor model that mimics human carcinogenesis. Influence of dysplasia or tumor on mTHPC distribution is assessed by relating the mTHPC fluorescence to the severity of dysplasia (none, EAI grade or tumor) or tissue compartment (epithelial or subepithelial stroma).

Materials and methods

Materials
Three different formulations of mTHPC were kindly provided by Biolitec AG (Jena, Germany); Foscan (4 mg mTHPC/ml), Fospeg (1.5 mg mTHPC/ml) and Foslip (1.38 mg mTHPC/ml) in the described stock concentrations. Prior to the experiment, all formulations were dissolved under minimal light and kept at 4 C in the dark as recommended by the manufacturer. Foscan was made by dissolving the stock-solution in a solution of PEG400: EtOH: water = 3:2:5 (v/v). Foslip and Fospeg were made by dissolving the stock-solution in 5% aqueous glucose solution and in sterile water respectively. All photosensitizers were diluted to reduce errors when injecting a small volume (concentration = 0.126mg/ml). Polyethylene glycol 400 (PEG400) was obtained from Sigma-Aldrich (Zwijndrecht, the Netherlands) and 96% ethanol (EtOH) from Merck (Amsterdam, The Netherlands).

Animal and tumor model
The experimental design for this study was approved by the experimental welfare committee of the University of Groningen and conformed to Dutch and European regulations for

animal experimentation. Fifty-four male Wistar rats (HsdCpb:W), 7 weeks old, weighing approximately 200 grams were purchased from Harlan Netherlands B.V. (Horst, The Netherlands). The animals were kept in stainless steel and plastic cages, at constant humidity and at a temperature of 20 C. They were fed with standard rat pellets and water ad libitum. 4NQO (Sigma Aldrich, Zwijndrecht, The Netherlands) was dissolved in drinking water to a final concentration of 0.001%. Drinking water with the 4NQO solution was shielded from light by the use of coated bottles; these were replaced at least twice a week or whenever needed with freshly prepared solution. Animals were inspected daily and weighed weekly. After 12 weeks, animals were anaesthetized once a week for a thorough inspection of the oral cavity. During our animal experimentations general anesthesia was performed using Isoflurane®/O_2/N_2O as an inhalation anesthetic. When either tumor growth was visually identified or the animal had lost too much weight (>10% of body mass; one of the humane endpoints according to the animal welfare committee), the experimental procedure would start.

Experimental procedures
Prior to the experimental procedures the rats were anaesthetized. One of 3 mTHPC formulations was chosen by randomization and injected intravenously. The dosage used for all formulations was 0.15 mg mTHPC/kg. After intravenous injection the animals were kept under reduced light conditions (< 60 lux) to avoid phototoxicity. At either 2, 4, 8, 24, 48 or 96 hours after injection (n= 3 animals per formulation per time point) the animals were sacrificed by cervical dislocation. Tongue and palate were immediately excised and snap frozen in liquid nitrogen. The frozen tissue samples were handled under subdued light conditions. Excised tongue and palate were subsequently cut in the sagittal plane into 3 and respectively 2 gross tissue samples. These tissue samples were cut in a sagittal plane with a microtome under subdued light conditions for both histological sections (5 μm) and sections used for fluorescence microscopy (20 μm). The cutting of the 20 μm section was directly followed by a corresponding 5 μm section, thereby enabling both histological and fluorescence assessment of nearly identical, adjacent tissue. All sections were cut and mounted on Starfrost® adhesive glass slides (Menzel, Braunschwig, Germany). Altogether, a total of 184 confocal and HE microscopy slides were used for further analysis. Sections used for fluorescence microscopy were analyzed by confocal microscopy directly after sectioning. Histological slides were stained with hematoxylin and eosin (HE). After staining the HE slides were digitally scanned (460 nm resolutions scans) and available for assessment at various magnifications (1.25x, 25x, 5x, 10x) using a Hamamatsu Nanozoomer in combination with NDPserve, NDPview and NDPscan software.

Confocal Fluorescence Microscopy
Immediately after sectioning (<3 hours), fluorescence images were acquired at 10 x magnification of the slide using a confocal fluorescence microscope (LSM510, Zeiss, Jena, Germany). Fluorescence images were acquired of parts of the 20 μm slides as selected by the

A

B
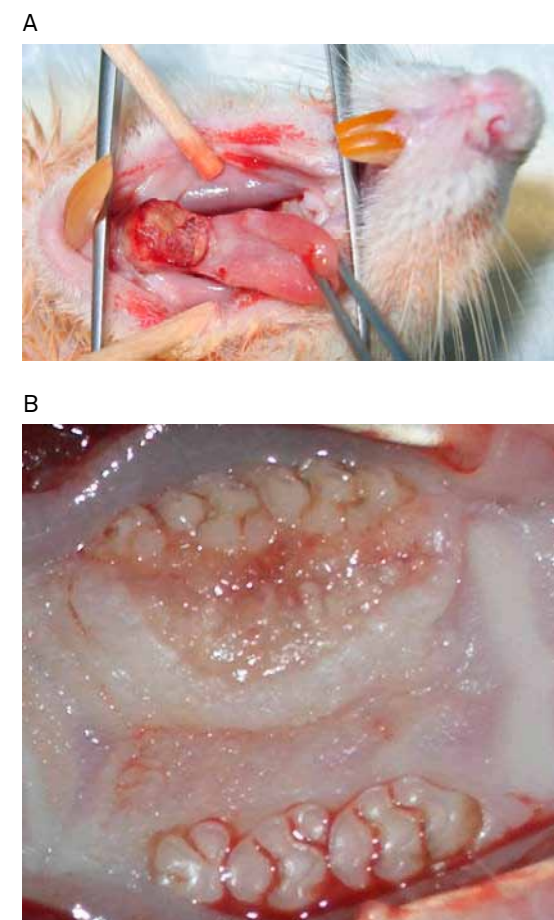
Figure 1. Wistar rat lying on its back for inspection under anesthesia. A base of tongue tumor (A) and tumor of the hard palate (B) developed after induction by 4NQO in drinking water.

first author using white light transmission images. Criteria for selection were the presence of epithelium, absence of cutting artifacts and recognizable tissue structures. Recognizable tissue structures aided correlation of the confocal fluorescence image to its corresponding section on the HE slide. Each image consisted of 921.4 microns square (512 x 512 pixels). Fluorescence tiles (multiple images) acquired from the section consisted of at least 3 images and at most 9 images to provide information on larger regions of tissue. After collecting fluorescence images (tile), corresponding white light transmission images (tile) of the same region on the 20 μm section was made.
Excitation and light collection was performed using a 405 nm laser equipped with a 505 nm long-pass detection filter combined with spectral detection between 545-706 nm (at 10nm intervals). Care was taken to acquire optical slices of 5 μm at the center of each 20 μm sec-

Table 1. Score sheet of histological grading by the use of Epithelial Atypia Index (EAI).

| Histological features		scores
DROP SHAPED RETE RIDGES	NONE	0
	SLIGHT	2
	MARKED	4
IRREGULAR STRATIFICATION	NONE	0
	SLIGHT	2
	MARKED	5
KERATINISATION OF CELLS BELOW THE KERATINISED LAYER	NONE	0
	FEW/SHALLOW	1
	MANY/DEEP	3
BASAL CELL HYPERPLASIA	NONE	0
	SLIGHT	1
	MARKED	4
LOSS OF INTERCELLULAR ADHERANCE	NONE	0
	SLIGHT	1
	MARKED	5
LOSS OF POLARITY	NONE	0
	SLIGHT	2
	MARKED	6
HYPERCHROMATIC NUCLEI	NONE	0
	SLIGHT	2
	MARKED	5
INCREASED NUCLEO-CYTO- PLASMATIC RATIO (INCREASED DENSITY) IN BASAL AND PRICKLE CELL LAYER	NO INCREASE	0
	SLIGHT INCREASE	2
	MARKED INCREASE	6
ANISOCYTOSIS AND ANISONUCLEOSIS	NONE	0
	SLIGHT	2
	MARKED	6
PLEOMORPHIC CELLS AND NUCLEI	NONE	0
	SLIGHT	2
	MARKED	6
MITOTIC ACTIVITY	NORMAL	0
	SLIGHT INCREASE	1
	MARKED INCREASE	5
LEVEL OF MITOTIC ACTIVITY	NORMAL	0
	LOWER ½ ONLY	3
	ALSO UPPER ½	10
PRESENCE OF BIZARRE MITOSIS	NONE	0
	SINGLE	6

tion. A single spatially uniform fluorescent glass reference slide was used throughout the experiment (2273-G, Van Loenen Instruments, Zaandam, The Netherlands). At the beginning of each imaging session a confocal fluorescence image was acquired at a predetermined depth (20 µm) within the fluorescent slide in order to determine day to day variations in the overall sensitivity of the microscopic setup. These variations are mostly related to changes in the collection efficiency system and the sensitivity of the spectral detection. Furthermore, a flat-field correction of the fluorescence images was performed by dividing each individual sample image tile by a fluorescence reference image per emission wavelength.

Spectral images were analyzed as a linear combination of basis spectra and fitted using a singular value decomposition algorithm using software written in LabVIEW (version 7.1, National Instruments Corporation) [41,42]. These procedures resulted in calibrated fluorescence intensities. Basis spectra of mTHPC, protoporphyrin IX (PpIX) and tissue background auto-fluorescence were measured using the same microscopic system as described above. For these spectra, measurements were performed on healthy oral rat mucosa used for a previous experiment.

Immediately after the acquisition of each fluorescence image a white light transmission images of each frozen sample was also acquired to aid the identification of corresponding regions of interest in HE slides. For the purposes of visualization RGB images of the fluorescent components: Red (mTHPC), Blue (PpIX) and Green (AF) were processed and transformed so that the maximum image contrast was selected for each channel. While the main focus of our current study is the analysis of mTHPC distribution related to tissue type and (dysplasia) grade, a short description is given on the distribution of mTHPC, AF, and PpIX in the confocal fluorescence images.

Histological grading by EAI

First, we determined the part of each HE section of which a corresponding sample image (a tile, consisting of multiple images) was available. This was done by matching the white light transmission images of the confocal sections to a corresponding part of the HE section. Using NDPserve software, corresponding sections of the HE were annotated. Secondly, within all of the corresponding and annotated HE sections, a total of 387 Regions of interest (ROI) were selected by the first author while blinded from the sample fluorescence images. Of these ROIs, 280 were located within epithelium and 107 within non-dysplastic stromal tissue. The EAI was used to score oral epithelial dysplasia of each selected ROI within epithelium [40]. This index involves the assessment of 13 histological features (table 1). These histological features are graded into further subcategories like "none", "slight" or "marked" with respective increase in scores. The final score of the EAI is made up of the sum of these 13 scores, up to a maximum of 75. The final score was further arranged using 5 ordered categories; EAI 0 (normal), EAI 1-20 (slight dysplasia), EAI 20-40 (moderate dysplasia), EAI > 40 (severe dysplasia) and carcinoma (tumor). Carcinoma (tumor) was defined by pathologically assessment of the HE sections as presence of tumor cells beyond the basal membrane.

A

B

C

D

E
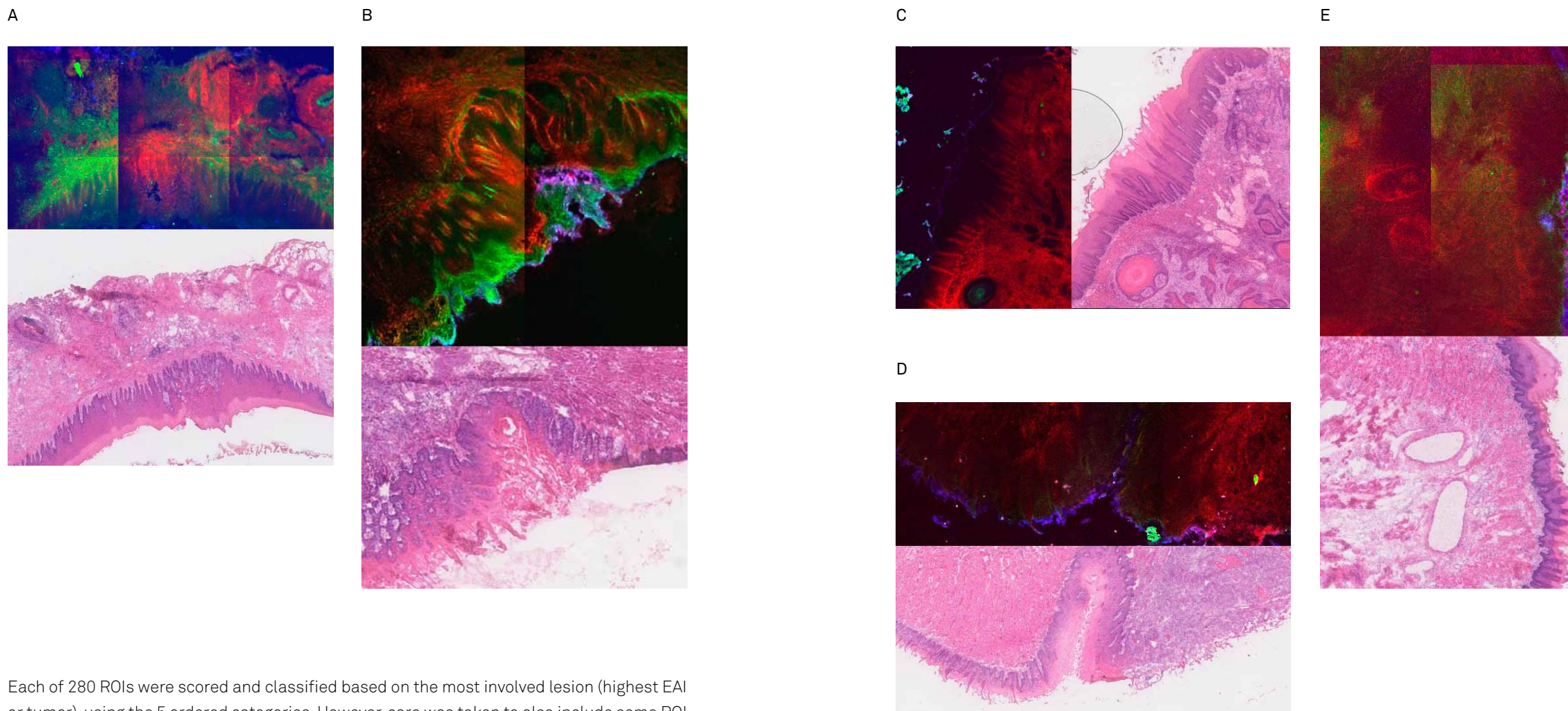
Each of 280 ROIs were scored and classified based on the most involved lesion (highest EAI or tumor), using the 5 ordered categories. However, care was taken to also include some ROI on normal appearing epithelium. The authors MW and SV scored the selected ROIs of the HE sections in random order by agreement. To validate and correlate our scoring on these ordered categories, 25% (random selection) of the ROIs were scored by pathologist BV, his score was used as the gold standard. When there was disagreement on the combined score of MW, SV vs BV, the score of pathologist BV was used.

Determination of fluorescence in a ROI
Calibrated fluorescence images were processed using ImageJ (version 1.46r, National Institutes of Health, USA). This permitted the measurement of mTHPC fluorescence intensity in a Region of interest (ROI) as previously selected in an HE section. The 387 ROI's selected had an average size of nearly 82 microns square. To prevent bias, image analysis was performed according to a pre-defined strategy; spectral analysis of mTHPC fluorescence intensity of

Figure 2. Examples of matched confocal fluorescence images (10X magnification) with their corresponding HE images. Fluorescence images (transformed to obtain maximum contrast) depict distribution of mTHPC (colored red), autofluorescence (colored green) and PpIX (colored blue). For aesthetic reasons both fluorescence and HE images were resized. A: Fospeg 48 hours after injection. The highest EAI score found in the HE section was 43. B: Fospeg 8 hours after injection. The highest EAI score found in the HE section was 11. C: Foscan 24 hours after injection. The tissue was determined to be cancerous. D: Foscan 96 hours after injection. The tissue was determined to be cancerous. E: Fospeg 4 hours after injection. The tissue was determined to be normal.

a ROI in a calibrated fluorescence image was performed by selecting the ROI on the corresponding and matched white-light images. These white-light images of the slide were taken by the confocal microscopy in the exact same position and directly after the acquisition of the corresponding fluorescence images. In this manner, the ROI selected previously in the HE section could be matched to the same anatomical location on the white light transmission image. Since the coordinates of the white light transmission image corresponds exactly with that of the fluorescence image (both performed with the same setup without manipulating the 20 μm section), the EAI score and fluorescence of a ROI are matched.

Statistical analysis
Inter-observer agreement on histological scoring and subsequent ordering in 5 tissue categories of ROI was calculated using a linear weighted kappa (κ) [43]. Pearson's correlation coefficient was used (two-tailed, 95% CI) in determining the correlation coefficients (r) between EAI, AF and measured mTHPC fluorescence within a ROI. Further analysis was performed on correlation per tissue type and formulation per similar time point. The two-tailed t-test was used (α=0.05) to compare means of measured fluorescence stratified according to formulation, time point or one of five ordered tissue categories. Both IBM® SPSS® Statistics (software version 20) and Graphpad Prism® (software version 5.0), were used for statistical analysis.

Results

Experimental data
After a mean of 36 weeks (range: 24-45) of exposure to 4NQO, 54 rats were included for the experimental procedures. All rats had a clinically observable intra-oral tumor (figure 1). No rats were lost during the induction of tumors by 4NQO. Typical examples of matched HE sections with corresponding confocal sections are shown in figure 2. The inter-observer agreement on EAI scored for 25% of these ROI located within epithelium had a linear weighted kappa (κ) of 0.54 (95% CI 0.32; 0.76), considered a moderate agreement [43]. Fifty-five of the ROI scored an EAI of 0 (normal tissue), while 92 ROI were scored as cancerous tissue (tumor). The remaining 133 ROI (slight, moderate or severe dysplasia) had a mean EAI score of 13.68 (SD; 10.9). As a consequence of the use of an induced tumor model, each category of dysplasia (slight, moderate or severe dysplasia) was not always observed in a ROI; some ROIs showed no dysplastic lesions and thus contained only normal tissue.

Correlation of mTHPC fluorescence with EAI score
The correlation of the EAI (as determined in an HE slide) with the calibrated mTHPC fluorescence (as determined in the corresponding confocal fluorescence slide) was plotted for all ROIs (figure 3). The correlation coefficient (r) of mTHPC fluorescence versus EAI stratified for Foscan, Foslip and Fospeg was 0.39, 0.030 and 0.29 respectively. For all formulations at
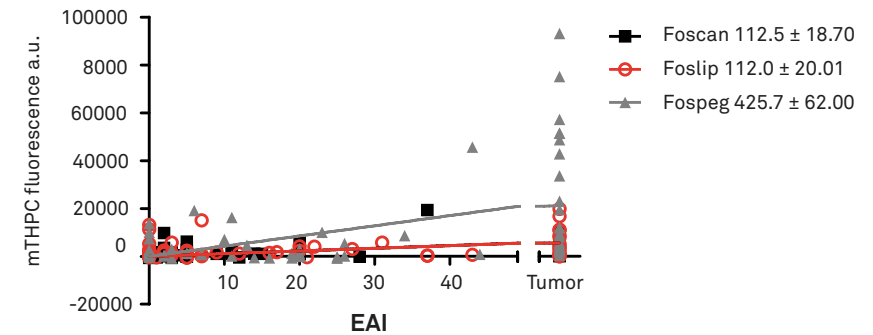

Figure 3. mTHPC fluorescence plotted versus EAI per investigated ROI for 3 different mTHPC formulations (Foscan, Foslip, Fospeg). Fluorescence measured in tumor tissue is also included. For clarity error-bars are omitted.

all time points, a tendency (non-significant) was found for increased mTHPC fluorescence within tumor tissue compared to non-tumor tissue. A detailed description of measured mTHPC fluorescence intensities stratified by formulation, time and tissue (grade) is given in the supplementary data.

Distribution of mTHPC in different tissue stratified by time and formulation
When comparing calibrated mTHPC fluorescence in normal epithelium between the different mTHPC formulations a tendency (non-significant) was shown for Foscan to show least fluorescence (figure 4A). However, only at the 4 hour time point a significant difference (p<0.05) in mTHPC fluorescence was found as Fospeg showed higher fluorescence compared to both Foscan (p=0.0107) and Foslip (p=0.0318). When comparing mTHPC fluorescence in subepithelial stroma between the different mTHPC formulations, a tendency was shown for Fospeg to show highest fluorescence with both Foslip and Foscan showing comparable fluorescence (figure 4B). Only at the 96 hour time point a significant higher fluorescence in stroma was found for Foslip compared to Foscan (p=0.0401). No further significant differences were found. Overall, each formulation showed a similar mTHPC fluorescence pharmacokinetic profile for both epithelial and sub-epithelial tissue with a tendency for higher fluorescence for stroma.
When comparing mTHPC fluorescence in tumor tissue between the different mTHPC formulations a tendency (non-significant) was shown for Fospeg to show highest mTHPC fluorescence at all time points (figure 4C). Both liposomal formulations showed higher fluorescence at 2, 4 and 8 hours compared to Foscan. However, at early time points only Fospeg showed significant higher fluorescence intensities in tumor; at 2 hours (p=0.0423) and 8 hours (p=0.0474) compared to Foscan and at 8 hours (p=0.0060) compared to Foslip. No
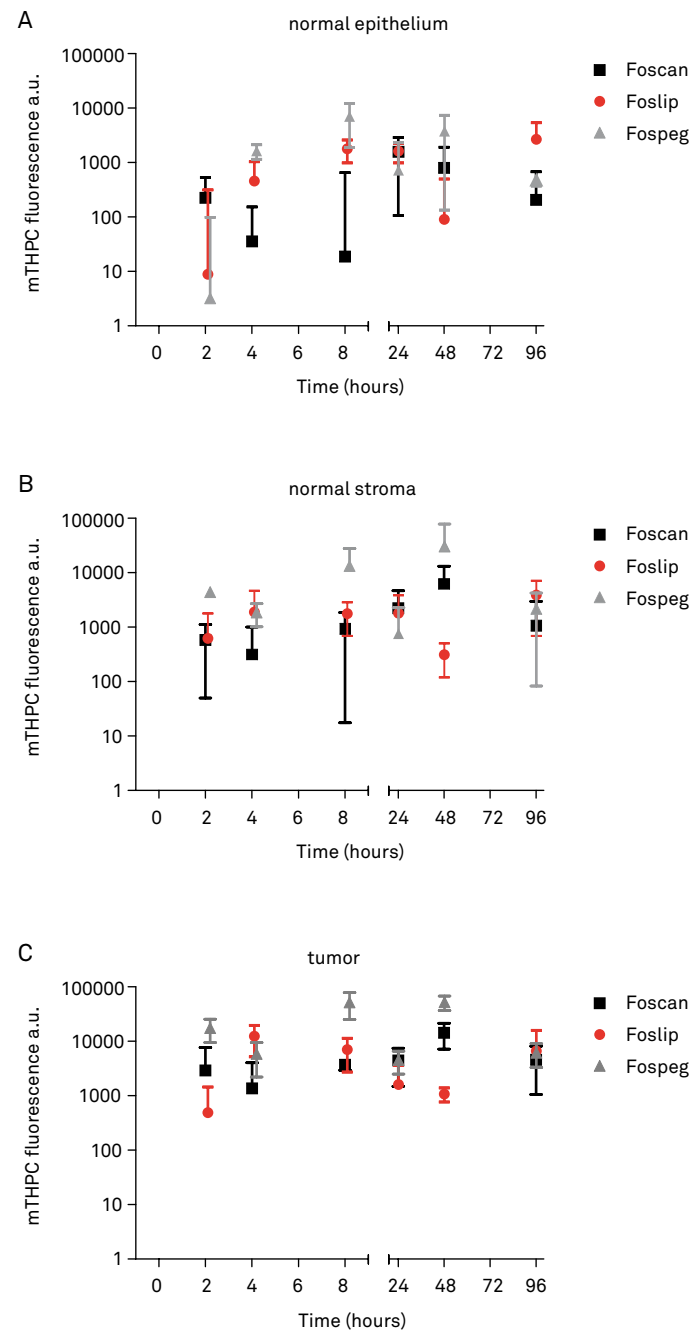
Figure 4. mTHPC fluorescence kinetic profile in normal epithelium (A), normal stroma (B) and tumor tissue (C) for Foscan, Foslip and Fospeg (error-bars indicate standard-deviation, logarithmic scale for mTHPC fluorescence).
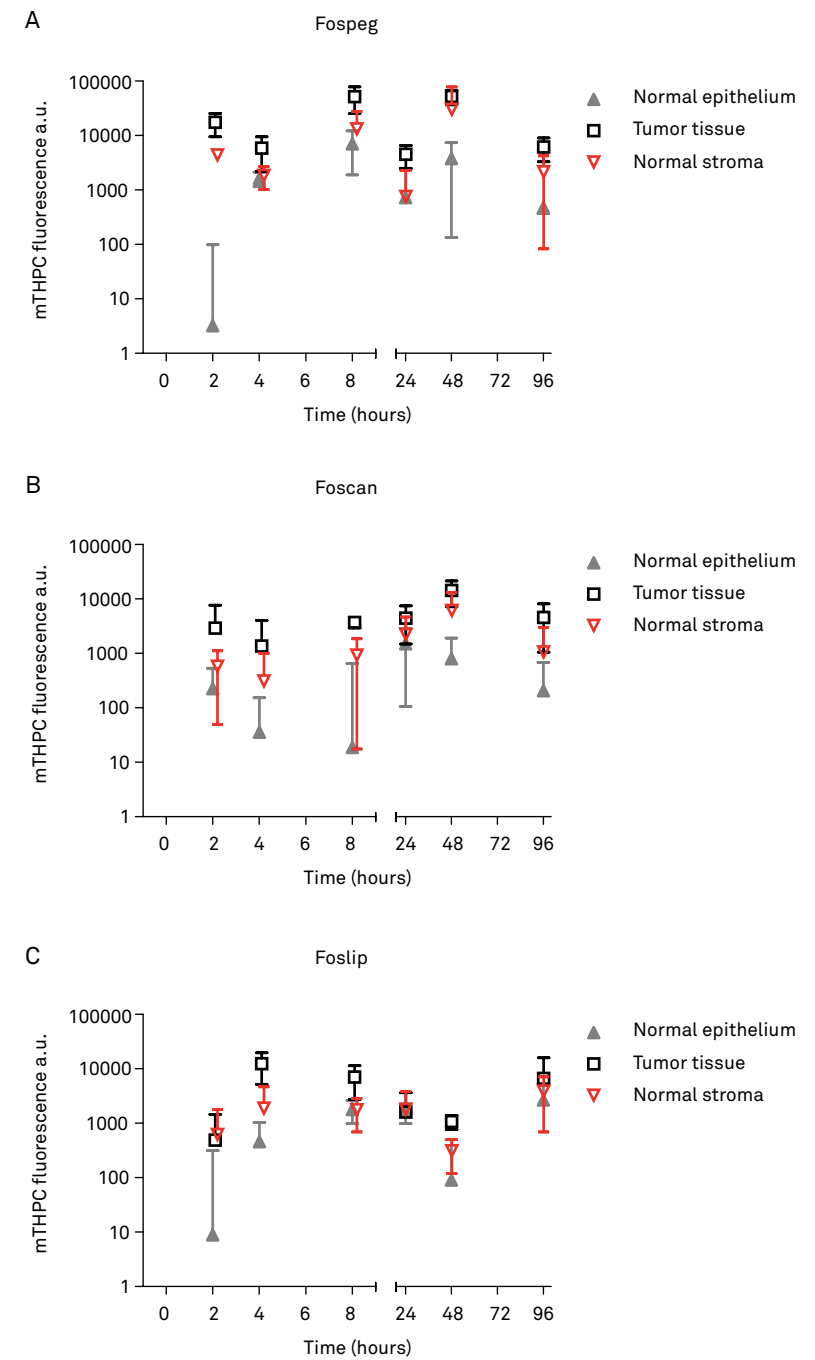

Figure 5. Difference in mTHPC fluorescence kinetic profile in normal epithelium, normal subepithelial tissue (stroma) and tumor tissue for 3 different formulations; Fospeg (A), Foscan (B) and Foslip (C) (error-bars indicate standard-deviation, logarithmic scale for mTHPC fluorescence).

other significant differences were observed at these early time points. At the 24 hour time point Fospeg showed significantly (p=0.0170) higher mTHPC fluorescence compared to Foslip, and at 48 hours to both Foscan (p=0.0242) and Foslip (p=0.0014). At the 48 hour time point Foslip reached the lowest mTHPC fluorescence in tumor of the formulations as it was also significantly (p=0.0388) lower compared to Foscan. No other significant differences were observed at these later time points in tumor (>48 hours).

Distribution of mTHPC for different formulations stratified by tissue type and time
When comparing calibrated mTHPC fluorescence between both normal epithelium or normal stroma vs tumor tissue stratified for formulation, mean fluorescence in tumor tissue showed a tendency towards higher intensity at all time points (figure 5A, B, C). However, no mTHPC formulation showed a significant difference between normal epithelium and tumor tissue at the 2 hour time point. Fospeg showed at all 5 later time points a significant (p<0.05) higher mTHPC fluorescence in tumor tissue compared to normal epithelium (figure 5A). Foscan showed significant (p<0.05) higher mTHPC fluorescence in tumor compared to normal epithelium at 4, 8, 48 and 96 hours (figure 5B). Foslip showed a significant (p<0.05) higher fluorescence in tumor compared to normal epithelium at 4, 8 and 48 hours (figure 5C). When comparing subepithelial stroma tissue with tumor, we found a significant (p<0.05) higher fluorescence intensity in tumor for Fospeg at the first 4 time points. For Foslip the 4, 8 and 48 hour time point showed significant (p<0.05) higher fluorescence in tumor, while for Foscan only at 8 hours a significant (p<0.05) higher mTHPC fluorescence in tumor was found.

Gross analysis of confocal images
While analysis of calibrated fluorescence intensities of mTHPC, AF or PpIX per ROI was the main goal of the study, non-quantitative visual analysis was also performed. All images of tongue tissue showed PpIX present on the filli of the tongue (figure 2B – 2E). Autofluorescence was particularly present on keratinized parts like the palate, keratin pearls, or dysplastic lesions (figure 2A – 2C). mTHPC fluorescence was noted more in tissue characterized as cancerous (figure 2C, D) and around vasculature at early time points (figure 2E). Moreover, more mTHPC fluorescence was visually observed in subepithelial tissue compared to the epithelium. Overall, the visual mTHPC distribution over the different tissue compartments and over of tissue with different grades of dysplasia showed clear differences in spatial distribution.

Discussion

Fospeg showed higher mTHPC fluorescence intensities in normal stroma, normal epithelium and tumor tissue compared to both Foscan and Foslip. For Fospeg, we found significantly higher mTHPC fluorescence intensity in tumor tissue compared to normal subepithelial stromal tissue between 2-24 hours. For Foslip the significant higher fluorescence intensity

at 4, 8 and 48 hours was less evident than that of Fospeg. Foscan showed less tumor selectivity as only at 8 hours a significant higher tumor fluorescence vs stroma was found. The highest mTHPC fluorescence in our experiment was measured for Fospeg in tumor tissue at 8 hours. At that time point the normal to tumor fluorescence ratio was >8. While we used calibrated fluorescence measurements to observe the fluorescence pharmacokinetic profile, non-calibrated visual assessment of mTHPC fluorescence patterns was performed. In these images mTHPC fluorescence within vasculature was observed at early time points (figure 2E), as extensively reported in other studies [20,22,44]. At later time points mTHPC fluorescence appeared to be more diffusely spread within tissue.

In complete agreement with our recent window chamber xenograft rat model, Fospeg showed highest mTHPC fluorescence in tumor tissue 8 hours after injection. Furthermore both studies showed significant higher mTHPC fluorescence in tumor tissue at 2, 8 and 48 hours after injection compared to Foscan and Foslip [20]. In accordance with other *in vivo* studies, Fospeg exhibited highest calibrated fluorescence intensities in tissue at earlier time points and with significant higher fluorescence intensities in tumor (selectivity) compared to Foslip and in particular Foscan [8,9,20,21,45].

As suggested in previous studies, both the water-soluble liposomal formulations probably accumulate in tumor tissue due to the EPR-effect thereby increasing selectivity compared to Foscan. The higher mTHPC fluorescence intensity and tumour selectivity of Fospeg over Foslip (that we observed) is most likely to be a consequence of the pegylation of the liposomes in Fospeg. [10,46]. These liposomes coated by hydrophilic polymers are known to prevent the uptake by the (MPS). Indeed, non-pegylated conventional liposomes used in Foslip are described with high accumulation in liver and spleen [45]. Conversely, mTHPC in pegylated liposomes is less taken up in liver tissue compared to Foscan [8]. The relative low fluorescence intensity we found for Foslip compared to Foscan was also observed by others using high performance liquid chromatography [45].

The 4NQO model enabled us to investigate the relation of mTHPC fluorescence intensity with the degree of epithelial dysplasia. A weak correlation coefficient (r) between EAI and mTHPC fluorescence for Foscan (r=0.39) and Fospeg (r=0.29) was found while for Foslip no correlation was found. This suggests that increased mTHPC fluorescence in tumor tissue as found especially for Fospeg, is caused by an increased tumor accumulation possibly due to the altered tissue architecture and tumor angiogenesis and not by pre-malignant cellular changes. Therefore, the EPR effect may not be present in dysplastic tissue but only in tissue with severe disturbances in architecture and lymphatic drainage (tumor tissue).

Differences with other studies were the time points at which highest tumor fluorescence was found. For instance, we observed for Foscan highest tumor fluorescence at 48 hours, while in several studies using xenograft models, including our window chamber model, maximum mTHPC tumor fluorescence at 24 hours was observed [8,20,47,48]. Since the mTHPC formulations were prepared and injected in the exact same manner as in our aforementioned study, a possible explanation for the discrepancies could be the influence of different animal mod-

els on mTHPC (fluorescence) pharmacokinetic profile [20]. Accordingly, while some discrepancies between studies are noted on exact pharmacokinetic profile, the use of different tumor models could be responsible for these. The 4NQO experimental model is very useful model for research in (fluorescence) pharmacokinetics in oral tissue as it closely mimics the clinical context in which mTHPC mediated PDT is used [4]. The induced carcinogenesis model used in our experiment allows for an investigation of fluorescence pharmacokinetics more closely related to the clinical situation than the use of more prolific growing xenografts. Supporting our reasoning, a recent workgroup on nanoparticles and the EPR effect for drug delivery stated that for preclinical research into drugs and their EPR effect, (animal) tumor models characterized by heterogeneous tumor tissue are preferred over xenograft models as they better reflect the clinical situation [49].

Hence, induced epithelial tumors are bound to consist of more heterogeneous tissue and possibly subepithelial tissue. To correct for this heterogeneity, we included analysis of the fluorescence intensity in normal subepithelial stromal tissue besides the careful analysis of the corresponding HE slides. In contrast to implanted and well vascularised xenografts, induced tumors are not encapsulated and therefore it is more difficult to determine exact tumor boundaries. Furthermore, normal tissue, various grades of dysplastic tissue and tumor tissue are all in close vicinity to each other in our induced tumor model. For these reasons, exact spatial distribution of mTHPC fluorescence distribution by fluorescence microscopy is necessary to describe the influence of tissue grade (none, dysplasia, tumor) and tissue compartment in detail.

One potential advantage of performing fluorescence microscopy on frozen sections is that the effects of differences in tissue optical properties are likely to be much smaller than that in the *in vivo* optical measurements [24]. Excitation light passes through the tissue section which reduces the influence of light scattering in frozen sections on the fluorescence spectra. We have previously investigated the use of optical imaging on thin (5 μm) frozen sections and found that thinner sections are much more susceptible to variations in quantitative fluorescence (data not shown). This is presumably due to the interaction of exogenous fluorophores with water in thawing samples; an effect that is overcome by imaging an optical slice at the center of a thicker frozen section. Due consideration should be given to the use of mTHPC fluorescence imaging to determine the behavior of different PS formulations since mTHPC fluorescence may be influenced by the effects of mTHPC serum stability, binding and/or aggregation [50]. Moreover, both the incorporation of mTHPC into liposomes and the composition of different liposomes is known to significantly influence the spectral properties [6,51]. In trying to predict clinical importance of the different mTHPC formulations one could argue that only mTHPC molecules able to fluoresce are important for PDT. However, predicting PDT response in general is difficult as numerous variables are influential in treatment outcome [2].

Besides various *in vitro* studies on potentially increased PDT efficacy of liposomal mTHPC, some studies have reported on using liposomal mTHPC for *in vivo* PDT experiments [1,18,19]. Recent *in vivo* studies on PDT using Fospeg in both rats and cats suggested higher tumor ne-

croses at earlier time points compared to using Foscan [8,9]. For Foslip one study showed that highest tumor necroses was achieved at an early time point (6 hours), PDT efficacy was unfortunately not compared to Foscan [45]. Curiously, that time point showed tumor and plasma concentrations of mTHPC below their maximal values. This further emphasizes the complexity in predicting PDT damage and the need for additional mTHPC mediated PDT damage experiments performed on induced tumor models.

Conclusion

To the best of our knowledge, our current study is the only one describing calibrated fluorescence intensities of Foscan, Foslip and Fospeg in an induced tumor model. This model also permitted the investigation of a possible relationship between grade of dysplasia and mTHPC fluorescence. Fospeg did show higher tumor fluorescence at earlier time points compared to Foslip and in particular Foscan. Potentially this could mean shortening the currently used drug-light interval of 96 hours and lowering of the currently used dosage to induce similar PDT damage. Thereby possibly lowering the photosensitivity associated with mTHPC mediated PDT [4,5]. Future studies should be undertaken to demonstrate the PDT efficacy at these earlier time points.

References

1. Berlanda J, Kiesslich T, Engelhardt V, Krammer B, Plaetzer K. Comparative in vitro study on the characteristics of different photosensitizers employed in PDT. J Photochem Photobiol B. 2010 Sep 2;100(3):173-80.

2. Senge MO, Brandt JC. Temoporfin (foscan(R), 5,10,15,20-tetra(m-hydroxyphenyl)chlorin)--a second-generation photosensitizer. Photochem Photobiol. 2011 Nov-Dec;87(6):1240-96.

3. European Medicines Agencies. H-C-318 foscan european public assessment report. 2009 04/30.

4. de Visscher SA, Dijkstra PU, Tan IB, Roodenburg JL, Witjes MJ. mTHPC mediated photodynamic therapy (PDT) of squamous cell carcinoma in the head and neck: A systematic review. Oral Oncol. 2013 Mar;49(3):192-210.

5. Karakullukcu B, Kanick SC, Aans JB, Sterenborg HJ, Tan IB, Amelink A, et al. Integration of fluorescence differential path-length spectroscopy to photodynamic therapy of the head and neck tumors is useful in predicting clinical outcome. Int J Radiat Oncol Biol Phys. Submitted.

6. Reshetov V, Kachatkou D, Shmigol T, Zorin V, D'Hallewin MA, Guillemin F, et al. Redistribution of meta-tetra(hydroxyphenyl)chlorin (m-THPC) from conventional and PEGylated liposomes to biological substrates. Photochem Photobiol Sci. 2011 Jun;10(6):911-9.

7. Paszko E, Ehrhardt C, Senge MO, Kelleher DP, Reynolds JV. Nanodrug applications in photodynamic therapy. Photodiagn Photodyn Ther. 2011 /;8(1):14-29.

8. Bovis MJ, Woodhams JH, Loizidou M, Scheglmann D, Bown SG, Macrobert AJ. Improved in vivo delivery of m-THPC via pegylated liposomes for use in photodynamic therapy. J Control Release. 2012 Jan 30;157(2):196-205.

9. Buchholz J, Kaser-Hotz B, Khan T, Rohrer Bley C, Melzer K, Schwendener RA, et al. Optimizing photodynamic therapy: In vivo pharmacokinetics of liposomal meta-(tetrahydroxyphenyl)chlorin in feline squamous cell carcinoma. Clin Cancer Res. 2005 10/15;11(1078-0432; 20):7538-44.

10. Derycke AS, de Witte PA. Liposomes for photodynamic therapy. Adv Drug Deliv Rev. 2004 01/13;56(0169-409; 1):17-30.

11. Senge MO. mTHPC--a drug on its way from second to third generation photosensitizer? Photodiagnosis Photodyn Ther. 2012 Jun;9(2):170-9.

12. Pegaz B, Debefve E, Ballini JP, Wagnieres G, Spaniol S, Albrecht V, et al. Photothrombic activity of m-THPC-loaded liposomal formulations: Pre-clinical assessment on chick chorioallantoic membrane model. Eur J Pharm Sci. 2006 05;28(0928-0987; 1-2):134-40.

13. Konan YN, Gurny R, Allemann E. State of the art in the delivery of photosensitizers for photodynamic therapy. J Photochem Photobiol B. 2002 03;66(1011-1344; 1011-1344; 2):89-106.

14. Huwyler J, Drewe J, Krahenbuhl S. Tumor targeting using liposomal antineoplastic drugs. Int J Nanomedicine. 2008;3(1176-9114; 1):21-9.

15. Westerman P, Glanzmann T, Andrejevic S, Braichotte DR, Forrer M, Wagnieres GA, et al. Long circulating half-life and high tumor selectivity of the photosensitizer meta-tetrahydroxyphenylchlorin conjugated to polyethylene glycol in nude mice grafted with a human colon carcinoma. Int J Cancer. 1998 06/10;76(0020-7136; 6):842-50.

16. Brannon-Peppas L, Blanchette JO. Nanoparticle and targeted systems for cancer therapy. Adv Drug Deliv Rev. 2004 Sep 22;56(11):1649-59.

17. Maeda H, Wu J, Sawa T, Matsumura Y, Hori K. Tumor vascular permeability and the EPR effect in macromolecular therapeutics: A review. J Control Release. 2000 03/01;65(0168-3659; 1-2):271-84.

18. Kiesslich T, Berlanda J, Plaetzer K, Krammer B, Berr F. Comparative characterization of the efficiency and cellular pharmacokinetics of foscan- and foslip-based photodynamic treatment in human biliary tract cancer cell lines. Photochem Photobiol Sci. 2007 Jun;6(6):619-27.

19. Petri A, Yova D, Alexandratou E, Kyriazi M, Rallis M. Comparative characterization of the cellular uptake and photodynamic efficiency of foscan(R) and fospeg in a human prostate cancer cell line. Photodiagnosis Photodyn Ther. 2012 Dec;9(4):344-54.

20. de Visscher SA, Kascakova S, de Bruijn HS, van den Heuvel AP, Amelink A, Sterenborg HJ, et al. Fluorescence localization and kinetics of mTHPC and liposomal formulations of mTHPC in the window-chamber tumor model. Lasers Surg Med. 2011 Aug;43(6):528-36.

21. Svensson J, Johansson A, Grafe S, Gitter B, Trebst T, Bendsoe N, et al. Tumor selectivity at short times following systemic administration of a liposomal temoporfin formulation in a murine tumor model. Photochem Photobiol. 2007 09;83(0031-8655; 0031-8655; 5):1211-9.

22. Mitra S, Maugain E, Bolotine L, Guillemin F, Foster TH. Temporally and spatially heterogeneous distribution of mTHPC in a murine tumor observed by two-color confocal fluorescence imaging and spectroscopy in a whole-mount model. Photochem Photobiol. 2005 Sep-Oct;81(5):1123-30.

23. Witjes MJ, Speelman OC, Nikkels PG, Nooren CA, Nauta JM, van der Holt B, et al. In vivo fluorescence kinetics and localisation of aluminum phthalocyanine disulphonate in an autologous tumour model. Br J Cancer. 1996 Mar;73(5):573-80.

24. de Visscher SA, Witjes MJ, Kascakova S, Sterenborg HJ, Robinson DJ, Roodenburg JL, et al. In vivo quantification of photosensitizer concentration using fluorescence differential path-length spectroscopy: Influence of photosensitizer formulation and tissue location. J Biomed Opt. 2012 Jun;17(6):067001.

25. Andrejevic-Blant S, Hadjur C, Ballini JP, Wagnieres G, Fontolliet C, van den Bergh H, et al. Photodynamic therapy of early squamous cell carcinoma with tetra(m-hydroxyphenyl)chlorin: Optimal drug-light interval. Br J Cancer. 1997;76(8):1021-8.

26. Blant SA, Glanzmann TM, Ballini JP, Wagnieres G, van den Bergh H, Monnier P. Uptake and localisation of mTHPC (foscan) and its 14C-labelled form in normal and tumour tissues of the hamster squamous cell carcinoma model: A comparative study. Br J Cancer. 2002 Dec 2;87(12):1470-8.

27. Kanojia D, Vaidya MM. 4-nitroquinoline-1-oxide induced experimental oral carcinogenesis. Oral Oncol. 2006 Aug;42(7):655-67.

28. Nunoshiba T, Demple B. Potent intracellular oxidative stress exerted by the carcinogen 4-nitroquinoline-N-oxide. Cancer Res. 1993 Jul 15;53(14):3250-2.

29. Ramotar D, Belanger E, Brodeur I, Masson JY, Drobetsky EA. A yeast homologue of the human phosphotyrosyl phosphatase activator PTPA is implicated in protection against oxidative DNA damage induced by the model carcinogen 4-nitroquinoline 1-oxide. J Biol Chem. 1998 Aug 21;273(34):21489-96.

30. Tada M, Tada M. Main binding sites of the carcinogen, 4-nitroquinoline 1-oxide in nucleic acids. Biochim Biophys Acta. 1976 Dec 13;454(3):558-66.

31. Wallenius K, Lekholm U. Oral cancer in rats induced by the water-soluble carcinogen 4-nitrochinoline N-oxide. Odontol Revy. 1973;24(1):39-48.

32. Vered M, Yarom N, Dayan D. 4NQO oral carcinogenesis: Animal models, molecular markers and future expectations. Oral Oncol. 2005 Apr;41(4):337-9.

33. Nauta JM, Roodenburg JL, Nikkels PG, Witjes MJ, Vermey A. Epithelial dysplasia and squamous cell carcinoma of the wistar rat palatal mucosa: 4NQO model. Head Neck. 1996 Sep-Oct;18(5):441-9.

34. Nauta JM, Roodenburg JL, Nikkels PG, Witjes MJ, Vermey A. Comparison of epithelial dysplasia--the 4NQO rat palate model and human oral mucosa. Int J Oral Maxillofac Surg. 1995 Feb;24(1 Pt 1):53-8.

35. Patel V, Poulopoulos AK, Levan G, Game SM, Eveson JW, Prime SS. Loss of expression of basement membrane proteins reflects anomalies of chromosomes 3 and 12 in the rat 4-nitroquinoline-N-oxide model of oral carcinogenesis. Carcinogenesis. 1995 Jan;16(1):17-23.

36. Shah JP, Gil Z. Current concepts in management of oral cancer--surgery. Oral Oncol. 2009 Apr-May;45(4-5):394-401.

37. Dayan D, Hirshberg A, Kaplan I, Rotem N, Bodner L. Experimental tongue cancer in desalivated rats. Oral Oncol. 1997 Mar;33(2):105-9.

38. Whelpton R, Michael-Titus AT, Basra SS, Grahn M. Distribution of temoporfin, a new photosensitizer for the photodynamic therapy of cancer, in a murine tumor model. Photochem Photobiol. 1995 Apr;61(4):397-401.

39. Ris HB, Li Q, Krueger T, Lim CK, Reynolds B, Althaus U, et al. Photosensitizing effects of m-tetrahydroxyphenylchlorin on human tumor xenografts: Correlation with sensitizer uptake, tumor doubling time and tumor histology. Int J Cancer. 1998 Jun 10;76(6):872-4.

40. Smith C. Histological grading of oral epithelial atypia by the use of photographic standards. Copenhagen: ; 1969.

41. Kruijt B, de Bruijn HS, van der Ploeg-van den Heuvel,A., de Bruin RW, Sterenborg HJ, Amelink A, et al. Monitoring ALA-induced PpIX photodynamic therapy in the rat esophagus using fluorescence and reflectance spectroscopy. Photochem Photobiol. 2008 Nov-Dec;84(6):1515-27.

42. Finlay JC, Mitra S, Foster TH. In vivo mTHPC photobleaching in normal rat skin exhibits unique irradiance-dependent features. Photochem Photobiol. 2002 Mar;75(3):282-8.

43. Landis JR, Koch GG. An application of hierarchical kappa-type statistics in the assessment of majority agreement among multiple observers. Biometrics. 1977 Jun;33(2):363-74.

44. Triesscheijn M, Ruevekamp M, Aalders M, Baas P, Stewart FA. Outcome of mTHPC mediated photodynamic therapy is primarily determined by the vascular response. Photochem Photobiol. 2005 Sep-Oct;81(5):1161-7.

45. Lassalle HP, Dumas D, Grafe S, D'Hallewin MA, Guillemin F, Bezdetnaya L. Correlation between in vivo pharmacokinetics, intratumoral distribution and photodynamic efficiency of liposomal mTHPC. J Control Release. 2009 Mar 4;134(2):118-24.

46. Romberg B, Hennink WE, Storm G. Sheddable coatings for long-circulating nanoparticles. Pharm Res. 2008 Jan;25(1):55-71.

47. Jones HJ, Vernon DI, Brown SB. Photodynamic therapy effect of m-THPC (foscan) in vivo: Correlation with pharmacokinetics. Br J Cancer. 2003 07/21;89(0007-0920; 0007-0920; 2):398-404.

48. Garrier J, Bressenot A, Grafe S, Marchal S, Mitra S, Foster TH, et al. Compartmental targeting for mTHPC-based photodynamic treatment in vivo: Correlation of efficiency, pharmacokinetics, and regional distribution of apoptosis. Int J Radiat Oncol Biol Phys. 2010 Oct 1;78(2):563-71.

49. Prabhakar U, Maeda H, Jain RK, Sevick-Muraca EM, Zamboni W, Farokhzad OC, et al. Challenges and key considerations of the enhanced permeability and retention effect for nanomedicine drug delivery in oncology. Cancer Res. 2013 Apr 15;73(8):2412-7.

50. Reshetov V, Zorin V, Siupa A, D'Hallewin MA, Guillemin F, Bezdetnaya L. Interaction of liposomal formulations of meta-tetra(hydroxyphenyl)chlorin (temoporfin) with serum proteins: Protein binding and liposome destruction. Photochem Photobiol. 2012 May 19.
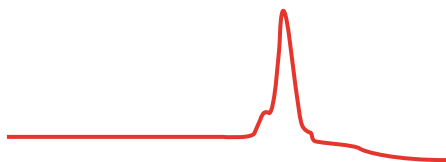
51. Kachatkou D, Sasnouski S, Zorin V, Zorina T, D'Hallewin MA, Guillemin F, et al. Unusual photoinduced response of mTHPC liposomal formulation (foslip). Photochem Photobiol. 2009 05;85(0031-8655; 0031-8655; 3):719-24.

Appendix I. mTHPC fluorescence intensities tabulated for Foscan, Foslip, Fospeg, tissue grade and time point.

		Foscan fluorescence intensity		Foslip fluorescence intensity		Fospeg fluorescence intensity	
		mean	SD	mean	SD	Mean	SD
2 hours	normal	225	309	9	306	3	95
	slight dysplasia	465	2052			596	1432
	moderate dysplasia	844	2544	278	463	368	533
	severe dysplasia						
	tumor	2909	4741	488,5	957	17467	7953
	normal stroma	582	533	619	1162	4421	578
4 hours	normal	36	118	458	572	1642	491
	slight dysplasia			2048	2384		
	moderate dysplasia	4	3165	4040	5815	3193	5505
	severe dysplasia			5747	10716		
	tumor	1367	2668	12381	7206	5855	3653
	normal stroma	313	691	1899	2766	1860	850
8 hours	normal	19	632	1790	801	7038	5147
	slight dysplasia	652	1526	1738	567	11812	7010
	moderate dysplasia					10099	16068
	severe dysplasia					8644	10359
	tumor	3703	760	7047	4330	51706	26585
	normal stroma	934	917	1776	1086	13235	14431
24 hours	normal	1503	1397	1622	637	726	1589
	slight dysplasia	1381	749	195	1238	578	340
	moderate dysplasia	2873	4333	1884	1878	10	867
	severe dysplasia			675	3683	895	3796
	tumor	4466	2971	1608	2029	4536	2032
	normal stroma	2226	2452	1796	2062	761	1511
48 hours	normal	801	1109	90	408	3777	3643
	slight dysplasia	9731	10217	456	191		
	moderate dysplasia						
	severe dysplasia			280	94		
	tumor	14299	7106	1079	310	52104	15423
	normal stroma	6134	7051	313	193	30238	47845
96 hours	normal	205	472	2672	2712	477	108
	slight dysplasia	15	26	5494	8272	1306	95
	moderate dysplasia			2396	983	2787	3693
	severe dysplasia						
	tumor	4583	3524	6676	9226	6186	2873
	normal stroma	1063	1913	3904	3213	2165	2082

Chapter 4

In vivo quantification of photosensitizer concentration using fluorescence differential path-length spectroscopy: influence of photosensitizer formulation and tissue location

Abstract

Background and objective. *In vivo* measurement of photosensitizer concentrations may optimize clinical PDT. Fluorescence differential pathlength spectroscopy (fDPS) is a non-invasive optical technique that has been shown to accurately quantify the concentration of Foscan® in rat liver. As a next step towards clinical translation, the effect of different liposomal mTHPC formulations (Fospeg® and Foslip®) on fDPS is investigated. Furthermore, fDPS was evaluated in target organs for Head-and-Neck PDT.

Materials and Methods. Fifty-four healthy rats were intravenously injected with 1 formulation at 0.15 mg/kg mTHPC. fDPS was performed on liver, tongue and lip. mTHPC concentration estimates using fDPS were correlated with the results of the subsequent harvested and chemically extracted organs.

Results. An excellent goodness of fit (R^2) between fDPS and extraction was found for all formulations in the liver ($R^2=0.79$). A much lower R^2 between fDPS and extraction was found in lip ($R^2=0.46$) and tongue ($R^2=0.10$).

Conclusion. fDPS was validated for measuring mTHPC tissue concentration in the liver for Foscan, Foslip and Fospeg. The lower performance in lip and in particular tongue was mainly attributed to the more layered anatomical structure, which influences scattering properties and photosensitizer distribution.

Introduction

Photodynamic therapy (PDT) has been established as a local treatment modality for several kinds of malignancies in various organs [1-7]. PDT is based on the use of a light sensitive drug, a photosensitizer, which is locally applied or systemically administered. The photosensitizer *meta*-tetra(hydroxyphenyl)chlorin (mTHPC INN: Temoporfin) is one of the most potent clinically used photosensitizers to date [8-10]. Its development, study and clinical use was recently summarized in a comprehensive review [11]. The formulation of mTHPC in ethanol and propylene glycol (Foscan®) is in use for both curative and palliative treatment of head and neck squamous cell carcinoma (SCC) [7,12]. The treatment involves excitation of the administered photosensitizer with non-thermal light at the tumor site which leads to the formation of cytotoxic reactive oxygen species (ROS) [9,13-17]. The amount of ROS formed depends on the type of photosensitizer, its concentration, tissue oxygenation and the light fluence (rate). In head and neck tumors, treatment is typically performed using a mTHPC dose of 0.15 mg kg^{-1} mTHPC and light fluence of 20 J cm^{-2} at a fluence rate of 100 mW cm^{-2} delivered at 652nm [11]. However, despite the fixed light fluence and administered drug dose differences in PDT response may occur. Monitoring PDT parameters (oxygen, light fluence (rate) and photosensitizer concentration) during therapy could provide insight in the complex and dynamic interactions that occur during PDT and could give information on the deposited PDT dose [18]. Our group recently developed *fluorescence* differential pathlength spectroscopy (fDPS) as a tool to quantify micro vascular oxygen saturation (a surrogate marker of tissue oxygen concentration) and photosensitizer concentration in tissue [19,20]. In previous research, we were able to show that fDPS can be used to measure photosensitizer concentration in vivo in rat liver [21]. In this proof-of-concept study, our group used the photosensitizer mTHPC (Foscan) at 0.3 mg/kg as the target photosensitizer. A good linear correlation was found between the mTHPC concentration measured with fDPS and the mTHPC concentration measured with the gold standard, chemical extraction. As a next step towards clinical translation of fDPS for monitoring PDT in head & neck tumors, we here evaluate the performance of fDPS using a clinically relevant drug dose (0.15 mg/kg) in target organs for head-and-neck PDT: the lip and the tongue. From a tissue optics point of view it is more challenging to analyze oral mucosal tissues compared to liver tissue. For example, some oral tissues are keratinized (dorsum of the tongue, palate) and are effectively layered media, while other areas are not (inner lip, flour of mouth). The keratinization of the dorsal tongue is present in all mammals, although the degree of keratinization varies between species [22]. In the present study we have investigated how accurate fDPS measures photosensitizer concentrations in these more optically heterogeneous media. Similar to our previous proof-of-concept study, chemical extraction will serve as the gold standard for mTHPC concentration in these tissues.

One of the problems affecting Foscan in (pre)clinical PDT is its poor water solubility resulting in aggregation [11,23]. Therefore, water soluble liposomal formulations have been designed as

nanocarriers for mTHPC. A further advantage of liposomal drug-carrier systems is a reduced uptake by the mononuclear phagocyte system (MPS) and an enhanced permeability and retention effect (EPR) [24]. Two liposomal mTHPC formulations that have been developed are Foslip® and Fospeg® [8,25-32]. In contrast to Foslip, the surface of the liposomes used in Fospeg is coated by a hydrophilic polymer to decrease recognition by the RES and thus increase circulation time [24,33]. Both the incorporation of mTHPC into liposomes and the composition of different liposomes are known to significantly influence the spectral properties [28,30]. Furthermore, Foslip and Fospeg are known to exhibit different redistribution patterns and liposomal stability in serum [30]. We have therefore also investigated the influence of the use of nanocarriers on fDPS performance.

Material and methods

Animal and procedures
Fifty-four male Wistar rats (HsdCpb:W) weighing between 250 – 350 g, were purchased from Harlan Netherlands B.V. (Horst, The Netherlands). Three different formulations of mTHPC were kindly provided by Biolitec AG (Jena, Germany); Foscan (4 mg mTHPC/ml), Fospeg (1.5 mg mTHPC/ml) and Foslip (1.38 mg mTHPC/ml). Prior to the experiment, Foscan, Foslip and Fospeg were dissolved for intravenous injection under minimal light and kept at 4 °C in the dark, as recommended by the manufacturer. The dose used was 0.15 mg mTHPC /kg and animals were kept under reduced light conditions (< 60 lux). Prior to the experimental measurements the rats were anaesthetized using Isoflurane®/O_2/N_2O as a general inhalation anesthetic. Variations in mTHPC concentrations are achieved by taking measurements at different time points in the pharmacokinetics profile of each formulation. At 2, 4, 8, 24, 48 or 96 hours after injection (n= 3 animals per formulation per time point) tissue concentrations of mTHPC were measured using fDPS. In the oral cavity, 4 measurements were performed on the mucosa of the lip and 6 on the dorsum of the tongue, all at randomly chosen locations. Next, tissue overlying the liver was dissected which allowed measurements at 6 randomly chosen locations on the liver. Directly after the optical measurements the animals were terminated by cervical dislocation. Lip, tongue and liver were immediately excised and snapfrozen in liquid nitrogen. fDPS measured the concentration of mTHPC in lip, tongue and liver based on the emitted fluorescence of mTHPC. The concentration estimates determined by fDPS were compared to the concentration determined by chemical extraction. The experimental design for this study was approved by the experimental welfare committee of the University Medical Center Groningen and conformed to Dutch and European regulations for animal experimentation.

Measurement of mTHPC tissue concentration using fDPS
A measurement setup was used (figure 1) based on the setup described by the group of Amelink et al. [19,21]. In short, the measurement probe contained two 800 μm fibers at a core-to-core distance of 880 μm. The surface of the probe was polished under an angle of 15 degrees to minimize specular reflections during the measurements. One 800 μm fiber, the delivery-and-collection fiber (dc), is coupled to a bifurcated 400 μm fiber, containing a "delivery" and a "collection" leg. The delivery leg is coupled to a 200 μm bifurcated fiber, one leg of which is connected to a xenon light source (HPX-2000, Ocean Optics, Duiven, The Netherlands) and the other leg is connected to a 405 nm diode laser (Power Technology Inc., Arkansas, USA). The collection leg is coupled to another bifurcated 200 μm fiber, of which one leg directly leads to the first channel of spectrograph setup (MC-2000-4-TR2, Ocean Optics, Duiven, The Netherlands), while the other leg leads to a 570 nm long-pass filter before leading into the second channel of the spectrograph. The second 800 μm fiber of the probe, the collection fiber (c), is coupled to a bifurcated 400 μm fiber. One leg is directly coupled to the third channel of the spectrograph, while the other leg leads to the 570 nm long-pass filter, before being coupled in to the fourth channel of the spectrograph.
Before every measurement, de fDPS system was calibrated as described previously [7,19]. The measured DPS spectra were fitted to a model extensively described by our group in the literature [20,21,34-36], which returned quantitative estimates of blood volume fraction, micro vascular blood oxygenation and vessel diameter. The measured fDPS spectra are corrected for the effect of absorption by multiplying it by the ratio of DPS-signals at the excitation wavelength without and with absorption present, resulting in absorption-corrected fDPS spectra [37]. The contribution of mTHPC to the spectra was extracted by using a singular value decomposition (SVD) algorithm [38,39] using autofluorescence, protoporphyrin IX (PpIX) and mTHPC fluorescence as basis spectra.

Measurement of mTHPC tissue concentration using chemical extraction
To determine the concentration of mTHPC in the excised frozen tissues, the chemical extraction method of Kascakova et al. was used [40]. In short, small tissue samples (~0.1 grams) of lip, dorsum of the tongue and liver were used. In liver it was possible to randomly obtain three samples of liver tissue per animal, representative of tissue located on the liver surface as measured by fDPS. This way, we could average multiple random locations in both optical and chemical concentrations measurements of the liver. In tongue and lip however, we could only obtain one macroscopically representative tissue sample as measured by fDPS, due to the small size of the lip and tongue of rats. All tissue samples obtained were dissolved in 2 ml of the tissue solvent Solvable™ (Perkin Elmer, Groningen, The Netherlands) during 2 hours at 50 ºC, while regularly stirred. Subsequently, the solubilised solution was diluted further with Solvable™ to an optical density (OD) <0.1. The diluted samples were analyzed in a fluorimeter (Perkin Elmer, Groningen, The Netherlands) by using an excitation wavelength of 423 nm and a spectral detection band of 450 to 800 nm with a resolution of 0.5 nm. The basis spectrum of mTHPC was derived after correction for Solvable™ and autofluorescence components. The concentration of mTHPC was derived from a known calibration curve [40].

Statistics and correlation

Confidence intervals on the individual parameters for the individual measurements were determined based on the covariance matrix generated for each fit as described by Amelink et al. [41]. Differences in fluorescence intensities between formulations and tissue types at similar time points, were determined using one-way ANOVA (two-tailed) with the Bonferroni test for selected pairs of columns. (Non-) linear regression was used to fit a straight line forced through the origin to characterize the relation between fDPS and chemical extraction for different locations and formulations. To quantify goodness of fit of the regression lines, R-squared and 95% confidence intervals (CI) were determined.

Differences in slope of regression lines between datasets were assessed by the sum-of-squares F-test using a confidence interval of p=0.05. Pearson's correlation coefficient was used (two-tailed, 95% CI) in determining the correlation coefficients (r) between mTHPC fluorescence (fDPS) and blood volume (DPS). Graphpad Prism® (software version 5.0) was used for all statistical analysis.

Confocal Fluorescence Microscopy

Frozen tissue samples of control and mTHPC administered animals were handled under subdued light conditions. Liver, tongue and lip tissue sections of 50 μm were cut and mounted on Starfrost® adhesive glass slides (Menzel, Braunschwig, Germany). Fluorescence images were acquired at 10 x magnification using a confocal fluorescence microscope (LSM510, Zeiss, Jena, Germany). Excitation and light collection was performed using a 405 nm laser equipped with a 505 nm long-pass detection filter combined with spectral detection between 545-706 nm (at 10nm intervals). Typically 5 μm optical slices were acquired from the center of each 50 μm section. Software written in LabVIEW (v7.1) was used to account for the autofluorescence component of raw fluorescence; where the intensity of resulting images was confirmed to be that attributable to mTHPC fluorescence.

Results

Typical DPS and fDPS spectra and their fits are shown in figure 1A, 1B, respectively. The fitted mTHPC contributions of all 54 rats in the lip, tongue and liver at different time points based on the FDPS measurements is shown in figure 2A. The actual mTHPC concentrations determined using chemical extraction are shown in figure 2B.

Comparison of fDPS versus extraction

An overall comparison of fDPS and extraction per tissue type (figure 2A, 2B), show a similar trend for both methods as a function of time. One noticeable difference is that fDPS clearly measures more mTHPC in the lip than in the tongue at all time points, whereas in the extraction the mTHPC concentrations in these tissue types appears to be very similar. A compari-
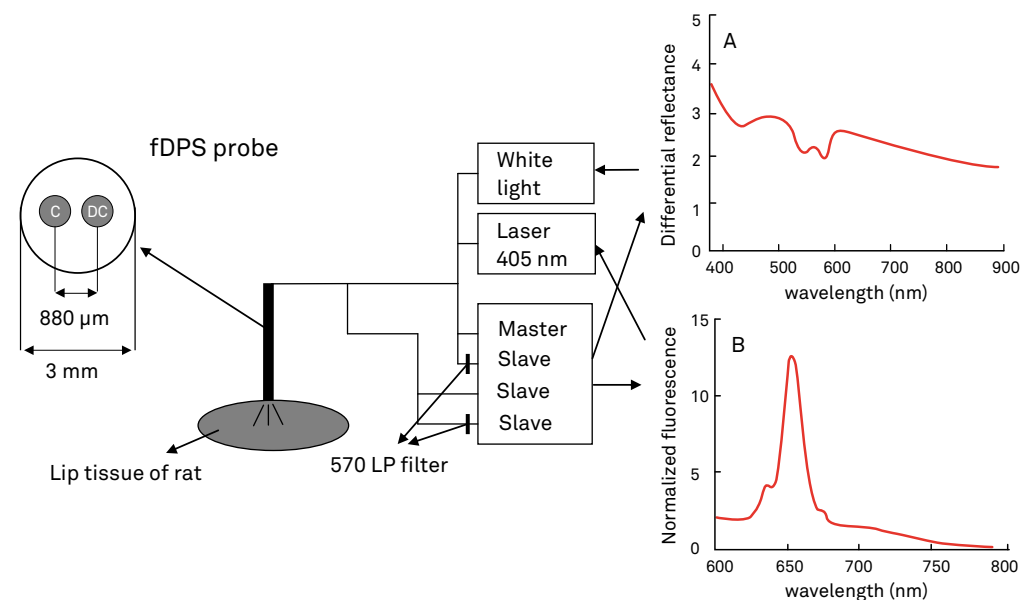

Figure 1. Schematic diagram of the fDPS measurement setup used in our study. On the right, acquired representative paired DPS spectra and fits (A) and fDPS spectra and fits (B) from the rat lip are shown. The fluorescence spectra demonstrate both autofluorescence and fluorescence attributable to mTHPC.

son of mean fluorescence measured by extraction shows no difference (p>0.05) between lip and tongue tissue (figure 2B). However, the same comparison in fluorescence signal measured by fDPS shows a significantly (p<0.0001) higher fluorescence in lip (figure 2A).

To further investigate this issue, we plotted the mTHPC component of the fDPS fluorescence versus the mTHPC concentration measured by chemical extraction (figure 3) for each formulation and tissue location within the same rat, thereby correcting for possible inter-animal differences in mTHPC uptake and intravenous administration. A linear regression line forced through the origin was used to characterize the relation between fDPS and chemical extraction for different locations and formulations.

In liver tissue (Figure 3A), an excellent goodness of fit was found for Foscan, Foslip and Fospeg (R^2= 0.74, 0.89, 0.82) for their 3 respective best-fit regression lines. The 6 regression lines for lip and tongue tissue (Figure 3B, 3C) showed overall much lower R^2, except for Foslip in lip tissue (R^2=0.79). Pooling of data per tissue-type (figure 3D), without discriminating for formulation-type, clearly showed differences in goodness of fit between different tissue types. Especially in the liver an excellent goodness of fit (R^2 = 0.79) was observed, while in lip (R^2=0.46) and in particular in tongue (R^2 =0.10), goodness of fit was much lower.
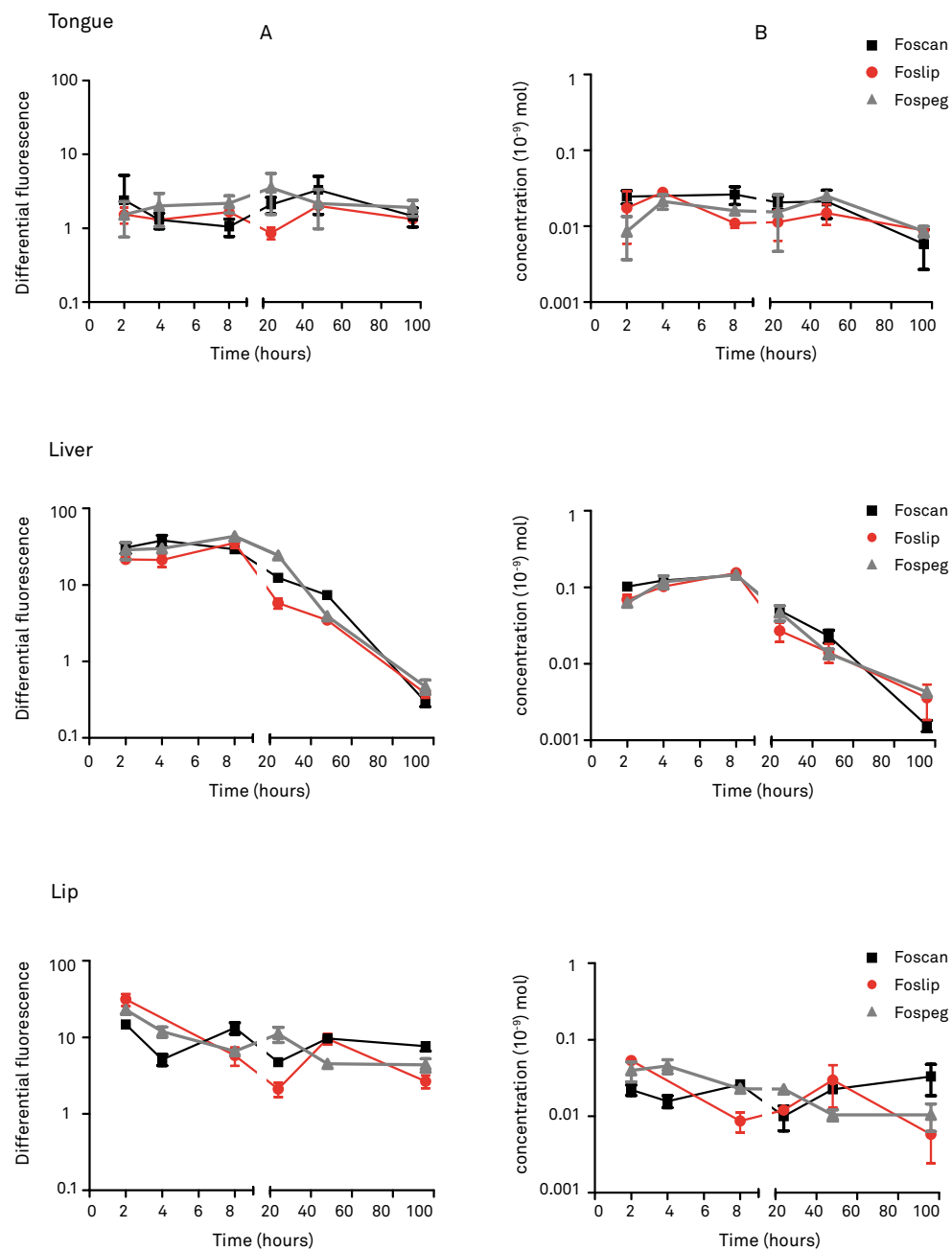
Figure 2. mTHPC concentration vs. time measured by fDPS (A) and chemical extraction (B) in tongue, liver and lip tissue for Foscan, Foslip and Fospeg (error bars indicate SEM). Note the logarithmic scale used for the y-axes.
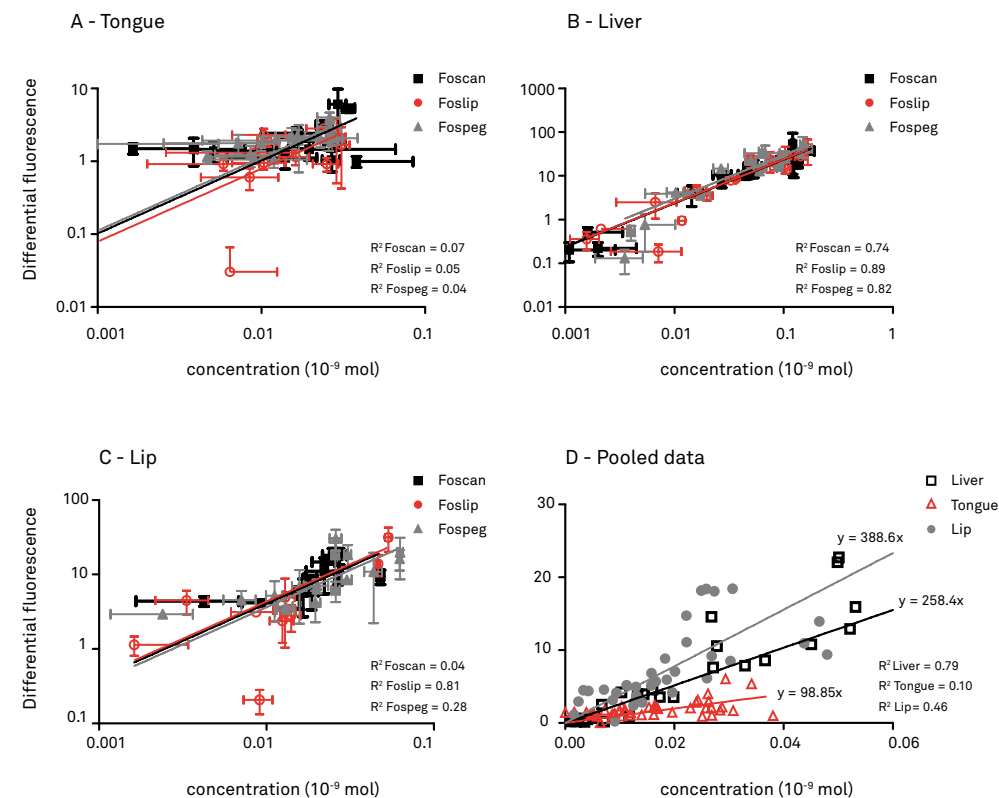
Figure 3. Optically measured mTHPC concentration (fDPS) versus true mTHPC concentration (extraction) for 3 different mTHPC formulations (Foscan, Foslip, Fospeg) in tongue (A), liver (B) and lip (C) tissue (error bars indicate SD, logarithmic scales). One measurement point represents multiple fDPS and extraction measurements of 1 rat. Best fit linear regression lines forced through the origin are plotted as solid lines. Pooled data per tissue type (D) show significant differences ($p < 0.001$) in the slopes of the regression lines between the tissue types (linear scales). In figure 3D, for clarity purposes only a portion of of the data points are shown and error bars are omitted

Influence of mTHPC formulations and tissue type

The influence of mTHPC formulation on fDPS was investigated by assessing differences in slope of regression lines within each tissue type. The sum-of-squares F-test showed a significant ($p < 0.05$, F: 3.252) difference in slope between mTHPC formulations in the liver, with Fospeg showing the highest slope (figure 3A). Similar analysis in lip and tongue tissue, showed no significant ($p < 0.05$) difference in slope between the formulations. Therefore, it is possible to calculate one slope for all three formulations in tongue and lip tissue (figure 3D). In lip and tongue tissue, the goodness of fit to the shared regression line (lip: $y = 388.6x$, 95%

Figure 4. Representative confocal fluorescence microscopy of tongue (A), liver (B) and lip (C) tissue. Images on the left depict distribution of mTHPC (colored red), corrected for autofluorescence. Images on the r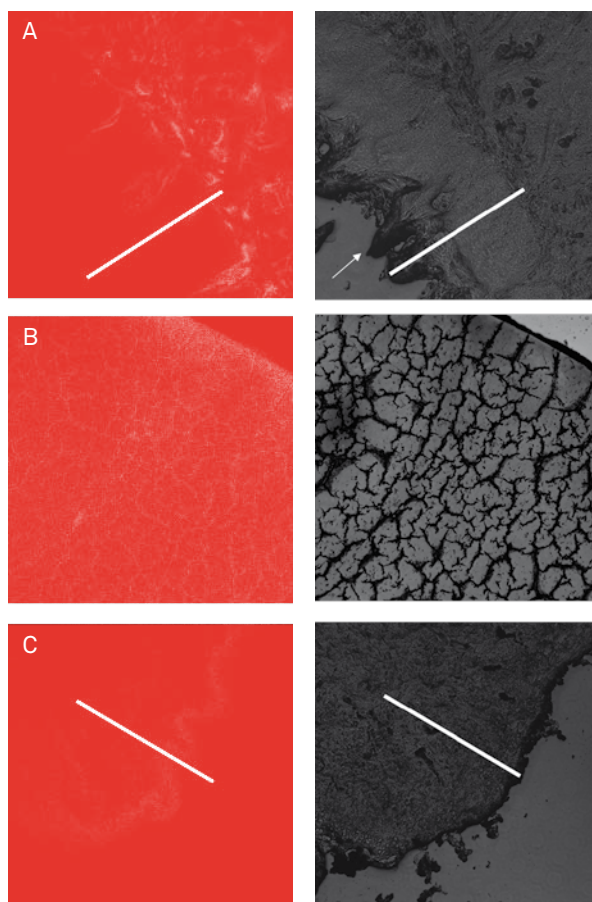ight show white light transmission images of the same slide. White scale bar: 500 μm, corresponding approximately with the interrogation depth of fDPS. Arrow in A) indicates one of the filliform papillae on the surface of the dorsal tongue.

CI: 321.1- 456.2, tongue: y=98.85x, 95% CI: 80.85 – 116.9) remained similar compared to the fit to 3 different lines (figure 3B, 3C). In order to assess the influence of tissue type on the slope regression lines, one overall regression line for liver was computed as well (y=258.4x, 95% CI: 242.8 – 280.5). The differences in slope of the overall regression lines of liver, lip and tongue are clear (figure 3D). Further statistical analysis confirmed the difference visually observed between the regression slopes of lip, tongue and liver: $p < 0.001$, F: 15.70.
To elucidate the differences between the slopes of the regression lines observed for different tissue types, the DPS data were further analyzed for scattering and blood volume

Table 1. Means and standard deviations of Mie scattering amplitudes in arbitrary units measured by fDPS for different tissue types.

	Tongue	Liver	Lip
Mean	1.220	0.5579	1.722
SD	0.1150	0.01844	0.1839

fraction differences. Overall analysis of the scattering amplitude per tissue type shows significant differences between tissue types ($p < 0.05$), with the least amount of scattering measured in the liver (table 1). No significant difference between the scattering amplitude for different mTHPC formulations was found at any time point in any tissue location. The blood volume fraction was found to have a significant correlation with mTHPC fluorescence only in the liver at the early (2, 4 and 8 hours) time points; a significant Pearson's correlation (r) was found of 0.90, 0.57 and 0.82, respectively.

Confocal microscopy
To further investigate our findings of a lower correlation in lip and tongue versus liver, fluorescence microscopy was performed to determine difference in mTHPC distribution. Confocal fluorescence microscopy was performed on 50 μm sections of liver, tongue and lip at various time points. Typical examples are shown in figure 4. Differences between tissue types are clearly observable; mTHPC is homogeneously spread throughout the liver section, while in lip and especially tongue tissue mTHPC is more heterogeneously distributed. Furthermore, the presence of layered structures can be clearly seen on the transmission images in lip and especially the tongue. In tongue tissue, the filliform papillae (arrow) can be clearly seen, and do not contain any mTHPC. In lip tissue, a much smaller superficial layer shows no uptake of mTHPC, combined with an increased uptake in the basement membrane.

Discussion

The direct relationship between mTHPC concentration and therapeutic outcome is complicated as numerous parameters influence the deposited PDT dose. However, the amount of mTHPC present in tissue is clearly an important factor in the deposition of PDT dose. Non-invasive monitoring of mTHPC concentration, as well as other important parameters during PDT, could allow for standardization and optimization of clinical PDT [4,18,42,43]. The aim of this study was to test the optical photosensitizer concentration measurement technique fDPS in a more clinically relevant environment compared to previous research performed on liver tissue [21]. Therefore, in our present study we used both a clinically relevant tissue location

and a clinically used drug dose. Furthermore, we tested the influence of promising new liposomal mTHPC formulations on fDPS performance.

In the liver, linear regression analysis showed an excellent goodness of fit (R^2) for the fDPS data to the extraction data, with Foscan, Foslip and Fospeg showing similar R^2. As a further validation for fDPS with our lower drug dose we compared our R^2 to the results of Kruijt *et al*. They found a R^2 value of 0.87 for Foscan measured by fDPS in the liver; we found a slightly lower R^2 value of 0.74. Our R^2 values were higher for Fospeg and Foslip at 0.82 and 0.89 respectively. Therefore, our measurements indicate that fDPS results could be reproduced in the liver at the clinically relevant dose of 0.15 mg/kg mTHPC, and extended to the Foslip and Fospeg formulations. Note that although the R^2 values can be compared between this study and the study of Kruijt et al, the regression line *slopes* cannot be compared between these two studies due to differences in the distance between the probe tip and the calibration standard combined with a difference in excitation wavelength in these studies. The lower wavelength in the current study excites mTHPC at its maximum absorption peak, to maximize mTHPC fluorescence at a lower drug dose. Since both the calibration method and the excitation wavelength were kept constant during our current study, comparison of regression line slopes within our study is possible.

fDPS measurements in a clinically relevant and optically more demanding environment of tongue and lip tissue showed a lower correlation between the fDPS data and the extraction data. Especially in tongue tissue, the correlation was poor with R^2 approaching 0 for all formulations. fDPS in lip tissue performed only slightly better. The possible reasons for this poor correlation are discussed below.

Influence of mTHPC formulation on fDPS performance
The influence of mTHPC formulation on fDPS signal proved to be significant in liver; Fospeg showed a higher slope of the regression line compared to both Foslip and Foscan. This suggests Fospeg has a significant higher quantum yield compared to the other formulations, in vivo. This could be explained by a relatively higher amount of non-aggregated mTHPC molecules in liposomal formulations [24]. Other *in-vivo* studies also describe a higher fluorescence of Fospeg compared to Foscan [25,26], although in these studies fluorescence intensity is also influenced by formulation specific pharmacokinetics such as aggregation and EPR. The significant difference in slope between the regression lines of Fospeg and Foslip probably depend on the detailed characteristics of the liposomes. It is known that pegylation of liposomes lengthens the plasma half-life of liposomes, thereby enabling a longer relative monomeric state of mTHPC in Fospeg, resulting in a relatively higher slope of the regression line compared to Foslip.

In both tongue and lip tissue, no significant difference in slope of the regression lines between the three mTHPC formulations was present. However, this may well be related to the lower goodness of fit and the higher CI of the regression lines in tongue and lip compared to liver, making a significant difference difficult to establish.

Influence of tissue type on fDPS performance
Our results clearly indicated a difference in fDPS performance depending on tissue type. Indeed, data analysis (figure 3D) showed very distinct differences in both the goodness of fit (R^2) and in the slope of the regression lines between tissue types.

To investigate the potential reasons for these differences, the different tissues were microscopically analyzed. Fluorescence microscopy showed clear differences in tissue specific distribution of mTHPC at all time points; in liver mTHPC was much more homogeneously distributed compared to both lip and tongue tissue (figure 4). Furthermore, in tongue tissue an absence of mTHPC fluorescence was seen in the most superficial, dorsal layer around the papillae. In contrast, in lip tissue a distinct layer (basement membrane) close to the surface shows more mTHPC fluorescence compared to the stroma, while similar to the tongue the most superficial layer shows almost no mTHPC fluorescence; however, in lip tissue this superficial layer is much smaller than in tongue tissue. These differences in distribution of mTHPC can be explained by the known difference in uptake of the dye in various structures like epithelium, lamina propria, striated muscle, smooth muscle, glands and fibro-connective tissue [44-47]. While liver tissue consists of multiple similar lobules, lip and tongue have a more complicated, layered composition.

The most important anatomical difference between lip and tongue tissue is the presence of keratinized stratified mucosa in the dorsal tongue while the inner side of the lip is covered by smooth non-keratinized mucosa. Besides tissue specific differences in mTHPC uptake, the biodistribution of mTHPC varies greatly with time [46,48]. However, the tissue specific mTHPC distribution is bound to have some influence on optical concentration measurements.

More challenging for our fluorescence measurement are the structural differences between tissue types. The layered, heterogeneous anatomy will certainly influence the tissue specific optical properties, in particular scattering properties. This difference is illustrated by significantly higher scattering amplitudes for lip and tongue tissue compared to liver tissue. Further indication of heterogeneity of lip and tongue tissue is given by the overall larger standard deviations of the scattering amplitude data compared to liver (table 1).

With knowledge of the microscopic differences observed in anatomy and mTHPC distribution between tissue types, we can explain the tissue specific differences in fDPS performance. The significant difference we found between correlation coefficients and slopes of the regression lines for different tissue types (figure 3D) is potentially caused by a combination of three factors: 1) the layered biodistribution of photosensitizer in combination with the superficial sampling volume of fDPS vs. larger sampling volume of chemical extraction, 2) inter-animal variations in the thickness of the keratin layer, and 3) the large differences in scattering properties between tissue types. With regards to the last point, although fDPS yields absorption corrected data, it does not correct for inter- and intra-tissue scattering differences [19,21,37]. As a result, the slope of the correlation between fDPS and extraction will be influenced by the average scattering coefficient of the tissue under investigation. Table 1 shows that the scattering properties vary with tissue type, resulting in different correlation

slopes; furthermore, intra- and inter-animal variations in scattering properties are more pronounced in more heterogeneous, layered tissue, such as tongue, resulting in a poorer correlation. A future challenge in improving optical concentration measurements performance would therefore be the ability to correct for scattering [49].

With regards to the first two factors, the correlation coefficients and slopes of the regression lines are also affected by a difference in interrogation volume of both techniques (extraction and fDPS). The minimum interrogation volume necessary to obtain accurate extraction data needs to be ~10^2mm³ (~0.1 gram of tissue), compared to ~0.2mm³ for fDPS. This difference will influence the slope of the regression line in tissue with a relatively heterogeneous (layered) mTHPC distribution, as found in tongue and lip tissue. In tongue a large part of the fDPS interrogation depth (~500 μm) of the dorsal tongue consists of papillae (keratin layer), as previously noted (figure 4). Papillae in the rat can be up to 200 μm in length [50] and showed decreased mTHPC uptake. Therefore only roughly half the fDPS interrogation volume contains mTHPC resulting in a lower slope of the regression line between fDPS-extracted mTHPC concentration and chemical extraction in the tongue. Conversely, because the surface of the lip tissue has an increased uptake of mTHPC compared to the surface of the tongue, the fDPS-measured mTHPC fluorescence in the lip increases for the same chemically extracted mTHPC concentration. This explains the significant higher mTHPC fluorescence as measured by fDPS in lip compared to tongue tissue, whereas in the extraction the mTHPC concentrations in these tissue types appear to be very similar (figure 2). Furthermore, a lower correlation will be found for tissues with more heterogeneous photosensitizer distributions. Although multiple fDPS measurements are averaged for each animal on each tissue type, inter-animal variations in photosensitizer biodistribution with tissue depth will not be averaged out and result in poor correlations. Similarly, inter-animal variations in average keratin layer thickness will also result in poor correlations between the superficially localized fDPS measurement and the "bulk" chemical extraction. The average thickness of the keratin layer in the Wistar rat tongue is described by others as 150μm (SD ± 100), measured at a central portion of the dorsal tongue [51]. However, the highly keratinized filliform papillae are well known to have substantial, intra-animal morphological variation among differing sites of the dorsal rat tongue [50]. This is supported by the even higher variation in average thickness we found for the whole dorsal tongue; 200 μm (SD: ± 120).

Extrapolation of our current results to the clinic is difficult; the dimensions and anatomy in normal human tissue are different compared to that of a rat [52]. For example, in humans the keratin layer of normal tissues is on average much smaller than in a rat, which is likely to pose less of a problem for the application of our technique on human tongue [22,52]. Furthermore, the pharmacokinetics of mTHPC differs between humans and rodents [23]. Another complicating factor is significant spatial variation in mTHPC biodistribution within tumors [48]. Moreover, tumors of the oral cavity could also disrupt or change the keratin layer, and therefore influence the performance of our technique. All these aspects may lead to very different observations and very different levels of homogeneity and heterogeneity in human

(tumor) tissues. In our current pre-clinical study, the emphasis has been on careful investigation of quantitative mTHPC measurements in optically more challenging tissues and of the influence of liposomal formulations. Promising nonetheless, were the results of a recent clinical study using fDPS [37]. The feasibility of clinical fDPS was shown, as clinical PDT treatments were monitored in three patients with SCCs of the oral cavity,

Conclusion

The non-invasive optical technique fDPS shows promising results in determining the mTHPC concentration in the rat liver for Foscan and for both liposomal formulations; Foslip and Fospeg. In liver, Fospeg showed a significant higher quantum yield compared to the other formulations. In optically homogeneous liver, the correlation with the extraction data was excellent. In the more heterogeneous lip tissue the correlation was lower. In tongue tissue the correlation was poor. The most likely cause of these differences in correlation is the more demanding optical characteristics of lip and especially tongue tissue. In tongue tissue fDPS performance is probably even further decreased by a thick layer of keratinized epithelium, which influences the optically sampled mTHPC distribution. Furthermore, in order to accurately monitor mTHPC concentration in heterogeneous tissue, a correction for scattering is needed. This is particularly important for (future) monitoring of mTHPC in spatially heterogeneous tumor tissues.

References

1. Dougherty TJ. An update on photodynamic therapy applications. J Clin Laser Med Surg. 2002 02;20(1044-5471; 1044-5471; 1):3-7.

2. Brown SB, Brown EA, Walker I. The present and future role of photodynamic therapy in cancer treatment. Lancet Oncol. 2004 08;5(1470-2045; 1470-2045; 8):497-508.

3. Lehmann P. Methyl aminolaevulinate-photodynamic therapy: A review of clinical trials in the treatment of actinic keratoses and nonmelanoma skin cancer. Br J Dermatol. 2007 May;156(5):793-801.

4. Wilson BC, Patterson MS. The physics, biophysics and technology of photodynamic therapy. Phys Med Biol. 2008 05/07;53(0031-9155; 0031-9155; 9):R61-109.

5. Moore CM, Pendse D, Emberton M, Medscape. Photodynamic therapy for prostate cancer--a review of current status and future promise. Nat Clin Pract Urol. 2009 Jan;6(1):18-30.

6. Bown SG, Rogowska AZ, Whitelaw DE, Lees WR, Lovat LB, Ripley P, et al. Photodynamic therapy for cancer of the pancreas. Gut. 2002 Apr;50(4):549-57.

7. Karakullukcu B, van Oudenaarde K, Copper MP, Klop WM, van Veen R, Wildeman M, et al. Photodynamic therapy of early stage oral cavity and oropharynx neoplasms: An outcome analysis of 170 patients. Eur Arch Otorhinolaryngol. 2011 Feb;268(2):281-8.

8. Berlanda J, Kiesslich T, Engelhardt V, Krammer B, Plaetzer K. Comparative in vitro study on the characteristics of different photosensitizers employed in PDT. J Photochem Photobiol B. 2010 Sep 2;100(3):173-80.

9. Dougherty TJ, Gomer CJ, Henderson BW, Jori G, Kessel D, Korbelik M, et al. Photodynamic therapy. J Natl Cancer Inst. 1998 06/17;90(0027-8874; 0027-8874; 12):889-905.

10. Mitra S, Foster TH. Photophysical parameters, photosensitizer retention and tissue optical properties completely account for the higher photodynamic efficacy of meso-tetra-hydroxyphenyl-chlorin vs photofrin. Photochem Photobiol. 2005 07;81(0031-8655; 0031-8655; 4):849-59.

11. Senge MO, Brandt JC. Temoporfin (foscan(R), 5,10,15,20-tetra(m-hydroxyphenyl)chlorin)--a second-generation photosensitizer. Photochem Photobiol. 2011 Nov-Dec;87(6):1240-96.

12. D'Cruz AK, Robinson MH, Biel MA. mTHPC-mediated photodynamic therapy in patients with advanced, incurable head and neck cancer: A multicenter study of 128 patients. Head Neck. 2004 03;26(1043-3074; 1043-3074; 3):232-40.

13. Henderson BW, Dougherty TJ. How does photodynamic therapy work? Photochem Photobiol. 1992 01;55(0031-8655; 0031-8655; 1):145-57.

14. Melnikova VO, Bezdetnaya LN, Potapenko AY, Guillemin F. Photodynamic properties of meta-tetra(hydroxyphenyl)chlorin in human tumor cells. Radiat Res. 1999 10;152(0033-7587; 0033-7587; 4):428-35.

15. Dewaele M, Maes H, Agostinis P. ROS-mediated mechanisms of autophagy stimulation and their relevance in cancer therapy. Autophagy. 2010 Oct;6(7):838-54.

16. Buytaert E, Dewaele M, Agostinis P. Molecular effectors of multiple cell death pathways initiated by photodynamic therapy. Biochim Biophys Acta. 2007 Sep;1776(1):86-107.

17. Ochsner M. Photophysical and photobiological processes in the photodynamic therapy of tumours. J Photochem Photobiol B. 1997 May;39(1):1-18.

18. Wilson BC, Patterson MS, Lilge L. Implicit and explicit dosimetry in photodynamic therapy: A new paradigm. Lasers Med Sci. 1997 Oct;12(3):182-99.

19. Amelink A, Kruijt B, Robinson DJ, Sterenborg HJ. Quantitative fluorescence spectroscopy in turbid media using fluorescence differential path length spectroscopy. J Biomed Opt. 2008 Sep-Oct;13(5):054051.

20. Amelink A, Sterenborg HJ. Measurement of the local optical properties of turbid media by differential path-length spectroscopy. Appl Opt. 2004 May 20;43(15):3048-54.

21. Kruijt B, Kascakova S, de Bruijn HS, van der Ploeg-van den Heuvel,A., Sterenborg HJ, Robinson DJ, et al. In vivo quantification of chromophore concentration using fluorescence differential path length spectroscopy. J Biomed Opt. 2009 May-Jun;14(3):034022.

22. Iwasaki S. Evolution of the structure and function of the vertebrate tongue. J Anat. 2002 Jul;201(1):1-13.

23. Triesscheijn M, Ruevekamp M, Out R, Van Berkel TJ, Schellens J, Baas P, et al. The pharmacokinetic behavior of the photosensitizer meso-tetra-hydroxyphenyl-chlorin in mice and men. Cancer Chemother Pharmacol. 2007 Jun;60(1):113-22.

24. Derycke AS, de Witte PA. Liposomes for photodynamic therapy. Adv Drug Deliv Rev. 2004 01/13;56(0169-409; 1):17-30.

25. de Visscher SA, Kascakova S, de Bruijn HS, van den Heuvel AP, Amelink A, Sterenborg HJ, et al. Fluorescence localization and kinetics of mTHPC and liposomal formulations of mTHPC in the window-chamber tumor model. Lasers Surg Med. 2011 Aug;43(6):528-36.

26. Buchholz J, Kaser-Hotz B, Khan T, Rohrer Bley C, Melzer K, Schwendener RA, et al. Optimizing photodynamic therapy: In vivo pharmacokinetics of liposomal meta-(tetrahydroxyphenyl)chlorin in feline squamous cell carcinoma. Clin Cancer Res. 2005 10/15;11(1078-0432; 20):7538-44.

27. Compagnin C, Moret F, Celotti L, Miotto G, Woodhams JH, Macrobert AJ, et al. Meta-tetra(hydroxyphenyl)chlorin-loaded liposomes sterically stabilised with poly(ethylene glycol) of different length and density: Characterisation, in vitro cellular uptake and phototoxicity. Photochem Photobiol Sci. 2011 Nov 2;10(11):1751-9.

28. Kachatkou D, Sasnouski S, Zorin V, Zorina T, D'Hallewin MA, Guillemin F, et al. Unusual photoinduced response of mTHPC liposomal formulation (foslip). Photochem Photobiol. 2009 05;85(0031-8655; 0031-8655; 3):719-24.

29. Kiesslich T, Berlanda J, Plaetzer K, Krammer B, Berr F. Comparative characterization of the efficiency and cellular pharmacokinetics of foscan- and foslip-based photodynamic treatment in human biliary tract cancer cell lines. Photochem Photobiol Sci. 2007 Jun;6(6):619-27.

30. Reshetov V, Kachatkou D, Shmigol T, Zorin V, D'Hallewin MA, Guillemin F, et al. Redistribution of meta-tetra(hydroxyphenyl)chlorin (m-THPC) from conventional and PEGylated liposomes to biological substrates. Photochem Photobiol Sci. 2011 Jun;10(6):911-9.

31. Svensson J, Johansson A, Grafe S, Gitter B, Trebst T, Bendsoe N, et al. Tumor selectivity at short times following systemic administration of a liposomal temoporfin formulation in a murine tumor model. Photochem Photobiol. 2007 09;83(0031-8655; 0031-8655; 5):1211-9.

32. Bovis MJ, Woodhams JH, Loizidou M, Scheglmann D, Bown SG, Macrobert AJ. Improved in vivo delivery of m-THPC via pegylated liposomes for use in photodynamic therapy. J Control Release. 2011 Oct 1.

33. Romberg B, Hennink WE, Storm G. Sheddable coatings for long-circulating nanoparticles. Pharm Res. 2008 Jan;25(1):55-71.

34. Amelink A, Sterenborg HJ, Bard MP, Burgers SA. In vivo measurement of the local optical properties of tissue by use of differential path-length spectroscopy. Opt Lett. 2004 May 15;29(10):1087-9.

35. Amelink A, Kaspers OP, Sterenborg HJ, van der Wal JE, Roodenburg JL, Witjes MJ. Non-invasive measurement of the morphology and physiology of oral mucosa by use of optical spectroscopy. Oral Oncol. 2008 Jan;44(1):65-71.

36. van Veen RL, Amelink A, Menke-Pluymers M, van der Pol C, Sterenborg HJ. Optical biopsy of breast tissue using differential path-length spectroscopy. Phys Med Biol. 2005 Jun 7;50(11):2573-81.

37. Karakullukcu B, Kanick SC, Aans JB, Sterenborg HJ, Tan IB, Amelink A, et al. Clinical feasibility of monitoring m-THPC mediated photodynamic therapy by means of fluorescence differential path-length spectroscopy. J Biophotonics. 2011 Oct;4(10):740-51.

38. Kruijt B, de Bruijn HS, van der Ploeg-van den Heuvel,A., de Bruin RW, Sterenborg HJ, Amelink A, et al. Monitoring ALA-induced PpIX photodynamic therapy in the rat esophagus using fluorescence and reflectance spectroscopy. Photochem Photobiol. 2008 Nov-Dec;84(6):1515-27.

39. Finlay JC, Mitra S, Foster TH. In vivo mTHPC photobleaching in normal rat skin exhibits unique irradiance-dependent features. Photochem Photobiol. 2002 Mar;75(3):282-8.

40. Kascakova S, Kruijt B, de Bruijn HS, van der Ploeg-van den Heuvel,A., Robinson DJ, Sterenborg HJ, et al. Ex vivo quantification of mTHPC concentration in tissue: Influence of chemical extraction on the optical properties. J Photochem Photobiol B. 2008 May 29;91(2-3):99-107.

41. Amelink A, Robinson DJ, Sterenborg HJ. Confidence intervals on fit parameters derived from optical reflectance spectroscopy measurements. J Biomed Opt. 2008 Sep-Oct;13(5):054044.

42. Kruijt B, van der Ploeg-van den Heuvel,A., de Bruijn HS, Sterenborg HJ, Amelink A, Robinson DJ. Monitoring interstitial m-THPC-PDT in vivo using fluorescence and reflectance spectroscopy. Lasers Surg Med. 2009 Nov;41(9):653-64.

43. Robinson DJ, de Bruijn HS, van der Veen N, Stringer MR, Brown SB, Star WM. Fluorescence photobleaching of ALA-induced protoporphyrin IX during photodynamic therapy of normal hairless mouse skin: The effect of light dose and irradiance and the resulting biological effect. Photochem Photobiol. 1998 Jan;67(1):140-9.

44. Andrejevic Blant S, Ballini JP, van den Bergh H, Fontolliet C, Wagnieres G, Monnier P. Time-dependent biodistribution of tetra(m-hydroxyphenyl)chlorin and benzoporphyrin derivative monoacid ring A in the hamster model: Comparative fluorescence microscopy study. Photochem Photobiol. 2000 Mar;71(3):333-40.

45. Peng Q, Moan J, Ma LW, Nesland JM. Uptake, localization, and photodynamic effect of meso-tetra(hydroxyphenyl)porphine and its corresponding chlorin in normal and tumor tissues of mice bearing mammary carcinoma. Cancer Res. 1995 Jun 15;55(12):2620-6.

46. Andrejevic S, Savary JF, Monnier P, Fontolliet C, Braichotte D, Wagnieres G, et al. Measurements by fluorescence microscopy of the time-dependent distribution of meso-tetra-hydroxyphenylchlorin in healthy tissues and chemically induced "early" squamous cell carcinoma of the syrian hamster cheek pouch. J Photochem Photobiol B. 1996 Nov;36(2):143-51.

47. Blant SA, Glanzmann TM, Ballini JP, Wagnieres G, van den Bergh H, Monnier P. Uptake and localisation of mTHPC (foscan) and its 14C-labelled form in normal and tumour tissues of the hamster squamous cell carcinoma model: A comparative study. Br J Cancer. 2002 Dec 2;87(12):1470-8.

48. Mitra S, Maugain E, Bolotine L, Guillemin F, Foster TH. Temporally and spatially heterogeneous distribution of mTHPC in a murine tumor observed by two-color confocal fluorescence imaging and spectroscopy in a whole-mount model. Photochem Photobiol. 2005 Sep-Oct;81(5):1123-30.

49. Kanick S, Robinson D, Sterenborg H, Amelink A. Semi-empirical model of the effect of scattering on single fiber fluorescence intensity measured on a turbid medium. Biomed Opt Expr. 2012 Jan 1;3(1):137-52.

50. Nagato T, Nagaki M, Murakami M, Tanioka H. Three-dimensional architecture of rat lingual filiform papillae with special reference to the epithelium-connective tissue interface. J Anat. 1989 Aug;165:177-89.

51. Kobayashi A, Iikubo M, Kojima I, Ikeda H, Sakamoto M, Sasano T. Morphological and histopathological changes in tongues of experimentally developed acromegaly-like rats. Horm Metab Res. 2006 Mar;38(3):146-51.

52. Toyoda M, Sakita S, Kagoura M, Morohashi M. Electron microscopic characterization of filiform papillae in the normal human tongue. Arch Histol Cytol. 1998 Aug;61(3):253-68.

Chapter 5

Summary, general discussion and future perspectives

Summary

Standard treatment of head and neck squamous cell carcinoma (HNSCC) consists of surgery, radiotherapy or chemoradiation, as monotherapy or multimodal strategy.
Most treatment strategies of HNSCC are associated with localized impairment of organ function and diminished aesthetic appearance. These side effects are more pronounced at certain anatomical locations, increased tumor size and with treatment of recurring or additional tumors. Photodynamic Therapy (PDT) is used in curative and palliative local treatment for tumors of various anatomical origins. Currently, the potent photosensitizer *meta*-tetra(hydroxyphenyl)chlorin (mTHPC) is used in its clinically available Foscan® formulation as an alternative treatment for early stage and advanced stage HNSCC with promising clinical results, supposedly with a decrease of treatment related morbidity. However, literature seldom reports efficacy or morbidity of PDT in relation to the standard treatment regimes. Even so, (pre)clinical studies describe some drawbacks of mTHPC due to its properties; prolonged phototoxicity, aggregation of the highly hydrophobic mTHPC in physiological conditions and high uptake by the mononuclear phagocyte system (MPS) resulting in reduced bioavailability at the target organ. To enhance the properties of mTHPC while retaining its potency, water-soluble liposomal mTHPC formulations have been designed. Another possible route for enhancement of PDT is by *in vivo* dosimetry of the complex, interdependent dynamic interactions of the parameters (oxygen, fluence (rate) and photosensitizer) involved in PDT.
In the research described in this thesis the efficacy of currently used mTHPC mediated PDT for HNSCC is presented. Moreover, the results of the evaluation of two liposomal mTHPC formulations in tumor models and a new tool (fDPS) to measure mTHPC tissue concentrations are presented.

Chapter 2.1 is a systematic review of the literature on mTHPC mediated PDT (Foscan) in treatment of HNSCC. Twelve studies were included for our review, none of which exceeded level 3 on the Oxford levels of evidence. Six of 12 studies described PDT with palliative intent of which 3 described surface illumination and the remaining 3 studies described interstitial PDT of tumors with a bigger volume. Findings from this review support the use of PDT and interstitial PDT for palliative intent in patients with no further treatment options available, as substantial tumor response and increase in quality of life was noted. These palliative studies suggested lower response with superficial PDT for tumors with a depth > 10 mm and suggested a high need for an alternative airway post-operatively with interstitial PDT. Evaluation of PDT for early stage disease is difficult, as no comparative studies with other modalities are available. However, evaluation on treatment response following PDT stratified according to groups was possible. Treatment response with PDT for T1 tumors is significantly better compared to T2 tumors. Furthermore, tumor response with PDT is significantly better for 1st primary tumors versus non-1st primary tumors. The most common complication of Foscan mediated PDT described is phototoxicity, pain or discoloration at the injection site is also commonly described.

In **chapter 2.2** a retrospective comparison between mTHPC (Foscan) mediated PDT and transoral surgery for early stage, primary oral SCC is given. PDT patients were included from studies identified in our systematic review (chapter 2.1), while the surgically treated patients were included from our hospital database. All PDT tumors had a maximum tumor depth of 5 mm as assesed by imaging. To select similar primary tumors, infiltration depth was restricted to 5mm for the surgery group as assessed by pathology. A total of 126 T1 and 30 T2 tumors were included in the PDT group and 58 T1 and 33 T2 tumors were included in the surgically treated group. Complete response (CR) rates of PDT and surgery showed no significant differences and were 86% and 76% for T1 respectively, and for T2 63% and 78%. When comparing local disease free survival (LDFS), PDT was significantly less effective than surgery for both T1 and T2 tumors. However, when comparing the need for local retreatment no significant difference for T1 tumors were found, while for T2 tumors surgery resulted in significantly less frequent need for local retreatment. Overall survival was not significantly different for PDT and surgery for both patients with T1 and T2 tumors. We therefore conclude that treatment of primary T1 tumors of the oral cavity by either mTHPC mediated PDT or transoral surgery seems to result in similar outcomes. For T2 tumors PDT seemed less effective; PDT and surgery showed similar overall survival rates for both patients with T1 and T2 tumors.

Chapter 3.1 describes the evaluation of two liposomal formulations of mTHPC, Foslip® and Fospeg®. Foslip consists of mTHPC encapsulated in conventional liposomes; Fospeg consists of mTHPC encapsulated in pegylated liposomes. Foslip, Fospeg and Foscan were injected at a dose of 0.15 mg/kg mTHPC and subsequently mTHPC fluorescence kinetics was studied using the rat window-chamber model. At 7 time points after injection (5 minutes – 96 hours) fluorescence images were made with a charge-coupled device (CCD). These fluorescence images were corrected by a ratio fluorescence imaging technique (chapter 3.2). The three mTHPC formulations showed marked differences in their fluorescence kinetic profile. In vasculature, Fospeg clearly shows higher fluorescence intensities during the experimental time points compared to Foscan and Foslip. Maximum tumor fluorescence is reached at 8 hours for Fospeg and at 24 hours for Foscan and Foslip with overall highest tumor fluorescence for Fospeg between 2 - 48 hours. Increased fluorescence intensities at 2 and 4 hours after injection in tumor over normal tissue (selectivity) proved significant for Foslip and nearly reached significance for Fospeg. Foscan showed no "tumor selectivity".
Our findings suggest that liposomal bound mTHPC and especially Fospeg, enhances the bioavailability of mTHPC in vasculature and tumor tissue. Next to that it might reduce the necessary drug light interval.

In **chapter 3.2** the ratio fluorescence imaging technique we developed and used for the quantification of fluorescence images in the window chamber model (chapter 3.1) is tested and explained. A problem associated with fluorescence measurements is the difficulty of obtaining quantitative fluorescence, due to varying optical properties of tissues in time. The ratiometric quantification method we developed to monitor mTHPC pharmacokinetics in the rat window-chamber model uses a combination of dual-wavelength excitation and dual-wavelength detection and accounts for the wavelength dependence of tissue optical properties. Fluorescence images were captured by a CCD after injection of 0.15 mg/kg mTHPC. Excitation wavelengths were at 629 nm and 652 nm. Two fluorescence emission bands were used; one at the secondary fluorescence maximum of mTHPC (720 nm) and one in a region of tissue autofluorescence and no photosensitizer fluorescence (> 763 nm). An algorithm was used to correct for optical properties.

During the experimentation time, the autofluorescence intensity showed a steady increase for all tissues above 24 hours. Furthermore, uncorrected fluorescence signals showed larger intra-chamber variations than the corrected fluorescence signal of the same tissue. Only at early time points in vasculature large variations in corrected mTHPC fluorescence were observed. A similar fluorescence pharmacokinetic profile was observed when comparing our correction algorithm with a previously validated double ratio ratiometric technique.

In **chapter 3.3**, we used the 4-nitroquinoline-1-oxide (4NQO) induced oral cavity carcinogen model to compare the localization of the different mTHPC formulations (Foscan, Foslip and Fospeg) within normal, precancerous and cancerous tissue in 54 rats. When oral examination revealed tumor, the rats received 0.15 mg/kg mTHPC. At several time points between 2 - 96 hours after injection the rats were terminated. Oral tissue was sectioned for hematoxylin and eosin (HE) coupes and for corresponding fluorescence confocal microscopy. The HE slides were assessed on tissue type and scored on the severity of dysplasia by the Epithelial Atypia Index (EAI). Our measurements were corrected for variations in the experimental setup. Fospeg showed higher fluorescence in normal and tumor tissue compared to Foslip and Foscan, in particular at early time points (<24 hours). Fospeg showed more tumor selectivity (mTHPC fluorescence intensity in tumor vs normal stroma) compared to Foslip and especially Foscan at early time points. Highest mTHPC fluorescence was shown for Fospeg in tumor tissue 8 hours after injection. Only a weak correlation between increasing grade EAI and higher mTHPC fluorescence was found. Our findings derived from the 4NQO model suggest that Fospeg has a superior fluorescence pharmacokinetic profile and tumor uptake at early time points over Foslip and in particular Foscan. In contrast to tumor tissue, precancerous tissue does not show significant increased mTHPC fluorescence intensities.

In **chapter 4.1**, we investigated the effect of different mTHPC formulations (Foscan, Foslip and Fospeg) and clinically relevant, heterogeneous tissue on the performance of fluorescence differential path-length spectroscopy (fDPS). fDPS is a non-invasive optical technique

developed to accurately quantify the concentration of mTHPC in tissue. In 54 healthy rats multiple fDPS measurements were performed on liver, tongue and lip tissue at several time point 2 - 96 hours after injection of 0.15 mg/kg mTHPC. After fDPS measurements, rats were terminated and the measured tissue was harvested. mTHPC concentrations determined by fDPS were correlated with the mTHPC concentrations of the harvested and chemically extracted tissue using linear regression analysis.

An excellent goodness of fit between fDPS and extraction was found for all formulations in the liver. In lip and especially in tongue tissue a much lower goodness of fit between fDPS and extraction was found. Fluorescence microscopy clearly showed differences in tissue specific distribution of mTHPC at all time points; in liver mTHPC was much more homogeneously distributed compared to both lip and tongue tissue. In tongue tissue a thick layer of keratinized epithelium without mTHPC uptake was present, taking up a big portion of the fDPS interrogation volume. Lip and tongue tissue differed further from liver as it showed significantly higher scattering amplitudes accompanied by larger standard deviations. The different formulations of mTHPC influenced fDPS; the slope of the regression line for Fospeg was higher compared to both Foslip and Foscan. fDPS can reliable measure mTHPC concentrations of Foscan, Foslip and Fospeg in the optically homogenous liver. fDPS in optically more heterogeneous tissue is hampered by scattering.

General discussion

Evaluation of mTHPC mediated Photodynamic therapy in clinical treatment of head and neck squamous cell carcinoma
In **chapter 2** we described the current evidence in literature on both curative and palliative mTHPC mediated PDT. Our review clearly showed a lack of prospective, comparative, randomized studies hurting the attributed evidence of papers on mTHPC mediated PDT (chapter 2.1). Despite this limitation, our review concluded that PDT should be considered for patients with untreatable local disease lacking any further treatment options as substantial tumor response and increase in quality of life was noted. Comparing the results of PDT with palliative intent to conventional modalities has not been performed in literature. However, the added value of such a study is uncertain as heterogeneity of patients and tumors with respect to previous treatments, tumor spread and co morbidities are to be expected. Instead of comparing PDT with the often used systemic treatments (combination chemotherapy) in patients with end stage disease, proper indications for the use of the local treatment modality PDT in these difficult to treat patients should be made [1-3]. Even though interstitial PDT was found to have an excellent local treatment response in big tumors considering the lack of further treatment options, gains in efficacy could probably be achieved by the use of digital pre-treatment dosimetric planning for the positioning of the interstitial fibers [2]. While the clinical application of dosimetry is to be encouraged, the complexity of the interdependent

treatment parameters underlying PDT needs better understanding to allow for true clinical, *in vivo*, feedback on the factors determining deposited PDT dose. Therefore, a first step should be quantification of oxygen saturation, mTHPC uptake, blood flow, fluence (rate) and the influence of optical properties on measurement techniques. The complexity of PDT is further illustrated by the time-dependent yet not fully predictable pathway of PDT inflicted cell death [4-6]. Similar to interstitial PDT, to a lesser degree these same problems arise in the prediction of treatment response after superficial PDT of smaller tumors. The absence of comparative studies on mTHPC mediated PDT for early stage disease is surprising for a drug that is on the market for nearly two decades. In contrast to palliative treatment, comparable treatment groups for PDT and surgery/radiotherapy could be performed in well-designed, randomized, studies. Most of the studies on PDT with curative intent described similar treatment response, better aesthetic outcome and preservation of organ function compared to surgery and radiotherapy evidenced by mainly anecdotal evidence and own experience [7-9]. While we can confirm the potential of PDT from our own experience, the use of PDT for treatment of early stage disease should be backed up by solid evidence; as both surgery and radiotherapy of early stage disease have high cure rates, PDT must reach at least similar rates to be considered a worthwhile treatment option. In order to get some comparison of PDT versus surgery in treatment of early stage disease, we performed a retrospective study. While several flaws in design can be identified in the study we performed, it allowed us to make some sort of comparison between PDT and surgery. Despite the problematic study design, our inclusion criteria were chosen so that the cases from our surgical database optimally reflect the cases from the PDT database. Our main conclusion was that PDT and surgery resulted in similar treatment results for T1 tumors, for T2 tumors PDT performed worse (chapter 2.2). Overall survival was similar for surgery and PDT stratified according to tumor size. This may well suggest that failure of primary treatment of T2 tumors after PDT is manageable by subsequent salvage treatment. Future comparative studies should address the treatment specific differences in assessment of a complete response for PDT (visual inspection) and surgery (histopathological analysis). For surgery this difference resulted in a benefit over PDT as re-excision after compromised surgical margins is often seen as one primary treatment. To account for this, we used the need for retreatment and survival as endpoints for our study. A known intrinsic advantage of PDT over radiotherapy and surgery is the possibility of re-treatment of recurrent or residual disease by either PDT or conventional treatment after previous PDT [10]. While the efficacy of PDT in achieving treatment response could be compared to surgery as described previously, a comparison in post-treatment morbidity was not identified and could not be performed in our retrospective comparative study. Therefore we can only conclude that the possible clinical advantage in aesthetic outcome and function preservation of PDT over surgery and radiotherapy, tough often mentioned, and observed in our institute, is without any evidence. As one of the main problems in treating HNSCC are patients with multiple primary or recurrent tumors in which treatment is associated with loss of organ function, possible organ sparing treatments like PDT should be

investigated. We were able to investigate the complications attributed to PDT which were mostly phototoxicity reactions due to non compliance of patients to the stringent light protocol in combination with mTHPC associated photosensitivity. Pain or discoloration at the injection site is also common and suggests a problematic injection, due to the problematic solubility of hydrophobic mTHPC in plasma. Clinical mTHPC mediated PDT is a welcome addition for treatment of patients with end-stage HNSCC without further treatment options. The benefit of PDT over conventional treatment for early-stage HNSCC is not sufficiently investigated; in retrospective studies, treatment results seem similar to surgery, however influence on morbidity compared to surgery is not assessed. The main advantage of PDT is that it does not utilize ionizing radiation and thus does not have a maximal cumulative dose. Information on PDT associated morbidity compared to surgery and radiotherapy in clinical treatment is missing and is necessary to give a verdict over PDT for clinical treatment of early stage disease. To evaluate a possible added benefit of mTHPC mediated PDT in the treatment of early stage disease, future prospective studies should compare efficacy of PDT with conventional treatment on a group of well defined tumors besides the desired comparison in treatment related morbidity. Some of the complications described in literature associated with the hydrophobicity of Foscan, may be avoided or decreased by the use of mTHPC encapsulated into liposomes. Currently, mTHPC mediated PDT seems worthwhile for patients with advanced local disease without further treatment options left. Treatment with curative intent for T1 tumors shows similar treatment results to surgical treatment in the need for retreatment, any difference in treatment related morbidity should be investigated further.

Enhancement of mTHPC fluorescence pharmacokinetics by liposomes
Liposomal drug-carrier systems have previously shown to increase tumor uptake and improve water-solubility of mTHPC in a few, flawed studies. For the first time Foslip, Fospeg (both liposomal mTHPC) were compared to Foscan within one animal tumor models up to 96 hours after injection. We compared fluorescence pharmacokinetics of Foscan with both Foslip and Fospeg to gain insight into the possibilities for future (pre) clinical PDT studies using liposomal mTHPC formulations. **Chapter 3** described the fluorescence pharmacokinetics over 96 hours of systemically administered Foscan, Foslip and Fospeg in a xenograft window-chamber model (chapter 3.1) and in the induced 4NQO tumor model (chapter 3.3). We concluded from our results that liposomal encapsulation of mTHPC clearly increases mTHPC fluorescence in tissue at earlier time points compared to Foscan. Of the two liposomal formulations, Fospeg showed the most mTHPC fluorescence during our experiments suggesting a clinical interesting ability of increased PDT efficacy. Fospeg even showed signs of accumulation in tumor tissue or so called tumor selectivity. The data extracted from the window chamber model allowed us to compare the non-invasive fluorescence pharmacokinetics of mTHPC in tumor, vasculature and normal tissue over 96 hours within the same animal. Quantification of measured mTHPC fluorescence is essential to determine small differences in fluorescence emitted from different tissue types and different formulations.

Quantification was partly possible due to the thin tissue layer present in the window chamber model, decreasing influence of optical properties. The most significant step in acquiring quantitative *in vivo* mTHPC fluorescence was the development of a technique that corrected for varying optical properties in time (chapter 3.2). The ratiometric quantification method uses a combination of dual-wavelength excitation and dual-wavelength detection in the near infrared region (NIR) where the tissue absorption and scattering are relatively small. The first excitation wavelength of 652 nm (720 nm detection) was used to excite the mTHPC and autofluorescence whereas the second excitation wavelength at 629 nm (> 763 nm detection) only excited autofluorescence, so that this could be subtracted. This subtraction was performed as autofluorescence was not significantly different for 629 and 652 nm excitation. Subsequently the autofluorescence-corrected mTHPC image was divided by the autofluorescence signal to correct for variations in tissue optical properties. Because even small differences in mTHPC fluorescence between tissue types or formulations should be investigated, accurate quantification of mTHPC is important. The need for accurate quantification was clearly shown as autofluorescence of the same tissue changed over time and uncorrected fluorescence signals showed relative large intra-chamber variations. The importance of the 4NQO model used lies in the possibility to investigate the influence of precancerous tissue on mTHPC uptake for different formulations in a non-xenograft model. While xenograft models are suited to investigating pharmacokinetics, induced tumor models are more likely to mimic pharmacokinetics of tumors encountered in the clinic. The choice of tumor model is important as the tumor model used is most likely the cause of the different results reported in several, similar pharmacokinetic studies [11-13]. The prolific growth pattern often characteristic of xenograft models influences almost all aspects of tumor biology and thereby its influence on pharmacokinetics. The most important factors affecting transport of drugs to tumor tissue are the tumor vasculature, tumor growth environment and functioning of the MPS. A known characteristic of tumor vasculature is the occurrence of the enhanced permeability and retention (EPR) effect, in which "leaky vasculature" without adequate lymphatic drainage cause passive accumulation of liposomes (macromolecules) in tumor tissue [14,15]. These factors affecting drug transportation are known to vary based on the cancer model used [16]. For instance, xenograft models often show a high uptake in tumor tissue due to enhanced EPR effect resulting from prolific growing vasculature therefore giving a false impression of tumor selective uptake of a drug. A recent workgroup on nanoparticles and the EPR effect for drug delivery in oncology stated that for preclinical research into drugs and their EPR effect, (animal) tumor models characterized by heterogeneous tumor tissue are preferred over xenograft models as they better reflect the clinical situation [16]. We used fluorescence microscopy to describe the spatial distribution of mTHPC in the heterogeneous tissue. By correlating the location and fluorescence intensity of mTHPC to the grade of tissue dysplasia and tissue compartment (epithelium, stromal tissue) we could assess the influence of dysplasia grade, tissue type, mTHPC formulation and drug-light interval on localization of mTHPC. This is a clear advantage over typical xenograft studies were extrac-

tion or gross fluorescence measurements are averaged out over the complete interrogated volume and precancerous tissue is not even present.

Fospeg showed in the window chamber model and the 4NQO model significant higher mTHPC fluorescence in tumor tissue and in vasculature at earlier time points; with the 8 hour time point showing the overall highest mTHPC fluorescence in tumor tissue. The proposed increased uptake of liposomal mTHPC in tumor tissue was indeed present for Foslip and especially Fospeg. This tumor selectivity was mostly present at early time points (< 24 hours). Our assumption that precancerous tissue accumulates significantly higher amounts of mTHPC proved incorrect; only a weak correlation between dysplasia grade induced in the 4NQO model and mTHPC fluorescence was found for all mTHPC formulations.

The higher fluorescence intensities for both liposomal formulations in tumor tissue is due to the EPR effect causing passive accumulation of liposomes (macromolecules) in tumor tissue without adequate lymphatic drainage [14,15]. Our data suggests that this EPR effect may not be present in dysplastic tissue but only in tumor tissue. The higher mTHPC fluorescence intensity and tumor selectivity of Fospeg over Foslip are explained by the increased circulation time and thereby increased possibility for uptake in tumor tissue due to the coating of the liposomes used in Fospeg by hydrophilic polymers. This coating results in a diminished recognition by the MPS of these "stealth" liposomes. Aggregation of hydrophobic mTHPC molecules in plasma are the cause of the observed lower fluorescence intensities of Foscan which is associated with diminished fluorescence, increased uptake by the MPS and delayed uptake into tissue [17]. Although emitted mTHPC fluorescence is influenced by mTHPC serum stability, binding and/or aggregation and the incorporation into liposomes of mTHPC, one could argue that only mTHPC molecules able to fluoresce are important for PDT [18-20]. Liposomal mTHPC is of interest for further (pre)clinical studies due to its enhanced pharmacokinetic profile compared to Foscan. However, PDT is based upon a complex interdependent reaction of various treatment parameters, therefore predicting PDT response in general is difficult [21] But for one of the parameters involved, the photosensitizer used, an improvement in properties by using liposomal mTHPC seems likely to benefit PDT. From a clinical perspective, the possible shortening of the drug-light interval, lowering of the drug-dose and the use of a photosensitizer (PS) with better solubility and similar efficacy could be worthwhile. The importance of the EPR effect we found for Fospeg in our preclinical model and its potential role in clinical treatment should be considered as increased tumor accumulation of several nanodrugs is attributed to EPR. Most interestingly, even micronodal metastases in the liver were shown to exhibit the EPR effect [22]. Notwithstanding these findings, blood flow, blood pressure, degree of tumor vascularisation, presence of necrotic cores and the function of lymphatic drainage are clearly factors of importance on the magnitude of the EPR effect [16,23]. Inter- and intra-variations in tumor characteristics will influence the clinical pharmacokinetics of Fospeg and may alter the selectivity for tumor over normal tissue. It is therefore important to recognize that further clinical work is necessary to confirm the translational relevance of the finding presented.

Liposomal mTHPC formulations investigated in this thesis showed superior fluorescence pharmacokinetics over the clinically used Foscan. In particular Fospeg showed increased fluorescence and tumor selectivity at earlier time points.

Our results warrant research into PDT efficacy for Fospeg at early time points and reduced drug dose compared to Foscan. The choice of preclinical model used is important, as it ideally must represent patients with solid tumors and all of the aspects influencing the EPR effect. Therefore, induced tumor models should be used for PDT studies comparing inflicted tissue damage between mTHPC formulations at different drug-light intervals. A possible method to calculate PDT damage is to calculate necroses from a tumor as a percentage of the whole tumor surface area [24]. The use of quantitative spectroscopy, such as fDPS, in early phase clinical studies would be particular advantageous for determining if Fospeg shows enhanced pharmacokinetics in human tumors. These types of measurements would provide additional clinical data to support the use of PDT light treatment planning.

in vivo quantification of photosensitizer concentration using fluorescence differential path-length spectroscopy

The relationship between mTHPC concentration and therapeutic outcome in PDT is known to be complicated. Nonetheless, mTHPC tissue concentration is an important factor in the deposition of PDT dose. Fluorescence differential path-length spectroscopy (fDPS) is a non-invasive optical technique that has shown previously to accurately quantify the concentration of Foscan in rat liver [25]. **Chapter 4** described the use of fDPS in a clinically relevant and optically more challenging environment. Furthermore, we tested the influence of different mTHPC formulations (Foscan, Foslip and Fospeg) at a clinically relevant drug dose of 0.15 mg/kg on fDPS performance instead of the previously used 0.30 mg/kg mTHPC. mTHPC concentration estimates using fDPS were correlated with the results of the subsequent harvested and chemically extracted organs using linear regression analysis. An excellent goodness of fit between fDPS and extraction was found for all formulations in the liver. This finding validates fDPS in the liver for the different mTHPC formulations at a clinically relevant dose. In lip and especially in tongue tissue a much lower goodness of fit between fDPS and extraction was found. The most likely cause of these differences in correlation is the more layered anatomical structure, which influences photosensitizer distribution and scattering properties. Fluorescence microscopy clearly showed differences in tissue specific distribution of mTHPC at all time points; in liver mTHPC was much more homogeneously distributed compared to both lip and tongue tissue. As the extraction technique averages mTHPC concentration over the entire measured volume and fDPS is able to take several measurements within that volume, spatial heterogeneous mTHPC distribution will result in decreased correlation. In tongue tissue fDPS performance is probably decreased by a thick layer of keratinized epithelium without mTHPC uptake, which further influences the optically sampled mTHPC distribution. The differences in interrogation volume of both techniques (extraction and fDPS) are therefore relatively more pronounced in heterogeneous tongue tis-

sue. Differences in scattering amplitude were illustrated by significantly higher scattering amplitudes accompanied by larger standard deviations for lip and tongue tissue compared to those of liver tissue. The different formulations of mTHPC influenced the fDPS measurements; the slope of the regression line for Fospeg in liver was higher compared to both Foslip and Foscan suggesting a higher quantum yield for Fospeg. This could be explained by a relatively higher amount of non-aggregated mTHPC molecules in liposomal formulations [14]. Other *in vivo* studies also describe a higher fluorescence of Fospeg compared to Foscan [12,26], although in these studies fluorescence intensity is also influenced by formulation specific pharmacokinetics such as aggregation and EPR. Within lip and tongue tissue, no significant difference in slope of the regression lines between the mTHPC formulations was present which is probably related to the overall lower goodness of fit and the higher confidence intervals of these regression lines.

The biggest challenging for optical fluorescence measurement are the structural differences between and within tissue types; our results clearly indicated a difference in fDPS performance depending on tissue type, notwithstanding the influence of different interrogation volumes for fDPS and extraction. Layered, heterogeneous anatomy influences the tissue specific optical properties, in particular scattering properties. In order to accurately monitor mTHPC concentration in heterogeneous tissue, a correction for scattering is needed. This is particularly important for (future) monitoring of mTHPC in spatially heterogeneous tumor tissues with even higher expected variations in scattering coefficient. However, a clinical PDT study performed on patients treated with interstitial PDT for head and neck tumors showed promising results [27]. In patients, fDPS was shown to measure Foscan 96 hours after injection and monitor the reduction of mTHPC fluorescence (photobleaching) during PDT. In healthy patients, fDPS correctly estimated the absence of mTHPC in healthy volunteers. Therefore, fDPS demonstrated the feasibility of monitoring *in vivo* several treatment parameters during PDT. Interestingly, these measurements showed low *in vivo* oxygen saturation within tumor tissue. An explanation for these positive results of these clinical fDPS studies in contrast to our findings could be our dependence on a mismatch in interrogations volumes of our measure methods in combination with choosing highly keratinized tissue with its associated increased scattering coefficients. Recently, multi-diameter single fiber reflectance (MDSFR) spectroscopy showed potential in *in vivo* quantification of optical properties [28,29]. The mechanisms underlying the deposition of PDT dose are complex, however with the FDPS technique measuring blood saturation, blood volume and mTHPC fluorescence over the same interrogated volume, optical monitoring of these parameters could guide clinical PDT [6,27,30].

fDPS was shown to be a reliable non-invasive tool for measuring mTHPC concentration for Foscan, Foslip and Fospeg in homogenous liver tissue. In tissue with spatially more heterogeneous mTHPC distribution one could argue that fDPS was able to measure small differences in spatial mTHPC distribution while the extraction technique averaged the mTHPC concentration over the entire interrogated volume. Due to differences in interrogation volume between fDPS and the golden standard of extraction, spatial heterogeneity of mTHPC

distribution combined with the influence of scattering, validation of fDPS in optically more layered tissue proved challenging. Possible correction for scattering would enhance these measurements and allow for real-time dosimetry of important PDT treatment parameters.

Future perspectives

Improvement of clinical PDT
As our studies showed (chapter 2), randomized, prospective studies comparing PDT with conventional treatment modalities on treatment response and treatment related morbidity are lacking. The experience of most clinicians using mTHPC (Foscan) is that PDT compares favorably to both surgery and radiotherapy in terms of patient esthetics and oral function after treatment, therefore comparative studies should be performed on treatment related morbidity besides treatment response. To measure morbidity after treatment of HNSCC, questionnaires assessing quality of life should be used as well as clinical assessments of speech and swallowing. Furthermore, the treatment cost and (psychological) burden of treatment should also be investigated. Of course, these studies on comparative morbidity are more needed for early stage tumors. For patients with incurable, local disease without further treatment options our review (chapter 2.1) clearly stated that PDT results in increased quality of life. Enhancement of currently used mTHPC mediated PDT could be achieved by the application of current developments and a better understanding of PDT. One of the drawbacks of clinically used Foscan, its phototoxicity, could be improved upon by using liposomal mTHPC. We suggest a comparison of Foscan with Foslip and Fospeg on induced tumor response at varying drug-light[39] intervals and at decreased mTHPC dose. In order to gain clinically more relevant information, induced preclinical tumor models instead of xenografts should be used for these experiments as an evaluation of potential clinical benefit (less phototoxicity due to decreased dose) of these formulations. The local pain, irritation and phototoxicity at the injection site associated with the hydrophobicity of administered Foscan may be improved upon by using the better water-soluble liposomal formulations of mTHPC. Combined uses of PDT with other therapeutic modalities such as surgery, radiotherapy, chemotherapeutics and drugs have been described extensively as a strategy to improve the effectiveness of PDT[5]. For instance, Cox-2 inhibitors enhance the anti-tumor effect of PDT[31]. In combination with radiotherapy, PDT sensitizes cancer cells to radiotherapy and radiotherapy enhances efficacy of PDT[32-34]. Identifying various agents that combined with PDT result in improved tumor cell kill without an increase in normal cell kill will undoubtedly be a major focus of clinical research.

An interesting approach, is to use a PS to enhance the release of endocytosed macromolecules into the cytosol; the photochemical internalization (PCI) technique[5,35,36]. PCI uses the principle of PS molecules located in endocytic vesicles. Light activation of the PS results in the production of reactive oxygen species (ROS) that damage the membranes of these vesi-

cles with the subsequent release of the endocytosed macromolecule (a drug) to the cytosol where its therapeutic targets are located. PCI may be used to activate the entrapped drug only in the light-exposed area. However, both the precise requirements for a PS to be used in PCI and knowledge on the clinical therapeutic effect of entrapped drugs on solid tumors are limited. Currently, a promising clinical phase I/II trial is ongoing using Amphinex®, an experimental chlorine type PS, in combination with low-dose of Bleomycin, a chemotherapeutic which is rapidly entrapped in endocytic vesicles[5]. The lower dose used is preferred as Bleomycin is related to severe lung morbidity[37]. The use of the clinically approved mTHPC in PCI with Bleomycin, instead of the less potent, experimental Amphinex, is the focus of current preclinical research. Potentially, an increased local tumor reaction could be reached by using liposomal mTHPC with its increased tumor uptake combined with light-activated release of Bleomycin. The PCI effect is not limited to Bleomycin as PCI of other macromolecules that cannot pass the plasma membrane (such as adenoviruses, immunotoxins, ribosome-inactivating proteins etc.) also showed increased biological activity[5,35]. Modified adenoviruses are widely studied for their possible use as oncolytic viruses. Similar to tumor cells, (oncolytic) viruses can alter the cell cycle and cellular pathways and therefore have the potential to target tumor cells, replicate and destroy tumor cells[38]. As a sufficient level of delivery of the oncolytic virus into target cells is essential, enhancement of this delivery is needed. Despite the promising preclinical work and the clinical trial, PS induced phototoxicity is also of concern in PCI. Furthermore, (partial) destruction of the entrapped drug besides destruction of endocytic vesicles and oxygen competition between PS and the entrapped drug (Bleomycin) will affect PCI. Although high doses of radiotherapy, chemotherapy and even major surgery have an immunosuppressive effect, PDT is increasingly described with having an immunostimulatory effect in preclinical models with a small immunosuppressive component[39]. Besides the direct cell kill and shutdown of vasculature, PDT induces local inflammation at the treatment site. After PDT, fragments of disintegrated tumor cells attract leukocytes, forms tumor-specific T cells and can evoke tumor specific immune response. Ideally, not only the primary treated tumor would be destroyed by PDT but also remaining tumor cells by the capability of boosting the immune response by way of tumor specific immunity[5]. Preclinical studies showed that PDT was able to control the growth of tumors outside of the light-exposed area[40,41]. However, clinical studies measuring a possible immune recognition of tumor cells after PDT are needed to assess the usefulness of this effect in PDT.

Improvement of photosensitizer pharmacokinetics
The problematic solubility of the potent mTHPC is largely due to its overall symmetrical structure. Advances in synthesis of unsymmetrical mTHPC related molecules allow for a modulation of pharmacological properties (increased water solubility) without big changes in its basic photochemistry[42]. Other synthetic advances could result in PS with longer wavelength absorption or conjugation with two-photon absorbers, potentially allowing for a more focused (thus more selective) two-photon excitation using NIR resulting in an

increased treatment depth [5,42]. Another way of enhancing PS delivery is the use of "nano" particles or drug carrier systems. Nanoparticles containing PS have been developed and investigated for their enhanced tumor selectivity and increased water-solubility for years. Potential "nano" carrier systems are quantum dots, liposomal formulations, dendritic micelles and silica nanoparticles to name a few [21]. In our current studies on drug carrier systems of mTHPC (chapter 3), liposomes were used that would accumulate in (tumor) tissue by virtue of the EPR effect. Literature suggests that the EPR effect could be augmented using systemic nitroglycerin, ACE-inhibitors and angiotensin-II induced hypertension [43]. A general advantage of PS s encapsulated in nanocarriers, is the uncoupling of the chemical properties of the encapsulated PS from the delivery process. This concept makes future targeting and delivery of an encapsulated PS dependant on the drug carrier system used.

An approach to target tumor tissue is the attachment of a tumor-selective particle, monoclonal antibodies, molecule to a photosensitizer or a drug-carrier system encapsulating a photosensitizer [5,44,45]. A possible target for PDT in treatment of HNSCC is the epidermal growth factor receptor (EGFR), which is seen in >90% of patients. Triggering of the molecular signaling pathway in tumor cells with EGFR by ligand binding or cross-talk with other receptors, results in activation of pathways which regulate cell proliferation, apoptosis, metastases and angiogenesis [46]. Therefore, monoclonal antibodies (e.g., Cetuximab) and tyrosine kinase inhibitors (e.g., Erlotinib) targeting EGFR have become clinically important in these cancers [47]. Another target could be vascular endothelial growth factor (VEGF) and its receptors, which is one of the most important factors regulating the angiogenesis and metastasis characteristic for tumor tissue. Upregulation of low-density lipoprotein (LDL) receptors and folate receptors on tumor cells could also be of use in active targeting of PDT [48,49]. Folic acid is very attractive as a targeting molecule because it is inexpensive, not toxic or immunogenic, it is stable and it can be easily coupled to the surface of nanocarriers or conjugated to a PS [50]. However, Folic acid receptors are only present in 45% of primary HNSCC [51]. A recent *in vitro* study attached folic acid to Fospeg and reported an improved uptake of mTHPC in cells expressing folate receptors and increased cell kill compared to "passive" Fospeg. However, the targeted Fospeg only showed a modest selectivity in mTHPC uptake in cell with folate receptors, indicating that non-specific endocytosis remains the prevailing mechanism of cell internalization [50]. Combining PSs with monoclonal antibodies have been mostly unsuccessful, with some recent exceptions, due to difficulties in conjugation [42,52,53].

The ability to target the drug-carrier to control the localization of the drugs, could result in a decrease of phototoxicity and damage of healthy tissue. However, development of a "standard" approach for targeting of HNSCC seems unlikely. Due to the heterogeneity and dynamic changes of the molecular basis of the tumor cells, the expression profiles of tumor-associated antigens will alter. Furthermore, changes in tumor vasculature and stroma will affect pharmacokinetics of targeted drugs. Thus, only when carefully adapting the PS to the tumor cells, its stage of disease, its micro-environment and its molecular targets a real targeted, tailor-made treatment with associated benefits will have arrived.

In vivo monitoring of PDT parameters
Monitoring parameters of importance during PDT is essential to understand mechanisms of action underlying PDT and to enhance treatment. For instance, varying clinical response to similar treatment could be explained. Future challenges lay in correction for the intra-and inter-subject variations in parameters such as PS pharmacokinetics, tissue optical properties, local oxygen saturation and delivered fluence (rate). The parameters influence the deposited PDT dose and even change during treatment. Ideally, monitoring of these parameters is done during treatment and can provide instant feedback to detect (technical) problems, optimize PDT and subsequently increase tumor response. Our study (chapter 4) indicated that for monitoring of PS concentration future studies should account for the influence of optical properties (scattering in particular) and spatial distribution of the PS in tissue and therefore the interrogation volume chosen. Clinical proof of principle studies using optical guidance to quantitatively measure PDT parameters, such as mTHPC concentration, could be used to get insight into PDT and allow for individualized clinical treatment regimes.

References

1. Cohen EE, Lingen MW, Vokes EE. The expanding role of systemic therapy in head and neck cancer. J Clin Oncol. 2004 May 1;22(9):1743-52.

2. Karakullukcu B, Nyst HJ, van Veen RL, Hoebers FJ, Hamming-Vrieze O, Witjes MJ, et al. mTHPC mediated interstitial photodynamic therapy of recurrent nonmetastatic base of tongue cancers: Development of a new method. Head Neck. 2012 Jan 31.

3. Haddad RI, Shin DM. Recent advances in head and neck cancer. N Engl J Med. 2008 Sep 11;359(11):1143-54.

4. Zhu TC, Finlay JC. The role of photodynamic therapy (PDT) physics. Med Phys. 2008 Jul;35(7):3127-36.

5. Agostinis P, Berg K, Cengel KA, Foster TH, Girotti AW, Gollnick SO, et al. Photodynamic therapy of cancer: An update. CA Cancer J Clin. 2011 /;61(4):250-81.

6. Robinson DJ, Karakullukcu MB, Kruijt B, Kanick SC, van Veen RPL, Amelink A, et al. Optical spectroscopy to guide photodynamic therapy of head and neck tumors. Ieee Journal of Selected Topics in Quantum Electronics. 2010 JUL-AUG;16(4):854-62.

7. Nyst HJ, Tan IB, Stewart FA, Balm AJ. Is photodynamic therapy a good alternative to surgery and radiotherapy in the treatment of head and neck cancer? Photodiagnosis Photodyn Ther. 2009 Mar;6(1):3-11.

8. Hopper C. Photodynamic therapy: A clinical reality in the treatment of cancer. Lancet Oncol. 2000 Dec;1:212-9.

9. Karakullukcu B, van Oudenaarde K, Copper MP, Klop WM, van Veen R, Wildeman M, et al. Photodynamic therapy of early stage oral cavity and oropharynx neoplasms: An outcome analysis of 170 patients. Eur Arch Otorhinolaryngol. 2011 Feb;268(2):281-8.

10. Hornung R, Walt H, Crompton NE, Keefe KA, Jentsch B, Perewusnyk G, et al. m-THPC-mediated photodynamic therapy (PDT) does not induce resistance to chemotherapy, radiotherapy or PDT on human breast cancer cells in vitro. Photochem Photobiol. 1998 Oct;68(4):569-74.

11. Svensson J, Johansson A, Grafe S, Gitter B, Trebst T, Bendsoe N, et al. Tumor selectivity at short times following systemic administration of a liposomal temoporfin formulation in a murine tumor model. Photochem Photobiol. 2007 09;83(0031-8655; 0031-8655; 5):1211-9.

12. Buchholz J, Kaser-Hotz B, Khan T, Rohrer Bley C, Melzer K, Schwendener RA, et al. Optimizing photodynamic therapy: In vivo pharmacokinetics of liposomal meta-(tetrahydroxyphenyl)chlorin in feline squamous cell carcinoma. Clin Cancer Res. 2005 10/15;11(1078-0432; 20):7538-44.

13. Lassalle HP, Dumas D, Grafe S, D'Hallewin MA, Guillemin F, Bezdetnaya L. Correlation between in vivo pharmacokinetics, intratumoral distribution and photodynamic efficiency of liposomal mTHPC. J Control Release. 2009 Mar 4;134(2):118-24.

14. Derycke AS, de Witte PA. Liposomes for photodynamic therapy. Adv Drug Deliv Rev. 2004 01/13;56(0169-409; 1):17-30.

15. Maeda H, Wu J, Sawa T, Matsumura Y, Hori K. Tumor vascular permeability and the EPR effect in macromolecular therapeutics: A review. J Control Release. 2000 03/01;65(0168-3659; 1-2):271-84.

16. Prabhakar U, Maeda H, Jain RK, Sevick-Muraca EM, Zamboni W, Farokhzad OC, et al. Challenges and key considerations of the enhanced permeability and retention effect for nanomedicine drug delivery in oncology. Cancer Res. 2013 Apr 15;73(8):2412-7.

17. Hopkinson HJ, Vernon DI, Brown SB. Identification and partial characterization of an unusual distribution of the photosensitizer meta-tetrahydroxyphenyl chlorin (temoporfin) in human plasma. Photochem Photobiol. 1999 Apr;69(4):482-8.

18. Kachatkou D, Sasnouski S, Zorin V, Zorina T, D'Hallewin MA, Guillemin F, et al. Unusual photoinduced response of mTHPC liposomal formulation (foslip). Photochem Photobiol. 2009 05;85(0031-8655; 0031-8655; 3):719-24.

19. Reshetov V, Kachatkou D, Shmigol T, Zorin V, D'Hallewin MA, Guillemin F, et al. Redistribution of meta-tetra(hydroxyphenyl)chlorin (m-THPC) from conventional and PEGylated liposomes to biological substrates. Photochem Photobiol Sci. 2011 Jun;10(6):911-9.

20. Reshetov V, Zorin V, Siupa A, D'Hallewin MA, Guillemin F, Bezdetnaya L. Interaction of liposomal formulations of meta-tetra(hydroxyphenyl) chlorin (temoporfin) with serum proteins: Protein binding and liposome destruction. Photochem Photobiol. 2012 May 19.

21. Senge MO, Brandt JC. Temoporfin (foscan(R), 5,10,15,20-tetra(m-hydroxyphenyl)chlorin)--a second-generation photosensitizer. Photochem Photobiol. 2011 Nov-Dec;87(6):1240-96.

22. Maeda H, Bharate GY, Daruwalla J. Polymeric drugs for efficient tumor-targeted drug delivery based on EPR-effect. Eur J Pharm Biopharm. 2009 Mar;71(3):409-19.

23. Maeda H. The link between infection and cancer: Tumor vasculature, free radicals, and drug delivery to tumors via the EPR effect. Cancer Sci. 2013 Mar 16.

24. Bovis MJ, Woodhams JH, Loizidou M, Scheglmann D, Bown SG, Macrobert AJ. Improved in vivo delivery of m-THPC via pegylated liposomes for use in photodynamic therapy. J Control Release. 2012 Jan 30;157(2):196-205.

25. Kruijt B, Kascakova S, de Bruijn HS, van der Ploeg-van den Heuvel,A., Sterenborg HJ, Robinson DJ, et al. In vivo quantification of chromophore concentration using fluorescence differential path length spectroscopy. J Biomed Opt. 2009 May-Jun;14(3):034022.

26. de Visscher SA, Kascakova S, de Bruijn HS, van den Heuvel AP, Amelink A, Sterenborg HJ, et al. Fluorescence localization and kinetics of mTHPC and liposomal formulations of mTHPC in the window-chamber tumor model. Lasers Surg Med. 2011 Aug;43(6):528-36.

27. Karakullukcu B, Kanick SC, Aans JB, Sterenborg HJ, Tan IB, Amelink A, et al. Clinical feasibility of monitoring m-THPC mediated photodynamic therapy by means of fluorescence differential path-length spectroscopy. J Biophotonics. 2011 Aug 22.

28. Hoy CL, Gamm UA, Sterenborg HJ, Robinson DJ, Amelink A. Use of a coherent fiber bundle for multidiameter single fiber reflectance spectroscopy. Biomed Opt Express. 2012 Oct 1;3(10):2452-64.

29. van Leeuwen-van Zaane F, Gamm UA, van Driel PB, Snoeks TJ, de Bruijn HS, van der Ploegvan den Heuvel,A., et al. In vivo quantification of the scattering properties of tissue using multidiameter single fiber reflectance spectroscopy. Biomed Opt Express. 2013 Apr 9;4(5):696-708.

30. Finlay JC, Mitra S, Foster TH. In vivo mTHPC photobleaching in normal rat skin exhibits unique irradiance-dependent features. Photochem Photobiol. 2002 Mar;75(3):282-8.

31. Ferrario A, Fisher AM, Rucker N, Gomer CJ. Celecoxib and NS-398 enhance photodynamic therapy by increasing in vitro apoptosis and decreasing in vivo inflammatory and angiogenic factors. Cancer Res. 2005 Oct 15;65(20):9473-8.

32. Luksiene Z, Juzenas P, Moan J. Radiosensitization of tumours by porphyrins. Cancer Lett. 2006 Apr 8;235(1):40-7.

33. Luksiene Z, Kalvelyte A, Supino R. On the combination of photodynamic therapy with ionizing radiation. J Photochem Photobiol B. 1999 Sep-Oct;52(1-3):35-42.

34. Pogue BW, O'Hara JA, Demidenko E, Wilmot CM, Goodwin IA, Chen B, et al. Photodynamic therapy with verteporfin in the radiation-induced fibrosarcoma-1 tumor causes enhanced radiation sensitivity. Cancer Res. 2003 Mar 1;63(5):1025-33.

35. Selbo PK, Weyergang A, Hogset A, Norum OJ, Berstad MB, Vikdal M, et al. Photochemical internalization provides time- and space-controlled endolysosomal escape of therapeutic molecules. J Control Release. 2010 Nov 20;148(1):2-12.

36. Berg K, Weyergang A, Prasmickaite L, Bonsted A, Hogset A, Strand MT, et al. Photochemical internalization (PCI): A technology for drug delivery. Methods Mol Biol. 2010;635:133-45.

37. Sleijfer S. Bleomycin-induced pneumonitis. Chest. 2001 Aug;120(2):617-24.

38. Alemany R. Chapter four--design of improved oncolytic adenoviruses. Adv Cancer Res. 2012;115:93-114.

39. Castano AP, Mroz P, Hamblin MR. Photodynamic therapy and anti-tumour immunity. Nat Rev Cancer. 2006 Jul;6(7):535-45.

40. Kabingu E, Vaughan L, Owczarczak B, Ramsey KD, Gollnick SO. CD8+ T cell-mediated control of distant tumours following local photodynamic therapy is independent of CD4+ T cells and dependent on natural killer cells. Br J Cancer. 2007 Jun 18;96(12):1839-48.

41. Gomer CJ, Ferrario A, Murphree AL. The effect of localized porphyrin photodynamic therapy on the induction of tumour metastasis. Br J Cancer. 1987 Jul;56(1):27-32.

42. Senge MO. mTHPC--a drug on its way from second to third generation photosensitizer? Photodiagnosis Photodyn Ther. 2012 Jun;9(2):170-9.

43. Maeda H, Nakamura H, Fang J. The EPR effect for macromolecular drug delivery to solid tumors: Improvement of tumor uptake, lowering of systemic toxicity, and distinct tumor imaging in vivo. Adv Drug Deliv Rev. 2013 Jan;65(1):71-9.

44. Shirasu N, Nam SO, Kuroki M. Tumor-targeted photodynamic therapy. Anticancer Res. 2013 Jul;33(7):2823-31.

45. Solban N, Rizvi I, Hasan T. Targeted photodynamic therapy. Lasers Surg Med. 2006 Jun;38(5):522-31.

46. Argiris A, Karamouzis MV, Raben D, Ferris RL. Head and neck cancer. Lancet. 2008 May 17;371(9625):1695-709.

47. Master A, Malamas A, Solanki R, Clausen DM, Eiseman JL, Sen Gupta A. A cell-targeted photodynamic nanomedicine strategy for head and neck cancers. Mol Pharm. 2013 May 6;10(5):1988-97.

48. Kessel D. The role of low-density lipoprotein in the biodistribution of photosensitizing agents. J Photochem Photobiol B. 1992 Jul 15;14(3):261-2.

49. Low PS, Henne WA, Doorneweerd DD. Discovery and development of folic-acid-based receptor targeting for imaging and therapy of cancer and inflammatory diseases. Acc Chem Res. 2008 Jan;41(1):120-9.

50. Moret F, Scheglmann D, Reddi E. Folate-targeted PEGylated liposomes improve the selectivity of PDT with meta-tetra(hydroxyphenyl) chlorin (m-THPC). Photochem Photobiol Sci. 2013 May;12(5):823-34.

51. Saba NF, Wang X, Muller S, Tighiouart M, Cho K, Nie S, et al. Examining expression of folate receptor in squamous cell carcinoma of the head and neck as a target for a novel nanotherapeutic drug. Head Neck. 2009 Apr;31(4):475-81.

52. Mitsunaga M, Nakajima T, Sano K, Kramer-Marek G, Choyke PL, Kobayashi H. Immediate in vivo target-specific cancer cell death after near infrared photoimmunotherapy. BMC Cancer. 2012 Aug 8;12:345,2407-12-345.

53. Mitsunaga M, Ogawa M, Kosaka N, Rosenblum LT, Choyke PL, Kobayashi H. Cancer cell-selective in vivo near infrared photoimmunotherapy targeting specific membrane molecules. Nat Med. 2011 Nov 6;17(12):1685-91.

Chapter 6

Samenvatting

Introductie

In 2002 werd kanker in het hoofd-hals gebied wereldwijd bij meer dan een half miljoen mensen gediagnosticeerd en overleden ongeveer 350.000 patiënten aan de ziekte. In Nederland werd in 2011 bij bijna 100.000 mensen de diagnose kanker gesteld waarvan ongeveer 3.000 mensen kanker in het hoofd-hals gebied hadden. Kwaadaardige aandoeningen van het hoofd-hals gebied staan in Nederland op de zevende plaats van meest voorkomende kanker bij mannen en de op de negende plaats bij vrouwen. De laatste twintig jaar neemt de incidentie van hoofd-hals kanker toe waarbij vooral de sterke toename van mensen met mondkanker opvalt. Het merendeel van de kwaadaardige hoofd-hals tumoren zijn plaveiselcelcarcinomen (90%) die uitgaan van het slijmvlies van de bovenste voedings- en ademweg. Tabak en alcohol zijn de belangrijkste etiologische factoren voor het ontstaan van een plaveiselcelcarcinoom in het hoofd- hals gebied, waarbij een combinatie van alcohol en roken een synergistisch effect heeft. De laatste 10 jaar blijkt dat naast alcohol en roken ook infectie met het humaan papillomavirus, vooral subtype 16, een rol speelt bij het ontstaan van plaveiselcelcarcinomen van de orofarynx. Het virus wordt mogelijk via direct contact overgebracht. Kenmerkend voor de door humaan papillomavirus geïnduceerde plaveiselcelcarcinomen is dat ze voorkomen bij jonge, niet-rokende patiënten.

Plaveiselcelcarcinomen metastaseren vrijwel uitsluitend naar de regionale lymfeklieren in de hals en slechts zelden hematogeen. Lymfekliermetastasering wordt vooral bepaald door de anatomische locatie en grootte van de primaire tumor.

De behandeling van de primaire tumor en eventueel aanwezige lymfekliermetastasen in de hals bestaat uit chirurgische verwijdering, bestraling of uit een combinatie van voornoemde behandelmethoden. Soms wordt gekozen voor concomitante chemo- en radiotherapie, voornamelijk bij tumoren in een vergevorderd stadium. Het resultaat van de behandeling heeft vaak grote cosmetische en functionele gevolgen, zoals vermindering van het vermogen tot kauwen, slikken en spreken. De aard en ernst van deze bijwerkingen zijn afhankelijk van de lokalisatie van de tumor en zijn meer uitgesproken bij grote tumoren. De behandeling van hoofd-hals tumoren is niet alleen gericht op genezing van de patiënt maar ook op een goede functie en daarmee een acceptabele kwaliteit van leven na de behandeling. Soms treden recidieven op, ook kunnen er nieuwe primaire tumoren ontstaan. Naast de eerder genoemde behandelmethoden kan in geselecteerde gevallen fotodynamische therapie (PDT) worden toegepast voor zowel curatieve als palliatieve behandeling van de primaire tumor.

In de klassieke oudheid werd licht al gebruikt voor behandeling van diverse huidaandoeningen. In het begin van de 20ste eeuw werd onderzoek verricht naar de mogelijke therapeutische werking van licht. In 1903 ontving de Deense arts Niels Ryberg Finsen de Nobelprijs voor de geneeskunde voor zijn ontdekking dat door middel van licht (fototherapie) bepaalde ziekten zoals cutane tuberculose en pokken konden worden behandeld. Later experimenteerden andere onderzoekers met lokale en intraveneuze injectie van lichtgevoelige stoffen, zogenoemde fotosensitizers (PS), gevolgd door belichting van het doelweefsel. Hierbij bleek dat PDT weefselschade kon veroorzaken door een chemische reactie van de fotosensitizer als gevolg van excitatie door fotonen die een voor de fotosensitizer specifieke golflengte hadden. De geabsorbeerde fotonen transformeren de PS uit zijn laagste energieniveau, de energetische eigen- of grondtoestand, naar een aangeslagen toestand. De fotosensitizer kan terugkeren naar zijn grondtoestand door 1) emissie van de geabsorbeerde energie door licht met een lager energieniveau (fluorescentie) of 2) door verval van de fotosensitizer naar een aangeslagen triplet toestand. De fotosensitizer kan in zijn aangeslagen triplet toestand energie overdragen aan nabijgelegen weefsel waarmee het reageert (type I reactie). Daarnaast kan een rechtstreekse overdracht van energie aan zuurstof plaatsvinden (type II reactie). Beide reactie types vinden gelijktijdig plaats, waarbij de verhoudingen tussen de type I en II reacties afhankelijk is van de gebruikte fotosensitizer, de concentratie van de fotosensitizer, de weefseloxygenatie en het dosistempo van de belichting. Vooral de type II reactie is, door het ontstaan van potente reactieve zuurstofradicalen, geassocieerd met door fotodynamische therapie veroorzaakte weefselschade. Door de korte halfwaardetijd en hoge reactiviteit van zuurstofradicalen, respectievelijk10-320 nanoseconden en 10-55 nanometer, wordt alleen weefsel beïnvloed in de directe nabijheid van het gebied waar de zuurstofradicalen worden gevormd. De distributie van de fotosensitizer in het weefsel is daarom van belang voor de gewenste weefselschade door PDT. De distributie van de fotosensitizer wordt bepaald door de lokale vasculaire permeabiliteit en de tijdsafhankelijke diffusie, die onder andere worden beïnvloed door de interacties met plasma, de aggregatie en deaggregatie, de grootte, de lading en de hydrofobe of hydrofiele eigenschappen van de fotosensitizer moleculen en de gebruikte oplossing. De reactieve zuurstofradicalen veroorzaken weefselschade in de tumor door een combinatie van directe tumorcelschade en vasculaire infarcering van het tumorweefsel. De directe tumorcelschade leidt tot apoptose, necrose en stimulatie van mononucleaire fagocytose systeem. Vasculaire schade en infarcering worden vermoedelijk veroorzaakt door een combinatie van vasoconstrictie, trombusvorming en een verhoogde gevoeligheid van het endotheel voor PDT.

In 1913 werden porphyrines als fotosensitizer geïntroduceerd door Meyer-Betz. Vijftig jaar later werd het haemotoporphyrin derivaat (HPD) ontwikkeld. Bij dierstudies met dit middel bleek sprake van een verhoogde opname in tumorweefsel. In 1970 werden de eerste patiënten succesvol behandeld met HPD. In 1993 werd Photofrin® (porfimernatrium, gedeeltelijk gezuiverd HPD) als eerste fotosensitizer goedgekeurd door de Food and Drug Administration voor toepassing bij de behandeling van maligne tumoren. Photofrin heeft als nadelen dat hoge doses van de fotosensitizer en licht nodig zijn voor de gewenste tumorrespons, de penetratiediepte in het weefsel beperkt is, de langdurige lichtgevoeligheid van de huid na toediening van het middel en een complex productieproces door de ingewikkelde chemische samenstelling. Deze beperkingen van Photofrin leidden tot de ontwikkeling van

nieuwe, chemisch gesynthetiseerde zuivere verbindingen, zogenoemde tweede generatie fotosensitizers, met betere klinische eigenschappen en minder bijwerkingen. Voorbeelden van deze tweede generatie fotosensitizers zijn 5-aminolevulinezuur (5-ALA) en het daarvan afgeleide (Metvix®). Beide fotosensitizers worden gebruikt bij de behandeling van actinische keratosen en basaalcelcarcinomen. Verteporfin (Visudyne®), dat intraveneus wordt toegediend, wordt gebruikt bij de behandeling van maculadegeneratie van het oog. Meta-tetra(hydroxyfenyl) chlorine (mTHPC) is een andere fotosensitizer van de tweede generatie. Deze fotosensitizer heeft een penetratiediepte van tenminste 10 mm en de potentie tot weefseldestructie is hoger dan van Photofrin. mTHPC met ethanol (Foscan®)wordt gebruikt voor de behandeling van kleine en grote plaveiselcelcarcinomen in het hoofd-halsgebied. Hoewel enkele klinische studies zijn gepubliceerd met veelbelovende resultaten over de effectiviteit van mTHPC gemedieerde fotodynamische therapie, wordt de werkzaamheid en morbiditeit van deze behandeling sporadisch vergeleken met de standaard behandeling. Het merendeel van de publicaties over Foscan gemedieerde PDT geeft vooral inzicht in het werkingsmechanisme van de fotodynamische therapie en de behandelingsresultaten van een beperkt aantal patiënten. Ondanks de gerapporteerde goede resultaten van fotodynamische therapie bij de behandeling van plaveiselcelcarcinomen in het hoofd-halsgebied, is de effectiviteit van Foscan gemedieerde PDT ten opzichte van standaard behandeling onduidelijk.

Naast de positieve beschrijvingen van Foscan gemedieerde PDT zijn ook enkele nadelen beschreven. Nadelen zijn de lange periode van 96 uur tussen injectie en belichting, de aggregatie van mTHPC moleculen in de bloedbaan en de lage tumorselectiviteit. Andere nadelen bij de behandeling met de fotosensitizer Foscan zijn langdurige lichtgevoeligheid en pijn ter plaatse van de injectieplaats. Om deze nadelen van mTHPC gemedieerde PDT te verminderen met behoud van de potentie om weefselschade te induceren, werden wateroplosbare liposomale mTHPC formuleringen ontwikkeld. Liposomale dragers van mTHPC hebben een goede wateroplosbaarheid waardoor minder aggregatie van mTHPC in de bloedbaan zal plaatsvinden. Onder fysiologische omstandigheden, zoals in de bloedbaan, veroorzaakt de aggregatie van de fotosensitizer moleculen namelijk een lagere productie van zuurstofradicalen. De slechte wateroplosbaarheid van Foscan zorgt ook voor een snelle opname en afvoer van de mTHPC moleculen door het mononucleair fagocytoseysteem (MPS) waardoor de concentratie mTHPC in het tumorweefsel laag is. Liposomale dragers kunnen, naast de verbeterde wateroplosbaarheid en het tegengaan van aggregatie, mogelijk ook de opname van mTHPC in tumorweefsel verhogen. Passieve accumulatie van grote liposomale dragers ("macromoleculen") zou kunnen bijdragen aan een hogere concentratie van mTHPC in het tumorweefsel omdat in tumorweefsel sprake is van een verhoogde permeabiliteit van de bloedvaten en de afwezigheid van een goed functionerend lymfevaatstelsel. Deze combinatie van factoren resulteert in een toename van de extravasatie van macromoleculen uit de bloedbaan in het tumorweefsel zonder dat ze worden afgevoerd door het lymfestelsel. Door Biolitec AG zijn twee liposomale dragers van mTHPC ontwikkeld: Foslip® en Fospeg®.

In tegenstelling tot Foslip zijn de liposomen van Fospeg aan de oppervlakte bekleed met een polymeer. Hierdoor zijn ze verminderd detecteerbaar voor het mononucleair fagocytoseysteem (MPS) waardoor de beschikbaarheid in de circulatie toeneemt. Onderzoeken suggereren dat liposomale dragers van mTHPC zorgen voor een snellere en een hogere opname van mTHPC in tumorweefsel. Er is onduidelijkheid over de kinetiek van deze liposomale mTHPC dragers in pre-klinische tumormodellen en vergelijkende onderzoeken met Foscan ontbreken.

De effectiviteit van mTHPC gemedieerde PDT kan worden verbeterd door nauwkeurige en directe bepaling van factoren die van invloed zijn op het resultaat van fotodynamische therapie ("in vivo dosimetrie"). De PDT reactie wordt bepaald door een complexe, dynamische interactie van het zuurstofgehalte in het weefsel, het licht dosistempo en de PS concentratie. Dosimetrie van deze parameters tijdens de fotodynamische therapie geeft de mogelijkheid tot het real-time aanpassen van de variabelen waardoor de PDT reactie tijdens de behandeling geoptimaliseerd zou kunnen worden.

In dit proefschrift werd door middel van literatuuronderzoek het klinische bewijs voor Foscan gemedieerde PDT bij de behandeling van plaveiselcelcarcinomen in het hoofd-halsgebied geëvalueerd en vergeleken met de chirurgische behandeling. De kinetiek van de liposomale mTHPC dragers in tumormodellen werd vergeleken met die van Foscan. Een methode om *in vivo* mTHPC weefselconcentraties te meten door middel van fDPS (fluorescence Differential Pathlength Spectroscopy) werd getest op klinisch relevant en optisch heterogeen weefsel in een diermodel.

Samenvatting

In **hoofdstuk 2.1** wordt een systematische evaluatie beschreven van de publicaties over Foscan gemedieerde PDT bij de behandeling van plaveiselcelcarcinomen in het hoofd-halsgebied. Slechts twaalf studies konden worden geïdentificeerd en geselecteerd voor een kritische beoordeling. Alle studies scoorden niet hoger dan niveau 3 volgens de Oxford levels of evidence. In zes van de 12 studies werd fotodynamische therapie als palliatieve behandeling toegepast waarbij in 3 studies patiënten werden behandeld door middel van oppervlaktebelichting. De andere 3 studies beschreven fotodynamische therapie van tumoren met een groot volume die werden behandeld met interstitiële belichting. Bij de interstitiële behandeling worden, voor een egale lichtdosisverdeling, catheters op strategische plaatsen in het tumorweefsel geplaatst. Analyse van de studies waarbij fotodynamische therapie werd gebruikt voor palliatieve behandeling van uitbehandelde patiënten, toonde aan dat er sprake was een goede tumorrespons en daardoor een verbetering van de levenskwaliteit. Wel bleek een lagere respons op te treden bij oppervlaktebelichting van tumoren met een tumordikte van meer dan 10 mm en bleek dat, vanwege de zwelling, een alternatieve luchtweg meestal

nodig was na behandeling met interstitiële fotodynamische therapie. Omdat geen publicaties werden gevonden waar de resultaten van fotodynamische therapie werd vergeleken met die van chirurgische behandeling of radiotherapie, was evaluatie van in opzet curatieve fotodynamische therapie voor de behandeling van kleine tumoren niet goed mogelijk. Evaluatie van de behandelrespons na PDT in relatie tot grootte van de tumor bleek wel mogelijk. De tumorrespons na fotodynamische therapie bleek bij T1 tumoren aanzienlijk beter dan bij T2 tumoren. Bovendien bleek de tumorrespons van primaire tumoren na fotodynamische therapie significant beter dan van nieuwe primaire tumoren. De meest voorkomende complicatie van Foscan gemedieerde PDT was fototoxiciteit. Daarnaast werden pijn en huidverkleuring rondom de injectieplaats beschreven.

Hoofdstuk 2.2 is een retrospectief onderzoek waarin de resultaten van Foscan gemedieerde PDT voor in opzet curatieve behandeling van primaire, kleine plaveiselcelcarcinomen van de mondholte werd vergeleken met die van transorale chirurgische behandeling. De gegevens van de patiënten die waren behandeld met fotodynamische therapie werden verkregen van de studies die zijn beschreven in de systematische evaluatie van de literatuur (hoofdstuk 2.1). De chirurgisch behandelde patiënten werden gerekruteerd uit de UMCG database met als selectiecriterium een tumorinfiltratiediepte tot en met 5mm. Selectie van tumoren met een vergelijkbare diepte was nodig om de resultaten van de behandeling door middel van fotodynamische therapie en chirurgie te kunnen vergelijken. De PDT groep bestond uit 126 T1 en 30 T2 tumoren. De chirurgiegroep bestond uit 58 T1 en 33 T2 tumoren. De volledige respons (complete response) na fotodynamische en chirurgische behandeling was niet significant verschillend. Het percentage tumoren met een volledige respons na fotodynamische en chirurgische behandeling was voor T1-tumoren respectievelijk 86% en 76% en voor T2- tumoren respectievelijk 63% en 78%. Fotodynamische therapie had zowel bij T1- als T2-tumoren een significant kortere lokale ziektevrije overleving in vergelijking met de chirurgische behandeling. Bij het vergelijken van de noodzaak tot lokale herbehandeling vanwege een recidief, bleek bij T1-tumoren geen significant verschil tussen beide behandelingen. Bij T2-tumoren bleek na chirurgische behandeling een significant lagere noodzaak voor lokale herbehandeling. De algehele overleving van patiënten met T1- of T2-tumoren die met fotodynamische therapie of chirurgie waren behandeld, was niet significant verschillend. Geconcludeerd werd dat de resultaten van behandeling van primaire T1 plaveiselcelcarcinomen van de mondholte met Foscan gemedieerde PDT en chirurgische verwijdering vergelijkbaar zijn. Fotodynamische therapie voor behandeling van primaire T2-tumoren lijkt minder effectief.

In **hoofdstuk 3.1** wordt de fluorescentie kinetiek van Foslip en Fospeg, twee liposomale dragers van mTHPC, vergeleken met die van Foscan. Foslip is mTHPC ingekapseld in conventionele liposomen en Fospeg mTHPC is ingekapseld in gepegyleerde liposomen. Foslip, Fospeg en Foscan werden intraveneus geïnjecteerd met een dosis van 0,15 mg/kg mTHPC in rat-

ten die waren geprepareerd met het kamertjesmodel. In het rattenmodel werd de huid, met een diameter van 1 centimeter, van de rug verwijderd en vervangen door een transparant raampje. Dit raampje bood de mogelijkheid om het onderliggende weefsel met daarin een getransplanteerde tumor over lange tijdsperiodes te vervolgen. Op 7 verschillende tijdstippen na injectie, variërend van 5 minuten tot 96 uur, werden mTHPC fluorescentie opnames gemaakt met een charge coupled device (CCD). De verkregen opnames werden gecorrigeerd voor veranderingen in de optische eigenschappen van de weefsels door middel van een ratiometrische correctie algoritme (hoofdstuk 3.2). De drie verschillende mTHPC formuleringen toonden een duidelijk verschil in fluorescentie kinetiek. Fospeg had op de onderzochte tijden een duidelijk hogere fluorescentie in het vaatstelsel dan Foscan en Foslip. Maximale mTHPC fluorescentie in tumorweefsel was bij Fospeg 8 uur na injectie en bij Foscan en Foslip 24 uur na injectie bereikt. Fospeg liet tussen 2 en 48 uur na injectie hogere mTHPC fluorescentiewaarden in tumorweefsel zien dan Foscan en Foslip. Significante tumorselectiviteit van mTHPC fluorescentie werd alleen 2 en 4 uur na injectie van Foslip gevonden. Fospeg had op enkele tijdstippen een bijna significante tumorselectiviteit. Foscan had op geen van de tijdpunten een significante of bijna-significant hogere mTHPC fluorescentie in tumorweefsel waarbij dit werd vergeleken met de fluorescentie in het omringende normale weefsel. De bevindingen suggereren dat, vergeleken met Foscan, liposomale dragers van mTHPC (vooral Fospeg) de biologische beschikbaarheid van mTHPC in het vaatstelsel en het tumorweefsel verhogen.

In **hoofdstuk 3.2** wordt een ontwikkelde ratiometrische correctie-algoritme beschreven die werd gebruikt voor het kwantificeren van mTHPC fluorescentie in het kamertjesmodel (hoofdstuk 3.1). Omdat de weefseloptische eigenschappen en dus de autofluorescentie veranderen in de tijd, bemoeilijkt dit het kwantificeren van de fluorescentiemetingen. Om kwantitatieve mTHPC fluorescentiewaarden te kunnen bepalen bij experimenten met het kamertjesmodel, werd de ratiometrische kwantificeringsmethode ontwikkeld. Dit algoritme corrigeert de gemeten mTHPC fluorescentie voor de veranderende optische weefseleigenschappen in het kamertjesmodel gedurende de experimentele periode. Het algoritme maakt gebruik van een combinatie van excitatie en detectie van mTHPC- en autofluorescentie bij verschillende golflengtes waarmee rekening wordt gehouden met de golflengte afhankelijke optische eigenschappen van weefsels. Fluorescentieafbeeldingen werden gemaakt met een CCD na intraveneuze injectie van 0,15 mg/kg mTHPC. De gebruikte excitatie golflengtes waren 629 nm en 652 nm. Twee fluorescentie-emissie-banden werden gebruikt waarbij een was gelegen op de secundaire fluorescentie emissiepiek van mTHPC (720 nm) en een op een golflengte met autofluorescentie van weefsel en zonder mTHPC fluorescentie (> 763 nm). De gemeten waarden werden door middel van het algoritme gecorrigeerd voor de optische eigenschappen. Hierdoor was het mogelijk om de gekwantificeerde mTHPC fluorescentie en de gekwantificeerde autofluorescentie te bepalen. Tijdens het experiment toonden alle typen weefsels een stijging van de autofluorescentie 24 uur na injectie. Bovendien liet de

ongecorrigeerde fluorescentie grotere intra-kamer variaties zien in vergelijking met de gecorrigeerde fluorescentie van hetzelfde weefsel. Beide bevindingen toonden aan dat correctie van de optische eigenschappen nodig was om de fluorescentie te kwantificeren.

In **hoofdstuk 3.3** wordt de distributie in de tumor van de verschillende mTHPC formuleringen (Foscan, Foslip, Fospeg) vergeleken in een 4-nitroquinoline-1-oxide (4NQO) tumormodel. In het onderzoek werden bij 54 ratten epitheeldysplasieën en plaveiselcelcarcinomen van het mondslijmvlies geïnduceerd door middel van het toedienen van het carcinogeen 4NQO. Op het moment dat de tumor klinisch zichtbaar werd, werd bij de ratten een van de 3 mTHPC formuleringen (0,15 mg/kg mTHPC) intraveneus toegediend. Op 1 van de 6 verschillende tijdstippen tussen de 2 en 96 uur na injectie werden de ratten getermineerd. Mondslijmvlies weefsel, met daarin tumoren, werd uitgenomen voor coupes die met hematoxyline-eosine (HE) werden gekleurd en coupes voor confocale fluorescentie microscopie. De HE coupes werden histologisch ingedeeld naar weefseltype en de mate van dysplasie werd beoordeeld met behulp van de Epithelial Atypia Index (EAI). Confocale microscopie werd gebruikt om de mTHPC fluorescentie te meten. De fluorescentiemetingen werden gecorrigeerd voor variaties in de microscopische opstelling. Fospeg toonde voornamelijk op de vroege tijdstippen (< 24 uur) een hogere fluorescentie in zowel normaal als tumorweefsel in vergelijking met Foslip en Foscan. Fospeg vertoonde tijdens de vroege tijdstippen meer tumorselectiviteit dan Foslip en Foscan. De hoogste mTHPC fluorescentie in tumorweefsel werd gemeten 8 uur na de injectie met Fospeg. Er werd slechts een zwakke correlatie gevonden tussen toenemende EAI en toenemende mTHPC fluorescentie. De bevindingen suggereerden dat Fospeg een vroegere en hogere opname van mTHPC heeft in (tumor)weefsel dan Foslip en Foscan. In tegenstelling tot hogere mTHPC fluorescentie in tumorweefsel, liet dysplastisch veranderd weefsel geen significant toename in mTHPC fluorescentie zien in vergelijking met normaal weefsel. Er was slechts een zwakke correlatie tussen de EAI en mTHPC fluorescentie.

In **hoofdstuk 4** wordt het effect beschreven van verschillende mTHPC formuleringen (Foscan, Foslip en Fospeg) op de meetmethode fluorescence Differential Pathlength Spectroscopy (fDPS). Ook wordt de invloed van klinisch relevant, maar optische heterogeen weefsel op fDPS onderzocht. fDPS is een niet-invasieve optische techniek waarmee de concentratie mTHPC in weefsels kwantitatief kan worden gemeten. 54 gezonde ratten werden intraveneus geïnjecteerd met een van de 3 mTHPC formuleringen (0,15 mg/kg mTHPC). Op 6 verschillende tijdstippen (2-96 uur) werden meerdere fDPS metingen verricht van de lever, de tong en de lip. Na de fDPS metingen, werden de ratten getermineerd en werd het gemeten weefsel verwijderd. In het weefsel werden de mTHPC concentraties gemeten door middel van chemische extractie. De gemeten mTHPC concentraties werden met behulp van een lineaire regressieanalyse vergeleken met de door middel van fDPS gemeten mTHPC waarden. In de lever werd een uitstekende correlatie gevonden tussen de fDPS en de chemische extractiemetingen van de drie mTHPC formuleringen. In de lip en vooral in de tong werden min-

der goede correlaties tussen fDPS en chemische extractiemetingen gevonden. Confocale fluorescentie microscopie toonde duidelijke verschillen aan in de weefselspecifieke verdeling van mTHPC op alle tijdstippen. In de lever bleek mTHPC meer homogeen gedistribueerd dan in de lip en de tong. De correlatie in de tong werd negatief beïnvloed door de dikte van het epitheel. Het tongepitheel, waarin nauwelijks mTHPC aanwezig was, besloeg een groot deel van het interrogatie volume bij de fDPS meting. Ook was in lip- en tongweefsel de verstrooiing van licht significant hoger dan in lever weefsel. De verschillende formuleringen van mTHPC hadden een invloed op de fDPS; De helling van de regressielijn was hoger voor Fospeg dan voor Foslip en Foscan. Geconcludeerd kan worden dat fDPS een betrouwbare methode is om de mTHPC concentraties van Foscan, Foslip en Fospeg in het optische homogene leverweefsel te meten. In optisch meer heterogeen weefsel, zoals de lip en de tong, werden de fDPS metingen negatief beïnvloed door verstrooiing van het licht en de heterogene distributie van mTHPC.

De onderzoeken in dit proefschrift tonen aan dat Foscan gemedieerde PDT kan worden toegepast bij de palliatieve behandeling van patiënten met een plaveiselcelcarcinoom in het hoofd-halsgebied. De resultaten van curatieve behandeling van kleine plaveiselcelcarcinomen (T1) met Foscan gemedieerde PDT en chirurgische behandeling zijn vergelijkbaar. Gerandomiseerde, prospectieve studies over de resultaten van fotodynamische therapie waarbij deze worden vergeleken met chirurgische behandeling of radiotherapie ontbreken echter. Liposomale dragers van mTHPC, in het bijzonder Fospeg, lieten een hogere en eerder opname in tumorweefsel zien in vergelijking met Foscan. De resultaten rechtvaardigen nader onderzoek naar de effectiviteit van Fospeg gemedieerde PDT in vergelijking met Foscan gemedieerde PDT. Hieruit moet blijken of een lagere dosis mTHPC en vroegere belichting de gewenste weefselschade veroorzaakt.

fDPS bleek een betrouwbare, niet-invasieve methode om de mTHPC concentratie in homogeen weefsel te meten. In weefsel met een meer heterogene mTHPC distributie bleek het mogelijk om met fDPS kleine verschillen in de ruimtelijke mTHPC distributie te meten. Door een verschil in het interrogatie volume tussen fDPS en de gouden standaard, chemische extractie, was de correlatie tussen beide meetmethodes echter laag. Waarschijnlijk berust dit op de grotere nauwkeurigheid van de fDPS metingen terwijl bij chemische extractie sprake is van middelende metingen. De fDPS meetmethode biedt door zijn real-time informatie over de mTHPC concentraties en de zuurstofoxygenatie, de mogelijkheid om de complexe PDT reactie te optimaliseren. Eventuele correctie voor verschillen in lichtverstrooiing zouden deze metingen versterken, zodat mogelijk een betere real-time dosisverdeling van belangrijke behandelingsparameters kan plaatsvinden tijdens PDT behandeling.

List of abbreviations

List of abbreviations used in this thesis

4NQO	4-nitroquinoline-1-oxide		MPS	mononuclear phagocyte system
(5-)ALA	5-aminolevulinic acid		MRI	magnetic resonance imaging
µs	scattering coefficient		mTHPC	meta-tetra(hydroxyphenyl)chlorin
µa	absorption coefficient		NIR	near infrared
AF	autofluorescence		OS	overall survival
AJCC	American Joint Committee on Cancer		OSCC	oral squamous cell carcinoma
a.u.	arbitrary units		PCI	photochemical internalization
CCD	charge-coupled device		PDT	Photodynamic therapy
CI	confidence interval		p.i.	post injection
CODT	Center of Optical Diagnostics and Therapy		PpIX	protoporphyrin IX
CR	complete response		PS	photosensitizer
CT	computed tomography		QLQ	Quality of Life Questionnaire
DAMP s	damage associated molecular patterns		RECIST	Response Evaluation Criteria In Solid Tumors
DPPC	dipalmitoylphosphatidylcholine		ROI	region of interest
DPPG	dipalmitoylphosphatidylglycerol		ROS	reactive oxygen species
DPS	differential pathlength spectroscopy		SCC	squamous cell carcinoma
DR	double ratio		SD	standard deviation
EAI	Epithelial Atypia Index		SE	standard error
EGFR	epidermal growth factor receptor		UICC	Union for International Cancer Control
EORTC	European Organisation for Research and Treatment of Cancer		UMCG	University Medical Center Groningen
EPR	enhanced permeability and retention		US	ultrasound
fDPS	fluorescence differential path-length spectroscopy		UW-QOL	University of Washington Quality of Life Questionnaire
HE	hematoxylin and eosin		VEGF	vascular endothelial growth factor
HNSCC	head and neck squamous cell carcinoma		WHO	World Health Organization
HPD	haemotoporphyrin derivative			
HPV	human papillomavirus			
ICD-10	International Classification of Diseases (10th edition)			
INN	International Nonproprietary Names			
IKNL	Integraal Kankercentrum Nederland			
IV	intravenous			
iPDT	interstitial PDT			
IQR	inter quartile range			
LDFS	local disease free survival			
LDL	low-density lipoprotein			
MDSFR	multi-diameter single fiber reflectance			

Dankwoord

Dankwoord

Een proefschrift is het resultaat van de inzet van een groot aantal geïnteresseerde, enthousiaste en stimulerende collega's. Graag wil ik iedereen bedanken die op enigerlei wijze een bijdrage heeft geleverd. In het bijzonder wil ik de volgende personen bedanken die een belangrijke rol hebben vervuld bij het tot stand komen van dit proefschrift. Zonder hun grote en onvoorwaardelijke inzet was er geen boekje geweest;

Mijn eerste promotor, prof. dr. J.L.N. Roodenburg, geachte professor. Ik wil u danken voor de mogelijkheden die u mij heeft geboden om dit onderzoek uit te voeren. We zijn nu enkele jaren verder en ik ben verheugd dat mijn promotietraject met succes is voltooid. Tijdens deze periode heb ik me altijd gewaardeerd en begrepen gevoeld. De combinatie van experimenten in de dierenlaboratoria in Groningen en Rotterdam, de studie Tandheelkunde, en de opleiding Kaakchirurgie was niet altijd makkelijk maar wel een uitdaging. U heeft mij altijd bijgestaan, ondersteund en het vertrouwen gegeven om de uitdaging aan te gaan. Hobbels op de weg werden door u glad gestreken en u gaf op de juiste momenten advies. Het schouderklopje op zijn tijd was natuurlijk niet nodig maar werd door mij stiekem wel op prijs gesteld. Ik heb veel respect voor uw onvoorwaardelijke inzet en de wijze waarop u mij heeft geholpen en ondersteund om mijn wetenschappelijke kwaliteiten te ontplooien.

Mijn tweede promotor, prof. dr. Ir. H.J.C.M. Sterenborg, geachte professor, beste Dick. Dit onderzoek is een voortzetting van een al jaren bestaand samenwerkingsverband tussen Groningen en Rotterdam en resulteerde opnieuw in een proefschrift. Ik wil u danken voor de geboden mogelijkheden om gebruik te kunnen maken van de faciliteiten en de expertise van het Centre of Optical Diagnostics and Therapy (CODT) van het Erasmus Medisch Centrum. De momenten waarop wij, aan het einde van een week met veel experimenten, de resultaten van de onderzoeken bespraken, zal ik blijven herinneren. Op een ontspannen, deskundige en relativerende wijze zette je mijn onderzoeksresultaten in een breder perspectief. Na ieder gesprek, verliet ik met een goed gevoel het CODT. Het SPIE congres in Innsbruck staat me ook goed bij. Niet alleen vanwege de voordrachten maar vooral onze goede en stimulerende gesprekken onder het genot van een glas wijn.

Mijn eerste co-promotor, dr. M.J.H. Witjes. Beste Max, waar moet ik beginnen? De onderzoeksopzet, je enthousiasme, je stimulerende en kritische vragen? Jij was de drijvende kracht achter mijn promotietraject. Jouw inzet en ideeën waren onontbeerlijk voor het opzetten van een goed doordacht promotieonderzoek. De dinsdagochtenden waarop ik je kamer binnenliep om "even" enkele punten te bespreken, waren vaak de start van lange gesprekken met nieuwe ideeën. De gesprekken bleven niet beperkt tot de dinsdagochtend; iedere dag stond je deur open, zelfs al was die dicht. Je creëerde daarmee voor mij een speelveld waarin ik vol

vertrouwen mijn weg kon gaan, maar altijd kon terugvallen op je wetenschappelijke kwaliteiten en kennis. In het begin van het onderzoek begeleidde je mij bij nieuwe stappen in het onderzoek, zoals het eerste dierexperiment, vervaardigen van 4NQO en de fDPS metingen, waardoor ik een goede start kon maken. Later sparden wij vooral over de opzet, de interpretatie van de resultaten en de klinische relevantie van de onderzoeken. Ik ben je dankbaar voor je hulp bij mijn wetenschappelijke vorming en de ruimte die je mij hierbij gaf. Ik weet zeker dat ik, na de promotie, hiervan nog vele jaren profijt van zal hebben. Ik heb bewondering voor de wijze waarop jij je wetenschappelijke activiteiten combineert met je drukke klinische werkzaamheden. Daarenboven vind ik het een plezier om met je samen te werken.

Mijn tweede co-promotor, dr. D.J. Robinson. Dear Dom, thank you for your support, patience, guidance, quick responses and enthousiasm for our project. It all seemed to make the 200 kilometers between Groningen and Rotterdam non-existent. When in Rotterdam, we always had lengthy discussions about our experimental setups and its limitations. Your experience with experimental PDT, knowledge of the intricate workings of PDT and your insight in the clinical role of PDT is impressive and was put to good use in this thesis. Most of all, you always made my trip to Rotterdam worthwhile and on the way back to Groningen the journey proved even faster as I had thoughts about new challenges, further analysis and additional research. Fortunately, we did not have to use photoshop corrections in the end; it all worked out!

Mijn derde co-promotor, dr. A. Amelink, beste Arjen. Dankbaar heb ik gebruik gemaakt van je deskundigheid die zich onder andere uit in het stellen van kritische vragen, je wetenschappelijke ideeën en je vermogen om snel tot de essentie van uitdagende onderzoeksvragen te komen. Je statistische kennis en interpretatie van de data, "the data is the data", waren van groot belang en ik heb er veel van geleerd. Onze fDPS experimenten tijdens het volgen van de olympische spelen op een laptopje, zijn voor mij verbonden aan dat onderzoek. Het tot stand brengen van een bruikbaar wifi signaal in de bunker was bijna uitdagender dan het experiment zelf. De muziek van "The National" behoort sindsdien ook tot mijn favorieten. Ik wens je veel succes in Eindhoven.

Ik wil ook de leden van de beoordelingscommissie bedanken: prof. dr. J.A. Langendijk, prof. dr. V. Vander Poorten en prof. dr. L.E. Smeele. Ik ben u zeer erkentelijk voor uw deskundige beoordeling van mijn proefschrift. Ik verheug me op de aankomende verdediging.

Prof. dr. F.K.L. Spijkervet, geachte professor, beste Fred. Ik wil u bedanken voor de mogelijkheden en vrijheid die u mij heeft geboden om op uw afdeling de opleiding tot MKA-chirurg te mogen volgen. Uw afdeling biedt een optimale, veilige en stimulerende omgeving voor een onderzoeker en een MKA-chirurg in wording. Ik heb u leren kennen als een toegankelijke, plezierige en onderwijs- en doelgerichte opleider. Ik verheug me op de resterende opleidingstijd.

Prof. dr. L.G.M. de Bont, geachte professor. Ik wil u bedanken voor de mogelijkheden die ik heb gekregen om het onderzoek uit te voeren aan de afdeling Kaakchirurgie. Een goede werkomgeving heeft er voor gezorgd dat ik met veel voldoening mijn onderzoek heb uitgevoerd.

Dr. S. Kascakova, dear Slavka, thank you for helping me with the window chamber experiments and the chemical extraction experiments. Even while it was tedious work, I enjoyed performing these experiments. I have fond memories about the wrapping of every tiny little detail of our experiment in aluminum foil, writing everything (and I mean everything) down, and of course listening to Slovakian music. I hope that you will have a splendid time in France. Pa, pa.

Dr. H.S. de Bruijn en mevr. A. Van der Ploeg – van de Heuvel, beste Riëtte en Lique, dank voor jullie fantastische hulp en ondersteuning. Wanneer ik in Rotterdam kwam, hadden jullie ervoor gezorgd dat ik direct aan de slag kon met de kamertjes modellen, het snijden van de vriescoupes en de confocale microscoop. Mijn bezoeken aan Rotterdam waren door jullie inzet efficiënt en plezierig. Jullie voorbereidende werkzaamheden bij het kamertjesmodel en de hulp in de vroege en late weekenddagen waren essentieel voor de studies. Vooral heel veel dank voor de gezellig gesprekken tijdens de dagenlange sessies achter de (vaak met olie ingesmeerde) microscoop.

Ik wil de collega's bedanken die als co-auteur een bijdrage hebben geleverd aan de onderzoeken die in dit proefschrift zijn beschreven.
Prof. dr. P.U. Dijkstra, beste Pieter, jouw kennis en begeleiding bij het systematisch uitvoeren van een systematic review heeft geleid tot 2 artikelen waaronder de eerste systematic review over de waarde van Foscan PDT. Prof. dr. I. Bing Tan, beste Bing, in 2006 heb ik mijn keuze co-schap bij jou in het Antoni van Leeuwenhoek ziekenhuis mogen lopen. Ik heb een fantastische tijd gehad en kwam tijdens deze periode voor het eerst in aanraking met allerlei aspecten van de PDT,. Bedankt voor het beschikbaar stellen van je data. Drs. B. Karakullukcu en drs. L.J. Melchers, beste Baris en Lieuwe, ik ben jullie dankbaar voor onze prettige samenwerking en het ter beschikking stellen van jullie database waardoor een vergelijkend onderzoek tussen PDT en chirurgische behandeling kon worden gepubliceerd. Dr. B. Van der Vegt, beste Bert, dank voor de efficiënte en ontspannen samenwerking bij het 4NQO artikel. Samen met jou heb ik enkele uren naar histologische coupes mogen kijken, dank voor je uitleg en interesse.

Beste Arie, Ar, Harm, Mark en Ralph, bedankt voor de ondersteuning bij de uitgebreide en vaak slecht planbare experimenten op het dierenlaboratorium. Hoewel rattenallergie mij vaak op de meest ongunstige momenten parten speelde, heb ik bij jullie, met behulp van allerlei maskers, veel plezier gehad!

Dr. W. Helfrich en ing. D. Samplonius, beste Wijnand en Douwe. Ik ben jullie erkentelijk dat ik tijdens het 4NQO experiment de mogelijkheid kreeg om gebruik te kunnen maken van het chirurgisch onderzoekslaboratorium en jullie ondersteuning.

W. Peng, beste Wei, je in-vitro werk laat interessante data zien, Ik ben erg benieuwd naar de uitkomsten van ons in-vivo PCI experiment met Foscan, succes met het onderzoek!

Beste Angelika, Harrie, Lisa, Nienke en Karin, bedankt voor de gezelligheid en hulp op de "derde".

Drs. P.M. Meiners, dr. M. Stokman en dr. N. Tymstra, beste Petra, Monique en Nienke "mijn kamergenoten". Gezelligheid, vreugde, frustratie en grappen, alle emoties kwamen voorbij in onze kamer. Petra, nog veel succes met het afronden van je proefschrift.

Dr. A. van Leeuwen, drs. S.H. Visscher, beste Anne en Susan. We begonnen gelijktijdig aan de opleiding Tandheelkunde. Vanwege het deel van het onderzoek dat in Rotterdam plaatsvond, heb ik de keuze gemaakt om me eerst volledig op het onderzoek te richten. Ik kon daarom helaas pas later starten met de studie Tandheelkunde. Ik vond het jammer dat ik daardoor de directe aansluiting met jullie verloor. Ik kijk terug op een tijd met leuke momenten maar ook onze gezamenlijke frustraties tijdens de preklinische fase. Anne, jij bent mijn gewaardeerde, gepromoveerde collega arts-assistent. Susan, binnenkort zal ook voor jou ook een einde komen aan je promotieonderzoek: veel succes met je tandheelkundige carrière.

Beste stafleden, arts-assistenten, onderzoekers en ondersteunend personeel van de afdeling Mondziekten, Kaak- en Aangezichtschirurgie van het UMCG. Jullie zorgen ervoor dat elke dag een leerzame en uitdagende dag is op een afdeling met een gemoedelijke sfeer; dank daarvoor.

Beste vrienden uit Grun, jullie hebben de afgelopen jaren gezorgd voor veel plezier en ontspanning. Nadat ik de studie Geneeskunde had afgerond, begon het nieuwe, andere leven met de studie Tandheelkunde. Het was gedaan met het wonen op kamers, pizza's bestellen, korte nachten, slechte films, de drankjes en de cafés. Of toch niet helemaal? Ik wil in willekeurige volgorde, Martijn, Frans, Jasper, Yvette, Jorrit, Sander, Ellen, Joost, Daan, Dimitri, Willemijn, Rick, Koen, Stijn, Jan-Peter en Thijs bedanken voor de borrels, de etentjes en de gezelligheid. Mogen er nog veel partijen volgen!

Beste Joost en Ingeborg, dank voor jullie gastvrijheid wanneer ik weer eens in Rotterdam was. Joost, ik wens je veel succes met je opleiding en promotieonderzoek aan de KNO-afdeling in Nijmegen.

Beste Lesley, wij kennen elkaar al vanaf onze jeugd in Hurdegaryp. Jij zat op een andere basisschool dan ik maar daarna hebben we veel gemeenschappelijke wegen bewandeld. Het Stedelijk Gymnasium in Leeuwarden, vakantiewerk op Vlieland, wonen in de Oosterpoort en de studie Geneeskunde. Mooi dat je nu in opleiding bent tot plastisch chirurg. Het is voor mij een voorrecht dat je mijn paranimf wilt zijn. Op naar jouw promotie?

Lieve Jan, mijn broer. Jij hebt de gave om mensen op hun gemak en welkom te laten voelen. Dat is een groot talent. We moeten wat vaker tijd voor elkaar maken. Ik vind het een eer dat je mijn paranimf wilt zijn.

Lieve Martine, mijn zus. Ik ben trots hoe jij je eigen weg vindt. Ik hoop dat ik nu wat meer tijd heb in de weekenden om vaker naar Amsterdam te kunnen komen.

Lieve Pa en Ma, jullie staan en stonden altijd voor mij klaar. Dat klinkt als vanzelfsprekend, maar dat is het niet. Samen met de Opa's en Oma's hebben jullie altijd veel belangstelling getoond voor mijn interesses, studies en werk. Ik kijk met warme gevoelens terug aan Hurdegaryp, Hengelo en Veldhoven. Jammer dat Opa de Visscher dit niet meemaakt. Lieve Ma, ik ben je erg dankbaar dat je mij een heerlijke jeugd hebt bezorgd, niet is bij jou onmogelijk voor je kinderen. Het heeft mij aan niets ontbroken. Lieve Pa, goed voorbeeld doet volgen. Ik heb veel respect hoe jij je inzet voor je werk en je gezin, je wilt altijd het beste voor ons.

Liefste Selma, ik ben zo blij met jou! Dank voor je eindeloze geduld tijdens mijn nog "eventjes" momenten, je hulp, je steun en je liefde. Ik ben ontzettend trots op je doorzettingsvermogen en positieve karakter, ook als het wat minder gaat. We hebben samen een hele mooie toekomst in het verschiet.

Sebastiaan de Visscher, december 2013

Curriculum Vitae

Sebastiaan Antonius Hendrik Johannes de Visscher was born on November 1st 1981 in Nijmegen, The Netherlands. In 2000 he graduated at the "Stedelijk Gymnasium" (pre-university education) in Leeuwarden. That same year he started his medical education at the University of Groningen. After obtaining his medical degree (MD), he started in 2007 his research at the University Medical Center Groningen, at the department of Oral and Maxillofacial Surgery. This work was combined with his dental training. After obtaining his dental degree (DDS) he started his Oral and Maxillofacial Surgery residency at the Department of Oral and Maxillofacial Surgery, University Medical Center Groningen (head: Prof. dr. F.K.L. Spijkervet, former head: Prof. dr. L.G.M. de Bont).